Universidad de Oviedo

Department of Mining Exploitation and Prospecting

Doctoral Thesis

Optimising characterization and remediation techniques for potentially toxic elements in polluted soils

---

Carlos Boente López

Under the supervision of:

José Luis Rodríguez Gallego, Carlos Sierra Fernández

Programme in Production, Mining-Environmental and Project Engineering

2019

Universidad de Oviedo
Universidá d'Uviéu
University of Oviedo

RESUMEN DEL CONTENIDO DE TESIS DOCTORAL

1.- Título de la Tesis	
Español/Otro Idioma: Optimización de técnicas de caracterización y remediación de suelos contaminados por elementos potencialmente tóxicos	Inglés: : Optimising characterization and remediation techniques for potentially toxic elements in polluted soils

2.- Autor	
Nombre: Carlos Boente López	DNI/Pasaporte/NIE:
Programa de Doctorado: Ingeniería de Producción, Minero-Ambiental y de Proyectos	
Órgano responsable: Explotación y Prospección de Minas	

RESUMEN (en español)

Esta investigación tiene por objeto desarrollar técnicas para la caracterización y remediación de suelos contaminados por elementos traza potencialmente tóxicos (Ing.: Potentially Toxic Elements, PTEs). Estos, por su toxicidad y peligrosidad para el medioambiente y la salud humana, constituyen el núcleo central de estudio. Mediante los procesos de caracterización, se busca identificar los contaminantes presentes en un suelo, estudiar su distribución espacial y evaluar sus posibles fuentes de emisión u orígenes. Por otro lado, la remediación de terrenos contaminados busca la eliminación o reducción de la concentración de los PTEs en el suelo. De esta manera, esta tesis abarca todo el proceso de vida de un contaminante en un suelo; desde que este accede al mismo procedente de una fuente, hasta que es eliminado. El trabajo es presentado como un compendio de 4 publicaciones. Dos relativas a las tecnologías de caracterización, y dos centradas en las de remediación.

Como avances más destacables en labores de caracterización, destaca la sinergia creada entre la estadística univariante, multivariante y la geoestadística (krigeado ordinario) para dar respuesta a los objetivos mencionados anteriormente. Además, estos se complementan con el desarrollo de un nuevo indicador de contaminación (Ing.: Soil Pollution Index, SPI) y la adaptación de la teoría de datos composicionales para introducir el nuevo concepto de Enriquecimiento Relativo del Contaminante (Ing.: Relative Enrichment of the Pollutant, RE). Todo ello teniendo considerando las diferentes escalas de trabajo y teniendo en perspectiva los Niveles Genéricos de Referencia.

Las acciones de remediación están focalizadas a mejorar la técnica del lavado de suelos. Se han utilizado diferentes equipos magnéticos y gravimétricos con suelos contaminados por distintas fuentes. Se proponen además varios métodos para la valoración de la eficiencia de los ensayos: validación del análisis atributivo y el nuevo Índice de Éxito (Ing.: Success Score). Adicionalmente, la tesis sienta las bases de una nueva técnica de remediación: El lavado de suelos asistido por nanopartículas de hierro cerovalente. Junto a esta se propone una nueva formulación basada en cuantificaciones magnéticas, cuyo objeto es evaluar la eficacia en la separación de los contaminantes de las técnicas empleadas, así como actuar de trazador de la distribución de nanopartículas en las muestras.

Universidad de Oviedo
Universidá d'Uviéu
University of Oviedo

RESUMEN (en Inglés)

This research aims to develop methodologies for the characterization and remediation of soils polluted by Potentially Toxic Elements (PTEs). Due to the toxicity and hazard caused to the environment and human health by PTEs, these constitute the core of the research. The characterization processes seek to (1) identify pollutants present in the soil, (2) study their spatial distribution, and (3) find their possible emission sources or origins. However, the remediation methodologies are intended to eliminate or reduce the concentration of PTEs in the soil. Thus, this thesis encompasses the entire life cycle of the pollutants in the soil; since they enter the soil arising from a source till they are eliminated. The thesis is presented as a compilation of 4 research papers, two related to the characterization methodologies, and two focused on the elimination of them.

Regarding characterization methods, one of the most important developments is the synergy that is established between the different univariate, multivariate, and geostatistical (ordinary kriging) analyses, in response to the objectives detailed earlier. Furthermore, these are complemented with a novel indicator of pollution (Soil Pollution Index, SPI) and also with the adaptation of the compositional data theory that allowed the introduction of a new concept: Relative Enrichment (RE). This was carried out considering the different scales of work and also the Risk-Based Soil Screening Levels (RBSSL).

However, the remediation processes are focused on the improvement in the soil washing technique. Different magnetic and gravimetric devices were used with soils polluted by different sources. Moreover, herein are proposed several methods for the assessment of the assays efficiency: Validation through attributive analysis and the new Success Score index. In addition, this thesis lays the foundation for the nanoscale ZVI-assisted soil washing. Moreover, there has been proposed an innovative formulation based on magnetic quantifications, the aim of which is to assess the efficiency of the methods used for pollutant separation, as well as to act as a tracer of the nanoparticles distribution on the samples.

SR. PRESIDENTE DE LA COMISIÓN ACADÉMICA DEL PROGRAMA DE DOCTORADO EN INGENIERÍA DE PRODUCCIÓN, MINERO-AMBIENTAL Y DE PROYECTOS

Universidad de Oviedo
Universidá d'Uviéu
University of Oviedo

FORMULARIO RESUMEN DE TESIS POR COMPENDIO

1.- Datos personales solicitante	
Apellidos: Boente López	Nombre: Carlos

Curso de inicio de los estudios de doctorado	2015

	SI	NO
Acompaña acreditación por el Director de la Tesis de la aportación significativa del doctorando	X	
Acompaña memoria que incluye		
Introducción justificativa de la unidad temática y objetivos	X	
Copia completa de los trabajos *	X	
Resultados/discusión y conclusiones	X	
Informe con el factor de impacto de la publicaciones	X	
Se acompaña aceptación de todos y cada uno de los coautores a presentar el trabajo como tesis por compendio	X	
Se acompaña renuncia de todos y cada uno de los coautores a presentar el trabajo como parte de otra tesis de compendio	X	

* Ha de constar el nombre y adscripción del autor y de todos los coautores asi como la referencia completa de la revista o editorial en la que los trabajos hayan sido publicados o aceptados en cuyo caso se aportará justificante de la aceptación por parte de la revista o editorial

FOR-MAT-VOA-033

Artículos, Capítulos, Trabajos

Trabajo, Artículo 1

Titulo (o título abreviado)	Trace elements of concern affecting urban agriculture in industrialized areas: A multivariate approach
Fecha de publicación	26 Mayo 2017
Fecha de aceptación	21 Mayo 2017
Inclusión en Science Citation Index o bases relacionadas por la CNEAI (indíquese)	Sí
Factor de impacto	4.427 (2017)

Coautor2 X Doctor □ No doctor . Indique nombre y apellidos	Nora Matanzas Valtuille
Coautor3 X Doctor □ No doctor . Indique nombre y apellidos	Nerea García González
Coautor4 □ Doctor X No doctor . Indique nombre y apellidos	Eduardo Rodríguez-Valdés Rodríguez
Coautor5 X Doctor □ No doctor . Indique nombre y apellidos	José Luis Rodríguez Gallego

Universidad de Oviedo
Universidá d'Uviéu
University of Oviedo

Trabajo, Artículo 2

Titulo (o título abreviado)	Combining raw and compositional data to determine the spatial patterns of Potentially Toxic Elements in soils
Fecha de publicación	5 Marzo 2018
Fecha de aceptación	5 Marzo 2018
Inclusión en Science Citation Index o bases relacionadas por la CNEAI (indíquese)	Sí
Factor de impacto	4.610 (2017)

Coautor2 X Doctor □ No doctor . Indique nombre y apellidos	Maria Teresa Duraes Albuquerque
Coautor3 □ Doctor X No doctor . Indique nombre y apellidos	Alicia Fernández Braña
Coautor4 □ Doctor X No doctor . Indique nombre y apellidos	Saki Gerassis Davite
Coautor5 X Doctor □ No doctor . Indique nombre y apellidos	Carlos Sierra Fernández
Coautor6 X Doctor □ No doctor . Indique nombre y apellidos	José Luis Rodríguez Gallego

Trabajo, Artículo 3

Titulo (o título abreviado)	Soil washing optimization by means of attributive analysis: Case study for the removal of potentially toxic elements from soil contaminated with pyrite ash
Fecha de publicación	1 Noviembre 2016
Fecha de aceptación	4 Noviembre 2016
Inclusión en Science Citation Index o bases relacionadas por la CNEAI (indíquese)	Sí
Factor de impacto	5.651 (2017)

Coautor2 X Doctor □ No doctor . Indique nombre y apellidos	Carlos Sierra Fernández
Coautor3 □ Doctor X No doctor . Indique nombre y apellidos	Eduardo Rodríguez-Valdés Rodríguez
Coautor4 X Doctor □ No doctor . Indique nombre y apellidos	Juan María Menéndez Aguado
Coautor5 X Doctor □ No doctor . Indique nombre y apellidos	José Luis Rodríguez Gallego

Trabajo, Artículo 4

Titulo (o título abreviado)	Nanoscale zero-valent iron-assisted soil washing for the removal of potentially toxic elements
Fecha de publicación	9 Febrero 2018
Fecha de aceptación	24 Enero 2018
Inclusión en Science Citation Index o bases relacionadas por la CNEAI (indíquese)	Sí
Factor de impacto	6.434 (2017)

Coautor2 X Doctor □ No doctor . Indique nombre y apellidos	Carlos Sierra Fernández
Coautor3 X Doctor □ No doctor . Indique nombre y apellidos	David Martínez Blanco
Coautor4 X Doctor □ No doctor . Indique nombre y apellidos	Juan María Menéndez Aguado
Coautor5 X Doctor □ No doctor . Indique nombre y apellidos	José Luis Rodríguez Gallego

Acknowledgements

This may be the only opportunity for me to thank all the people who were involved in this research directly or indirectly. So, you may find me a little more verbose in expressing my gratitude than expected.

If I had to underscore the support of two people, they would be my thesis directors: Prof. José Luis R. Gallego and Prof. Carlos Sierra Fernández. José Luis is a very inspirational and patient person from whom I learnt a lot all these years since 2013. I specially thank Carlos for introducing me to the concept of "researching," which was not clear for me initially. They both always provided me fast and effective assistance in the compilation of every chapter of this thesis. I consider myself fortunate to have had the opportunity to work with them.

I am likewise grateful to Prof. Teresa Albuquerque from IPCB (Castelo Branco) and Alejandro Bel-Lán from IGME (Madrid) for allowing me for my research stays. Both of them made me feel at home, offering me support and collaboration, both in working and social aspects. Furthermore, I must mention all the wonderful people I met at both places whom I cannot forget.

Some personnel from the University of Oviedo played significant roles, especially the support and advice of Prof. Juan María Menéndez-Aguado and David Martínez-Blanco were key during the compilation of the toughest part of the work: the chapter on soil remediation.

Of course, I will always remember and be thankful to the entire staff of INDUROT, and particularly, my work colleagues from the Geochemistry Area. Some of them also contributed greatly to various researches required to complete this thesis, and also to other non-academic tasks.

My parents' contribution must be also mentioned here. Apart from contributing to my genetic constitution, they are the prime designers of my personality. I thank them for the moral values and discipline that they inculcated in me since my childhood, as well as for their immense love and support. This was essential for this kind of work that demanded insistence and overcoming various issues. As remarked in every chapter of this thesis, I repeat that a healthy environment is desirable. Mine has been certainly excellent, and principally because of them.

Last, but not the least, I thank Zulema García, my girlfriend. She accompanied me to both research stays, and is ready to repeat it if a need arises. Whatever the destiny has planned for us, she is ready to face it alongside me. She definitely deserves a huge thanks.

Índice

Financing

This thesis has been financed by the *Formación del Profesorado Universitario* program, from the *Ministerio de Educación y Formación Profesional* (Reference FPU14/02215).

Both research stays, performed in the *Instituto Politécnico de Castelo Branco, Portugal* (3 months) and in the *Instituto Geológico y Minero de España, Madrid* (*IGME)* (1.5 months) were also financed by the program *Ayuda a la Movilidad para Estancias Breves*, from the same organism (References EST16/00264 and EST17/00209).

Contribution of the author to the published work

The candidate declares the authorship of all the chapters of this thesis, presented as a compendium of research articles. Chapter I (Introduction) has been completely compiled by him. Chapters II and III comprise the research articles. The field, laboratory and computing tasks, as well as the redaction of the articles have also been conducted by the student under the supervision of the rest of the authors of each paper. Chemical analyses were subcontracted to Actlabs (Canada) or to the Scientific and Technical Services of the University of Oviedo. Chapters IV and V (Discussion and Conclusions) were also contributed by the candidate.

List of Acronyms

ALR → *Additive Log-ratio (transformation)*

API → *Average Pollution Index*

CA → *Cluster Analisis*

CF → *Contaminant Factor*

CLR → *Centred Log-ratio (transformation)*

CVAAS → *Cold Vapor Atomic Absorption Spectrometry*

Dry-HIMS / DHIMS → *Dry-High Intensity Magnetic Separator*

ECEC → *Effective Cation Exchange Capacity*

EEA → *European Environment Agency*

EF → *Enrichment Factor*

GIS → *Geographic Information System*

HIMS → *High Intensity Magnetic Separation*

HLS → *Heavy Liquid Separation*

HPLC → *High Performance Liquid Chromatography*

ICP-MS/OES → *Inductively Coupled Plasma Mass/Optical Spectrometry*

IDW → *Inverse Distance Weighting*

ILR → *Isometric Log-ratio (transformation)*

NNIDW → *Natural Neighbour Inverse Distance Weighted*

NST → *Normal Score Transform*

nZVI → *Nano zero-valent Iron*

PAH → *Polycyclic Aromatic Hydrocarbon*

PCA → *Principal Component Analysis*

PIN → *Nemerow's Pollution Index*

PTE → *Potentially Toxic Element*

PXRD → *Powder X-Ray diffraction*

RBSSL → *Risk-Based Soil Screening Level*

RE → *Relative Enrichment*

RI → (*Ecological) Risk Index*

RSD → *Relative Standard Deviation*

SD → *Standard Deviation*

SGS → *Sequential Gaussian Simulation*

SPI → *Soil Pollution Index*

SSL → *Soil Screening Level*

TCLP → *Toxicity Characteristics Leaching Procedure*

VSM → *Vibrating Sample Magnetometer*

Wet-HIMS / WHIMS → *Wet-High Intensity Magnetic Separator*

WHO → *World Health Organization*

ZVI → *Zero-valent Iron*

Abstract

This research aims to develop methodologies for the characterization and remediation of soils polluted by Potentially Toxic Elements (PTEs). Due to the toxicity and hazard caused to the environment and human health by PTEs, these constitute the core of the research. The characterization processes seek to (1) identify pollutants present in the soil, (2) study their spatial distribution, and (3) find their possible emission sources or origins. However, the remediation methodologies are intended to eliminate or reduce the concentration of PTEs in the soil. Thus, this thesis encompasses the entire life cycle of the pollutants in the soil; since they enter the soil arising from a source till they are eliminated. The thesis is presented as a compilation of 4 research papers, two related to the characterization methodologies, and two focused on the elimination of them.

Regarding characterization methods, one of the most important developments is the synergy that is established between the different univariate, multivariate, and geostatistical (ordinary kriging) analyses, in response to the objectives detailed earlier. Furthermore, these are complemented with a novel indicator of pollution (Soil Pollution Index, SPI) and also with the adaptation of the compositional data theory that allowed the introduction of a new concept: Relative Enrichment (RE). This was carried out considering the different scales of work and also the Risk-Based Soil Screening Levels (RBSSL).

However, the remediation processes are focused on the improvement in the soil washing technique. Different magnetic and gravimetric devices were used with soils polluted by different sources. Moreover, herein are proposed several methods for the assessment of the assays efficiency: Validation through attributive analysis and the new Success Score index. In addition, this thesis lays the foundation for the nanoscale ZVI-assisted soil washing. Moreover, there has been proposed an innovative formulation based on magnetic quantifications, the aim of which is to assess the efficiency of the methods used for pollutant separation, as well as to act as a tracer of the nanoparticles distribution on the samples.

Resumen

Esta investigación tiene por objeto desarrollar técnicas para la caracterización y remediación de suelos contaminados por elementos traza potencialmente tóxicos (Ing.: Potentially Toxic Elements, PTEs). Estos, por su toxicidad y peligrosidad para el medioambiente y la salud humana, constituyen el núcleo central de estudio. Mediante los procesos de caracterización, se busca identificar los contaminantes presentes en un suelo, estudiar su distribución espacial y evaluar sus posibles fuentes de emisión u orígenes. Por otro lado, la remediación de terrenos contaminados busca la eliminación o reducción de la concentración de los PTEs en el suelo. De esta manera, esta tesis abarca todo el proceso de vida de un contaminante en un suelo; desde que este accede al mismo procedente de una fuente, hasta que es eliminado. El trabajo es presentado como un compendio de 4 publicaciones. Dos relativas a las tecnologías de caracterización, y dos centradas en las de remediación.

Como avances más destacables en labores de caracterización, destaca la sinergia creada entre la estadística univariante, multivariante y la geoestadística (krigeado ordinario) para dar respuesta a los objetivos mencionados anteriormente. Además, estos se complementan con el desarrollo de un nuevo indicador de contaminación (Ing.: Soil Pollution Index, SPI) y la adaptación de la teoría de datos composicionales para introducir el nuevo concepto de Enriquecimiento Relativo del Contaminante (Ing.: Relative Enrichment of the Pollutant, RE). Todo ello teniendo considerando las diferentes escalas de trabajo y teniendo en perspectiva los Niveles Genéricos de Referencia.

Las acciones de remediación están focalizadas a mejorar la técnica del lavado de suelos. Se han utilizado diferentes equipos magnéticos y gravimétricos con suelos contaminados por distintas fuentes. Se proponen además varios métodos para la valoración de la eficiencia de los ensayos: validación del análisis atributivo y el nuevo Índice de Éxito (Ing.: Success Score). Adicionalmente, la tesis sienta las bases de una nueva técnica de remediación: El lavado de suelos asistido por nanopartículas de hierro cerovalente. Junto a esta se propone una nueva formulación basada en cuantificaciones magnéticas, cuyo objeto es evaluar la eficacia en la separación de los contaminantes de las técnicas empleadas, así como actuar de trazador de la distribución de nanopartículas en las muestras.

Chapter I. Introduction to Soil Pollution and Potentially Toxic Elements

I.I Soil pollution: Concept and sources

Soil pollution is defined as the presence or the introduction harmful or poisonous substance(s) into the soils at such a concentration that it may pose a risk to human health and/or ecosystem. Such an introduction can be a consequence of both natural and human factors (Thornton, 2012).

A vast variety of elements and compounds are naturally present in the soils. Some of them are metals, metalloids, inorganic ions (e.g., potentially toxic elements, PTEs), salts, and organic compounds (namely, hydrocarbons, polycyclic aromatic hydrocarbons [PAHs], heterocyclics, alcohols), among others. Thus, when the concentration of these contaminants exceeds certain threshold levels, a concept that has been developed in the following, it might result in soil pollution.

In this context, it is worth stressing that pollution should not be used as a synonym of contamination, although both terms sometimes are used interchangeably. Within this context, the main difference lies in the capability of the environment to absorb or endure a harmful agent. Thus, if the environment can resist that agent without hampering the chemical cycles of life, we refer to it as contamination. However, if the agent causes damage to the environment or human health, it is referred to as pollution (Chapman, 2007). In brief, all pollutants are contaminants, but not all contaminants are pollutants.

The sources of pollution may be generally divided into two main categories: natural and anthropogenic. The former are less common in the present, although they can be more devastating. Some of them are as follows (Alloway, 2013):

- Natural accumulation by means of atmospheric deposition and leaching away with precipitation.
- Natural enrichment of certain elements in the Earth's crust, which might be advantageous for mining.
- Natural production in the soil when certain environmental conditions are established.
- Natural disasters such as volcanos, earth/seaquakes, etc.

Furthermore, anthropogenic sources might be "deliberate" (industrial, mining) or accidental. They account for the major part of the cases of soil pollution (Alloway, 2013). A list of examples is provided in the following:

- Industry: Foundries and manufacturing plants, involving furnaces or processes that might disperse contaminants, are the most common source of pollution, according to the European Environment Agency (EEA).
- Mining: The crushing or processing of raw materials are a common source of pollutants. In some cases, this sort of pollution occurs along with the natural one.
- Agricultural activity: The use of herbicides, pesticides, insecticides, or fertilizers.
- Traffic: Vehicle exhausts are of special concern in cities or soils surrounding frequented roads or motorways, although it exhibits decreasing trends with the use of less contaminating fuels.
- The dumping or storage of wastes in landfills. Large quantities of waste might provoke the migration of pollutants from soil to groundwater, causing the contamination of other environmental matrices.

The EEA periodically updates a document with the principal sources of contamination in soils. The last revision, in 2012, revealed that industry was, by far, the main source of pollution, which combined with the oil industry surpasses 50% of the total sources. The abovementioned natural sources are included among the 9% of the "Others" category (Figure 1.1).

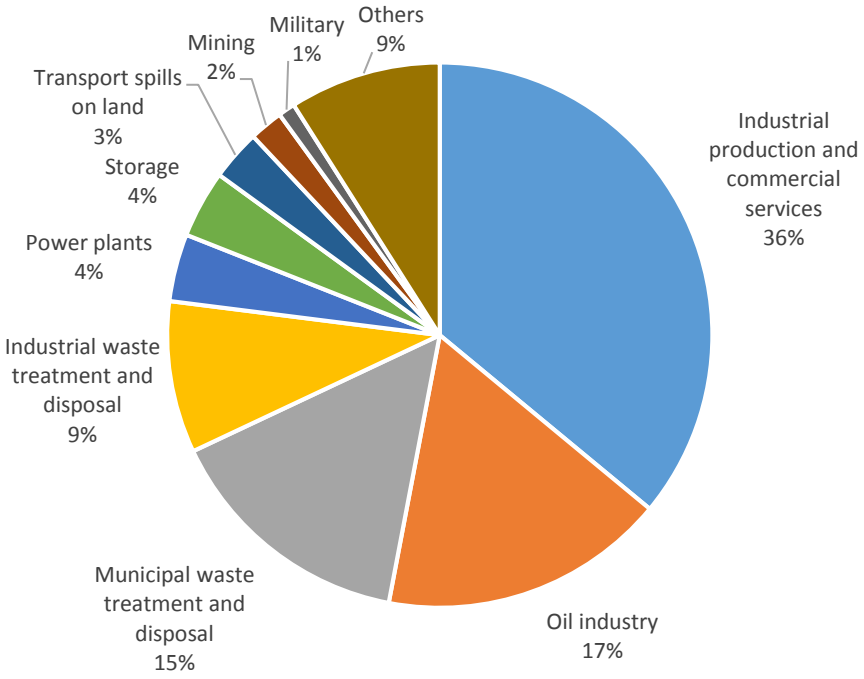

Figure 1.1. Sources of soil pollution in the EU (Source: European Environment Agency, 2012)

Once the causes were reviewed, there were found a huge variety of contaminants that could endanger soils. Of them, the present thesis focuses only on PTEs, particularly with regard to their identification, distribution, interaction, and remediation options.

I.II Potentially Toxic Elements

In geochemical studies, the term PTE is often treated as a synonym for "heavy metals" and "trace elements." This is not completely correct. Technically, or by definition, heavy metals are elements with five times higher density than that of water. Of them, a few are essential for the enzyme system (e.g., Zn, Mo, Co), whereas others are hazardous or carcinogenic (e.g., Hg, As, Pb, Sb). Moreover, a trace element is one with a concentration less than 1000 $mg \cdot kg^{-1}$ in a rock composition, thus including the majority of the elements in the periodic table (Duffus, 2002).

PTEs are a group of chemical elements of environmental concern the principal feature of which are their persistence in the environment and the ease with which they biomagnify and bioaccumulate (Clemens, 2006). Their accumulation would not have had any interest if some of them were not highly toxic, putting in risk the health of various ecosystems and that of humans when they reach certain concentrations in different compartments (e.g., soil, water, sediments, air). Consequently, their identification, characterization, and remediation are key factors for sustainable development.

In the scientific community, there is disagreement as to which elements compose the entire list. A reliable one is provided by the project Geochemical Mapping of Agricultural and Grazing Land Soil (GEMAS). It is a European geochemical atlas of agricultural soils that assesses their exposure to PTEs and their relatives (Fabian et al., 2014). Project results were presented in December 2013 in Rome, Italy. The number of elements studied reached 53, all of which have been summarized in Table 1.1. Of these, those that present a certain degree of toxicity (T, T+, or T++) correspond to PTEs.

Table 1.1 List of elements analyzed under the project GEMAS and their level of toxicity: T++ as high, T+ as moderate, T as low, V as variable toxicity, N as nontoxic, R as radioactive, and U as undefined (Source: Adapted from GEMAS project, 2014).

Sym.	Element	Tox.	Sym.	Element	Tox.	Sym.	Element	Tox.
Ag	Silver	T+	In	Indium	U	Sn	Tin	U
Al	Aluminum	T	K	Potassium	N	Sr	Strontium	T+
As	Arsenic	T++	La	Lanthanum	U	Ta	Tantalum	U
Au	Gold	T+	Li	Lithium	T	Te	Tellurium	U
B	Boron	T	Mg	Magnesium	N	Th	Thorium	R
Ba	Barium	T+	Mn	Manganese	T	Ti	Titanium	T
Be	Beryllium	T++	Mo	Molybdenum	T+	Tl	Thalium	T++
Bi	Bismuth	U	Na	Sodium	N	U	Uranium	R
Ca	Calcium	N	Nb	Niobium	U	V	Vanadium	T+
Cd	Cadmium	T++	Ni	Nickel	T+	W	Wolfram	U
Ce	Cerium	U	P	Phosphorus	V	Y	Yttrium	U
Co	Cobalt	T+	Pb	Lead	T++	Zn	Zinc	T+
Cr	Chromium	T++	Pd	Palladium	U	Zr	Zirconium	U
Cs	Caesium	U	Pt	Platinum	T+			
Cu	Copper	T	Rb	Rubidium	U			
Fe	Iron	N	Re	Rhenium	U			
Ga	Gallium	T	S	Sulphur	V			
Ge	Germanium	U	Sb	Antimony	T++			
Hf	Hafnium	U	Sc	Scandium	U			
Hg	Mercury	T++	Se	Selenium	T++			

Usually, those elements classified as T, T+, or T++ may pose damage to both human health and/or environment when they occur in high concentrations (He et al., 2005), thus coinciding with the traditionally termed PTEs. The list is headed by As, Be, Cd, Cr, Hg, Pb, Sb, Se, and Tl, although others should not be underestimated.

As mentioned earlier, PTEs form part of the environment. But their concentrations in the soils increased mostly as a consequence of human activities (Alloway, 2013). Among the main reasons for this increase, escalation of the human population, and the increasing demand for goods can be highlighted. In the following pages, a brief description of the principal PTEs affecting the soils of the Principality of Asturias (Spain), specifically those studied in the literature and presented in this thesis, is provided. The description is focused on the chemistry, mineral paragenesis, toxicity, sources of pollution, as well as risks for the human health and the environment.

Arsenic

Arsenic (As; atomic number: 33) is a metalloid that usually occurs in combination with metals or sulfurs. The typical minerals it forms are arsenopyrite (FeSAs) and arsenolite (As_2O_3), but it can also occur in the form of realgar (AsS) and orpiment (As_2S_3), two minerals the geology of both of which is very much linked to that of cinnabar (HgS), the principal ore of Hg. This fact relates these two PTEs, which show geochemical affinity and are usually present together in their natural backgrounds without necessary occurrence of anthropogenic activity (Duker et al., 2005). Other examples of natural associations are Au/Ag–As (hydrothermal veins), Ni–Cu(–As) massive sulfides, Cu shales, or phosphate deposits, but in Asturias their importance is minor.

When the human activity factor is considered, as can occur in different forms such as mining, waste disposal, use of fertilizers, pesticides, herbicides, groundwater exploitation, geological alterations (floods) or chemical by-products, and spillage. For instance, the roasting of pyrite (FeS_2) for the production of sulfuric acid results in a very dangerous waste termed *pyrite ash*, which comprises high concentrations of hematite and PTEs, especially As (Oliveira et al., 2012). Principal applications of As include its usage in the performance of insecticides, fungicides (Cu-Arsenates), and also as herbicides along railroads.

Arsenic toxicity presents dependence on valence: As (III) compounds are more toxic than As (V) compounds. As (V) species predominate in aerobic conditions, whereas As (III) is predominant under reducing conditions. It is especially toxic when it interacts with sulfydryl groups of proteins or enzymes, and also through the increase of oxygen species that are reactive in the cells (Gebel, 2000). Long-term effects of high levels of inorganic arsenic exposure might provoke the occurrence of severe diseases, including dermal lesions, skin cancer, or vascular diseases. Dermal lesions are predominant and have been observed in populations with high concentrations of As in drinking water (Smith et al., 2000). However, vital organs such as liver, kidney, or the circulatory system are also severely affected as they are involved in arsenic absorption.

The mean amount of As content in soils is 5 $mg \cdot kg^{-1}$ in the world (natural soils); in the soils of Asturias, this mean is almost thrice that of the world, reaching 13.7 $mg \cdot kg^{-1}$ (Fernández et al., 2018). Furthermore, Asturias has several sites where the concentrations surpass 1000 $mg \cdot kg^{-1}$. Some well-known sites contaminated by As are the fertilizer

factory of Nitrastur (pyrite cinder wasting), and the Hg mines of El Terronal and La Soterraña, among others (Gallego et al., 2016, 2015).

There are plants that can highly concentrate this element in an eco-friendly, but by slow, remediation through the process of phytoextraction. For instance, *Raphanus sativus* (Smith et al., 2008) or *Pteris vittata* (Wang et al., 2007) are typical As-hyperaccumulators. Even trees such as *Betula celtiberica* have showed a great potential of As-decontamination in soils of Asturias (Mesa et al., 2017), where it is autochthonous.

Soil washing has also shown a notable potential for decontamination of As-enriched soils (Sierra et al., 2011; 2010). These procedures explore the size and density differences between soil particles and As compounds to enable separation. This happens due to the adsorption of PTE onto the clayey particles of the soil, which are feasible to be separated by size. Moreover, magnetic susceptibility and electric conductivity can be also exploited by means of magnetic and electric separators (Jobin et al., 2016; Sierra et al., 2013). This is a trend that occurs not only with As, but also with other PTEs.

Antimony

The chemistry of antimony (symbol Sb and atomic number 51) is very similar to that of As. It is a chalcophile metalloid the toxic species of which are equal, Sb (III) being more hazardous than Sb (V), presenting a tendency to react with sulfurs, forming complex compounds such as stibnite (Sb_2S_3) or kermesite (Sb_2S_2O). This metalloid also presents oxide compounds such as valentinite (Sb_2O_3) and cervantite (Sb_2O_4).

In nature, antimony presents natural associations with Pb, Cu, Zn, and Ag deposits, although it is not frequently the principal aim of a mining exploitation or the principal product of an industry. For this reason, this PTE is often considered as a secondary contaminant in environmental studies, because its apparition is not straightforward.

Generally, it occurs in regions where smelting of Cu or Pb is carried out, emitted by car exhausts, and also produced during the combustion of coal. Precisely, coal burning forced the accomplishment of several studies about this metal in China (Qi et al., 2008) and this may also be the principal reason for the high presence of the PTE in the soils of Asturias, a region whose major driver has historically been the coal mining, and from which up to five thermal power stations in the region take advantage of. Three of the four areas studied in this thesis are located less than half a kilometer away from a coal power

plant, which led Sb to be considered as the principal contaminant through the research. It has left an appreciable footprint in practically all polluted regions' soils of Asturias as a consequence of the abovementioned reasons that encourage its emergence.

Thus, although Sb has not received as much attention as other PTEs in environmental science, its harmfulness to human health is high, being even more toxic than As or Pb (McCallum, 2005). Thus, lung tumors, intestinal problems, or dermal irritation are just some of the issues that a high exposure to this PTE might cause.

The extraction of this PTE has been recently assessed (Mubarak et al., 2015). The recommended techniques to decontaminate soils affected by this pollutant are the use of chelating agents or the chemical fixation. Authors also highlight the green technologies (phyto- and bio-remediation) as alternative, whereas others such as soil washing is unfeasible unless the site is highly contaminated. Throughout this research, it will be sustained that the later statement is not completely correct in all cases.

Mercury

Among PTEs that present high concern, perhaps mercury (symbol Hg and atomic number 80) is the top most hazardous. It is a non-essential, extremely toxic but non-carcinogenic transition metal that can be found in the native form (rare), or in the form of a mineral: cinnabar (HgS), the most common ore or livingstonite ($HgSb_4S_6$). Deposits of this PTE are principally hydrothermal, and occur in natural associations of Hg–Sb–As or Hg–Ag/Au in quartz, and as Au or Hg vein deposits.

Inorganic Hg presents a high mobility in acid conditions and it can evaporate when released into water or soil due to its low melting and evaporation points. Microbes can convert the inorganic Hg to organic forms (methyl/ethyl-Hg), speciation which is even more toxic, and that can accumulate in aquatic life (Syversen and Kaur, 2012). Precisely, the accumulation of methyl-Hg on fishes and shellfishes of the Minamata Bay caused the major poisoning event of this PTE ever known (Harada, 1995).

Unfortunately, this was not the unique case of poisoning by this PTE. The metal has been in contact with humans in multiple cases because of its multitude of uses: caustic soda or chlorine production, gold ore processing, dentistry, wood impregnation, barometers and thermometers, and detonators or vapor lamps are only some of the applications this heavy metal has, some of them even for household use.

Hg extraction had its apogee during the decades of the years 1940s–1960s, but it was started to be substituted by other elements with the increase in the social awareness about its toxicity and hazard. This is the reason why in the decade of 1970, the USSR sold most of its Hg reserves, causing a strong drop in prices that affected all over the world the so-called "Mercury crisis" (Luque and Gutierrez-Claverol, 2006). In Europe, its extraction was forbidden around the year 2000 in some countries. Moreover, the European Union launched a strategy in 2005 to reduce the emission of mercury in all its territories, growing in relevance since the recent coming into force of the Minamata UN convention, in 2017, a universal environmental agreement that obligates the countries to control the sources of mercury pollution (Evers et al., 2016). This arrangement is intended to ban all exports, imports, and fabrication of products composed of Hg between the years 2018 and 2020 (United Nations, 2017).

Regarding Spain, Hg is linked to the mining history of this country since the Roman era, playing a significant role in it. The mines of Almadén (Ciudad Real) constitute the greatest cinnabar reservoir of the world, and despite its closure due to the price depression, the deposit continues hosting a vast volume of this metal (Higueras et al., 2011). Something similar has occurred in the Principality of Asturias, where there were a considerable number of Hg-mines widely dispersed in the territory: some of the most popular and important mines are El Terronal, La Soterraña, Olicio, and Caunedo, which are included in the Inventory of Polluted Soils of the Principality of Asturias too. The study of their impact on the environment was a topic of interest for geochemists of the region during the last decade (Fernández-Martínez et al., 2015; Larios et al., 2012; Loredo et al., 2006; Sierra et al., 2011), including phytoremediation approaches (Matanzas et al., 2017; Fernández et al., 2017). For instance, soils of Olicio were selected for in-depth case studies for the remediation methodologies applied in the current research. Moreover, a review of the Asturian Hg overview was recently published (Ordóñez et al., 2013).

Among all the problems it can cause to human health, Hg inhalation or exposure to it at high concentrations might provoke respiratory distress, symptoms of the central nervous system (CNS) such as tremors, memory loss, or neurocognitive disorders. Many of these signs disappear once the exposure ends, but a long-term contact may produce irreversible damage to the kidney and brain. An extensive review of the effects of Hg on human health is highlighted in Clarkson and Magos (2006).

Copper

Copper (Cu; atomic number 29) is one of the most exploited metals in mining. Cu has multiple uses: smelting, for the production of bronze alloys when combined with tin (Sn), electrics or electronics, water piping, pigments, coins, jewelry, kitchenware, transport sector, and new materials, among others. Cu demand does not seem to stop as human increasingly uses Cu utensils and similar products that are manufactured with this metal. Its properties include excellent electric and thermal conductivities as well as magnetic susceptibility.

Cu occurs in the nature as a native element or by forming a huge variety of minerals such as chalcopyrite ($CuFeS_2$), bornite (Cu_5FeS_4), malachite ($Cu_2Co_3[OH]_2$), covellite (CuS), and chalcosite (Cu_2S), among others. It is associated with volcanogenic massive sulfide deposits (together with Pb, Zn, Cd, Ag, Fe, As, and Sb), porphyry Cu deposits (Fe, Mo), or Cu shale deposits (Ag, Zn, Pb, and Mo) (Álvarez et al., 2018). Mining, industry, or even agriculture, are the principal activities through which it enters into the soils, the distribution of which might be attributable to air (factory chimneys), water (mining leachates), and waste deposits (i.e., pyrite ashes). Soils of the world present a medium concentration of Cu around the 25 $mg \cdot kg^{-1}$. Cu toxicity is relatively rare and minor as compared with Hg or As and occurs when Cu(II) is reduced to Cu(I) in the presence of superoxide or reducing agents (Gaetke et al., 2014). However, chronic exposure to Cu may result in Menkes and Wilson's diseases (Chen et al., 2011). Mineral processing technologies are common ways to decontaminate a soil polluted by this PTE.

Regarding Asturias, it is known that the number of Cu active mines was 15 at the end of the nineteenth century (Rodríguez-Terente et al., 2006). Mining of this metal persists nowadays but very minimal, principally as a secondary product by means of flotation processes in several gold mines (Cepedal et al., 2006). In this context, the Texeo district, located in the Aramo mountain range has historically been the most prominent Cu mine in the area (Martínez Cortizas et al., 2016). Beyond them, the high degree of past and current industrialization of the region has led to an undoubted pollution of soils, as it is stated across the environmental studies that were conducted in the area (Miranda et al., 2005).

Lead

One of the most typical pollutants is lead (Pb; atomic number 81). This is chalcophile metal the principal ore of which is the galena (PbS). It could occur as lead deposits (together with Zn–Cd, which share a similar chemistry, or Cu), and also in fide or Mississippi Valley epigenetic type reservoirs.

Pb presents the particular feature of being an immobile metal. It binds strongly to the humic fraction of the soil, and does not often migrate to the ground water, therefore inducing the contamination of the topsoil, but not of the deeper parts. Car exhausts were the main source of pollution of this PTE in the world during the leaded gasoline era until its ban in the year 2000, but this legacy stills persists in areas next to roads or cities (Mielke et al., 2010). Nowadays, this pathway has been substituted by steel works, smelters, coal combustion, or more generally, blast furnace flux dust, which made from Pb one of the principal inorganic pollutants in the world. Moreover, its mining and metallurgical process are among those that produce the most wastes (Gallego et al., 2001).

Regarding health, Pb is not considered an essential element. In fact, the maximum contaminant-level goal for this PTE in drinking water is zero mg/l. Pb intake might cause, according to the World Health Organization, severe damage to brain, kidneys, liver, and bones, by accumulating on both bones and teeth.

Due to its significant presence and risk to the environment and/or human health, there were performed multitude of studies to reduce its content all over the world: physical soil washing is a suitable treatment technique as a consequence of the density of the metal (Demir and Köleli, 2013; C. Sierra et al., 2013). Finally, stabilization is a common technology that tries to take advantage of the difficulties of this PTE to be transported (Alpaslan and Yukselen, 2002), retaining the contaminant to the soil matrix and impeding its mobility by different processes, such as its absorption by the roots of plants (Matanzas et al., 2017) or by the addition of nanoparticles.

The Principality of Asturias is not characterized by having a large number of Pb mines. Five exploitations were significant, but its relevance in the sector was minor (Rodríguez-Terente et al., 2006). The heavy industries in the region is the major cause of pollution by this PTE (Gallego et al., 2013; Sierra et al., 2014a), which is present in almost all the cases of this study, although in different concentrations and origins.

Zinc

As well as Pb, Zinc (Zn; atomic number 30) is a chalcophile element the chief mineral ore of which is the sphalerite (ZnS), although it can be extracted from wurtzite (ZnS), smithsonite ($ZnSO_4$), or zincite (ZnO). It is found associated with Cd and also with Pb in Mississippi valley deposits.

Zn is an essential element for all organisms. Its toxicity is generally moderate/low and is not carcinogenic. From this point of view, it is less dangerous than all the abovementioned PTEs, and for this reason it has lesser restrictive threshold values. However, exposure to high concentrations can produce similar damage to that caused by Pb. Smelters, combustion, and traffic are their principal environmental pathways.

In Asturias, although the number of mines that extracted zinc were minor (four sites in the oriental border), there still is in operation one of the largest Zn-smelters in the world as well as other galvanized products factories (Sierra et al., 2014a). It is not a primary pollutant in the soils of Asturias, but its sporadic presence in soils that is relevant enough to deserve special attention in the current research.

I.III Soil pollution level assessment: The screening values

The degree of affectation of a soil is usually determined according to legal standards, that is to say, administrative frontiers delimited by an administrative body. However, proper categorization of a soil as polluted requires further discussion including ideas such as "natural concentration," thus giving rise to concepts such as geochemical background level, soil screening level, and the Risk-Based Soil Screening Level.

Geochemical background

The term background level, or geochemical background, comes originally from exploration geochemistry, and was defined by Hawkes and Webb (1962) as "the normal abundance of an element in barren earth material," also indicating that "a background must be considered a range rather than an absolute value." The same author also defines the geochemical anomalies as "a departure from the geochemical patterns that are normal for a given area or geochemical landscape." Therefore, the geochemical background is used as a frontier to differentiate the normal element concentrations and the anomalies. Considering that a range has always two limits, "the upper limit of normal background fluctuation is called the threshold" (Porteous, 1996).

Background, anomaly, and threshold are three concepts that carry implicitly the key word "normal" in their definitions. This is when one may think: What "normal abundance" is?

It depends principally on two factors: scale and location. Considering continental scale, in some areas the natural element concentration can be as high or higher than almost any visible anthropogenic contamination (Reimann and Garrett, 2005). Moreover, if we reduce the scale, new signs of pollution, not visible at a larger scale, appear. When the study scale is incorrect, specific features of the study area are lost, and then soils that are unpolluted might be considered as polluted and vice versa (Darnley et al., 1995). Along the same lines, each specific location has its own geology, therefore making background levels dependent on the mineralogical composition of the parent material (Prabhakaran Nair and Cottenie, 1971).

In summary, to determine the "geochemical background" concentrations, in other words, the intervals of "normal abundance," a substantial number of samples need to be collected over a sufficiently large area to be able to differentiate between natural and

anthropogenic footprints. After this, all anomalies must be excluded, and later the background range can be determined by means of mathematical expressions such as the classical mean ±2 σ (Reimann et al., 2005). The upper limit, defined as the threshold earlier, takes the name of soil screening level (SSLs).

Soil Screening Level

SSLs are the threshold of concentrations in the soils above which there is concern enough to warrant site-specific risk assessment. This means that a concentration above the SSL does not automatically imply **remedial** action or its designation as polluted. Contrarily, in general, if the soil concentrations fall below the SSL, no study would be required (U.S. Environmental Protection Agency, 2007).

Therefore, SSL is a symbolic value that serves two purposes: (a) evaluation/comparison of the PTE contents of any soil sample, independently of its natural or anthropogenic origin; and (b) threshold value initially used to obtain the legal limits of a PTE in a soil.

Risk-Based Soil Screening Level

The definition of RBSSL can be found in the legislation as "the concentration of a pollutant in the soil which does not imply a risk higher than the maximum acceptable for human health or ecosystems" (BOPA, 2014). Strictly speaking, RBSSLs determine the threshold values of pollution for each contaminant. Their values are established in terms of the SSLs with the addition of toxicological data. Toxicological data are generally constant and public (e.g., US EPA, 2005), but SSLs, as mentioned above, vary as per scale and location, so RBSSLs have a direct dependence on the SSLs adopted.

In Spain, the RBSSL establishment is in the sphere of competence of the autonomous communities. The works of this research are always referred to the official RBSSLs for Asturias (Table 1.2), as this is the region where the studies take place. Therefore, if a researcher desires to use the methodologies discussed herein, the RBSSL for its study area should be considered.

Table 1.2 The Risk-Based Soil Screening Levels of Asturias in accordance with the use of soil (Modified from BOPA, 2014).

Element	Symbol	Use of soil			
		Industrial ($mg \cdot kg^{-1}$)	**Recreative ($mg \cdot kg^{-1}$)**	**Residential ($mg \cdot kg^{-1}$)**	**Other uses ($mg \cdot kg^{-1}$)**
Antimony	Sb	295	120	25	5
Arsenic	As	200	40	40	40
Barium	Ba	10000	10000	10000	1540
Beryllium	Be	205	140	30	20
Cadmium	Cd	200	20	20	2
Chromium (III)	Cr(III)	10000	10000	10000	10000
Chromium (VI)	Cr(VI)	50	25	5	2
Cobalt	Co	300	105	25	25
Copper	Cu	4000	400	400	55
Lead	Pb	800	400	400	70
Manganese	Mn	9635	4970	2135	2135
Mercury	Hg	100	10	1	1
Molybdenum	Mo	600	60	60	6
Nickel	Ni	6500	4150	650	65
Selenium	Se	2500	1740	250	25
Silver	Ag	200	20	20	2
Thallium	Tl	10	3	1	1
Tin	Sn	10000	10000	10000	4360
Vanadium	V	1505	845	190	50
Zinc	Zn	10000	4550	4550	455

As indicated by Table1.2, the RBSSLs change in terms of soil use. These uses, in the case of Asturias, are determined according to the General Urban Development Plan (In Spanish: Plan General de Ordenación Urbana, PGOU). In general terms, the bibliography distinguishes, ranked from less to more environmental exigency, four uses, which are as follows:

- **Industrial**: The use of soil is limited to productive or extractive activities such as industry, factories, mines, and so on. Agricultural use is excluded. It is assumed that the access to this soil is restricted and limited, so the individual exposed is considered an adult who works on that site, the rest of the population being subjected to minor exposition parameters.
- **Recreational**: The use of soil is limited to leisure, recreational, or sportive activities. This category includes children's playgrounds, urban parks, beaches,

and sports fields, among others. People are occasionally exposed and without preparation, so the levels are more restrictive than the industrial ones.

- **Residential**: This soil is intended to the principal purpose of providing housing in every form: houses, offices, stores, and so on.
- **Other uses**: It is referred to those use of soils that do not fit into one of the three types described above. For instance, here are included agricultural or forestry soils. They are the most restrictive as these soils might be a source of nutrition for plants, animals, and humans.

Once the RBSSLs are determined, a soil must be declared as polluted in the following situations (RD 9/2005, BOE-A-2005-895):

(a) automatically, when the concentration of a pollutant in the soils exceeds at least 100 times the RBSSL;

(b) whether the RBSSL is exceeded for a pollutant and a risk assessment indicates that there is a risk for the human health/ecosystems.

Thus, considering all the abovementioned concepts, the overall view of the different concepts described is briefed in Figure 1.2.

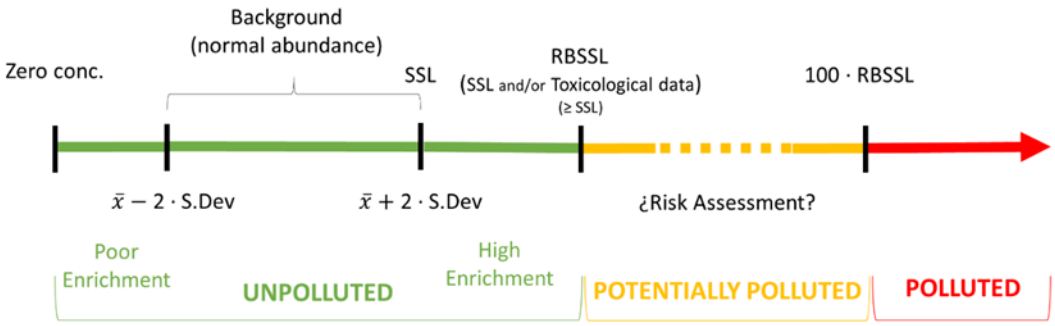

Figure 1.2 Scheme of the evolution in the concentration of a PTE in soils and the degree of pollution. Axis represents the concentration of a pollutant.

From which some conclusions may be extracted:

- The geochemical background is a range that represents the normal abundance of a PTE in a soil.
- SSL is a value that can serve as a basis for the determination of RBSSL. It allows to distinguish those PTEs in which the soil is enriched.
- RBSSL acts as a threshold value to separate what is unpolluted from what could be. Its value is fixed by current laws and is determined on the basis of the SSL

for a certain scale. It changes in terms of the use of soil, being conditioned by the risk assessment.

- There is a range of uncertainty in the values between the RBSSL and 100·RBSSL, where the soil might be polluted. In this case, the risk assessment determines if the soil is finally declared polluted or not.
- Backgrounds and SSLs depend on terms of the scale and location. Consequently, RBSSLs are conditioned by them.

I.IV Soil pollution in Asturias

Historically, the Principality of Asturias has been one of the major industrial cores of Spain. There is no denying that industry represented the cornerstone of the Asturian economy since the industrialization era, it being an unquestionable engine for the region's development (Voth, 2004). Concerning this sector, first of all, surface and underground mining must be highlighted: Coal is probably one of the hallmarks of Asturian mining. The year 2019 supposed the end of subsidized coalmining in Spain, causing the closure of multitude of mines, as a consequence, only a few coal exploitations still remain, but with low activity, whereas more than 10 destined to the extraction of metallic or industrial minerals and rocks are active. These numbers pale in comparison with those reached during the first half of the 20th century, when the number of mining concessions amounted to more than a hundred (IGME, 2016), but still showing the importance of the sector.

Moreover, metallic exploitations were almost as relevant as the coal ones in the past. For instance, as mentioned earlier, Asturias has great Hg deposits that made her its greatest producers in Spain, just under Almadén (Higueras et al., 2005). As described above, mercury mining reached its apogee in the 1950s, until it plunged into a crisis during the 1970s, which ended with the closure of the facilities in those years (Luque and Gutierrez-Claverol, 2006). The case of Hg is remarkable, but no less important are the extractions of Au, Ag, Cu, or fluorspar, which also enjoyed great interest in the region.

For this, the region presents an obvious mining wealth, which acted as a catalyzer for the settlement of heavy industries, namely: steel, chemicals, explosives and fertilizers, as well as coal power plants. All these industrial activities have left an important footprint of pollution in soils all over the region. Moreover, the particular geomorphology of Asturias, consisting principally in valleys, hillsides, and meadows, encouraged soil pollutants' accumulation. Their effect on health is evidenced in numerous environmental studies that have been carried out during the last few years. For example, PTEs are linked to the increase in the number of lung cancers attributable to PM10 particles in the atmosphere in the region (López-Cima et al., 2011; Megido et al., 2017).

In this context, contaminated sites were inventoried in 2001 (Consejería de Medio Ambiente del Principado de Asturias & Rymoil S.A., 2001). This work was performed as required in the Law 10/1998. This law in its article 27 establishes that each autonomous

community must declare and delimit an inventory of polluted soils. Their identification, as explained in the last section, must be performed in terms of soil usage and risk assessment, exposure routes and time, potential receivers and contaminant nature, and so on.

Thus, in the Asturian case, 12 abandoned sites, are inventoried as polluted, 11 of them still awaiting an official declaration on the part of the government. This has been shown in Figure 1.3:

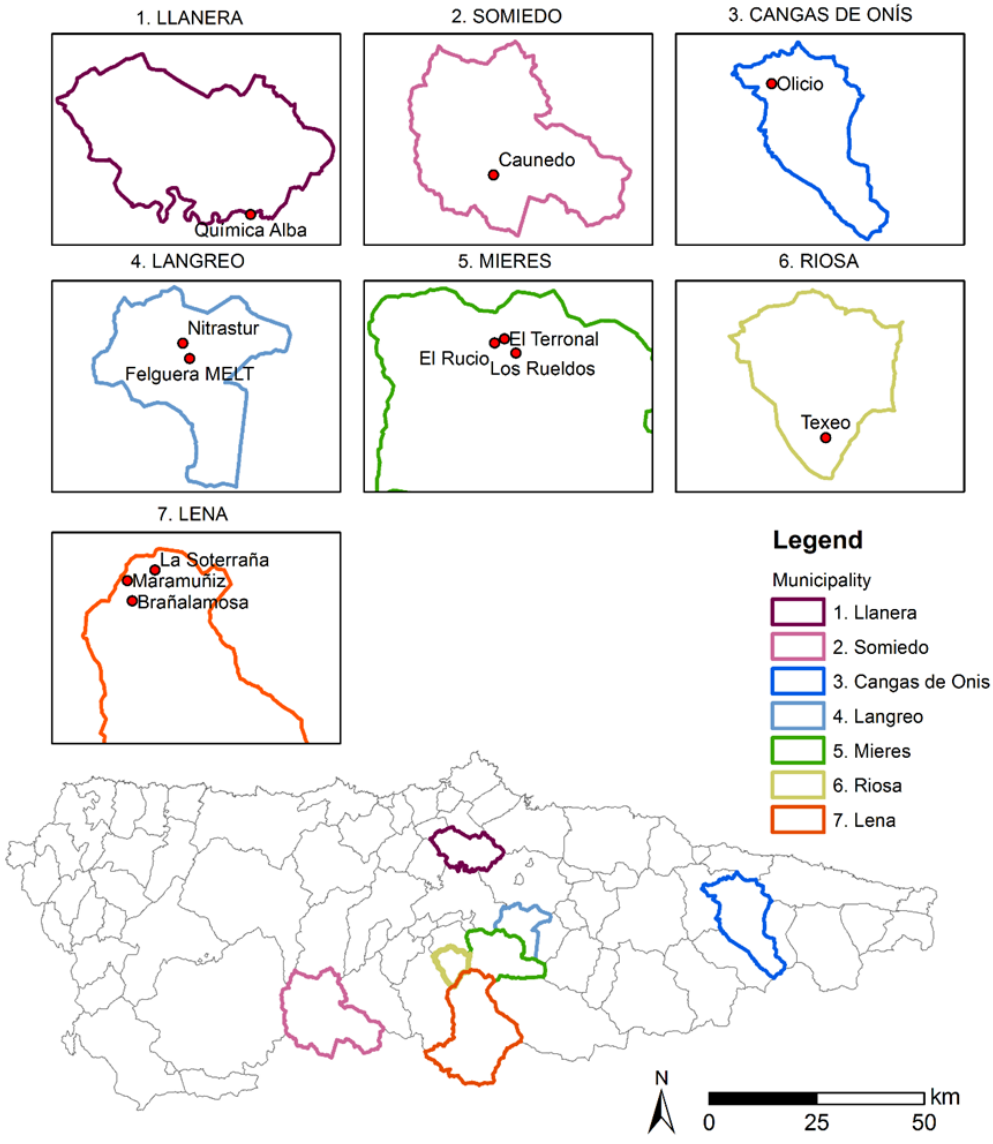

Figure 1.3 Location of the 12 declared polluted soils of the Principality of Asturias.

They correspond to the following:

1. **Química Alba**: A derelict naphthalene products and derivatives factory. Polluted uniquely by organic pollutants. It was declared as a polluted soil by the end of the 2000s and then remediated (Pelaez et al., 2013).
2. **Caunedo**: An Hg exploitation located in the Nature Reserve of Somiedo. Hg. It is the principal contaminant in this site as no ore treatment was performed (Boente et al., 2019).
3. **Olicio**: As Caunedo, another Hg mine located in the heart of the Picos de Europa National Park. Its soils were subjected to remediation studies in the current research. Hg, Pb, Sb, and As are the principal pollutants due to the presence of ore treatment.
4. **Nitrastur**: A brownfield corresponding to a derelict fertilizer plant. As, Pb, and Zn are the principal PTEs of concern (Gallego et al., 2016), although it presents high quantities of other PTEs and other organic pollutants. Remediation methodologies proposed were also applied with this soil.
5. **Felguera MELT**: Factory intended to the production of railway material. Pb and organochlorines are the principal pollutants.
6. **El Terronal**: The most important Asturian Hg deposit. It is a complex with furnaces and treatment plants (Gallego et al., 2015). One of the most highly polluted sites in the region. Particularly remarkable are the extremely high concentrations of Hg and As.
7. **El Rucio**: This Hg mine belongs to the same mineralization as el Terronal, and it is very close to it. Despite this, the concentrations of PTEs are considerably minor and its effect on environment is nowhere near El Terronal.
8. **Los Rueldos**: The Hg mineralization is impregnated in a conglomerate-breccia. It is similar to El Rucio although an area affected by acid mine drainage is its most remarkable feature (Sierra et al., 2013).
9. **Texeo**: Located in the Aramo range, it corresponds to former Cu mines (Loredo et al., 2008).

10. **La Soterraña**: After el Terronal, by relevance, it is the second largest Hg deposit of Asturias. The facility had furnaces and mineral processing plant. The degree of pollution is high (Sierra et al., 2011).
11. **Maramuñiz**: A minor Hg extracting site located near la Soterraña. The core is reduced to several dumps of the area that are covered by the vegetation today.
12. **Brañalamosa**: Another cinnabar mineralization belonging to the complex of La Soterraña. It is similar to Maramuñiz.

It must be highlighted that except the mines of Caunedo and Olicio, and also the old factory of Quimica Alba, the remaining nine sites are located in the central sector of of Asturias, specifically in the mining basins of Mieres and Langreo. Despite this, Asturias has a vast amount of polluted soils that do not appear in the Inventory. Therefore, although they are not declared as polluted, the damage to human health or environment persists.

The characterization technologies applied in the research were developed in some places of this nature. For example, the urban gardens of Jove or Lloreda, in Gijón, and the entire area of Langreo are not inventoried, but the soil affection is clearly visible. Precisely, the "absence" of polluted soils in the highly industrialized municipalities of Gijón and Avilés draws attention.

A revision of the Inventory of Polluted Soils is still necessary, as some locations were omitted, and new cases came forth. The second chapter of this thesis aims to examine the degree of pollution in soils of this nature that are hypothetically, but not officially, polluted, by means of advanced characterization methods.

I.V Methods for the characterization of polluted soils

The characterization process

The aim of a soil pollution characterization is to determine pollution sources, identify the principal contaminants, assess the degree of affection (therefore, its degree of risk to living organisms), and finally define their spatial distribution.

The basis and tools used in a characterization process shares similarities to those applied in prospecting of mineral resources. For example, the Autonomous Community of Andalusia structures the complete sequence of a characterization study in the following stages (modified from: Consejería de Medio Ambiente y Ordenación del Territorio. Junta de Andalucía, 2016):

A. Preliminary Investigation;
B. Characterization plan;
C. Exploratory design and detailed exploratory design;
D. Analytic essays;
E. Database treatment; and
F. Pollution assessment (data interpretation)

In the following sections, these stages are described together with the following:

A. Preliminary Investigation

It is intended to compile all the available information about the site. This step can be dived into four stages:

- **Historical study**: Here, information is gathered about the features of the study site and its historical evolution.
- **Analysis of the physical medium**: Principally, the geographical/administrative context, the geologic domain, the hydrology and hydrogeology, capturing wells, or the existence of protected areas should be considered. At the end of this stage, the category of the RBSSL to be considered should be clear, together with the possible ways of pollutant migration and the magnitude of the area to research.
- **Field visits**: Several field tours are required to contrast all the information gathered in the two previous stages.

- **Performance of a primary conceptual model of risks**: The scope is that the posterior sampling designs cover the delimitation of the sources of pollutants, points of exposure, vulnerable pollution receivers, and so on.

B. Characterization plan

Previous stage conclusions are extrapolated to the specific design of the soil quality research. The characterization plan is a group of organizational, administrative, and technical measures, which are carried out to reduce the number of possible improvisations. It includes aspects such as, the deadline, the design criteria control, the establishment of quality controls as well as measures to prevent environmental and occupational risks.

C. Exploratory design and detailed exploratory design

The aim of the exploratory characterization is to determine pollution levels of a soil. In this phase, sampling plays a fundamental role.

Sampling strategies

The number and location of the sampling points should be determined after considering the abovementioned variables together with other parameters such as the mobility features of the pollutants, previous studies performed in the area, geology, geomorphology, hydrographical basins, and depth of affection, among others.

There exist multiple soil sampling strategies. The distribution by mesh or transects are the most common (de Zorzi et al., 2008). For both cases, the distribution of sampling points can be regular or random. For instance, a regular sampling has important drawbacks when it is planned to perform geostatistics, as it causes the addition of artificial anisotropies. Therefore, it is more advisable to use a random, or alternative methods providing randomness to the data, such as the "cross" sampling (Dinsdale and Salibian-Barrera, 2018). Moreover, there are indicators to optimize the number of points and the distance between them.

Another important aspect to consider during sampling is the possibility of collecting simple or composite samples (Dinsdale and Salibian-Barrera, 2018). A simple sample is that in which the soil is collected in a unique point and at a given depth. A composite sample is constituted by several simple samples, being useful for instance to cover the

surface of a mesh considerably large (>10 m). Composite samples should be mixed in appropriate proportions to obtain the medium value of the target feature (e.g., concentration). However, the use of this sort of sample presents an important handicap, namely, cross-contamination.

For both simple and composite samples, it is recommended to divide each in five increases from 1 m distance maximum, obtaining a representative soil of the sampling point.

D. Analytical assays

Hereunder, some of the most important assays are mentioned, although others could be needed under certain circumstances.

- **Pedological characterization**: Soil texture, soil density, pH, electrical conductivity, and organic matter, among others (Wilding and Drees, 1983).
- **Grain size distribution**: It is mandatory in the design of remediation processes, as contaminants are linked to certain fractions of the soil (especially fine) (Sierra et al., 2010).
- **Chemical analyses**: They are essential in characterization studies, encompassing analytics such as multielement analysis, sequential fractioning. or chemical speciation.
    - Multielement analysis provides the concentration of PTEs in soil, and it is often calculated by Inductively Coupled Plasma Pass/Optical Spectrometry (ICP-MS/OES) or by Cold Vapor Atomic Absorption Spectrometry (CVAAS) for certain PTEs (Hg).
    - Sequential extraction provides the degree of bioavailability of the PTE in the soil. It may be determined by the Tessier's Toxicity Characteristics Leaching Procedure (TCLP) or Measurements and Testing Programme (formerly, BCR) methods (Davidson et al., 1998; Peters, 1999; Tessier et al., 1979).
    - Chemical speciation allows to reveal the proportion of a PTE in a soil that is present in its toxic species (e.g., methyl/ethyl-Hg, As [III] or Cr [VI]. Their quantification can be also determined by ICP-MS coupled to a High Performance Liquid Chromatography (HPLC).

- **Mineralogical study:** Predominant mineral phases can be also quantified to support the identification of rocks or the origins of the pollutants when they have a mineral origin. This can be determined by means of petrographic microscopy, X-ray diffractometry, and scanning electron microscope.

E. Database treatment

The results of all the analytical assays, together with all the information gathered related to the environment and the area of study (preliminary investigation), allow to construct the *geochemical database*. This database, which could be different depending on the objectives proposed and the requirements/features of the study, is the tool that the researcher used to evaluate the soil pollution load.

In pollution studies, it is common to find *outliers* in the geochemical database. Outliers are extremely shifted values that deviate from other data, for instance, a sample with an abnormal concentration of a PTE. They can arise from errors during the experimental process, but they can also appear as a result of an anthropogenic/natural enrichment or a pollution event (focus), either individually or in clusters (Smoliński et al., 2003).

This is not necessarily negative. In fact, the identification of hotspots is key in environmental studies. However, they hamper the statistical and geostatistical analysis, and consequently, the interpretation of the results. So, their inclusion/exclusion must be performed very carefully and always keeping in mind the objectives of the study.

There exist multiple methods to identify PTEs outliers. Among them, those based on the spatial autocorrelation theory and the range method are of particular interest (Yang et al., 2018). The spatial autocorrelation theory defends that the horizontal variation of the concentration of a PTE is continuous; that is, whether a high value exists in a region (or vice versa), it is probably an outlier (Sokal and Thomson, 2006). However, the range method states that the values that are higher or lower than the average $\pm n$ times the standard deviation are outliers (Zhang and Selinus, 1998).

The methods for the outlier exclusion are based on statistical practices. Two useful methods for the identification/removal of outliers in soil pollution are the box plot and the Mahalanobis' distance. The box plot method uses the far upper fence; the third quartile

of the data plus three times the interquartile range: $Q3 + 3 \cdot (Q3 - Q1)$. It is useful to identify elements that are highly enriched in certain samples for statistical studies, and to discard them if necessary.

Moreover, when searching not for elements but for entire multielemental anomalous samples, the percentile 99 of the Mahalanobis' distance is a proper method (Alameddine et al., 2010). Other alternatives to these methods are the Local Moran's I at 95% confidence interval (Anselin, 1995), the Tango's C index (Tango, 1995), and the Getis' G index (Getis and Ord, 1992). There are numerous possibilities and at the end it is the researcher who decides which method is the most suitable for investigation.

F. Pollution assessment (Data interpretation)

When the geochemical database has been cleaned and it is ready for use, the following step is the one that most knowledge requires of all the characterization process: the interpretation of the results. Although there are multiple methods to achieve a proper pollution assessment, here are proposed some frequented tools in modern science to support the interpretation of the data. Therefore, the section has been divided into three: enrichment factors and pollution indexes, statistics, and geostatistics.

F.1 Enrichment factors. Pollution indices and indicators

To assess precisely which sampling points show more or less pollution, it is common to use enrichment factors or pollution indexes. They are commonly constructed in terms of the concentration of PTEs together with a reference value. Thus, the degree of contamination and the resulting pollution indexes, may vary when different backgrounds are considered. Two of the most common indices currently in use are:

Enrichment factors

The Enrichment Factor (EF) is a tool that was developed initially to speculate on the origin of elements in the atmosphere, though progressively has been extended to the study of soils and sediments (Sierra et al., 2014a; Sucharovà et al., 2012). It is defined as follows:

$$EF = \frac{\left(\frac{C_i}{C_{ie}}\right)_s}{\left(\frac{C_i}{C_{ie}}\right)_{RS}} \quad (1)$$

where C_i is the concentration of PTE *i* in the samples of interest or the selected reference sample, and C_{ie} is the concentration of an immobile element in the sample. Proper immobile elements are V or T_i, which trend to show a behavior that is independent from PTEs.

Thus, $\left(\frac{C_i}{C_{ie}}\right)_s$ is the PTE to immobile element ratio in the sample of interest, and $\left(\frac{C_i}{C_{ie}}\right)_{RS}$ is the PTE to immobile element ratio in the sample of reference. The sample of reference is usually a statistical estimator contained in the geochemical background (e.g., average excluding outliers).

Index of Geoaccumulation (I_{geo})

The original index was defined by Muller (Muller, 1969), with the scope of determining the levels of metal contamination in sediments, by comparing current concentrations with pre-industrial levels. The geoaccumulation index is defined by Equation 2:

$$I_{geo} = \log_2\left(\frac{C_i}{1{,}5 \cdot C_{ri}}\right) \quad (2)$$

where C_i is the concentration of the PTE of interest *i* in the soil, and C_{ri} is the geochemical background concentration of the PTE *i*. Factor 1.5 is used to correct possible variations in background values. In terms of the result obtained, pollution is classified as follows:

- $I_{geo} \leq 0$ - Unpolluted
- $0 < I_{geo} \leq 1$ - From unpolluted to moderately polluted
- $1 < I_{geo} \leq 2$ - Moderately polluted
- $2 < I_{geo} \leq 3$ - From moderately polluted to strongly polluted
- $3 < I_{geo} \leq 4$ - Strongly polluted
- $4 < I_{geo} \leq 5$ - From strongly polluted to extremely polluted
- $I_{geo} > 5$ - Extremely polluted

Other similar indexes are the potential Ecological Risk Index (RI) (Hakanson, 1980), the Average Pollution Index (API) (Reimann and De Caritat, 2005), the Contamination Factor (CF) (Hakanson, 1980), and the Nemerow's Pollution Index (PIN) (Xu et al., 2010). However, all of them have constant revisions. It seems advisable to calculate some and to compare results, instead of relying on the use of only one of them for the research.

F.2 Statistical analyses

Geochemical information can be better treated by statistical procedures. Statistics is the principal key to determine pollutants, origins, and sources: Natural or anthropogenic (Facchinelli et al., 2001). The following Table 1.3 summarizes some statistical tools that allow to understand a pollution assessment; all of them used in multitude of recent studies (e.g., Albuquerque et al., 2017; Spahić et al., 2018; Wang et al., 2019).

Table 1.3 Some typical statistical tools applied in soil science for pollution assessment.

Statistical Process	Type	Operation	Usefulness in soil science	Examples
Variable transformations	Univariate	Log / Arcsin / Box-Cox	Achievement of normality in data for easier interpretation	(Facchinelli et al., 2001; Filzmoser et al., 2009)
Statistical descriptions	Univariate	Mean / median / standard deviation / relative standard deviation / trimmed mean, etc.	Fast summarization of data; outlier identification	
Bivariate correlations	Bivariate	Providing the connection between two variables	One-to-one relationships between PTEs or certain variables such as pH	
Factor analysis	Multivariate	Describing a dataset in terms of new and unrelated variables (components)	Grouping of elements; geological identification.	
Hierarchical clustering analysis	Multivariate	Grouping a set of variables by their similarity	Grouping of samples; outlier identification	
Machine learning (Bayesian networks)	Multivariate	Representing a set of variables and their conditional dependencies	Describing how different elements weight in the construction of another variable (e.g., pollution index)	(Cracknell and Reading, 2014)
Compositional data	Multivariate	Additive / centered / isometric log-ratio transformations	Representing elemental concentrations as part of a whole whose sum is a positive constant (e.g., 1 or 100)	(McKinley and Lloyd, 2011)

F.3 Geostatistics

So far, our discussion about pollution assessment has made reference to points, and not to areas or volumes. Considering that an area or a volume has an infinite number of points, it is unaffordable to collect a sample for each. Consequently, the only way to find out the concentration of a contaminant in a point that has not been sampled is by using predictions.

Geostatistics is a powerful tool for the analysis of spatially correlated data (Goovaerts, 1999a). It was originally used in mining and petroleum exploration industries to predict the direction of the veins and oil deposits (Goovaerts, 1999b). However, due to the many advantages of these methods, geostatistics quickly extended its applicability to other branches such as environmental engineering (Pereira and Soares, 2018). Its principal objectives are to describe and analyze the spatial variability of a variable, unlike classical statistical methods that do not use the spatial information; a key characteristic of environmental data.

According to Goovaerts, 2001, geostatistical analysis is a three-step process: The description and modeling of spatial variation, spatial prediction, and uncertainty modeling.

Description and modeling of spatial variation

Geostatistics rely on Waldo Tobler's first law of geography: Things that are close are more related than things that are further apart (Tobler, 1993). Thus, the presence of a spatial structure is a prerequisite to the application of geostatistics. Fortunately, the distribution of a PTE in a soil is not usually random and follows certain patterns. Tendencies of whether the variables are categorical may be identified by computing omnidirectional variograms (or more frequently, semivariograms) in the case of continuous variables, or by indicator semivariograms (Oliver and Webster, 2014).

Formulation governing the modeling and behavior of the variograms is highly complex. This happens because geostatistics is based on random functions, whereby the set of unknown values is considered a set of spatially dependent random variables (Journel and Huijbregts, 1978). The random function usually carries a semivariogram, which is modeled from experimental values. Thus, the semivariogram is the tool that allows the geostatisticians to predict the variables (e.g., the concentration of a PTE in

soils or water). Semivariograms represents the semivariance of a variable in terms of the distance (Goovaerts, 2019), and it should display a function similar to that in Figure 1.4.

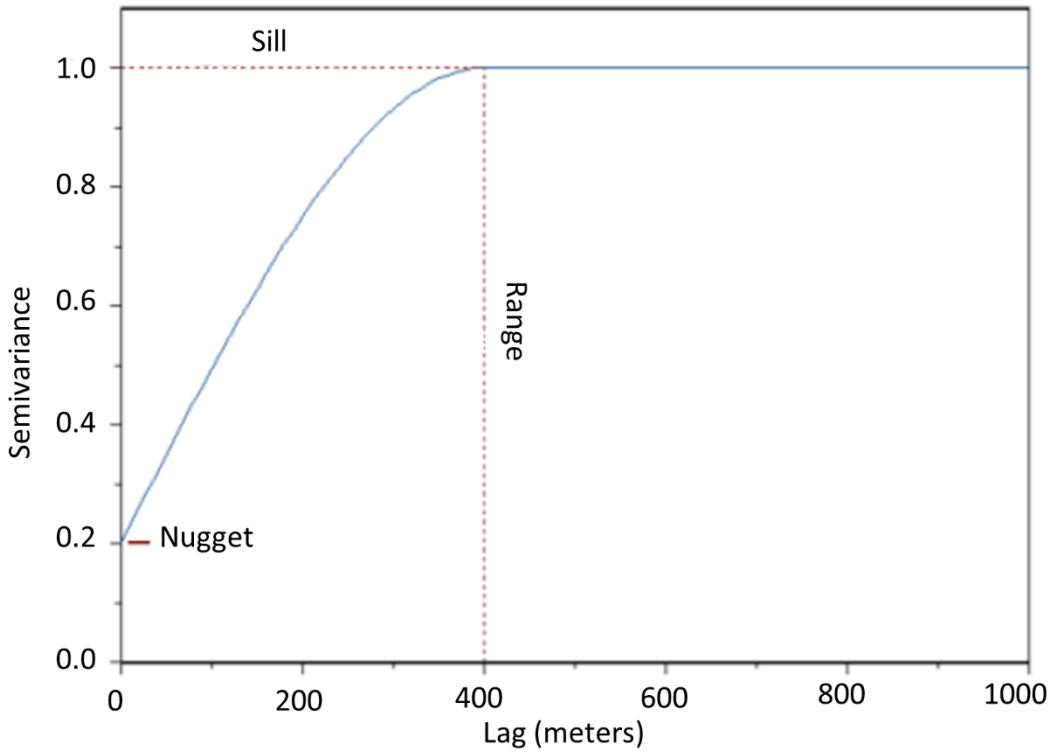

Figure 1.4 Graphical representation of a semivariogram and their principal parameters.

Some of the principal parameters are as follows:

- **Nugget** (C_0): It is the value of the semivariance for a 0-distance, which corresponds to the unexplained semivariance of the model. Ideally, its value should be zero, as the variance between two points that are separated by 0 meters should be null. The nugget is attributable to errors during the sampling and it is solved incrementing the interval of sampling.
- **Sill** ($C+C_0$): It is the value of the maximum semivariance found, where the function stops increasing and is stabilized. At this point, the variables lose their correlation.
- **Range**: It is the value of the distance where sill is reached. At this point, the variables are spatially independent from each other. In other words, it is not possible to predict the variable (e.g., concentration of the pollutant) with confidence.

Moreover, anisotropy is also a factor to consider. Spatial variability may not be the same in all directions. To address this problem, it is typical to perform variograms in

different directions: NE–SW, W–E, etc. Once variograms are established for each direction, it is possible to represent them in terms of an ellipse (ellipsoid in three-dimensional case), whose axes are the range of the variograms. The greater the eccentricity of the ellipse, the greater the anisotropy. In isotropic cases, the range would be the case and the ellipse would be therefore a circle (or a sphere in three-dimensional case).

Spatial prediction

The estimation and mapping of soil attributes in unsampled areas is the principal aim of geostatistics. To do this, methods for interpolation are multiple and each has its own characteristics.

Of them, kriging is the most common. It is a generic name that geostatisticians provide to a family of generalized least-squares regression algorithms (Goovaerts et al., 2016). In practice, there is a wide palette of kriging methods available (e.g., simple, ordinary, universal cokriging). Although the description of each surpasses the limits of this introduction, data should follow a Normal/Gaussian distribution to be used in kriging methods (Kleijnen, 2009). However, the normality of the geochemical data may be achieved by means of statistical transformations. Common transformations include square, cube root, standard deviation, logarithmic, and Box-Cox, among others (Shumway et al., 2002), or even compositional transformations (McKinley et al., 2016).

An evolution of kriging is the Sequential Gaussian Simulation (SGS). It starts by defining the univariate distribution of variables, performing a Normal Score Transform (NST) of the original values to a classical normal distribution, assuming multivariate-normality of the normal scores (Nussbaumer et al., 2018). This assumption ensures that the distribution at a given location is normal with mean and variance provided by simple kriging. Therefore, simulations are performed sequentially by using the normal score variogram and a zero mean until the method converges (Nussbaumer et al., 2018). Finally, data are back-transformed to original grade values.

Another common method is the Inverse Distance Weighting (IDW). It is a simpler technique that does not use statistical models. In IDW, only known *z* values and distance weights are used to determine unknown areas (Lu and Wong, 2008). This makes it a useful tool to use when it is not possible to reach the normality of the data (Mueller et al., 2004).

Nowadays, although these are the most frequent methods, it is normal to use more methods of interpolation to consolidate the results. Some examples are the methods of Splines, Natural Neighbor Inverse Distance Weighted (NNIDW), and so on. All these can be applied by terms of geostatistical software such as ArcGIS®, Surfer®, and SpaceStat®, among others.

Modeling uncertainty

Assessing uncertainty about soil attributes is a preliminary step to evaluate the risk involved in any decision-making process; for instance, to intensify an area of sampling during a detailed exploratory study. Another reason to model the uncertainty is to predict how errors propagate (Goovaerts, 2001). A usual approach is to compute a kriging estimate map and then the associated error variance, using a cross-validation process to validate the model (Chilès and Delfiner, 2012).

I.VI Methods for the remediation of polluted soils

1.6.1 Remediation techniques: A brief overview

Once the characterization has been performed and the areas of risks have been properly identified, it is time, if necessary or possible, to remediate the polluted areas. Nowadays, there are multiples technologies to decontaminate polluted soils. They are usually classified in accordance with the location of the soil during the treatment. Thus, they can be considered in-situ, on-situ, and ex-situ. The former implies that the decontamination is carried out at the same site where the polluted soil was originally found and without excavation, the on-situ treatment implies that the decontamination of the soil is carried out in the same location where the polluted soil is found but after digging on it. The ex-situ procedures require to transfer the polluted the soil to another location (Sharma and Reddy, 2004).

Generally, corrective actions to deal with polluted soils can be classified as (Sharma and Reddy, 2004):

- **Natural attenuation**: This process takes advantage of the reactions that naturally occur in the polluted soil over time. The method is very cheap but considerably slow, so it is only used in cases where the contaminants do not pose a risk for human health or environment, or if the level of pollution is relatively low.
- **Isolation/landfill transportation**: Conceptually, they cannot be categorized as remediation procedures, as they do not remove the pollutants from the soil or change its physicochemical characteristics.
- **Solidification/stabilization**: Solidification encapsulates the waste to form a solid material. Stabilization converts the contaminants into less soluble, mobile, or toxic forms.
- **Pollutant removal**: This group of technologies can be divided in turn into:
    - *Physicochemical*: which remove, extract, or transform the pollutant via physicochemical procedures.
    - *Thermal methods*: These warm the contaminants to high temperatures to destroy or immobilize it.
    - *Biological methods*: These use the activity of living organisms (plants, bacteria) to degrade or accumulate the contaminants.

In brief, the pollutants can either be recovered or destroyed. Although the first option was predominant in the past, present day policies of the majority of the developed nations prefer the latter. More specifically, the most common techniques of each of the abovementioned categories are shown in Table 1.4 (Sharma and Reddy, 2004):

Table 1.4 Classification of remediation techniques.

Name	Type	Place
Air injection	Physicochemical	In-situ
Vapour extraction	Physicochemical	In-situ
Flushing	Physicochemical	In-situ
Electrokinetic treatment	Physicochemical	In-situ
Phytoremediation	Biological	In-situ
Bioventing	Biological	In-situ
Bioslurping	Biological	In-situ
Soil washing	Physicochemical	On/Ex-situ
Incineration	Thermal	On/Ex-situ
Thermal desorption	Thermal	On/Ex-situ
Ultraviolet oxidation	Physicochemical	Ex-situ
Landfarming	Biological	Ex-situ
Bio cells	Biological	Ex-situ
Composting	Biological	Ex-situ

The selection of the optimal technology for each case study is fundamental. Remediation is, generally, a very expensive process. This implies that a study of technical viability at the pilot scale must be performed prior to the on-field implementation. However, apart from the cost, there are other several parameters that might be considered before the selection (Thomas, 2002):

- **The efficiency**. Each technique has been tested by researchers all over the world. However, some are more suitable than others depending on the case. For instance, the phytoremediation, a long-term passive remediation method, is recommendable to refine the result when PTEs content is low (Gerhardt et al., 2009). However, to reach this point, perhaps a physicochemical technique, which is more aggressive with the contaminant, should be performed.
- **The presence of housing**. Some methods, such as thermal desorption, may provoke dust, noise, or emission of gases. This makes them inapplicable when the polluted soil is next to neighborhoods.

In this context, the remediation methodologies applied during the current research are always carried out at the pilot/laboratory scale. However, the positive results achieved encourage their scale-up. Given the difficulty of implementing some of them, soil washing is the chosen remediation technology to focus on , which was stated earlier to be adequate for soils of similar characteristics to those used in this research (Sierra et al., 2014b, 2013, 2011, 2010).

1.6.2 Soil washing

Soil washing is a remediation technology based on two kinds of cleaning technologies, namely, physical separation and chemical extraction. Sometimes, it receives other terms, such as soil recycling or volume reduction (Dermont et al., 2008).

The conceptual idea of physical separation is to remove pollutants from the soil by concentrating them into a minor volume. This is achieved by taking advantage of the existing differences between the characteristics of PTEs and the soil particles or between soil particles in case the contaminant has preferential sorption to some of them. These may range from size, density, or hydrophobic behavior to electric, magnetic, or kinetic properties in a process similar to that used in mineral processing to separate the ore from the tailings (Abumaizar and Smith, 1999). However, chemical soil washing solubilizes metals contained in the soil by using chemical reagents, just as a hydrometallurgical lixiviation.

Among the parameters that control the efficiency of the soil washing, the two most important are the liberation degree and the proportion of fines (silt and clays) in the soil to be treated. The former is the percentage of a particular phase that occurs in free and locked forms (Gupta and Yan, 2016). Regarding the second one, fines have a larger specific surface area on to which the pollutants may get adsorbed. This is the main reason why PTEs tend to accumulate in the fines, a high proportion of which may hamper the soil washing. Other remarkable parameters are the particle size distribution, particle shape, clay, and humic matter content, among others.

As mentioned above, physical separation of contaminants applies methodologies used for processing minerals. The main separation procedures adopted for soil washing or decontamination are as the following:

1. **Size washing**: It is based on the passage of particles of different sizes across holes of open diameters. It provides a high level of continuous processing with simple and low-cost equipment; for example, screens and trammel screen.
2. **Washing by sedimentation velocity**: Different ratios of sedimentations due to size, shape, or density. Although the advantages are the same as those of size washing, this method loses effectivity when soil contains high proportions of clay and silt; for example, hydrocyclones.
3. **Gravity washing**: This separation is carried out based on density differences. As in the washing methods, high content of clay and silt hampers the separation; for example, jigs, shaking tables, and spirals.
4. **Magnetic washing**: It exploits the magnetic susceptibility of PTEs. It allows to recover a wide variety of materials, being especially useful for the treatment of heavy metals; for example, wet/dry and high-/low-intensity magnetic separators.

Soil washing presents some pros and cons that must be valued before its implementation (Dermont et al., 2008). Some of the advantages of the physical separation are:

- The possibility of treating both organic soil pollution and PTEs in the same system.
- The volume of soil to be further treated for metal recovery is reduced.
- The variety of separation procedures offer a wide range of possibilities and flexibility to separate each contaminant.
- It is relatively simple and can be cost-effective.

However, the soil washing will not work properly when:

- PTEs are strongly bound to soil grains.
- There is no strong difference between the properties of the natural soil and those of PTEs.
- There are great differences between the chemical forms of PTEs and the soil matrices.
- The concentration of PTEs is excessively high.
- Soil has a high content of humic matter.

The description of all the devices and techniques of remediation are beyond the scope of this introduction. Should the reader want to deepen his or her knowledge in one of these topics, he or she could find more information about remediation by mineral processing in Wills and Finch (2015) or Dermont et al. (2008).

In this research, at least one device from each of the abovementioned soil washing procedures has been tested. All of them have been briefly described in the following paragraphs:

Washing by size and sedimentation velocity: Hydrocyclone

The hydrocyclone, a static device, applies a centrifugal force to a liquid mixture. This results in the separation of PTEs in a water suspension, which is achieved by determining a force balance between the fluid resistance and the centripetal force. The value of this force is low in case of fines/light particles and high if the particles are dense and coarse (Mercier et al., 2007).

The mixture of soil–water is introduced in the drum. A motor pumps the mixture and introduces it in a tangential injection flow process, which transforms the velocity of the incoming mixture into a rotary motion. These forces create an internal vortex that moves fines/lights along the axis of the hydrocyclone to the overflow, while the heavy/dense components move downwards following a spiral path close to the walls of the hydrocyclone and toward the underflow discharge (Neesse et al., 2004). The hydrocyclone used for the task performed in this thesis was a lab-scale plant C700 Mozley (Figure 1.5).

Figure 1.5 Hydrocyclone lab-scale plant C700 Mozley.

Gravity washing: Float–sink separation

The aim of the float–sink gravity concentration method is to segregate particles with different specific gravities by immersing them in a fluid (e.g., heavy solutions, heavy liquids, suspension fluids) (Wills and Finch, 2015).

Within these techniques, the Heavy Liquid Separation (HLS) is a laboratory scale test. The HLS method consists on introducing a known-density liquid in a separating funnel. The liquid is obtained by mixing pure chloroform and bromoform in different proportions. The polluted soil is therefore introduced in such a way that particles with a density lower than that of the liquid float, while those with a higher density sink. The two fractions receive the names "heavies" and "lights."

It should be remarked that the HLS is a test of laboratory and it cannot be applied on field. However, the results of the tests are appropriate to assess the capability of other soil gravity washing techniques.

Magnetic separation: Wet and Dry High-Intensity Magnetic Separators

Some PTEs present magnetic properties that can be exploited. This mechanical process separates those contaminants (or the particles to which they have been preferentially attached) that present high magnetic susceptibility with respect to rest of the soil matrix. In this respect, it has to be highlighted that most soil matrices are not expected to be magnetic.

Thus, materials with positive magnetic susceptibility are attracted by a magnetic field, whereas those with no magnetic susceptibility are repelled by the magnet. This results in the attainment of a magnetic fraction, where supposedly PTEs remain, and a nonmagnetic fraction, ideally larger in volume, but also with a minor concentration of pollutants.

The "magnetic" fraction carries those elements that are ferri- and ferro-magnetics. They are characterized by their capacity to multiply the magnetic flux density (B) within them. However, the "non-magnetic" fraction contains those particles that cannot be separated by magnetism and that consequently show diamagnetic behavior (Svoboda and Fujita, 2003).

Moreover, there also exist materials that are "weakly magnetic." In this group, the para- and antiferromagnetic materials coexist, which barely increase the magnetic flux

density in their surroundings. This group also includes materials that are ferri- or ferromagnetic but, for being surrounded by nonmagnetic materials, lose or hide their magnetic power and consequently end in the middlings. On the contrary, this also happens with the nonmagnetic proportions of soils. Some authors refer to this material as a third fraction, although they coincide that it should be retreated (Sierra et al., 2014).

The origins of all these substances is the interactions of unpaired electrons at the molecular level. In this sense, a substance would be ferromagnetic whether its unpaired electrons are aligned, which causes a positive contribution to the net magnetization. If some of the unpaired electrons reduce the net magnetization, or if they are partially anti-aligned, the substance is ferrimagnetic. Ferromagnetic elements are, for instance, the metals, such as Fe, Cu, Ni, and the majority of their alloys.

However, paramagnetism occurs in the presence of an external magnetic field. The unpaired electrons are therefore randomly arranged. Atoms of the materials have inner electron shells that are incomplete, so their unpaired electrons spin and orbit in a specific way, making the atoms a permanent magnet tending to align with the external magnetic field. This is the case with Al, Na, and iron minerals such as hematite and goethite.

Finally, antiferromagnetism occurs when the magnetism is cancelled out by the set of magnetic atoms or ions that are aligned in the reverse direction. This is dependent on the temperature and is typical of hematite and chromium alloys.

During this research, devices used for the magnetic separation tests were Wet-High-Intensity Magnetic Separator (Wet-HIMS), model OUTOTEC Laboratory 3X4L, and, to a minor extent, a Dry-High-Intensity Magnetic Separator (Dry-HIMS), model L/P 10:30 of International Process Systems Inc. (U.S. PATENT) (Figure 1.6).

In the Wet-HIMS, the feed passes through a separating chamber composed of soft Fe spheres. The magnetic field is created by a current that passes through a coil, creating a magnetic field that magnetizes the Fe spheres. The feed (polluted soil in a suspension of water) crosses the canister with the Fe spheres and, if the materials present magnetic susceptibility, they remain attached to the spheres. The non-magnetic material keep the water stream on, falling down by gravity and the drag force to the “non-magnetics” tray. Once all the material pass through, the spheres are cleaned and the adhered particles are collected in a tray of “magnetics.”

However, the Dry-HIMS does not consume water. In this case, the feed follows on a drum that rotates around a magnet. Materials that have low magnetic susceptibility fall immediately by gravity when the drum reaches a vertical position, being collected on a tray for “non-magnetics.” The “magnetics” remain attached to the drum until they hit a brush that make them fall into another tray.

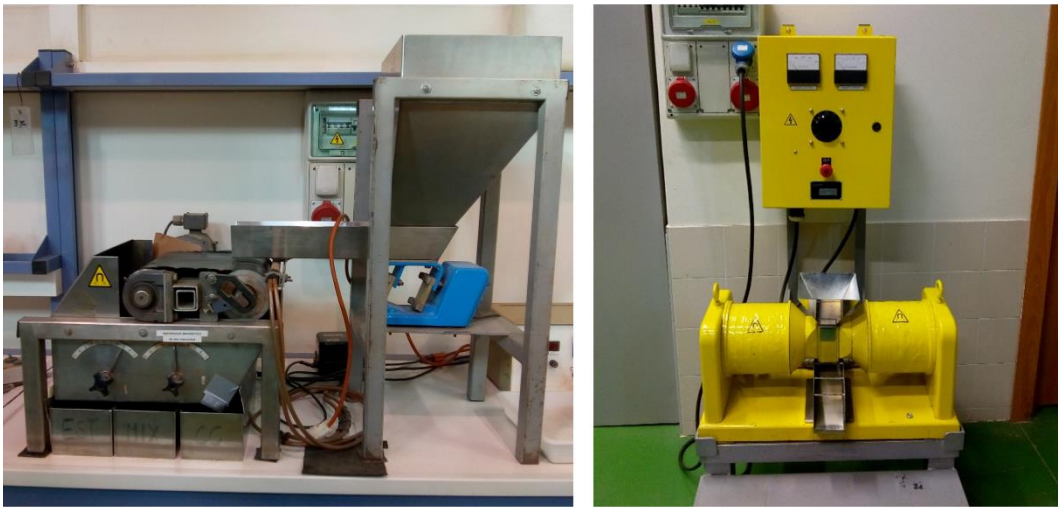

Figure 1.6 Left.- Dry-HIMS Model L/P 10:30 of International Process Systems Inc. (U.S. PATENT) **Right.-** Wet-HIMS Model OUTOTEC Laboratory 3X4L

1.6.3 Nanotechnology applied for soil remediation

Some researchers have demonstrated that the yield of soil washing can be enhanced if certain additives are introduced in the polluted soil, stimulating the properties that are exploited by soil washing (Beiyuan et al., 2018; Fedje and Strömvall, 2019).

One of the most increasingly used additives that are being added to soil or water to remediate them are the nanoparticles of different materials. Nanoremediation is an emerging technology the basis of which is the use of aqueous suspensions of very small particles (nanoparticles) to treat and degrade contaminants. This technology has been broadly use in groundwater, and its use is incipient for soils treatment (Karn et al., 2009); also, as supporting remediation methods involving plants (Gil-Díaz and Lobo, 2018).

Nowadays, there exist multiple types of nanoparticles for soil remediation. Some of the most frequently used synthetizations currently are as follows (Litter et al., 2018):

- Zero-valent iron nanoparticles: The application of the nanoscale zero-valent iron (nZVI or Fe[0]) for soil remediation has been widely accepted by

researchers and regulatory agencies, principally due to the low costs and the absence of any known toxicity that the use of iron could induce. These features made nZVI the favorite nanoparticle to be used in soil remediation. Fe(0) has been successfully used in subsurface reactive permeable barriers for the removal of polycyclic aromatic compounds from polluted soil and water sites.

- Iron oxide nanoparticles: Some examples of this type are the magnetite (Fe_3O_4), maghemite (γ-Fe_2O_3), hematite (α-Fe_2O_3), or goethite (α-FeOOH). The mechanism of adsorption in this case is attributable to two reasons. The van der Waals interactions with the surface of oxides, and to the ion exchange of pollutant ions in aqueous solutions with iron ions in the iron oxide lattice structure.
- Bimetallic nanoparticles: These nanoparticles are synthetized by the union of two metals, some of which are Fe–Ni, Ag–Cd, or Rh–Pd. The bimetallic nanoparticles offer the possibility of exploiting the specific properties of the metals and/or their unions. But they have a great counterpoint, which is the possible injection of PTEs in the soil. For this reason, their use in remediation is minor in comparison with ZVI or iron oxide nanoparticles.

There are two features that define the nanoparticles and made them an extremely versatile remediation tool (Araújo et al., 2015; O'Carroll et al., 2013; Stefaniuk et al., 2016; Zhang, 2003). The first is their size, which is between 1 and 100 nm (a typical bacterial cell has a diameter of 1000 nm). This small size allows their effective transport through groundwater flow, being versatile for both in-/ex- situ applications. Moreover, the size feature is related to another of their advantages: large specific surface and high surface activity. This allows them to be effective in a large volume of polluted soil even in low doses, which is especially important as their manufacturing price is high. Their second virtue, which comes along with their high surface activity, is their capability to be anchored for extended periods of time to the soil matrix, acting over the pollution permanently almost without any maintenance (Zhang, 2003).

However, the use of nanomaterials is not exempt of limitations, some of these are (Araújo et al., 2015):

- They are prone to easy aggregation and corrosion affecting their reactivity.

- Changes in soil properties as pH or redox conditions may affect their behavior. Nevertheless, for on-field applications this inconvenience is minimized as there exist other mechanisms to reduce changes in these properties.
- There is a possible threat they can pose to human health or environment. Although it is a nontoxic material, the addition of nanoparticles to an ecosystem should be done carefully, controlling the reaction of the nearest environment to the addition of this material not to break the ecosystem.

The addition of nanoparticles principally stimulates three phenomena in the soil that benefit its decontamination: Adsorption, reduction, and precipitation (Zhang, 2003). The type of nanoparticle injected assists one or more of these processes.

The former is uniquely dependent on the size, or in other words, the specific surface. It implies the reaction between an adsorbent (PTE) and an adsorbate (the nanoparticle itself), much reduced in size, which interacts due to physicochemical reactions, forming larger and heavier aggregates that are easier to separate.

However, the reduction phenomenon is predominant in the ZVI variant. This is a material with high reduction power and consequence of its high redox potential of $E^0_{Fe(II)/Fe(0)} = -0.440$ V. This enables it to reduce the majority of the transition metals. Something that does not happen with Fe(II) reduction, which is not thermodynamically favored and only takes place in metals with redox potential higher than +0.771 V (Li et al., 2006).

Finally, the precipitation causes the transformation of PTEs in other species of low solubility or even insoluble ones, which sometimes produces the mineralization, or the transformation of an organic compound in an inorganic but non-dangerous mineral (Klimkova et al., 2011).

These three mechanisms used in the removal of the contaminants might be also combined, depending on the characteristics and nature of the PTE. In this sense, Figure 1.7 shows the structure of the core-shell (Yan et al., 2010) that ZVI nanoparticles adopt and on which the mechanisms of removal are based. Here, the core is constituted by Fe(0) and the shell, or the external layer, is formed by several oxides or hydroxides, products of the oxidation of the Fe(0). This external layer provides the interstices in structure that boost the adsorption phenomena, whereas the core provides the reduction power.

Thus, in the case of oxide or hydroxide Fe nanoparticles, the predominant mechanism is that of the adsorption. Cations of PTEs are adsorbed by metallic substitution or by interaction with hydroxides that are present on the surface of the material in dissolution. Once PTEs are adsorbed onto this layer, magnetic properties of the ZVI or the forming of denser aggregates may be exploited by the soil washing equipment to remove PTEs (O'Carroll et al., 2013).

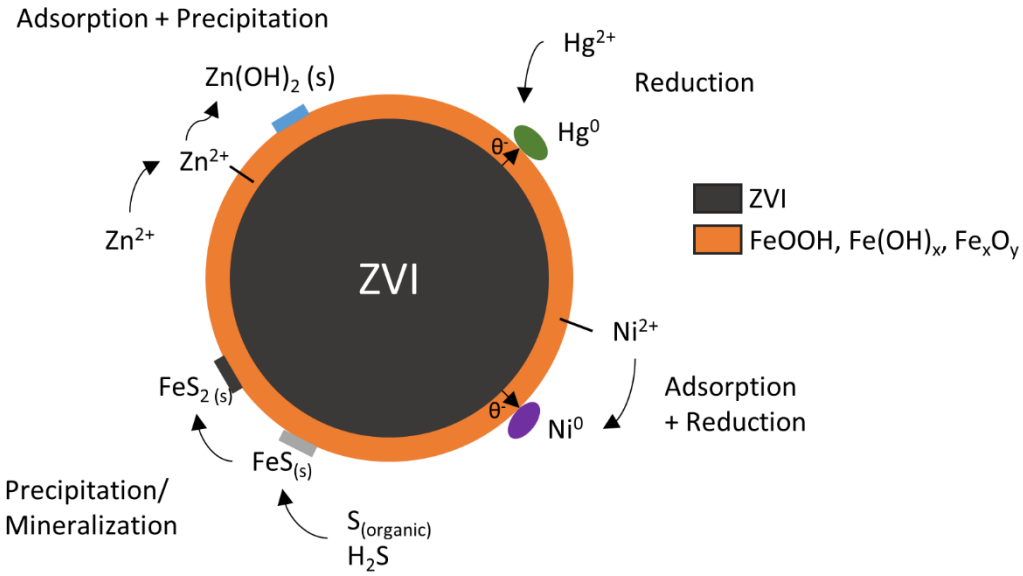

Figure 1.7 Core-shell model and the mechanisms of decontamination through zero-valent iron. Adapted from Yan et al., 2010.

All things considered, nano-remediation, and more specifically the use of ZVI, is widely accepted by the scientific community and has been demonstrated to be effective. In addition to the classical use as PTE immobilizer (Gil-Díaz et al., 2014), nowadays nanoparticles have been reported to be suitable for the extraction of PTEs as As (V) and As (III) species (Babaee et al., 2018), Cr (III) and Cr (VI) (Reyhanitabar et al., 2012), Cu/Pb (Gil-Díaz et al., 2018; Rajput et al., 2017), Zn (Kržišnik et al., 2014), or even several PTEs at the same time (Gil-Díaz et al., 2017), both for groundwater and soils.

In view of the above, through the current research exploiting ZVI nanoparticles properties by adding them to a polluted soil with the scope of improving the yield of the soil washing technique has been proposed.

I.VII Objectives

This thesis set the objective of developing new methodologies for the characterization and remediation of soils polluted by PTEs, given their hazards, high toxicity, and rising accumulation into the environment. Thus, the entire life cycle of these inorganic pollutants in the soils right from their identification till their separation, and eventually, elimination have been studied.

The improvement in the characterization processes has had the following main objectives: (1) to identify pollutants present in the soil, (2) to study the spatial distribution of the elements, and (3) to find their natural or anthropogenic origins or sources. These objectives can be divided more specifically into the following:

- The development of statistical working procedures to solve the earlier issues. Variables that contribute to a particular pollution issue are multiple, namely, elemental concentration, pH, bioavailability, and geology, among many others. In this regard, univariate statistics as well as multivariate statistics such as the hierarchical clustering and especially factor analysis have a fundamental role in linking all the variables and also in finding the main pollutants and their sources (Objectives 1 and 3).
- The use of geostatistics to study the spatial distribution of PTEs. In this context, the geostatistical interpolation method applied was Ordinary kriging, as a reliable algorithm frequently used in environmental science (Objective 2).
- The proposal of a new pollution indicator, compatible with kriging, which considers the legal limits and all the elements that surpass the threshold limits; thus, working directly with the elements of concern from a legal point of view (Objectives 1, 2, and 3).
- Adaptation of the compositional data theory to detect areas of natural or anthropogenic sources of PTEs through the introduction of a new concept of Relative Enrichment of a PTE (Objectives 2 and 3).
- To test the validity of the above methodologies at different scales: site, local, or regional scales.

However, the processes of remediation seek to eliminate or reduce the concentrations of PTEs in the soils. The main points of focus of this thesis are:

- To assess the viability of soil washing (fundamentally, magnetic or gravimetric/gran size concentration) as a technology to decontaminate soils especially enriched in PTEs. The aim is to test samples of soils from different genesis and to assess the efficiency of the assays through the attributive analysis formulation. A novel indicator is intended to be developed to assess the yield of the tests considering, again, the threshold levels.
- Introduction of the nanoscale zero-valent iron (nZVI)-assisted soil washing for the removal of PTEs. A novel remediation technology would be adopted that involves the application of nZVI into the soil to improve the concentration process. Attributive analysis equations must be modified to adapt them to this case. Moreover, a formulation based on magnetic quantifications to monitor and control the displacement of the nZVI during the process of soil washing would be generated.
- Finally, to establish a comparison between both remediation techniques and to ascertain those PTEs for which the techniques are more effective.

Ultimately, being consistent with the philosophy of researching, all tools provided here are designed to be applicable and transposable to any other study case of a similar nature.

I.VIII References

Abumaizar, R.J., Smith, E.H., 1999. Heavy metal contaminants removal by soil washing. J. Hazard. Mater. 70, 71–86. doi:10.1016/S0304-3894(99)00149-1

Alameddine, I., Kenney, M.A., Gosnell, R.J., Reckhow, K.H., 2010. Robust multivariate outlier detection methods for environmental data. J. Environ. Eng. 136, 1299–1304. doi:10.1061/(ASCE)EE.1943-7870.0000271

Albuquerque, M.T.D., Gerassis, S., Sierra, C., Taboada, J., Martín, J.E., Antunes, I.M.H.R., Gallego, J.R., 2017. Developing a new Bayesian Risk Index for risk evaluation of soil contamination. Sci. Total Environ. 603–604, 167–177. doi:10.1016/j.scitotenv.2017.06.068

Alloway, B.J., 2013. Heavy Metals in Soils, Heavy metals in soils. doi:10.1007/978-94-011-1344-1

Alpaslan, B., Yukselen, M.A., 2002. Remediation of lead contaminated soils by stabilization/solidification. Water. Air. Soil Pollut. 133, 253–263. doi:10.1023/A:1012977829536

Álvarez, R., Ordóñez, A., Pérez, A., De Miguel, E., Charlesworth, S., 2018. Mineralogical and environmental features of the asturian copper mining district (Spain): A review. Eng. Geol. doi:10.1016/j.enggeo.2018.07.007

Anselin, L., 1995. Local Indicators of Spatial Association—LISA. Geogr. Anal. 27, 93–115. doi:10.1111/j.1538-4632.1995.tb00338.x

Araújo, R., Castro, A.C.M., Fiúza, A., 2015. The Use of Nanoparticles in Soil and Water Remediation Processes, in: Materials Today: Proceedings. pp. 315–320. doi:10.1016/j.matpr.2015.04.055

Babaee, Y., Mulligan, C.N., Rahaman, M.S., 2018. Removal of arsenic (III) and arsenic (V) from aqueous solutions through adsorption by Fe/Cu nanoparticles. J. Chem. Technol. Biotechnol. 93. doi:10.1002/jctb.5320

Beiyuan, J., Tsang, D.C.W., Valix, M., Baek, K., Ok, Y.S., Zhang, W., Bolan, N.S., Rinklebe, J., Li, X.D., 2018. Combined application of EDDS and EDTA for removal of potentially toxic elements under multiple soil washing schemes. Chemosphere.

doi:10.1016/j.chemosphere.2018.04.081

BOE, Boletín Oficial del Estado - Real Decreto 9/2005, de 14 de enero, por el que se establece la relación de actividades potencialmente contaminantes del suelo y los criterios y estándares para la declaración de suelos contaminados. BOE-A-2005-895

Boente, C., Albuquerque, M.T.D., Gerassis, S., Rodríguez-Valdés, E., Gallego, J.R., 2019. A coupled multivariate statistics, geostatistical and machine-learning approach to address soil pollution in a prototypical Hg-mining site in a natural reserve. Chemosphere 218, 767–777. doi:10.1016/j.chemosphere.2018.11.172

BOPA, 2014. Generic Reference Levels for Heavy Metals in Soils from Principality of Asturias, Spain.

Cepedal, A., Fuertes-Fuente, M., Martín-Izard, A., González-Nistal, S., Rodríguez-Pevida, L., 2006. Tellurides, selenides and Bi-mineral assemblages from the Río Narcea Gold Belt, Asturias, Spain: Genetic implications in Cu-Au and Au skarns. Mineral. Petrol. 87, 277–304. doi:10.1007/s00710-006-0127-7

Chapman, P.M., 2007. Determining when contamination is pollution - Weight of evidence determinations for sediments and effluents. Environ. Int. doi:10.1016/j.envint.2006.09.001

Chen, T., Zhou, Z., Zhang, J., McClain, C.J., Song, M., 2011. Copper Deficiency Exacerbates Bile Duct Ligation-Induced Liver Injury and Fibrosis in Rats. J. Pharmacol. Exp. Ther. doi:10.1124/jpet.111.184325

Chilès, J.P., Delfiner, P., 2012. Geostatistics: Modeling Spatial Uncertainty: Second Edition, Geostatistics: Modeling Spatial Uncertainty: Second Edition. doi:10.1002/9781118136188

Clarkson, T.W., Magos, L., 2006. The toxicology of mercury and its chemical compounds. Crit. Rev. Toxicol. doi:10.1080/10408440600845619

Clemens, S., 2006. Toxic metal accumulation, responses to exposure and mechanisms of tolerance in plants. Biochimie. doi:10.1016/j.biochi.2006.07.003

Consejería de Medio Ambiente del Principado de Asturias & Rymoil S.A., 2001. Inventario y Caracterización de Suelos Contaminados del Principado de Asturias (EXPEDIENTE AT/2000/58-97).

Consejería de Medio Ambiente y Ordenación del Territorio. Junta de Andalucía, 2016. Guía para la Clasificación de Suelos Potencialmente Contaminados en Función del Riesgo.

Cracknell, M.J., Reading, A.M., 2014. Geological mapping using remote sensing data: A comparison of five machine learning algorithms, their response to variations in the spatial distribution of training data and the use of explicit spatial information. Comput. Geosci. 63, 22–33. doi:10.1016/j.cageo.2013.10.008

Darnley, a. G., Bjorklund, a., Bolviken, B., Gustavsson, N., Koval, P.V., Plant, J. a., Steenfelt, a., Tauchid, M., Xie, X., Garrett, R.G., Hall, G.E.M., 1995. A global geochemical database for environmental and resource management - Final Report of IGCP Project 259, Data Management.

Davidson, C.M., Duncan, A.L., Littlejohn, D., Ure, A.M., Garden, L.M., 1998. A critical evaluation of the three-stage BCR sequential extraction procedure to assess the potential mobility and toxicity of heavy metals in industrially-contaminated land. Anal. Chim. Acta. doi:10.1016/S0003-2670(98)00057-9

de Zorzi, P., Barbizzi, S., Belli, M., Mufato, R., Sartori, G., Stocchero, G., 2008. Soil sampling strategies: Evaluation of different approaches. Appl. Radiat. Isot. 66, 1691–1694. doi:10.1016/j.apradiso.2007.12.020

Demir, A., Köleli, N., 2013. The sequential use of washing and an electrochemical reduction process for the remediation of lead-contaminated soils. Environ. Technol. (United Kingdom) 34, 799–805. doi:10.1080/09593330.2012.717107

Dermont, G., Bergeron, M., Mercier, G., Richer-Laflèche, M., 2008. Soil washing for metal removal: A review of physical/chemical technologies and field applications. J. Hazard. Mater. 152, 1–31. doi:10.1016/j.jhazmat.2007.10.043

Dinsdale, D., Salibian-Barrera, M., 2018. Methods for preferential sampling in geostatistics. J. R. Stat. Soc. In press. doi:10.1111/rssc.12286

Duffus, J.H., 2002. "Heavy metals" a meaningless term? (IUPAC Technical Report). Pure Appl. Chem. doi:10.1351/pac200274050793

Duker, A.A., Carranza, E.J.M., Hale, M., 2005. Arsenic geochemistry and health. Environ. Int. doi:10.1016/j.envint.2004.10.020

Evers, D.C., Keane, S.E., Basu, N., Buck, D., 2016. Evaluating the effectiveness of the Minamata Convention on Mercury: Principles and recommendations for next steps. Sci. Total Environ. doi:10.1016/j.scitotenv.2016.05.001

Fabian, C., Reimann, C., Fabian, K., Birke, M., Baritz, R., Haslinger, E., Albanese, S., Andersson, M., Batista, M.J., Bel-lan, A., Cicchella, D., Demetriades, A., De Vivo, B., De Vos, W., Dinelli, E., Duriš, M., Dusza-Dobek, A., Eggen, O.A., Eklund, M., Ernstsen, V., Filzmoser, P., Flight, D.M.A., Forrester, S., Fuchs, M., Fügedi, U., Gilucis, A., Gosar, M., Gregorauskiene, V., De Groot, W., Gulan, A., Halamić, J., Hayoz, P., Hoffmann, R., Hoogewerff, J., Hrvatovic, H., Husnjak, S., Janik, L., Jordan, G., Kaminari, M., Kirby, J., Kivisilla, J., Klos, V., Krone, F., Kwećko, P., Kuti, L., Ladenberger, A., Lima, A., Locutura, J., Lucivjansky, D.P., Mann, A., Mackovych, D., McLaughlin, M., Malyuk, B.I., Maquil, R., Meuli, R.G., Mol, G., Negrel, P., O'Connor, P., Oorts, R.K., Ottesen, R.T., Pasieczna, A., Petersell, W., Pfleiderer, S., Poňavič, M., Pramuka, S., Prazeres, C., Rauch, U., Radusinović, S., Salpeteur, I., Scanlon, R., Schedl, A., Scheib, A.J., Schoeters, I., Šefčik, P., Sellersjö, E., Skopljak, F., Slaninka, I., Šorša, A., Srvkota, R., Stafilov, T., Tarvainen, T., Trendavilov, V., Valera, P., Verougstraete, V., Vidojević, D., Zissimos, A., Zomeni, Z., 2014. GEMAS. Appl. Geochemistry. doi:10.1016/j.apgeochem.2014.07.017

Facchinelli, A., Sacchi, E., Mallen, L., 2001. Multivariate statistical and GIS-based approach to identify heavy metal sources in soils. Environ. Pollut. 114, 313–324. doi:10.1016/S0269-7491(00)00243-8

Fedje, K.K., Strömvall, A.-M., 2019. Enhanced soil washing with copper recovery using chemical precipitation. J. Environ. Manage. 236, 68–74. doi:10.1016/j.jenvman.2019.01.098

Fernández-Martínez, R., Larios, R., Gómez-Pinilla, I., Gómez-Mancebo, B., López-Andrés, S., Loredo, J., Ordóñez, A., Rucandio, I., 2015. Mercury accumulation and speciation in plants and soils from abandoned cinnabar mines. Geoderma 253–254, 30–38. doi:10.1016/j.geoderma.2015.04.005

Fernández, S., Cotos-Yáñez, T., Roca-Pardiñas, J., Ordóñez, C., 2018. Geographically Weighted Principal Components Analysis to assess diffuse pollution sources of soil heavy metal: Application to rough mountain areas in Northwest Spain. Geoderma 311, 120–129. doi:10.1016/j.geoderma.2016.10.012

Filzmoser, P., Hron, K., Reimann, C., 2009. Principal component analysis for compositional data with outliers, in: Environmetrics. pp. 621–632. doi:10.1002/env.966

Gaetke, L.M., Chow-Johnson, H.S., Chow, C.K., 2014. Copper: toxicological relevance and mechanisms. Arch. Toxicol. 88, 1929–1938. doi:10.1007/s00204-014-1355-y

Gallego, J.L.R., Ordóñez, A., Loredo, J., 2001. Investigation of trace element sources from an industrialized area (Avil??s, northern Spain) using multivariate statistical methods. Environ. Int. 27, 589–596. doi:10.1016/S0160-4120(01)00115-5

Gallego, J.L.R., Ortiz, J.E., Sierra, C., Torres, T., Llamas, J.F., 2013. Multivariate study of trace element distribution in the geological record of Ro??anzas Peat Bog (Asturias, N. Spain). Paleoenvironmental evolution and human activities over the last 8000calyr BP. Sci. Total Environ. 454–455, 16–29. doi:10.1016/j.scitotenv.2013.02.083

Gallego, J.R., Esquinas, N., Rodríguez-Valdés, E., Menéndez-Aguado, J.M., Sierra, C., 2015. Comprehensive waste characterization and organic pollution co-occurrence in a Hg and As mining and metallurgy brownfield. J. Hazard. Mater. 300, 561–571. doi:10.1016/j.jhazmat.2015.07.029

Gallego, J.R., Rodríguez-Valdés, E., Esquinas, N., Fernández-Braña, A., Afif, E., 2016. Insights into a 20-ha multi-contaminated brownfield megasite: An environmental forensics approach. Sci. Total Environ. 563–564, 683–692. doi:10.1016/j.scitotenv.2015.09.153

Gebel, T., 2000. Confounding variables in the environmental toxicology of arsenic. Toxicology. doi:10.1016/S0300-483X(99)00202-4

Gerhardt, K.E., Huang, X.D., Glick, B.R., Greenberg, B.M., 2009. Phytoremediation and rhizoremediation of organic soil contaminants: Potential and challenges. Plant Sci. doi:10.1016/j.plantsci.2008.09.014

Getis, A., Ord, J.K., 1992. The Analysis of Spatial Association by Use of Distance Statistics. Geogr. Anal. 24, 189–206. doi:10.1111/j.1538-4632.1992.tb00261.x

Gil-Díaz, M., Alonso, J., Rodríguez-Valdés, E., Pinilla, P., Lobo, M.C., 2014. Reducing the mobility of arsenic in brownfield soil using stabilised zero-valent iron

nanoparticles. J. Environ. Sci. Health. A. Tox. Hazard. Subst. Environ. Eng. 49, 1361–9. doi:10.1080/10934529.2014.928248

Gil-Díaz, M., Lobo, M.C., 2018. Phytotoxicity of Nanoscale Zerovalent Iron (nZVI) in Remediation Strategies, in: Phytotoxicity of Nanoparticles. Springer International Publishing, Cham, pp. 301–333. doi:10.1007/978-3-319-76708-6_13

Gil-Díaz, M., López, L.F., Alonso, J., Lobo, M.C., 2018. Comparison of Nanoscale Zero-Valent Iron, Compost, and Phosphate for Pb Immobilization in an Acidic Soil. Water. Air. Soil Pollut. doi:10.1007/s11270-018-3972-1

Gil-Díaz, M., Pinilla, P., Alonso, J., Lobo, M.C., 2017. Viability of a nanoremediation process in single or multi-metal(loid) contaminated soils. J. Hazard. Mater. doi:10.1016/j.jhazmat.2016.09.071

Goovaerts, P., 2019. Geostatistical prediction of water lead levels in Flint, Michigan: A multivariate approach. Sci. Total Environ. 647, 1294–1304. doi:10.1016/j.scitotenv.2018.07.459

Goovaerts, P., 2001. Geostatistical modelling of uncertainty in soil science. Geoderma 103, 3–26. doi:10.1016/S0016-7061(01)00067-2

Goovaerts, P., 1999a. Geostatistics in soil science: State-of-the-art and perspectives. Geoderma 89, 1–45. doi:10.1016/S0016-7061(98)00078-0

Goovaerts, P., 1999b. Geostatistics for Natural Resources Evaluation. J. Environ. Qual. 28, 1044. doi:10.2134/jeq1999.00472425002800030046x

Goovaerts, P., Albuquerque, M.T.D., Antunes, I.M.H.R., 2016. A Multivariate Geostatistical Methodology to Delineate Areas of Potential Interest for Future Sedimentary Gold Exploration. Math. Geosci. 48, 921–939. doi:10.1007/s11004-015-9632-8

Gupta, A., Yan, D., 2016. Introduction mineral Processing Design and Operation, Mineral Processing Design and Operations - 2nd Edition.

Hakanson, L., 1980. An ecological risk index for aquatic pollution control.a sedimentological approach. Water Res. 14, 975–1001. doi:10.1016/0043-1354(80)90143-8

Harada, M., 1995. Minamata disease: Methylmercury poisoning in Japan caused by environmental pollution. Crit. Rev. Toxicol. 25, 1–24. doi:10.3109/10408449509089885

Hawkes, H.E., Webb, J.S., 1962. Geochemistry in mineral exploration. New York.

He, Z.L., Yang, X.E., Stoffella, P.J., 2005. Trace elements in agroecosystems and impacts on the environment. J. Trace Elem. Med. Biol. doi:10.1016/j.jtemb.2005.02.010

Higueras, P., Oyarzun, R., Lillo, J., Sánchez, J.C., Molina, J.A., Esbrí, J.M., Lorenzo, S., 2005. The Almadén district (Spain): anatomy of one of the world's largest Hg-contaminated sites. Sci. Total Environ. 112–124.

Higueras, P.L., Mansilla Plaza, L., Lorenzo Álvarez, S., Esbrí Víctor, J.M., 2011. The Almadén mercury mining district, in: History of Research in Mineral Resources.

IGME, 2016. Panorama minero de España.

Jobin, P., Mercier, G., Blais, J.F., 2016. Magnetic and density characteristics of a heavily polluted soil with municipal solid waste incinerator residues: Significance for remediation strategies. Int. J. Miner. Process. doi:10.1016/j.minpro.2016.02.010

Journel, A., Huijbregts, C., 1978. Mining geostatistics. San Diego: Academic Press.

Karn, B., Kuiken, T., Otto, M., 2009. Nanotechnology and in situ remediation: A review of the benefits and potential risks. Environ. Health Perspect. doi:10.1289/ehp.0900793

Kleijnen, J.P.C., 2009. Kriging metamodeling in simulation: A review. Eur. J. Oper. Res. doi:10.1016/j.ejor.2007.10.013

Klimkova, S., Cernik, M., Lacinova, L., Filip, J., Jancik, D., Zboril, R., 2011. Zero-valent iron nanoparticles in treatment of acid mine water from in situ uranium leaching. Chemosphere 82, 1178–1184. doi:10.1016/j.chemosphere.2010.11.075

Kržišnik, N., Mladenovič, A., Škapin, A.S., Škrlep, L., Ščančar, J., Milačič, R., 2014. Nanoscale zero-valent iron for the removal of Zn2+, Zn(II)-EDTA and Zn(II)-citrate from aqueous solutions. Sci. Total Environ. 476–477, 20–28. doi:10.1016/j.scitotenv.2013.12.113

Larios, R., Fernández-Martínez, R., LeHecho, I., Rucandio, I., 2012. A methodological

approach to evaluate arsenic speciation and bioaccumulation in different plant species from two highly polluted mining areas. Sci. Total Environ. 414, 600–607. doi:10.1016/j.scitotenv.2011.09.051

Li, X., Elliott, D.W., Zhang, W., 2006. Zero-Valent Iron Nanoparticles for Abatement of Environmental Pollutants: Materials and Engineering Aspects. Crit. Rev. Solid State Mater. Sci. 31, 111–122. doi:10.1080/10408430601057611

Litter, M.I., Quici, N., Meichtry, M., 2018. Iron nanomaterials for water and soil treatment.

López-Cima, M.F., García-pérez, J., Pérez-gómez, B., Aragonés, N., López-Abente, G., Tardón, A., Pollán, M., 2011. Lung cancer risk and pollution in an industrial region of Northern Spain: a hospital-based case-control study. Int. J. Health Geogr. 10, 10. doi:10.1186/1476-072X-10-10

Loredo, J., Álvarez, R., Ordóñez, A., Bros, T., 2008. Mineralogy and geochemistry of the Texeo Cu-Co mine site (NW Spain): Screening tools for environmental assessment. Environ. Geol. doi:10.1007/s00254-007-1078-y

Loredo, J., Ordonez, A., Alvarez, R., 2006. Environmental impact of toxic metals and metalloids from the Munon Cimero mercury-mining area (Asturias, Spain). J. Hazard. Mater. 136, 455–467.

Lu, G.Y., Wong, D.W., 2008. An adaptive inverse-distance weighting spatial interpolation technique. Comput. Geosci. 34, 1044–1055. doi:10.1016/j.cageo.2007.07.010

Luque, C., Gutierrez-Claverol, M., 2006. La minería del mercurio en Asturias. Rasgos históricos.

Martínez Cortizas, A., López-Merino, L., Bindler, R., Mighall, T., Kylander, M.E., 2016. Early atmospheric metal pollution provides evidence for Chalcolithic/Bronze Age mining and metallurgy in Southwestern Europe. Sci. Total Environ. doi:10.1016/j.scitotenv.2015.12.078

Matanzas, N., Sierra, M.J., Afif, E., Díaz, T.E., Gallego, J.R., Millán, R., 2017. Geochemical study of a mining-metallurgy site polluted with As and Hg and the transfer of these contaminants to Equisetum sp. J. Geochemical Explor. 182, 1–9.

doi:10.1016/j.gexplo.2017.08.008

McCallum, R.I., 2005. Occupational exposure to antimony compounds. J. Environ. Monit. 7, 1245. doi:10.1039/b509118g

McKinley, J., Lloyd, C.D., 2011. Multivariate Geochemical Data Analysis in Physical Geography, in: Compositional Data Analysis: Theory and Applications. doi:10.1002/9781119976462.ch21

McKinley, J.M., Hron, K., Grunsky, E.C., Reimann, C., de Caritat, P., Filzmoser, P., van den Boogaart, K.G., Tolosana-Delgado, R., 2016. The single component geochemical map: Fact or fiction? J. Geochemical Explor. 162, 16–28. doi:10.1016/j.gexplo.2015.12.005

Megido, L., Suárez-Peña, B., Negral, L., Castrillón, L., Fernández-Nava, Y., 2017. Suburban air quality: Human health hazard assessment of potentially toxic elements in PM10. Chemosphere 177, 284–291. doi:10.1016/j.chemosphere.2017.03.009

Mercier, G., Blais, J.F., Chartier, M., 2007. Pilot-scale decontamination of soils polluted with toxic metals by mineral processing technology and chemical leaching. J. Environ. Eng. Sci.

Mesa, V., Navazas, A., González-Gil, R., González, A., Weyens, N., Lauga, B., Gallego, J.L.R., Sánchez, J., Peláez, A.I., 2017. Use of endophytic and rhizosphere bacteria to improve phytoremediation of arsenic-contaminated industrial soils by autochthonous Betula celtiberica. Appl. Environ. Microbiol. 83. doi:10.1128/AEM.03411-16

Mielke, H.W., Laidlaw, M.A.S., Gonzales, C., 2010. Lead (Pb) legacy from vehicle traffic in eight California urbanized areas: Continuing influence of lead dust on children's health. Sci. Total Environ. doi:10.1016/j.scitotenv.2010.05.017

Miranda, M., López-Alonso, M., Castillo, C., Hernández, J., Benedito, J.L., 2005. Effects of moderate pollution on toxic and trace metal levels in calves from a polluted area of northern Spain. Environ. Int. 31, 543–548. doi:10.1016/j.envint.2004.09.025

Mubarak, H., Chai, L.Y., Mirza, N., Yang, Z.H., Pervez, A., Tariq, M., Shaheen, S., Mahmood, Q., 2015. Antimony (Sb) – pollution and removal techniques – critical assessment of technologies. Toxicol. Environ. Chem. 97, 1296–1318.

doi:10.1080/02772248.2015.1095549

Mueller, T.G., Pusuluri, N.B., Mathias, K.K., Cornelius, P.L., Barnhisel, R.I., Shearer, S.A., 2004. Map Quality for Ordinary Kriging and Inverse Distance Weighted Interpolation. Soil Sci. Soc. Am. J. doi:10.2136/sssaj2004.2042

Muller, G., 1969. Index of geoaccumulation in sediments of the Rhine River. Geological 2, 108–118.

Neesse, T., Dueck, J., Minkov, L., 2004. Separation of finest particles in hydrocyclones, in: Minerals Engineering. doi:10.1016/j.mineng.2004.01.016

Nussbaumer, R., Mariethoz, G., Gloaguen, E., Holliger, K., 2018. Which Path to Choose in Sequential Gaussian Simulation. Math. Geosci. 50, 97–120. doi:10.1007/s11004-017-9699-5

O'Carroll, D., Sleep, B., Krol, M., Boparai, H., Kocur, C., 2013. Nanoscale zero valent iron and bimetallic particles for contaminated site remediation. Adv. Water Resour. 51, 104–122. doi:10.1016/j.advwatres.2012.02.005

Oliveira, M.L.S., Ward, C.R., Izquierdo, M., Sampaio, C.H., de Brum, I.A.S., Kautzmann, R.M., Sabedot, S., Querol, X., Silva, L.F.O., 2012. Chemical composition and minerals in pyrite ash of an abandoned sulphuric acid production plant. Sci. Total Environ. 430, 34–47. doi:10.1016/j.scitotenv.2012.04.046

Oliver, M.A., Webster, R., 2014. A tutorial guide to geostatistics: Computing and modelling variograms and kriging. Catena. doi:10.1016/j.catena.2013.09.006

Ordóñez, A., Álvarez, R., Loredo, J., 2013. Asturian mercury mining district (Spain) and the environment: A review. Environ. Sci. Pollut. Res. 20, 7490–7508. doi:10.1007/s11356-013-1663-4

Pawlowsky, V., Burger, H., 1992. Spatial structure analysis of regionalized compositions. Math. Geol. doi:10.1007/BF00894233

Pelaez, A.I., Lores, I., Sotres, A., Mendez-Garcia, C., Fernandez-Velarde, C., Santos, J.A., Gallego, J.L.R., Sanchez, J., 2013. Design and field-scale implementation of an "on site" bioremediation treatment in PAH-polluted soil. Environ. Pollut. 181, 190–199. doi:10.1016/j.envpol.2013.06.004

Pereira, M.J., Soares, A., 2018. Geostatistics for Environmental Applications, in: Mathematical Geosciences. pp. 123–125. doi:10.1007/s11004-018-9733-2

Peters, R.W., 1999. Chelant extraction of heavy metals from contaminated soils. J. Hazard. Mater. doi:10.1016/S0304-3894(99)00010-2

Porteous, A., 1996. Dictionary of environmental science and technology, 2nd editio. ed. John Wiley & Sons, Inc., Chichester.

Prabhakaran Nair, K.P., Cottenie, A., 1971. Parent material-soil relationship in trace elements - a quantitative estimation. Geoderma 5. doi:10.1016/0016-7061(71)90014-0

Qi, C., Liu, G., Chou, C.L., Zheng, L., 2008. Environmental geochemistry of antimony in Chinese coals. Sci. Total Environ. doi:10.1016/j.scitotenv.2007.09.007

Rajput, S., Singh, L.P., Pittman, C.U., Mohan, D., 2017. Lead (Pb2+) and copper (Cu2+) remediation from water using superparamagnetic maghemite (γ-Fe2O3) nanoparticles synthesized by Flame Spray Pyrolysis (FSP). J. Colloid Interface Sci. 492, 176–190. doi:10.1016/j.jcis.2016.11.095

Reimann, C., De Caritat, P., 2005. Distinguishing between natural and anthropogenic sources for elements in the environment: Regional geochemical surveys versus enrichment factors. Sci. Total Environ. doi:10.1016/j.scitotenv.2004.06.011

Reimann, C., Filzmoser, P., Garrett, R.G., 2005. Background and threshold: critical comparison of methods of determination. Sci. Total Environ. 346, 1–16. doi:10.1016/j.scitotenv.2004.11.023

Reimann, C., Garrett, R.G., 2005. Geochemical background - Concept and reality. Sci. Total Environ. 350, 12–27. doi:10.1016/j.scitotenv.2005.01.047

Reyhanitabar, A., Alidokht, L., Khataee, A.R., Oustan, S., 2012. Application of stabilized Fe0nanoparticles for remediation of Cr(VI)-spiked soil. Eur. J. Soil Sci. 63, 724–732. doi:10.1111/j.1365-2389.2012.01447.x

Rodríguez-Terente, L.M., Luque, C., Gutierrez-Claverol, M., 2006. Los registros mineros para sustancias metálicas en Asturias. Trab. Geol. Univ. Oviedo.

Sharma, H.D., Reddy, K.R., 2004. Geoenvironmental Engineering: Site Remediation,

Waste Containment, and Emerging Waste Management Technologies. Dev. Geotech. Eng. doi:10.1016/S0165-1250(98)80038-2

Shumway, R.H., Azari, R.S., Kayhanian, M., 2002. Statistical approaches to estimating mean water quality concentrations with detection limits. Environ. Sci. Technol. doi:10.1021/es0111129

Sierra, C., Álvarez Saiz, J.R., Gallego, J.L.R., 2013. Nanofiltration of Acid Mine Drainage in an Abandoned Mercury Mining Area. Water, Air, Soil Pollut. 224, 1734. doi:10.1007/s11270-013-1734-7

Sierra, C., Boado, C., Saavedra, A., Ordóñez, C., Gallego, J.R., 2014a. Origin, patterns and anthropogenic accumulation of potentially toxic elements (PTEs) in surface sediments of the Avilés estuary (Asturias, northern Spain). Mar. Pollut. Bull. 86, 530–8. doi:10.1016/j.marpolbul.2014.06.052

Sierra, C., Gallego, J.R., Afif, E., Menéndez-Aguado, J.M., González-Coto, F., 2010. Analysis of soil washing effectiveness to remediate a brownfield polluted with pyrite ashes. J. Hazard. Mater. 180, 602–8. doi:10.1016/j.jhazmat.2010.04.075

Sierra, C., Martínez-Blanco, D., Blanco, J. a, Gallego, J.R., 2014b. Optimisation of magnetic separation: A case study for soil washing at a heavy metals polluted site. Chemosphere. doi:10.1016/j.chemosphere.2013.12.063

Sierra, C., Martínez, J., Menéndez-Aguado, J.M., Afif, E., Gallego, J.R., 2013. High intensity magnetic separation for the clean-up of a site polluted by lead metallurgy. J. Hazard. Mater. 248–249, 194–201. doi:10.1016/j.jhazmat.2013.01.011

Sierra, C., Menéndez-Aguado, J.M., Afif, E., Carrero, M., Gallego, J.R., 2011. Feasibility study on the use of soil washing to remediate the As-Hg contamination at an ancient mining and metallurgy area. J. Hazard. Mater. 196, 93–100. doi:10.1016/j.jhazmat.2011.08.080

Smith, A.H., Lingas, E.O., Rahman, M., 2000. Contamination of drinking-water by arsenic in Bangladesh: A public health emergency. Bull. World Health Organ. 78, 1093–1103. doi:10.1590/S0042-96862000000900005

Smith, P.G., Koch, I., Reimer, K.J., 2008. Uptake, transport and transformation of arsenate in radishes (Raphanus sativus). Sci. Total Environ. 390, 188–197.

doi:10.1016/j.scitotenv.2007.09.037

Smoliński, A., Walczak, B., Einax, J.W., 2003. Robust Multivariate Calibration in Environmental Studies. Anal. Lett. 36, 2317–2336. doi:10.1081/AL-120023722

Sokal, R.R., Thomson, B.A., 2006. Population structure inferred by local spatial autocorrelation: An example from an Amerindian tribal population. Am. J. Phys. Anthropol. 129, 121–131. doi:10.1002/ajpa.20250

Spahić, M.P., Sakan, S., Cvetković, Ž., Tančić, P., Trifković, J., Nikić, Z., Manojlović, D., 2018. Assessment of contamination, environmental risk, and origin of heavy metals in soils surrounding industrial facilities in Vojvodina, Serbia. Environ. Monit. Assess. doi:10.1007/s10661-018-6583-9

Stefaniuk, M., Oleszczuk, P., Ok, Y.S., 2016. Review on nano zerovalent iron (nZVI): From synthesis to environmental applications. Chem. Eng. J. doi:10.1016/j.cej.2015.11.046

Sucharovà, J., Suchara, I., Hola, M., Marikova, S., Reimann, C., Boyd, R., Filzmoser, P., Englmaier, P., 2012. Top-/bottom-soil ratios and enrichment factors: What do they really show? Appl. Geochemistry. doi:10.1016/j.apgeochem.2011.09.025

Svoboda, J., Fujita, T., 2003. Recent developments in magnetic methods of material separation. Miner. Eng. 16, 785–792. doi:10.1016/S0892-6875(03)00212-7

Syversen, T., Kaur, P., 2012. The toxicology of mercury and its compounds. J. Trace Elem. Med. Biol. doi:10.1016/j.jtemb.2012.02.004

Tango, T., 1995. A class of tests for detecting ‘general’ and ‘focused’ clustering of rare diseases. Stat. Med. 14, 2323–2334. doi:10.1002/sim.4780142105

Tessier, a, Campbell, P.G.C., Bisson, M., 1979. Sequential Extraction Procedure for the Speciation of Particulate Trace Metals. Anal. Chem. 51, 844–851. doi:10.1021/ac50043a017

Thomas, M.R., 2002. A GIS-based decision support system for brownfield redevelopment. Landsc. Urban Plan. doi:10.1016/S0169-2046(01)00229-8

Thornton, I., 2012. Environmental geochemistry: 40years research at Imperial College, London, UK. Appl. Geochemistry. doi:10.1016/j.apgeochem.2011.07.015

Tobler, W., 1993. Three Presentations on Geographical Analysis and Modeling: Non-Isotropic Geographic Modeling Speculations on the Geometry of Geography Global Spatial Analysis, National Center for Geographic Information and Analysis. Technical Report 93 (1).

United Nations, 2017. Minamata Convention on Mercury: Text and Annexes.

US Environmental Protection Agency, 2007. Soil Screening Guidance: User's Guide.

US EPA, 2005. Guidelines for Carcinogen risk assessment, Risk Assessment Forum. doi:10.1109/CSSS.2012.139

Voth, A., 2004. Asturias: Economic crisis and new development perspectives in Northern Spain. Geogr. Rundsch. 56, 38–45.

Wang, A.-T., Wang, Q., Li, J., Yuan, G.-L., Albanese, S., Petrik, A., 2019. Geo-statistical and multivariate analyses of potentially toxic elements' distribution in the soil of Hainan Island (China): A comparison between the topsoil and subsoil at a regional scale. J. Geochemical Explor. 197, 48–59. doi:10.1016/j.gexplo.2018.11.008

Wang, H.B., Wong, M.H., Lan, C.Y., Baker, A.J.M., Qin, Y.R., Shu, W.S., Chen, G.Z., Ye, Z.H., 2007. Uptake and accumulation of arsenic by 11 Pteris taxa from southern China. Environ. Pollut. 145, 225–233. doi:10.1016/j.envpol.2006.03.015

Wilding, L.P., Drees, L.R., 1983. Spatial Variability and Pedology, in: Pedogenesis and Soil Taxonomy. doi:doi:10.1016/S0166-2481(08)70599-3

Wills, B., Finch, J., 2015. Mineral Processing Technology:An Introduction to the Practical Aspects of Ore Treatment and Mineral Recovery. doi:10.1016/B978-075064450-1/50003-5

Xu, G., Xie, J., Zhang, Y., Zhao, C., Wu, Q., 2010. Application of nemerow pollution index in landscape river water quality assessment of Tianjin, in: 2010 4th International Conference on Bioinformatics and Biomedical Engineering, ICBBE 2010. doi:10.1109/ICBBE.2010.5514830

Yan, W., Herzing, A.A., Kiely, C.J., Zhang, W.X., 2010. Nanoscale zero-valent iron (nZVI): Aspects of the core-shell structure and reactions with inorganic species in water. J. Contam. Hydrol. 118, 96–104. doi:10.1016/j.jconhyd.2010.09.003

Yang, J., Wang, J., Zheng, Y., Lei, M., Yang, J., Wan, X., Chen, T., 2018. Method for identifying outliers of soil heavy metal data. Environ. Sci. Pollut. Res. 25, 12868–12875. doi:10.1007/s11356-018-1555-8

Zhang, C., Selinus, O., 1998. Statistics and GIS in environmental geochemistry - some problems and solutions. J. Geochemical Explor. 64, 339–354. doi:10.1016/S0375-6742(98)00048-X

Zhang, W.X., 2003. Nanoscale iron particles for environmental remediation: An overview. J. Nanoparticle Res. doi:10.1023/A:1025520116015

Chapter II. New advances for the characterization of pollution in soils by potentially toxic elements

II.I Trace elements of concern affecting urban agriculture in industrialized areas: A multivariate approach

C. Boente, N. Matanzas, N. García-González, E. Rodríguez-Valdés, J.R. Gallego

Chemosphere (2017)

Volume 183, May 2017, Pages 546-556

Rank: 21 out of 109 (1st Quartile) in *Environmental Chemistry* (JCR)

Chemosphere 183 (2017) 546–556

Contents lists available at ScienceDirect

Chemosphere

journal homepage: www.elsevier.com/locate/chemosphere

Trace elements of concern affecting urban agriculture in industrialized areas: A multivariate approach

C. Boente, N. Matanzas, N. García-González, E. Rodríguez-Valdés, J.R. Gallego*

INDUROT and Environmental Biotechnology & Geochemistry Group, University of Oviedo, C/Gonzalo Gutiérrez Quirós s/n, 33600, Mieres (Asturias), Spain

HIGHLIGHTS

- Trace element in peri-urban soils devoted to agriculture exceeded threshold levels.
- Multivariate statistics revealed anthropogenic activity, mainly coal combustion.
- A novel soil pollution index was applied to identify subareas of concern.
- Bioavailability assessment demonstrated low potential risks for human health.

GRAPHICAL ABSTRACT

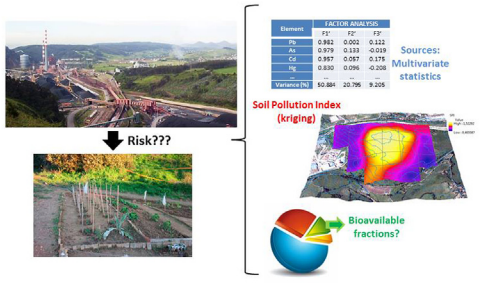

ARTICLE INFO

Article history:
Received 22 March 2017
Received in revised form
3 May 2017
Accepted 21 May 2017
Available online 26 May 2017

Handling Editor: Martine Leermakers

Keywords:
Soil
Trace elements
Multivariate statistics
Kriging
Bioavailability
PAHs

ABSTRACT

The urban and peri-urban soils used for agriculture could be contaminated by atmospheric deposition or industrial releases, thus raising concerns about the potential risk to public health. Here we propose a method to evaluate potential soil pollution based on multivariate statistics, geostatistics (kriging), a novel soil pollution index, and bioavailability assessments. This approach was tested in two districts of a highly populated and industrialized city (Gijón, Spain). The soils showed anomalous content of several trace elements, such as As and Pb (up to 80 and 585 mg kg^{-1} respectively). In addition, factor analyses associated these elements with anthropogenic activity, whereas other elements were attributed to natural sources. Subsequent clustering also facilitated the differentiation between the northern area studied (only limited Pb pollution found) and the southern area (pattern of coal combustion, including simultaneous anomalies of trace elements and benzo(a)pyrene). A normalized soil pollution index (SPI) was calculated by kriging, using only the elements falling above threshold levels; therefore point-source polluted zones in the northern area and diffuse contamination in the south were identified. In addition, in the six mapping units with the highest SPIs of the fifty studied, we observed low bioavailability for most of the elements that surpassed the threshold levels. However, some anomalies of Pb contents and the pollution fingerprint in the central area of the southern grid call for further site-specific studies. On the whole, the combination of a multivariate (geo) statistic approach and a bioavailability assessment allowed us to efficiently identify sources of contamination and potential risks.

1. Introduction

During the last century, the growth of cities worldwide led to an increase in urban agricultural practices (Szolnoki et al., 2013). The

* Corresponding author.
E-mail address: jgallego@uniovi.es (J.R. Gallego).

http://dx.doi.org/10.1016/j.chemosphere.2017.05.129
0045-6535/

term “urban agriculture” encompasses farms in inner cities, which are called urban gardens, and also to those located on the outskirts of cities (Leake et al., 2009; Rodríguez Martín et al., 2015). Regardless of the location of cities, their growth implies increased exposure of urban farming to air and soil pollution caused by heavy industry and dense traffic (Wiseman et al., 2013). Among the many contaminants derived from these anthropogenic sources, trace elements (such as Pb, As, Cu or Zn) are of particular concern (Argyropoulos et al., 2012; Boente et al., 2016). Trace elements, but also organics such as PAHs (Polycyclic Aromatic Hydrocarbons), enter soil through atmospheric deposition (Davis and Birch, 2011), and they can pose a public health problem when they exceed certain thresholds. In this regard, heavy metal(loid)s have long residence times and are easily assimilated by natural organisms (Kabata-Pendias, 2011). As a result, in the case of urban agriculture, trace elements can be taken up by plants, thus entering the food chain in significant amounts (Säumel et al., 2012). Therefore, the consumption of fruit and vegetables grown in soils with elevated concentrations of potentially toxic elements (Szolnoki et al., 2013; Tóth et al., 2016) poses a public health concern.

In order to determine whether trace elements contamination affects urban and peri-urban agriculture, plant and soil sampling in natural or uncultivated pasturelands—which are supposedly virtually pollution-free—is an appropriate approach to gather valuable information on the source and extent of atmospheric trace metal pollution in urban and industrial environments (Chai et al., 2015). Studies of this sort frequently follow the same approach, namely soil sample collection, preparation and chemical analysis of samples (Theocharopoulos et al., 2001), multivariate statistical and spatial analyses (Facchinelli et al., 2001; Gallego et al., 2002), and the identification of potential areas of risk on the basis of concentration thresholds considered hazardous for human health (Fairbrother et al., 2007). In this regard, SSLs (Soil Screening Levels), better known as RBSSLs (Risk-Based Soil Screening Levels), are threshold levels based on a specified degree of risk or hazard, usually taking also into account natural backgrounds. Thus these levels determine a threshold for several chemical elements at which a soil would require site-specific risk assessment. This value varies depending on soil use; i.e. industrial, residential, recreational, or other uses (natural soils, such as agricultural or forests) (BOPA, 2014). In this context, bioavailability and toxicity data of the potential contaminants should be considered in order to refine the bulk data of total concentrations (Izquierdo et al., 2015; Yutong et al., 2016). In addition, a site-specific risk assessment is sometimes also performed to determine potential effects of contaminants on human health (Hough et al., 2004).

RBSSLs are generally used (Wcisło et al., 2016) in brownfield sites to determine whether risk assessment is required. However, in extensive areas where diffuse pollution caused by atmospheric deposition is expected, an intermediate step should involve the identification of priority subareas in which site-specific risk assessment and/or bioavailability studies should be performed. In this context, soil pollution indexes (SPIs) are commonly used to determine the concentration of heavy metal(loid)s in soil (Zhiyuan et al., 2011). Many SPIs have been reported (Massas et al., 2013; Muller, 1969; Zaharia, 2011); however, in this study, we attempted to go one step further, in order to develop an innovative SPI that determines the global contamination of a position taking into account valid RBSSLs in the study area. This SPI has been configured as a regionalized variable (Matheron, 1971), and therefore it can be implemented and calculated via kriging. Kriging requires a point map (centroids of square grids for example) as input and returns a raster map with predictions. It uses experimental semi-variograms, that must be computed and interpreted (Goovaerts, 1999; Antunes and Albuquerque, 2013), to characterize the spatial relationship between samples (McGrath et al., 2004). It is an interpolation procedure that provides the best unbiased linear estimator and that allows prediction of element concentrations at non-sampled locations (Sierra et al., 2014). Kriging contemplates two groups of distances: the first is the distance between the point of interest and the sample location and the second is the distance between sample locations, giving rise to sample clustering, which impairs the quality of the estimation (Ha et al., 2014).

Given the abovementioned considerations, this study sought to improve and complement the classical characterization methodologies, like (multivariate) statistical and geostatistical analyses (kriging), with a new SPI especially designed for heavy metal pollution and that also considers RBSSLs. To this end, one of the largest industrialized areas of Spain was selected to test the capacity of this SPI. Thus, a comprehensive sampling campaign was undertaken in two districts in the surroundings of the city of Gijón (Asturias, Northern Spain). In this densely populated area, agricultural land coexists alongside several industries that process coal, heavy metals and cement—thus exposing nearby soils to potential contamination via atmospheric deposition of trace elements and other contaminants. The combined methodology carried out had three objectives:

- To determine whether heavy metal(loid)s affect the soil of two rural areas located in the surroundings of an industrialized area next to a large city and, thus, verify whether agricultural practices in this area give rise to a public health risk. A possible concurrent contamination with PAHs has been also addressed.
- To identify patterns and possible sources of pollution by means of multivariate statistics, thereby assigning the origins of the geochemical anomalies either to natural backgrounds, to diffuse contamination (atmospheric deposition), or to point-source contamination (industrial releases, waste disposal or others).
- To define, via kriging, a novel soil pollution index with which to identify areas of concern that merit bioavailability assessment.

2. Materials and methods

2.1. Site description

The districts of Jove and Lloreda are located in the NW and SW of Gijón (Fig. SM1), which is the largest city (almost 300,000 people) in the region of Asturias. Nowadays this city continues to be surrounded by several heavy industries that have been operating since the middle of the 20th century. Industrial processes include a coal power plant, metallurgy industries (including integrated steelworks), a cement plant, a main harbour (dry bulk port), and a number of auxiliary industries distributed in industrial estates, all of them potentially emitting trace elements and organic contaminants. The location of the main principal factories, sampling grids (see below), and points of interest is shown in Fig. 1.

The district of Jove (Northern grid) covers a hill about 150 m high running northeast-southwest, with the main urban area of Gijón situated to the west of the hill and the mouth of the Aboño estuary to the east. On this side, there is an industrial estate with a coal power station and a cement plant. In addition, about 3 km southwest of this district there is an iron/steel factory. Recent studies have revealed Hg pollution in groundwater in this area (González-Fernández et al., 2014).

The district of Lloreda (Southern grid) is also located on another small hill of around 100 m in height, about 4 km to the south of the district of Jove. Lloreda is flanked to the north by the heavily frequented A-8 motorway, to the northwest by the iron/steel factory, and to the northeast by a Zn-oxide plant.

Fig. 1. Study area, sampling grids, and factories in the area (small industrial activities not indicated).

2.2. Soil sampling strategy

The same sampling strategy was applied for both areas. After visual reconnaissance, analyses of preliminary data on soil trace element content (data not shown), and review of recent papers about the study zone (González-Fernández et al., 2014; Lage et al., 2016), we chose to encompass two study grids each covering 56.25 ha; each grid was in turn divided 25 mapping units, each measuring 150 × 150 m (Fig. 1). Five systematically distributed 1.5-kg samples were taken from the top 20–25 cm of the soil of each unit using an Edelman Auger (each sample was obtained from three increases in each sampling station, see Fig. 2).

The increments sampled were passed through a 2-cm mesh screen 'in situ' to remove rocks, gravel, and other large material before being taken to the laboratory. All samples were dried in an oven at 35 °C to prevent the evaporation of volatile compounds. Before and after sieving, samples were homogenized and quartered to preserve their representativeness. A composite sample from the five subsamples collected was obtained for each square-grid using a Jones riffle splitter. The final set of 50 composite samples was used for analyses (see below).

2.3. Analyses

2.3.1. Physico-chemical properties

The main physico-chemical properties were determined as follows: pH was measured in a suspension of soil and water (1:2.5) with a pH meter (Crison), and electrical conductivity was determined in the same extract (diluted 1:5). Organic matter was measured by weight loss at 450 °C (ignition method) (Schulte and Hopkins, 1996). Total N was determined by Kjeldahl digestion (Klute, 1996). Particle-size distribution was measured by Bouyoucos densimetry, after particle dispersion with sodium hexametaphosphate and sodium carbonate (Gee and Bauder, 1996). Carbonates were measured using a Bernard calcimeter and sulfates by liquid chromatography.

2.3.2. Multielement analyses

Composite samples (<2 mm) were sent to Envira, ISO-17025 accredited laboratories, where the heavy metal content was

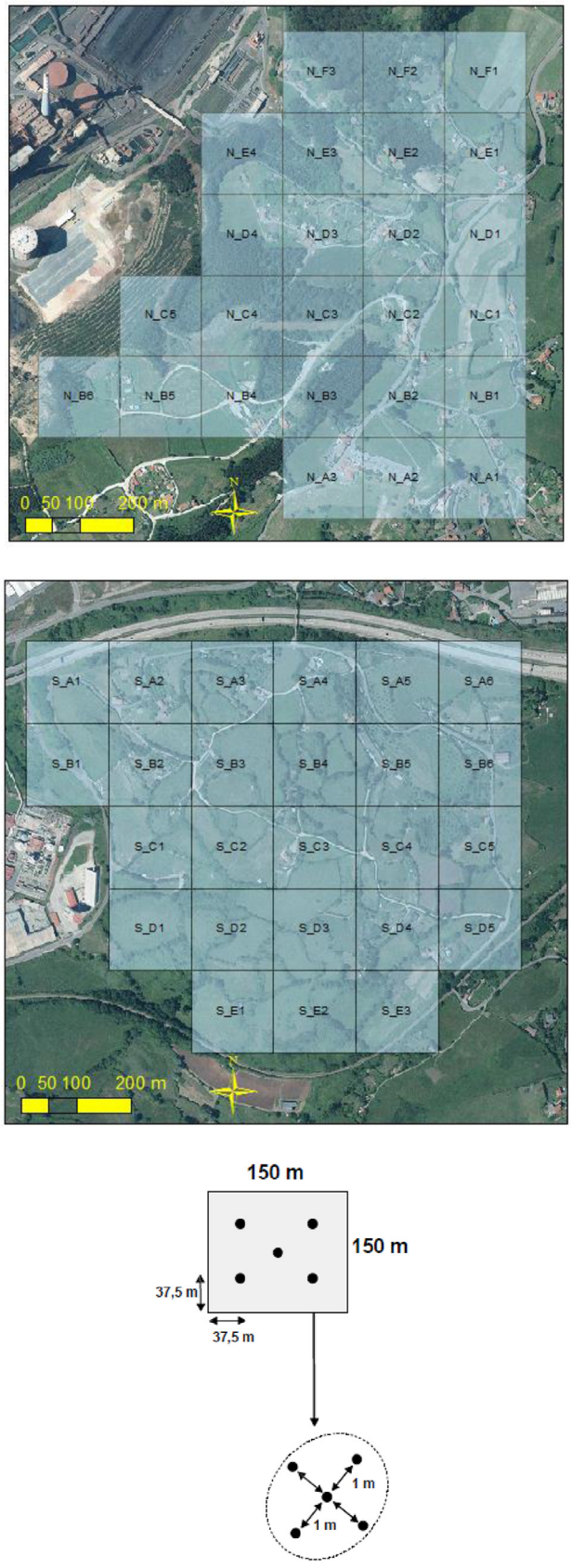

Fig. 2. (Top) Northern (Jove) and southern (Lloreda) sampling grids. (Bottom) Sketch of the sampling strategy for each mapping unit.

measured by means of method EPA 3051 in accordance with ISO 17294-1 and ISO 17924-2. In brief, samples were microwave-digested in aqua regia. Inductively coupled plasma mass spectrometry (ICP-MS) was then used to determine total concentration of As, Ba, Be, Cd, Co, Cr, Cu, Hg, Mo, Mn, Ni, Pb, Sb, Se, Sn, Tl, V and Zn, and cold vapor atomic absorption spectrometry (CVAAS) was used to determine Hg.

2.3.3. Polycyclic Aromatic Hydrocarbons

Selected samples from the southern grid (see results) were also analyzed for PAH (Polycyclic Aromatic Hydrocarbon) contents. In brief, soil samples were Soxtherm-extracted with dichloromethane:acetone (1:1). The 16 priority PAHs were determined after injection into a 7890A GC System coupled to a 5975C Inert XL MSD with a Triple-Axis Detector (Agilent Technologies) by means of EPA method 8272 modified. A capillary column DB-5ms (5% phenyl 95% dimethylpolysiloxane) 30 m × 0.25 mm i.d. × 0.25 μm film (Agilent Technologies) was used, with helium as carrier gas at a flow rate of 1 mL min^{-1}. The GC injector was operated in splitless mode for 2 min at 260 °C. The mass spectrometer was operated in selected ion monitoring mode (SIM), and the quantification *m/z* relations were 128, 152, 153, 154, 165, 166, 178, 202, 228, 252, 276 and 278.

2.4. Statistical analysis

Multielement results were compiled to create a database to be used for statistical analyses through SPSS V. 22 software. These studies included bivariate statistics and also multivariate statistics via factor analysis and cluster analysis (CA).

Factor analysis was performed by means of principal components analysis (PCA). The number of factors was determined by the Kaiser/Gutmann criterion; i.e. only eigenvalues larger than one were considered. The principal components method was used to extract the factors, following recommendations for geochemical data (Reimann and De Caritat, 2005), whereas the Varimax (orthogonal) rotation was applied because it minimizes the number of variables that have high loading on each factor (Gallego et al., 2013 and references therein). The factors obtained were studied and interpreted in function of their hypothetical origin (natural, anthropogenic or mixed).

In addition, the factor scores matrix produced was subjected to CA in order to obtain groups (clusters) of samples with a similar geochemical profile. CA was undertaken following the Ward algorithmic method, which maximizes the variance between groups and minimizes it between members of the same group (Murtagh and Legendre, 2014). The measurement used in this CA was the Squared Euclidean distance. The dendrograms obtained were mapped in order to provide a more intuitive representation.

2.5. Soil pollution index

A soil pollution index (SPI) for location *i* was calculated at each pixel of a raster as the summation of the quotients of the concentration of each specific element and its corresponding RBSSL, and then the results were averaged by the number of pollutants considered:

$$SPI_i = \frac{\sum_j \frac{C_j^i}{RBSSL_j}}{N}$$

where i = pixel to calculate; j = pollutant; C_j^i = the j pollutant concentration at point i (obtained by kriging); $RBSSL_j$ = the Risk Based Soil Screening Level for the pollutant j, which is established

Table 1
Descriptive statistics (range, mean, standard deviation, RSD) for the analysis of 25 composite soil samples for the district of Jove and 25 for the district of Lloreda. RBSSL, Range, Mean and SD are expressed in mg·kg^{-1}, RSD expressed in %.

Element	RBSSL	Northern grid				Southern grid			
		Range	Mean	SD	RSD	Range	Mean	SD	RSD
As	**40**	9.4–36.7	18.2	7.1	39	11.8–79.4	39.1	22.4	57
Ba	**1540**	56.0–265.0	116.0	48.3	42	179.0–563.0	306.2	107.9	35
Be	**20**	0.5–1.5	0.6	0.3	50	1.7–2.7	2.2	0.3	14
Cd	**2**	0.4–1.0	0.6	0.2	33	0.4–2.3	1.1	0.5	45
Co	**25**	0.8–21.7	3.4	4.1	121	8.3–15.2	11.4	1.7	15
Cr	**10,000**	10.1–36.1	20.2	7.4	37	39.0–70.5	53.9	7.1	13
Cu	**55**	5.7–244.0	25.2	46.3	184	22.0–116.0	36.8	19.7	54
Hg	**1**	0.2–1.9	0.5	0.4	80	0.1–0.4	0.2	0.1	50
Mn	**2135**	99.8–1060.0	277.5	197.2	71	833.0–4663.0	1683.0	926.4	55
Mo	**6**	0.7–20.6	1.9	3.9	205	1.1–2.8	1.9	0.5	26
Ni	**65**	3.4–30.2	9.5	5.2	55	24.5–39.0	33.1	4.4	13
Pb	**70**	32.7–585.0	95.9	116.4	121	32.9–170.0	94.6	43.4	46
Sb	**5**	1.0–5.2	2.5	1.3	52	1.4–9.7	4.3	2.6	60
Se	**25**	0.9–2.1	1.5	0.3	20	0.7–2.0	1.4	0.4	29
Sn	**4360**	1.1–407.0	20.2	81.1	401	3.4–5.7	4.0	0.6	15
Tl	**1**	0.3–0.6	0.4	0.1	25	0.5–2.8	1.4	0.7	50
V	**50**	17.0–53.1	31.6	9.3	29	49.4–77.1	63.0	6.8	11
Zn	**455**	64.0–1047.0	149.7	189.8	127	136.0–458.0	243.8	89.6	37

by the applicable legislation (BOPA, 2014); and N = the number of pollutants considered.

As shown below, for each grid, we considered only elements that exceeded the RBSSL for the soil category of "other uses" (agricultural soils) in at least one of the mapping units. The SPI values acquired were assigned to the centroid of each mapping unit, and SPI maps were obtained by kriging. It must be pointed out that the SPI is addictive by construction and therefore it may be assumed as a regionalized variable, being geostatistical methods adequate for its calculation.

2.6. Bioavailability and toxicity assessment

Given that knowledge of the mechanisms that regulate the release and mobility of contaminants is essential for risk evaluation purposes, a sequential extraction similar to that proposed by Tessier (Tessier et al., 1979) was also performed for selected samples (see results). In brief, extracts with reagents of increasing strengths were taken from 2.5-g soil samples, and the following fractions were obtained:

- Exchangeable: 2.5 g of dried waste was weighed and transferred to 50-mL centrifuge tubes, to which 25 mL of $MgCl_2$ (1 M, pH 7) was added. The tubes were vigorously shaken at room temperature for 1 h and then centrifuged at 13,000 rpm for 30 min. The supernatant was passed through a Whatman filter paper (no. 542) and then made up to 25 mL.
- Carbonate-bound: The residue from the exchangeable fraction was mixed with 25 mL of CH_3COONa/CH_3COOH buffer (1 M, pH 5); the tubes were shaken at room temperature for 5 h and then centrifuged and treated under the same conditions as those described above.
- Fe-Mn oxide-bound: The residue from the carbonate fraction was mixed with 25 mL of $NH_2OH \cdot HCl$ (0.04 M in acetic acid 25%); the tubes were shaken at 96 °C in a water bath for 6 h and then centrifuged and treated under the same conditions as those described above.
- Organic matter-bound: The residue from Fe/Mn oxide-bound fraction was mixed with 5 mL of 30% H_2O_2 and 3 mL of 0.01 M HNO_3; the tubes were shaken at 85 °C in a water bath for 5 h, followed by the addition of 2 mL of 30% H_2O_2 and 1 h at 85 °C in a water bath. Finally, 15 mL of 1 M NH_4NO_3 was added and followed by 10 min of shaking at room temperature. The tubes were then centrifuged and treated under the same conditions as those described above.
- Residual fraction: The residue from the organic matter-bound fraction was air-dried and ground with an agate mortar. 0.250 g of the ground residue was leached by means of an 'Aqua regia' digestion ($HCl + HNO_3$) in an Anton Paar 3000 microwave. This fraction and the preceding liquid ones were analyzed for heavy metal(loid) content by means of ICP-MS, as detailed in Section 2.3.1.

Hg, As and Cr speciation were also determined in order to identify the proportion of methyl- and ethyl-Hg, As (III) and Cr (VI), which are more toxic than inorganic Hg, As (V) and Cr (III), respectively. The species were separated and subsequently quantified in a 1260 Infinity HPLC coupled to a 7700 ICPMS (Agilent Technologies) as detailed in Gallego et al. (2015).

3. Results and discussion

3.1. Soil properties

From an edaphological point of view and as shown in Table SM1, soils from the two study areas were different. For the southern grid, no large local variations were observed; i.e. low RSDs (Relative Standard Deviations) were obtained for all the parameters, with the exception of carbonate content, which is dependent on the local geology. Conversely, in the northern area wide ranges of clay-sand and organic matter percentages suggest different soil typologies. In general terms, northern soils are more heterogeneous but also more sandy, more acidic and slightly richer in organic matter than the southern ones.

Various trends can be also appreciated from the multielement data in Table 1. Initially, northern samples revealed stronger variabilities (higher RSDs for most elements) than southern ones. More specifically, some elements, such as Cd, Se, Tl in the north or Ni, Zn, or V in the south, among others, presented very low RSDs and thus a tendency to follow a normal distribution. Conversely, for example, As in the south and Pb in the north revealed high RSDs, suggesting a non-normal distribution, which could be influenced by external agents other than soil composition. These observations initially indicate a certain degree of spatial variability related to the

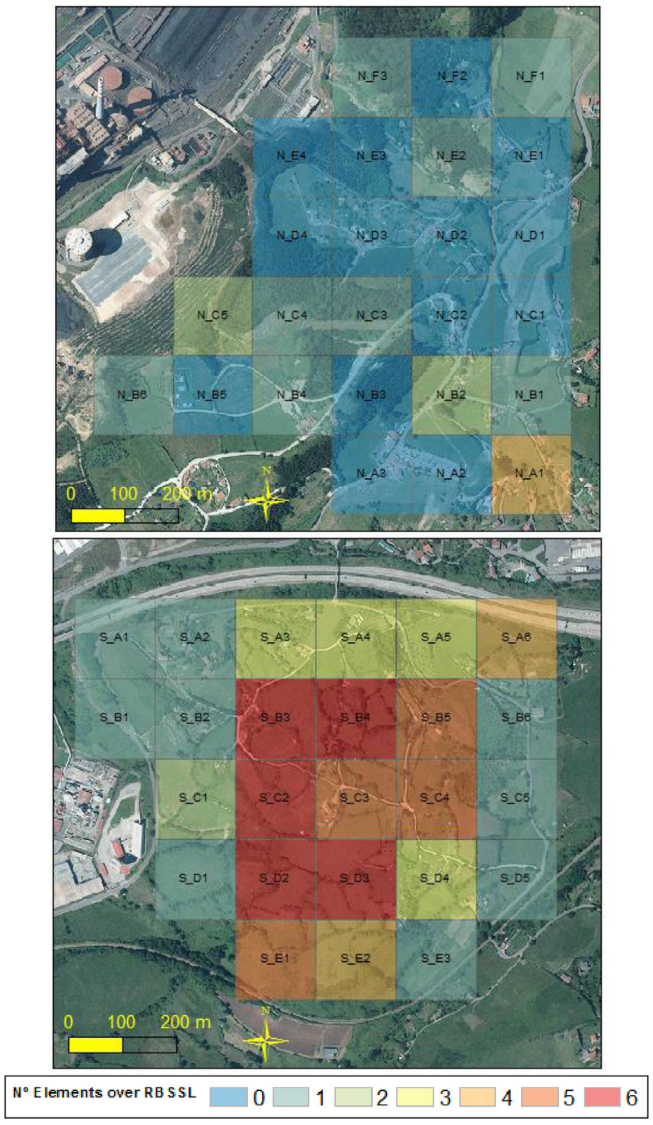

Fig. 3. Distribution of the number of trace elements that surpassed RBSSLs in each grid; (top) Northern grid, (bottom) Southern grid.

presence of anthropogenic contamination sources.

Focusing on average values, the southern area had, on the whole, higher concentrations of elements than the northern one, thereby suggesting a more significant geochemical anomaly in the south. In this area, the average content of Pb, Tl, As, Sb and other elements exceeded or were very close to RBSSLs (Table 1). In contrast, in the north, only average anomalous concentrations of Pb were found.

In a second step, the mapping units were ranked on the basis of trace elements surpassing the RBSSLs (Fig. 3). For the northern area, more than half the grids did not exceed the RBSSLs and the distribution of mapping units in which thresholds were exceeded was irregular. In contrast, in the southern area, the units that showed concentrations above the RBSSLs were regularly grouped in the middle of the grid, which corresponded to high grounds, as determined by topography. In these central units, six elements exceeded their respective RBSSLs.

As regards specific elements, Pb frequently exceeded the threshold concentration in the northern area (9 cases out of 25), but the other potential contaminants (Cu, Hg, Sb, Mo, Zn, and V) only slightly surpassed their respective RBSSLs in 1 or 2 cases. In contrast, a distinct scenario emerged in the southern area, where many more pollutants exceeded RBSSLs, with As (9 cases out of 25), Mn (6 out of 25), Pb (15 out of 25), Sb (9 out of 25), Tl (14 out of 25) and V (24 out of 25) being notable and Cu (2 out of 25) and Cd (1 out of 25) being less marked.

3.2. Sources of pollution: multivariate statistics

Bivariate correlations were also performed from the 25 samples and 18 elements analyzed for each grid individually. Interestingly, for the southern area, As showed a high correlation (>0.8) with other common elements of concern (Hg, Cd, Pb). In contrast, in the northern area, neither As nor Pb revealed significant correlations with other elements. However, in both areas less relevant elements, such as V, Be and Cr, showed a strong correlation with Ni and Co, all of them having low RSDs (Table 1). This observation initially suggests the presence of a similar natural background in the two areas, accompanied by potential multicomponent pollution in the south and only isolated point-source singularities in the north. In this context, a subdivision of the northern grid data in order to perform a more detailed statistical analysis with lower heterogeneity within samples was considered. However, the initial number of mapping units (samples) for each zone is 25, and therefore any subdivision would suppose a too low number of observations to satisfy factor analysis requirements.

3.2.1. Factor analysis

The results of the factor analysis for the metal concentration in the study areas are shown in Table 2. In both cases, four factors were extracted (Kaiser-Guttman criterion), accounting for at least 75% of the total variance.

In the northern area, the main factor (F1) presented high loads for seven elements that can be associated with the geochemical background, as explained above (low RSDs). The less significant second, third and fourth factors (F2, F3 and F4) did not include any element surpassing the RSBBLs. The most problematic element in this area, Pb, showed only a very slight association with F2, where it was linked to Cd and Zn—an observation commonly reported for these three elements (Burton et al., 2005; Sierra et al., 2014). However, the absence of a clear link points to a probable point-source origin of contamination for the abnormal values of Pb in some mapping units.

In the southern area (approx. 87% of explained variance), the first factor (F1′) had a high load for a list of mostly chalchophile elements, with high RSDs (Table 2), which frequently exceeded the RBSSLs in this area and which are very common in atmospheric pollution issues in northern Spain (Gallego et al., 2013; Irabien et al., 2008). Remarkably, Tl presented a very high load in this factor, and it has recently been identified as a good marker of the coal combustion fingerprint (López Antón et al., 2013; Vaněk et al., 2016). As stated above, in the outskirts of Gijón there is a coal-fired power station and also a steel industry, including coke ovens and sintering processes, both of them using coal and both common sources of trace element emission (Lau et al., 2016; Zajusz-Zubek and Konieczyński, 2003). In contrast, the second factor (F2′) is very similar to the first one (F1) found in the northern area; i.e. it presented high values for elements of minor importance and with a monotone distribution in all the zones studied such as Cr, Ni, Co, Be and V. We hypothesized that this factor is simply a geochemical association of lithophile elements, although a certain contribution of coal or even oil derivatives (traffic air pollution (Shi et al., 2008)) might be relevant (note that V was above the RBSSLs in almost all mapping units). The third and fourth factors (F3′ and F4′) explained

Table 2
Factor loadings and percentage of variance explained by the Varimax-rotated factors (extracted by principal components). Factor loadings higher than 0.6 are marked in italics, elements exceeding the RSBBL at least once are shown in bold.

Element	Northern grid				Element	Southern grid			
	F1	F2	F3	F4		F1′	F2′	F3′	F4′
Co	***0.937***	−0.095	0.003	0.224	**Pb**	***0.982***	0.002	0.122	0.026
Ni	***0.913***	0.149	0.002	0.318	**Tl**	***0.980***	0.092	0.028	0.026
Be	***0.909***	−0.088	0.172	−0.035	**As**	***0.979***	0.133	−0.019	−0.020
Cr	***0.895***	−0.022	0.062	0.248	**Sb**	***0.974***	0.011	0.037	−0.002
Mn	***0.855***	−0.018	0.159	0.080	**Cd**	***0.957***	0.057	0.175	0.010
V	***0.822***	0.215	−0.067	0.295	Mo	***0.860***	0.101	0.101	0.253
Tl	***0.808***	0.266	0.200	−0.219	Hg	***0.830***	0.096	−0.208	0.247
Ba	***0.762***	0.036	0.398	0.346	Ba	***0.807***	0.163	0.375	−0.175
Cd	−0.218	***0.891***	−0.004	−0.118	Se	***0.717***	0.182	−0.055	−0.543
Zn	0.136	***0.885***	−0.007	0.294	**Mn**	***0.616***	0.063	−0.135	−0.019
Se	0.395	***0.673***	0.066	0.163	Cr	−0.246	***0.921***	−0.039	0.174
As	0.183	0.04	***0.921***	0.189	Ni	0.246	***0.920***	0.216	−0.029
Sb	0.105	−0.079	***0.851***	−0.032	Be	0.306	***0.881***	−0.021	−0.065
Mo	0.481	0.266	***0.523***	−0.048	**V**	0.407	***0.850***	−0.053	0.074
Sn	0.181	0.013	0.3	***0.873***	Co	−0.546	***0.722***	0.284	0.063
Cu	0.281	0.251	−0.158	***0.785***	Cu	−0.115	0.083	***0.867***	0.220
Hg	−0.064	−0.03	0.406	−0.145	**Zn**	***0.646***	0.082	***0.680***	−0.005
Pb	−0.083	0.325	0.048	−0.127	Sn	0.210	0.162	0.201	***0.853***
Explained variance (%)	36.669	13.54	13.298	11.422	Explained variance (%)	50.884	20.795	9.205	6.004

Table 3
Average PAH concentrations of samples S-B3, S-C2, S-C3.

Compounds		RBSSLs (ppb)	Concentration (ppb)	Std. dev.
2–3 ring PAHs	Naphthalene	1000	29.41	18.42
	Acenaphthylene	–	6.17	0.81
	Acenaphthene	6000	0.00	0.00
	Fluorene	5000	4.46	0.07
	Phenanthrene	–	57.30	10.45
	Anthracene	45,000	8.87	1.61
4–6 ring PAHs	Fluoranthene	8000	93.54	13.23
	Pyrene	6000	71.36	9.19
	Benzo(a)anthracene	200	26.36	16.91
	Chrysene	20,000	32.30	19.98
	Benzo(k) fluoranthene	2000	111.05	13.08
	Benzo(b) fluoranthene	200	14.98	7.15
	Benzo(a)pyrene	20	**39.25**	34.86
	Indene(1,2,3-c,d)pyrene	300	70.22	4.85
	Dibenzo(a,h) anthracene	30	15.46	4.02
	Benzo(g,h,i)perylene	–	50.66	11.03
Total 16 PAHs			631.40	77.58
Diagnostic ratios	Phenanthrene/Anthracene		**6.46**	
	Fluoroanthene/Pyrene		**1.31**	

a very low proportion of variance and were therefore considered clearly secondary. These factors included elements such as Cu, Zn and Sn, which showed mixed behavior with regard to the first two factors.

Furthermore, in order to gather additional information about potential sources of pollution (reflected in Factor F1′), and taking into account the abovementioned geochemical association with coal combustion, we subjected some samples (S-B3, S-C2, S-C3) to PAH quantification. These samples were selected given that they showed a high number of elements exceeding RBSSLs and high loads in factor F1′ (both things suggest possible deposition of coal combustion fly ashes), in addition they are located in the higher area of the southern grid thus more exposed than others to atmospheric deposition. We conjectured that concurrent organic pollution occurs because of the atmospheric deposition of residues deriving from coal combustion (Liu et al., 2008). In this regard, results (Table 3) indicated that the presence of PAHs (total content below 1 ppm) was not very relevant. Nevertheless, the content of benzo(a)pyrene was above RBSSLs, thereby suggesting an anomaly. In addition, regarding PAH sources, samples revealed values of diagnostic ratios (Table 3) typically found in pyrogenic sources (Phenanthrene/Anthracene < 10 and Fluoroanthene/Pyrene > 1, see (Boehm, 2005; Uhler et al., 2010)). All things considered, these results provide complementary evidence of the influence of anthropogenic pollution sources, particularly coal combustion, in this area.

3.2.2. Cluster analysis (CA)

Having selected the main factors for each study area, we used factor score matrixes as an input for a cluster analysis. After the application of Ward's clustering algorithm, the dendrograms obtained were cut at a distance of 40 units (square Euclidean), obtaining a four- and three-cluster classification for the northern and southern area, respectively (Fig. 4). Therefore, the clustering of factorial scores facilitated the drawing of maps that indicate the degree of similarity between the mapping units, thereby

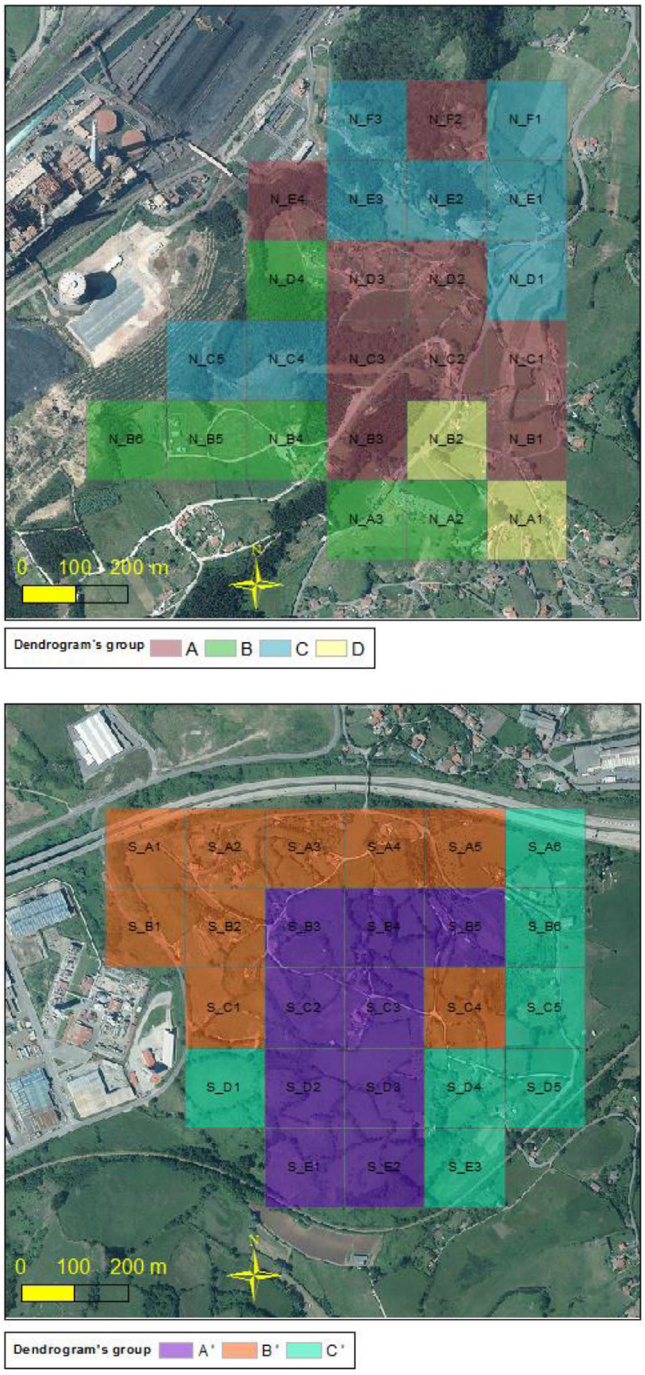

Fig. 4. Graphical clustering according to Ward's algorithm for the northern grid (top) and the southern grid (bottom).

identifying zones that are most affected by the contaminants (areas where, generally, the concentrations of elements like As and Pb were higher).

The four groups found after CA in the northern area were irregularly distributed. Interestingly, Group D represented the two mapping units with the most anomalous presence of trace elements (mainly Pb). Conversely, Groups A, B and C corresponded to zones of minor concern in which pollution appeared to be considerably low.

Regarding the southern grid, the first of the three groups, identified as A′, encompassed those grids in which the mapping units held element concentrations that exceeded the RBSSLs; i.e. units very well represented by Factor F1′. Conversely, Groups B′ and C′ corresponded to mapping units with a lower presence of elements of concern.

3.3. Soil pollution index

The information obtained in the preceding sections is not completely clarifying in order to identify sub-areas for site-specific studies. To overcome this limitation, we calculated the SPI for the centroids of each mapping unit. Following the formula described in Section 2.5, the SPI has been calculated for the heavy metal(loid)s of concern exceeding the RBSSLs. The results were then interpolated via kriging, as shown in the three-dimensional thematic maps in Fig. 5, thereby providing an overall view of the anomalies detected, in such way that the most contaminated zones could be easily distinguished.

The northern area presented a SPI that varied from 0.30 to 1.89. As seen in Fig. 5, this zone is very steep and the bottom left corner is potentially the area with greatest contamination, while the rest of the district showed lower concentrations, with the exception of mapping unit N-C4.

In the southern grid, the SPI ranged from 0.46 to 1.52 and the most affected area comprised the flat elevated zone in the center of the grid. In this case, the degree of contamination appeared to have a clear relationship with topography, thereby suggesting that soil erosion in the steep areas accounts for lower trace element concentrations. However, the degree of contamination was much more regularly distributed than in the northern area.

3.4. Bioavailability and toxicity

Given that the study areas are located in zones devoted to arable and livestock farming, we estimated the bioavailability and toxicity of the trace elements registering concentrations above their respective RBSSLs, in order to determine the risk to human health. These measurements were applied for samples corresponding with mapping units revealing the highest SPIs (Fig. 5).

In a first step, speciation analyses revealed the absence of traces of methyl- or ethyl-Hg, As (III) or Cr (VI) in the samples. Subsequently, the sequential extraction procedure described in Section 2.6 was applied, and the main results are indicated in Table 4.

The bioavailability for most of the trace elements analyzed was low for both study areas (Table 4) and, consequently, potential absorption by plants is very limited; this is especially important in the case of As, given its carcinogenic properties. Exceptionally, Pb and Zn in the case of the northern grid, and Cd for the southern one showed more than 10% bioavailability in some samples, although, as previously stated, on the basis of our findings, only Pb can be considered a significant contaminant. In fact, Pb in the northern area exceeded the RBSSL on several occasions, although its bioavailability differed in the three samples studied, thereby suggesting that the anomalies in Pb contamination can be attributed to different factors. This would imply that specific releases of Pb or Pb-waste disposal sites were at some time present in the northern area, in coherence with the multivariate results presented above; in addition, the different soil properties indicated in Table SM1 could be probably conditioning bioavailability results (more acidic pHs and less clay contents in the northern area). Consistently, the bioavailability of Pb in the southern area was very low and very similar in the three samples studied. These observations thus also support the notion that the southern area is affected by atmospheric deposition.

On the whole, the low bioavailability of the elements exceeding

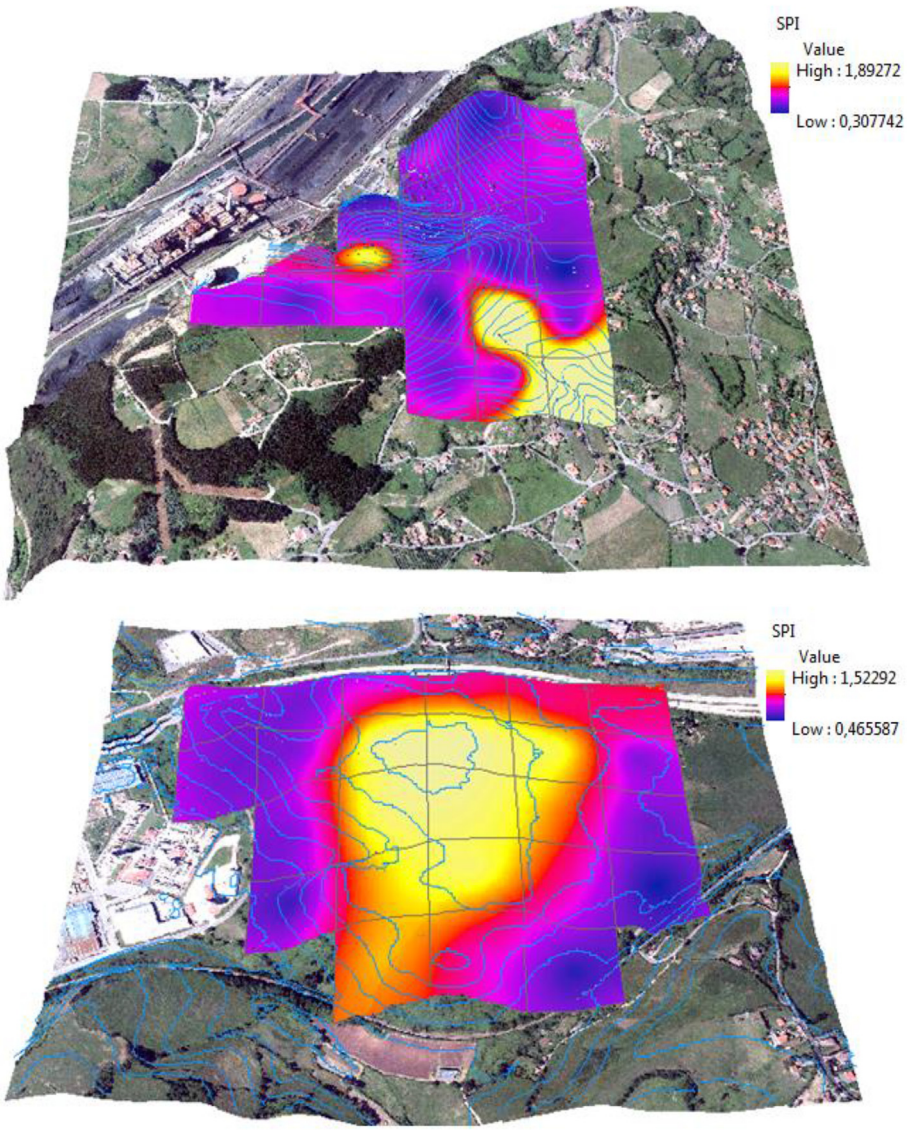

Fig. 5. Kriging estimation of the SPI obtained for the study areas; top: northern grid; bottom: southern grid (contour lines shown in blue). (For interpretation of the references to colour in this figure legend, the reader is referred to the web version of this article.)

the RBSSLs and the absence of the most toxic species suggest that agricultural practices in these areas pose a very low risk to human health. However, some specific anomalies in Pb content in the northern area, together with the demonstrated pollution fingerprint in the central area of the southern grid, might require further site-specific studies in smaller parcels, especially considering that the approach followed herein was based on composite samples characterizing 150-m side squares.

4. Conclusions

Two areas located in districts with predominant agricultural practices in the city of Gijón, were studied in order to assess the degree of potential soil pollution caused by the presence of heavy industries in the surroundings. Initially, the concentrations of several trace elements in soil were well-above the RBSSLs. Concretely, As and Pb were identified as the main contaminants of concern, whereas other elements, such as V, although surpassing the RBSSLs, were attributed to natural sources, as determined by factor analysis. The multivariate statistics carried out also included clustering, which facilitated the differentiation between the northern area (only local Pb pollution found) and the southern one (a wide clear fingerprint of coal combustion, including concurrent anomalies of trace elements and benzo(a)pyrene).

Additionally, we tested a novel SPI to detect specific subareas with higher risks. This SPI is calculated for every point in the study areas by kriging, using only the elements above the threshold levels. This SPI results served to support the conclusion of distinct distributions (local and diffuse) of trace elements in the study areas. In addition, given their high SPIs, three subareas from each of the grids were studied. The results showed low bioavailability of most of the elements surpassing the RBSSLs, and the absence of toxic species, such as As (III) and Cr (VI). These findings indicate low risk of agricultural practices in the study zone for human health. However, some specific anomalies, such as significant content of highly bioavailable Pb in the northern area, together with the demonstrated pollution fingerprint in the central area of the southern grid, may merit further attention by means of site-specific risk assessment.

Table 4
Concentrations ($mg \cdot kg^{-1}$) of the two main fractions obtained by sequential extraction, and percentages of bioavailability (bioavailable fraction –BF- includes exchangeable and carbonate-bound fractions; non-bioavailable fraction –nBF- includes oxides, organic matter, and residual fractions). The samples analyzed correspond to the three highest SPIs calculated for each grid.

Element	Mapping units (northern grid)								
	N-A1			N-B2			N-C4		
	BF	nBF	% Bioav.	BF	nBF	% Bioav.	BF	nBF	% Bioav.
Cu	5.7	238.3	2.4	1.3	32.3	3.9	0.0	8.9	0.0
Hg	0.0	0.2	0.9	0.0	0.3	0.0	0.0	0.4	0.0
Mo	0.0	20.6	0.0	0.0	1.2	0.0	0.0	0.9	0.0
Pb	11.1	88.0	11.2	6.3	578.7	1.1	109.8	209.2	34.4
Sb	0.0	3.1	0.0	0.0	5.2	0.0	0.0	3.2	0.0
V	0.7	43.0	1.7	0.4	32.6	1.2	0.4	25.4	1.6
Zn	273.4	773.6	26.1	50.7	102.3	33.1	76.9	64.2	54.5
Element	Mapping units (southern grid)								
	S-C2			S-B3			S-C3		
	BF	nBF	% Bioav.	BF	nBF	% Bioav.	BF	nBF	% Bioav.
As	0.0	76.4	0.0	0.0	79.4	0.0	0.0	74.4	0.0
Cd	0.7	0.8	44.7	0.8	1.1	40.2	0.8	1.1	40.6
Cu	0.0	35.8	0.0	0.0	36.7	0.0	0.0	34.6	0.0
Mn	100.8	2671.2	3.6	111.8	2466.2	4.3	113.1	1974.9	5.4
Pb	3.2	151.8	2.0	3.7	166.3	2.2	4.7	143.3	3.2
Sb	0.0	7.2	0.0	0.0	8.2	0.0	0.0	7.9	0.0
Tl	0.0	2.3	0.0	0.0	2.7	0.0	0.0	2.5	0.0
V	0.3	76.8	0.3	0.2	70.9	0.3	0.0	70.2	0.0

Acknowledgments

This research was funded by the Consejería de Infraestructuras, Ordenación del Territorio y Medioambiente of the Principality of Asturias. We would like also to thank the Environmental Assay Unit of the Scientific and Technical Services of the University of Oviedo for their technical support. Carlos Boente obtained a grant from the "Formación del Profesorado Universitario" program, financed by the "Ministerio de Educación, Cultura y Deporte de España".

Appendix A. Supplementary data

Supplementary data related to this article can be found at http://dx.doi.org/10.1016/j.chemosphere.2017.05.129.

References

Antunes, I.M.H.R., Albuquerque, M.T.D., 2013. Using indicator kriging for the evaluation of arsenic potential contamination in an abandoned mining area (Portugal). Sci. Total Environ. 442, 545–552. http://dx.doi.org/10.1016/j.scitotenv.2012.10.010.

Argyropoulos, G., Manoli, E., Kouras, A., Samara, C., 2012. Concentrations and source apportionment of PM10 and associated major and trace elements in the Rhodes Island, Greece. Sci. Total Environ. 432, 12–22. http://dx.doi.org/10.1016/j.scitotenv.2012.05.076.

Boehm, P.D., 2005. Polycyclic Aromatic Hydrocarbons (PAHs). Environmental Forensics: Contaminant Specific Guide. Elsevier, pp. 313–337.

Boente, C., Sierra, C., Rodríguez-Valdés, E., Menéndez-Aguado, J.M., Gallego, J.R., 2016. Soil washing optimization by means of attributive analysis: case study for the removal of potentially toxic elements from soil contaminated with pyrite ash. J. Clean. Prod. 142, 2693–2699. http://dx.doi.org/10.1016/j.jclepro.2016.11.007.

BOPA, Boletín Oficial del Principado de Asturias, 91, April 21, 2014. Generic Reference Levels for Heavy Metals in Soils from Principality of Asturias, Spain. http://sede.612asturias.es/bopa/2014/04/21/2014–06617.pdf (Accessed March 2017).

Burton, E.D., Phillips, I.R., Hawker, D.W., 2005. Geochemical partitioning of copper, lead, and zinc in benthic, estuarine sediment profiles. J. Environ. Qual. 34, 263. http://dx.doi.org/10.2134/jeq2005.0263.

Chai, Y., Guo, J., Chai, S., Cai, J., Xue, L., Zhang, Q., 2015. Source identification of eight heavy metals in grassland soils by multivariate analysis from the Baicheng-Songyuan area, Jilin Province, Northeast China. Chemosphere 134, 67–75. http://dx.doi.org/10.1016/j.chemosphere.2015.04.008.

Davis, B.S., Birch, G.F., 2011. Spatial distribution of bulk atmospheric deposition of heavy metals in metropolitan Sydney, Australia. Water Air. Soil Pollut. 214, 147–162. http://dx.doi.org/10.1007/s11270-010-0411-3.

Facchinelli, A., Sacchi, E., Mallen, L., 2001. Multivariate statistical and GIS-based approach to identify heavy metal sources in soils. Environ. Pollut. 114, 313–324. http://dx.doi.org/10.1016/S0269-7491(00)00243-8.

Fairbrother, A., Wenstel, R., Sappington, K., Wood, W., 2007. Framework for metals risk assessment. Ecotoxicol. Environ. Saf. 68, 145–227. http://dx.doi.org/10.1016/j.ecoenv.2007.03.015.

Gallego, J.R., Ordóñez, A., Loredo, J., 2002. Investigation of trace element sources from an industrialized area (Avilés, northern Spain) using multivariate statistical methods. Environ. Int. 27, 589–596. http://dx.doi.org/10.1016/S0160-4120(01)00115-5.

Gallego, J.R., Ortiz, J.E., Sierra, C., Torres, T., Llamas, J.F., 2013. Multivariate study of trace element distribution in the geological record of Roñanzas Peat Bog (Asturias, N. Spain). Paleoenvironmental evolution and human activities over the last 8000calyr BP. Sci. Total Environ. 454–455, 16–29. http://dx.doi.org/10.1016/j.scitotenv.2013.02.083.

Gallego, J.R., Esquinas, N., Rodríguez-Valdés, E., Menéndez-Aguado, J.M., Sierra, C., 2015. Comprehensive waste characterization and organic pollution co-occurrence in a Hg and As mining and metallurgy brownfield. J. Hazard. Mater. 300, 561–571. http://dx.doi.org/10.1016/j.jhazmat.2015.07.029.

Gee, G.W., Bauder, J.W., 1996. Particle size analysis. In: Klute, A. (Ed.), Methods of Soil Analysis. American Society of Agronomy, Madison, WI, pp. 383–411.

González-Fernández, B., Menéndez-Casares, E., Meléndez-Asensio, M., Fernández-Menéndez, S., Ramos-Muñiz, F., Cruz-Hernández, P., González-Quirós, A., 2014. Sources of mercury in groundwater and soils of west Gijón (Asturias, NW Spain). Sci. Total Environ. 481, 217–231. http://dx.doi.org/10.1016/j.scitotenv.2014.02.034.

Goovaerts, P., 1999. Geostatistics in soil science: state-of-the-art and perspectives. Geoderma 89, 1–45. http://dx.doi.org/10.1016/S0016-7061(98)00078-0.

Ha, H., Olson, J.R., Bian, L., Rogerson, P.A., 2014. Analysis of heavy metal sources in soil using kriging interpolation on principal components. Environ. Sci. Technol. 48, 4999–5007. http://dx.doi.org/10.1021/es405083f.

Hough, R.L., Breward, N., Young, S.D., Crout, N.M.J., Tye, A.M., Moir, A.M., Thornton, I., 2004. Assessing potential risk of heavy metal exposure from consumption of home-produced vegetables by urban populations. Environ. Health Perspect. 112, 215–221. http://dx.doi.org/10.1289/ehp.5589.

Irabien, M.J., Cearreta, A., Leorri, E., Gómez, J., Viguri, J., 2008. A 130 year record of pollution in the Suances estuary (southern Bay of Biscay): implications for environmental management. Mar. Pollut. Bull. 56, 1719–1727. http://dx.doi.org/10.1016/j.marpolbul.2008.07.006.

Izquierdo, M., De Miguel, E., Ortega, M.F., Mingot, J., 2015. Bioaccessibility of metals and human health risk assessment in community urban gardens. Chemosphere 135, 312–318. http://dx.doi.org/10.1016/j.chemosphere.2015.04.079.

Kabata-Pendias, A., 2011. Trace Elements in Soils and Plants. CRC Press. http://dx.doi.org/10.1201/b10158-25.

Klute, A., 1996. Nitrogen-total. In: Klute, A. (Ed.), Methods of Soil Analyses. American Society of Agronomy, Madison,WI, pp. 595–624.

Lage, J., Wolterbeek, H., Almeida, S.M., 2016. Contamination of surface soils from a heavy industrial area in the North of Spain. J. Radioanal. Nucl. Chem. 309, 429–437. http://dx.doi.org/10.1007/s10967-016-4757-x.

Lau, L.L., de Castro, L.F.A., Dutra, F., de, C., Cantarino, M.V., 2016. Characterization

and mass balance of trace elements in an iron ore sinter plant. J. Mater. Res. Technol. 5, 144–151. http://dx.doi.org/10.1016/j.jmrt.2015.10.007.
Leake, J.R., Adam-Bradford, A., Rigby, J.E., 2009. Health benefits of "grow your own" food in urban areas: implications for contaminated land risk assessment and risk management? Environ. Health 8 (Suppl. 1), S6. http://dx.doi.org/10.1186/1476-069X-8-S1-S6.
Liu, G., Niu, Z., Van Niekerk, D., Xue, J., Zheng, L., 2008. Polycyclic aromatic hydrocarbons (PAHs) from coal combustion: emissions, analysis, and toxicology. Rev. Environ. Contam. Toxicol. 192, 1–28. http://dx.doi.org/10.1007/978-0-387-71724-1_1.
López Antón, M.A., Spears, D.A., Díaz Somoano, M., Martínez Tarazona, R., 2013. Thallium in coal: analysis and environmental implications. Fuel 105, 13–18. http://dx.doi.org/10.1016/j.fuel.2012.08.004.
Massas, I., Kalivas, D., Ehaliotis, C., Gasparatos, D., 2013. Total and available heavy metal concentrations in soils of the Thriassio plain (Greece) and assessment of soil pollution indexes. Environ. Monit. Assess. 185, 6751–6766. http://dx.doi.org/10.1007/s10661-013-3062-1.
Matheron, G., 1971. The Theory of Regionalized Variables and its Applications. Les Cahiers du Centre de Morphologie Mathématique no.5, Ecole des Mines de Paris.
McGrath, D., Zhang, C., Carton, O.T., 2004. Geostatistical analyses and hazard assessment on soil lead in Silvermines area. Irel. Environ. Pollut. 127, 239–248. http://dx.doi.org/10.1016/j.envpol.2003.07.002.
Muller, G., 1969. Index of geoaccumulation in sediments of the Rhine River. Geol. J. 2, 108–118.
Murtagh, F., Legendre, P., 2014. Ward's hierarchical agglomerative clustering method: which algorithms implement Ward's criterion? J. Classif. 31, 274–295. http://dx.doi.org/10.1007/s00357-014-9161-z.
Reimann, C., De Caritat, P., 2005. Distinguishing between natural and anthropogenic sources for elements in the environment: regional geochemical surveys versus enrichment factors. Sci. Total Environ. 337, 91–107. http://dx.doi.org/10.1016/j.scitotenv.2004.06.011.
Rodríguez Martín, J.A., De Arana, C., Ramos-Miras, J.J., Gil, C., Boluda, R., 2015. Impact of 70 years urban growth associated with heavy metal pollution. Environ. Pollut. 196, 156–163. http://dx.doi.org/10.1016/j.envpol.2014.10.014.
Säumel, I., Kotsyuk, I., Hölscher, M., Lenkereit, C., Weber, F., Kowarik, I., 2012. How healthy is urban horticulture in high traffic areas? Trace metal concentrations in vegetable crops from plantings within inner city neighborhoods in Berlin. Ger. Environ. Pollut. 165, 124–132. http://dx.doi.org/10.1016/j.envpol.2012.02.019.
Schulte, E.E., Hopkins, B.G., 1996. Estimation of soil organic matter by weight loss-on-ignition. In: Magdoff, F.R., Tabatasbai, M.A., Hanlon, E.A. (Eds.), Soil Organic Matter: Analysis and Interpretation. Soil Science Society of America, Madison, WI, pp. 21–31.
Shi, G., Chen, Z., Xu, S., Zhang, J., Wang, L., Bi, C., Teng, J., 2008. Potentially toxic metal contamination of urban soils and roadside dust in Shanghai, China. Environ. Pollut. 156, 251–260. http://dx.doi.org/10.1016/j.envpol.2008.02.027.
Sierra, C., Boado, C., Saavedra, A., Ordóñez, C., Gallego, J.R., 2014. Origin, patterns and anthropogenic accumulation of potentially toxic elements (PTEs) in surface sediments of the Avilés estuary (Asturias, northern Spain). Mar. Pollut. Bull. 86, 530–538. http://dx.doi.org/10.1016/j.marpolbul.2014.06.052.
Szolnoki, Z., Farsang, A., Puskás, I., 2013. Cumulative impacts of human activities on urban garden soils: origin and accumulation of metals. Environ. Pollut. 177, 106–115. http://dx.doi.org/10.1016/j.envpol.2013.02.007.
Tessier, A., Campbell, P.G.C., Bisson, M., 1979. Sequential extraction procedure for the speciation of particulate trace metals. Anal. Chem. 51, 844–851. http://dx.doi.org/10.1021/ac50043a017.
Theocharopoulos, S.P., Wagner, G., Sprengart, J., Mohr, M.E., Desaules, A., Muntau, H., Christou, M., Quevauviller, P., 2001. European soil sampling guidelines for soil pollution studies. Sci. Total Environ. 264, 51–62. http://dx.doi.org/10.1016/S0048-9697(00)00611-2.
Tóth, G., Hermann, T., Da Silva, M.R., Montanarella, L., 2016. Heavy metals in agricultural soils of the European Union with implications for food safety. Environ. Int. 88, 299–309. http://dx.doi.org/10.1016/j.envint.2015.12.017.
Uhler, A.D., Stout, S.A., Emsbo-Mattingly, S.D., Rouhani, S., 2010. Chemical fingerprinting: streamlining site assessment during the sustainable redevelopment process. In: Sustainable Land Development and Restoration, pp. 325–343. http://dx.doi.org/10.1016/B978-1-85617-797-9.00016-2.
Vaněk, A., Grösslová, Z., Mihaljevič, M., Trubač, J., Ettler, V., Teper, L., Cabala, J., Rohovec, J., Zádorová, T., Penížek, V., Pavlů, L., Holubík, O., Němeček, K., Houška, J., Drábek, O., Ash, C., 2016. Isotopic tracing of thallium contamination in soils affected by emissions from coal-fired power plants. Environ. Sci. Technol. 50, 9864–9871. http://dx.doi.org/10.1021/acs.est.6b01751.
Wcisło, E., Bronder, J., Bubak, A., Rodríguez-Valdés, E., Gallego, J.R., 2016. Human health risk assessment in restoring safe and productive use of abandoned contaminated sites. Environ. Int. 94, 436–448. http://dx.doi.org/10.1016/j.envint.2016.05.028.
Wiseman, C.L.S., Zereini, F., Püttmann, W., 2013. Traffic-related trace element fate and uptake by plants cultivated in roadside soils in Toronto, Canada. Sci. Total Environ. 442, 86–95. http://dx.doi.org/10.1016/j.scitotenv.2012.10.051.
Yutong, Z., Qing, X., Shenggao, L., 2016. Chemical fraction, leachability, and bioaccessibility of heavy metals in contaminated soils, Northeast China. Environ. Sci. Pollut. Res. 23, 24107–24114. http://dx.doi.org/10.1007/s11356-016-7598-9.
Zaharia, C., 2011. Assessing the impact of some industrial and transport activities on soil by the global pollution index. Environ. Eng. Manag. J. 10, 387–391.
Zajusz-Zubek, E., Konieczyński, J., 2003. Dynamics of trace elements release in a coal pyrolysis process. Fuel 82, 1281–1290. http://dx.doi.org/10.1016/S0016-2361(03)00031-0.
Zhiyuan, W., Dengfeng, W., Huiping, Z., Zhiping, Q., 2011. Assessment of soil heavy metal pollution with principal component analysis and geoaccumulation index. Procedia Environ. Sci. 10, 1946–1952. http://dx.doi.org/10.1016/j.proenv.2011.09.305.

II.II Combining raw and compositional data to determine the spatial patterns of Potentially Toxic Elements in soils

---

C. Boente, M.T.D. Albuquerque, A. Fernández-Braña, S. Gerassis, C. Sierra, J.R. Gallego

Science of the Total Environment (2018)

Volume 631-632, August 2018, Pages 1117-1126

Rank: 19 out of 109 (1st Quartile) in *Environmental Chemistry* (JCR)

Science of the Total Environment 631–632 (2018) 1117–1126

Contents lists available at ScienceDirect

Science of the Total Environment

journal homepage: www.elsevier.com/locate/scitotenv

Combining raw and compositional data to determine the spatial patterns of Potentially Toxic Elements in soils

C. Boente [a], M.T.D. Albuquerque [b,c,*], A. Fernández-Braña [a], S. Gerassis [d], C. Sierra [e], J.R. Gallego [a]

[a] INDUROT, Environmental Technology, Biotechnology, and Geochemistry Group, Universidad de Oviedo, Campus de Mieres, 33600 Mieres, Asturias, Spain
[b] Instituto Politécnico de Castelo Branco, 6001-909 Castelo Branco, Portugal
[c] CERENA Research Center, University of Lisbon, Portugal
[d] Department of Natural Resources and Environmental Engineering, Univ. of Vigo, Lagoas Marcosende, 36310 Vigo, Spain
[e] Departamento de Transportes, Tecnología de Procesos y Proyectos, Universidad de Cantabria, Campus de Torrelavega, 39300 Torrelavega, Cantabria, Spain

HIGHLIGHTS

- Raw and compositional data were used to construct hazard maps.
- *Relative enrichment* was introduced as a tool for PTEs' fate interpretation.
- A geostatistical approach was implemented to identify polluted clusters.
- As, Cu, Hg, Pb, and Zn are the principal soil pollutants in the study area.
- The regions of risk overlap the urban, mining, or industrial centers.

GRAPHICAL ABSTRACT

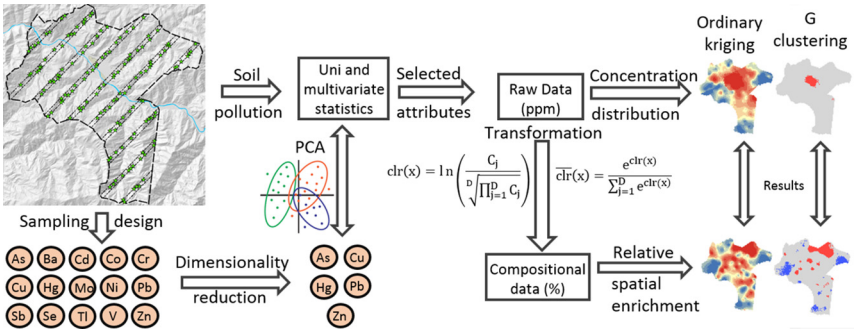

ARTICLE INFO

Article history:
Received 18 December 2017
Received in revised form 1 March 2018
Accepted 5 March 2018
Available online xxxx

Editor: F.M. Tack

Keywords:
Soil pollution
PTEs
Compositional data
Ordinary kriging
Local G-clustering
Relative enrichment

ABSTRACT

When considering complex scenarios involving several attributes, such as in environmental characterization, a clearer picture of reality can be achieved through the dimensional reduction of data.
In this context, maps facilitate the visualization of spatial patterns of contaminant distribution and the identification of enriched areas. A set, of 15 Potentially Toxic Elements (PTEs) – (As, Ba, Cd, Co, Cr, Cu, Hg, Mo, Ni, Pb, Sb, Se, Tl, V, and Zn), was measured in soil, collected in Langreo's municipality (80 km^2), Spain.
Relative enrichment (RE) is introduced here to refer to the proportion of elements present in a given context. Indeed, a novel approach is provided for research into PTE fate. This method involves studying the variability of PTE proportions throughout the study area, thereby allowing the identification of dissemination trends.
Traditional geostatistical approaches commonly use raw data (concentrations) accepting that the elements analyzed make up the entirety of the soil. However, in geochemical studies the analyzed elements are just a fraction of the total soil composition. Therefore, considering compositional data is pivotal. The spatial characterization of PTEs considering raw and compositional data together allowed a broad discussion about, not only the PTEs concentration's distribution but also to reckon possible trends of relative enrichment (RE).
Transformations to open closed data are widely used for this purpose. Spatial patterns have an indubitable interest. In this study, the Centered Log-ratio transformation (*clr*) was used, followed by its back-transformation, to build a set of compositional data that, combined with raw data, allowed to establish the sources of the PTEs and trends of spatial dissemination.

* Corresponding author at: IPCB, Av. Pedro Álvares Cabral, n° 12, 6000-084 Castelo Branco, Portugal.
E-mail address: teresal@ipcb.pt (M.T.D. Albuquerque).

https://doi.org/10.1016/j.scitotenv.2018.03.048

Based on the obtained findings it was possible to conclude that the Langreo area is deeply affected by its industrial and mining legacy. City center is highly enriched in Pb and Hg and As shows enrichment in a northwesterly direction.

1. Introduction

Environmental characterization involves complex scenarios in which several attributes must be considered. A dimensional reduction of data is pivotal to gain a clear picture of reality (Moen and Ale, 1998). Maps are useful to visualize pollutant concentrations, as well as to determine zones of contaminant enrichment, whether natural or caused by anthropogenic activity. Potentially Toxic Elements (PTEs) are increasingly affecting soils all over the world, thus posing a threat to both public health and the environment (McIlwaine et al., 2016). The presence of these elements in soils can be explained by many factors (Alloway, 1990). The growth of urbanization and resulting increase in industrial activities is among the most important (Biasioli et al., 2006). Given that high concentrations of PTEs can endanger human and environmental health, it is of utmost importance to characterize their spatial distribution, determine their source, and screen for enrichment trends (Fayiga and Saha, 2016; Li et al., 2014; Boente et al., 2017; Cachada et al., 2013).

The area of Langreo (Asturias, NW Spain) (Fig. 1) is one of the regions in the Iberian Peninsula most marked by industrialization (Gallego et al., 2016). Coal mining and industries devoted to energy, metallurgy, pharmacology, and fertilizers, among others, have been operating in this region for decades, leaving a lasting imprint on the environment (Martínez et al., 2014; Megido et al., 2017). In this regard, great amounts of PTEs have been identified in soils from former industrial plots in this area (Boente et al., 2016; Gallego et al., 2016).

A comparative study of a set of 15 chemical elements was performed, analyzed in soils gathered in the Langreo area (80 km^2), a paradigmatic industrial area as described above. In this sort of studies, the distribution of PTEs cannot be studied by merely considering the total concentrations (raw data), especially when the concentration of chemical elements in almost all datasets is compositional (Pawlowsky, 1989; Filzmoser et al., 2009a, 2009b), where attributes vary together with all the others. In this context, transformations that open closed data are widely used and, as compositions are recorded along with their spatial locations, spatial patterns are of interest (Pawlowsky, 1989). The contributions of Pawlowsky-Glahn to regionalized compositions (Pawlowsky, 1989; Pawlowsky and Burger, 1992; Pawlowsky et al., 1995) and their applications are widely applied (Odeh et al., 2003; Lark and Bishop, 2007) and also in environmental sciences (Olea et al., 2017). In this sense, multiple log-ratio transformations are commonly used, the most common being the additive log-ratio transformation (alr), the centered log-ratio transformation (clr) (e.g. Aitchison, 1986), and the isometric log-ratio transformation (ilr) (Egozcue et al., 2003). This compositional dataset was used to map patterns of RE, thereby allowing to identify spatial dissemination trends for PTEs.

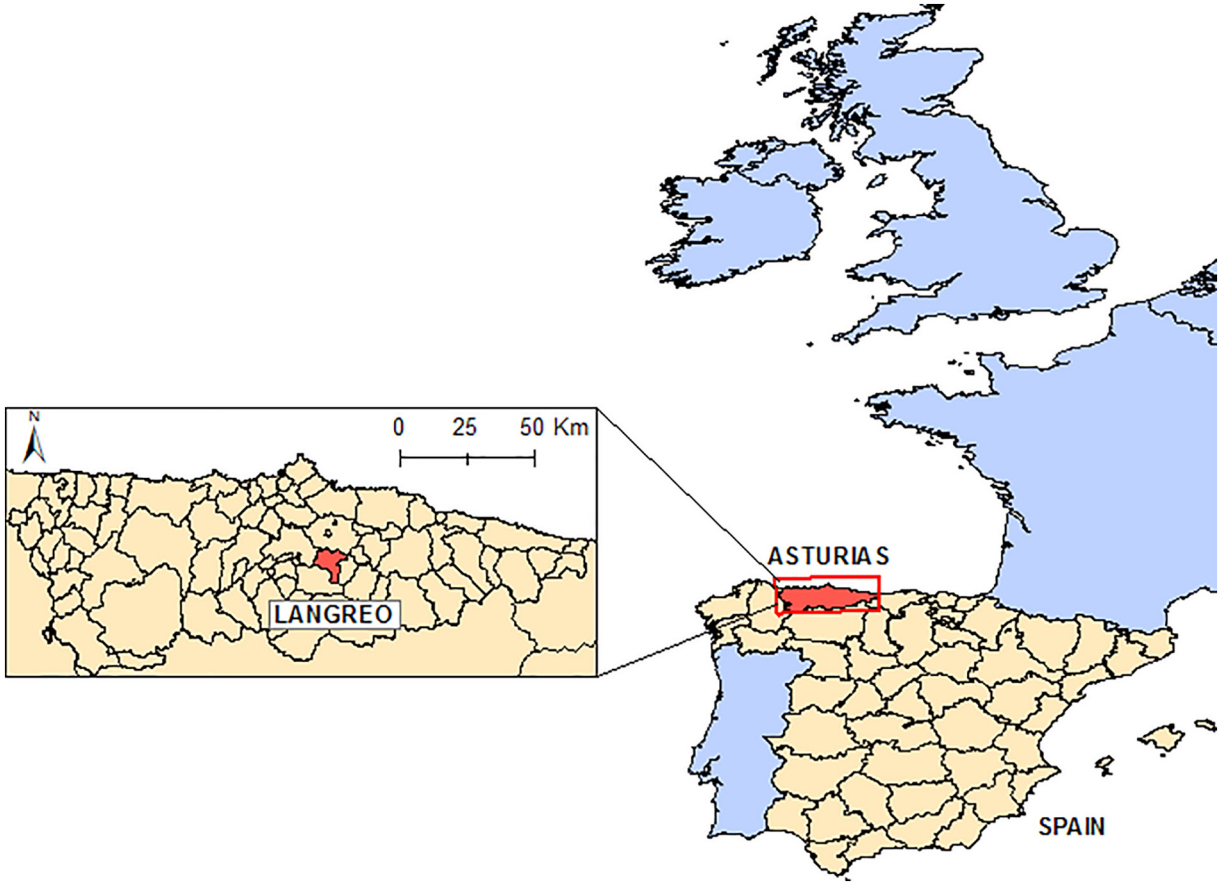

Fig. 1. Location of the study area in the municipality of Langreo in Asturias, Spain.

In summary, the main goal of this study was to test a methodology that, by means of combining raw and compositional data, has the capacity to identify spatial patterns, areas of pollution risk and anthropogenic or natural sources of PTEs. All the evidence provided is supported by uni- and multivariate statistical analysis, together with ordinary kriging and Local G clustering for the area of Langreo. Finally, core strengths and weaknesses are extrapolated to make this methodology useful and applicable to studies of a similar nature.

2. Materials and methods

2.1. Study area

Covering 80 km^2, the municipality of Langreo (Asturias, NW Spain, Fig. 1) has a history of mining and industrial activity that dates back to the 1850s (Martínez et al., 2014). This activity left behind a legacy of polluted sites, making this zone one of the most contaminated areas in northern Spain (Gallego et al., 2016) and thus an ideal site in which to test the method presented in this study.

The region lies along the Nalón River, which is the longest and the most voluminous in Asturias. Altitudes in the area vary from 200 m (location of the urban areas and industry) to 900 m (rural environments, forests), with the presence of steep mountains. This geography gives rise to an enclosed area that facilitates the accumulation of PTEs by atmospheric deposition.

2.2. Data collection and chemical analyses

Samples were collected using a stratified systematic sampling method at random distances to obtain a representative set of data on the total variability of PTE content and site diversity (natural or anthropic environments, geomorphology, land uses, etc.). To this end, 10 equidistant transects, 250 m wide and each one 1000 m apart, were distributed perpendicular to the Nalón River (Fig. 2). A total of 150 samples were collected, the number *per* transect being determined proportionally to its length. The sample location within each transect was selected at random (Fig. 2).

Each sample composed of five increases taken from each vertex of a 1-m edge square and its central point from the top 20–25 cm of the soil, using an Edelman Auger. Afterwards, samples were passed through a 2-cm mesh screen in situ to remove large material such as organic matter, rocks, and gravel. The samples were then dried in an oven at 35 °C to prevent the evaporation of volatile compounds and finally quartered by means of a Jones riffle splitter for soil homogenization and representativeness.

These fractions were ground in an RS100 Resch mill at 400 RPM for 40 s. Then, 1-g representative sub-samples were sent to the ISO-9002 and ISO-17025 accredited Bureau Veritas Laboratories (Vancouver, Canada) and subjected to 1:1:1 (HCl:HNO_3:H_2O) "aqua regia" digestion. The total concentrations of the elements were determined by Inductively Coupled Plasma-Mass Spectrometry (ICP-MS) by means of the Ultratrace AQ250 analytical package of

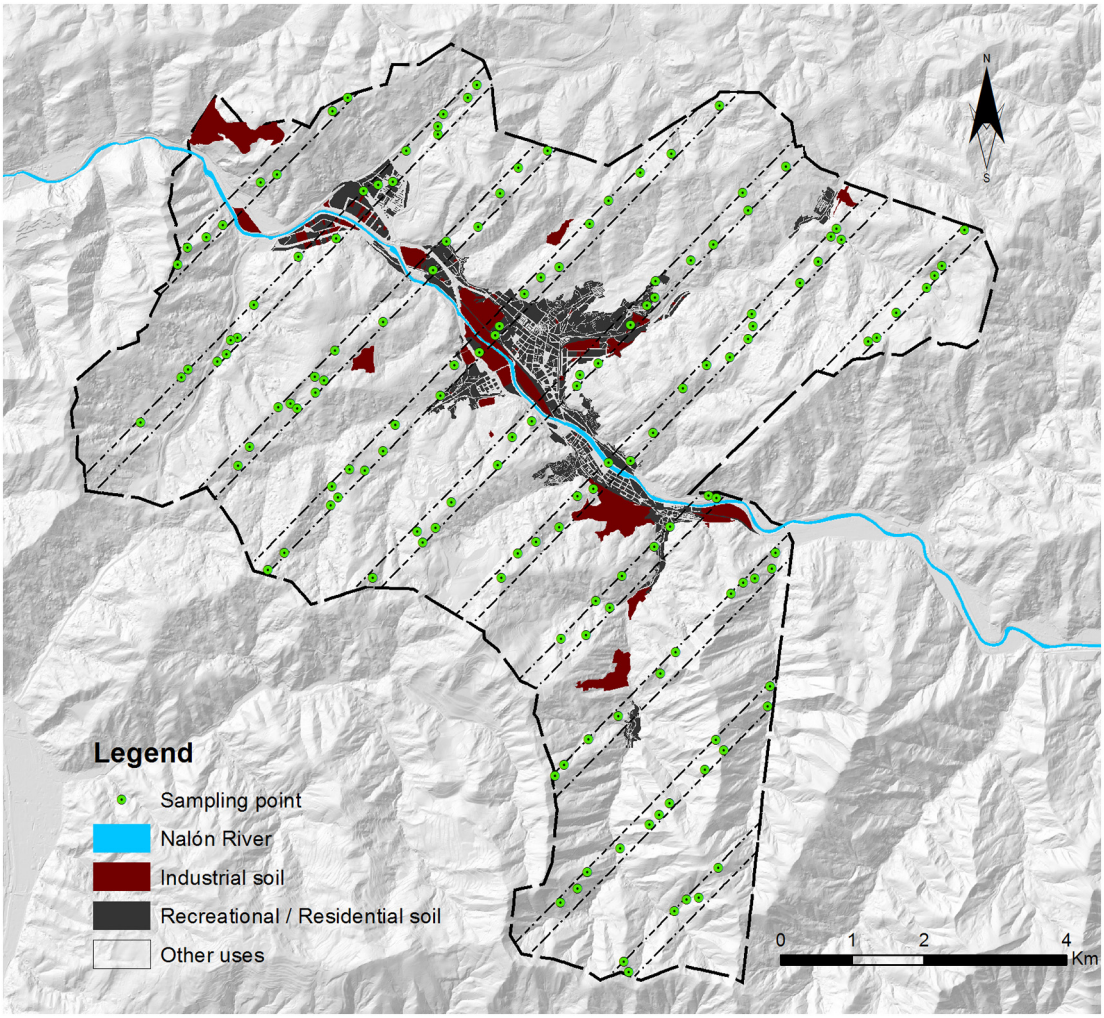

Fig. 2. Sampling design and land use categories in the study area.

Table 1
Descriptive statistics for 15 PTEs: Range, Mean, Median, Standard Deviation (SD), and Trimmed Mean (T.Mean 5%) are expressed in mg·kg^{-1}, Relative Standard Deviation (RSD) is expressed in %.*clr-log-ratio transform function. The geometric mean is used as the normalizer parameter.

PTE	Raw data						*Clr-transformed data				
	Range	Mean	Median	SD	RSD	T.Mean 5%	Mean	Median	SD	RSD	T.Mean 5%
As	6.4–91.1	21.8	18.5	10.9	49.8	21.0	21.9	20.9	6.3	28.9	21.7
Ba	11.0–1747.1	107.9	66.9	168.7	156.3	90.2	79.2	74.6	16.7	21.1	78.3
Cd	0.02–26.9	0.6	0.3	2.2	382.6	0.4	0.4	0.3	0.1	19.2	0.3
Co	1.1–34.0	10.0	9.8	5.0	49.8	9.9	9.4	10.2	11.4	121.7	9.4
Cr (III)	5.7–69.0	18.9	18.6	6.7	35.6	18.5	19.6	20.1	4.8	24.5	19.6
Cu	3.0–2022.2	39.0	22.7	163.6	419.2	24.6	24.4	24.2	7.3	29.7	24.1
Hg	0.1–2.6	0.4	0.3	0.4	95.5	0.4	0.3	0.3	0.1	21.3	0.3
Mo	0.4–4.6	1.0	0.9	0.6	53.6	1.0	1.0	1.0	0.2	16.0	1.0
Ni	1.4–52.8	18.3	16.5	9.1	49.7	18.0	17.5	17.5	7.2	41.1	17.5
Pb	10.5–3729.5	91.6	52.2	302.7	330.6	64.0	62.8	60.7	11.1	17.7	61.8
Sb	0.3–256.6	2.5	0.6	20.8	821.8	0.8	0.8	0.7	0.2	26.6	0.8
Se	0.1–1.9	0.9	0.8	0.4	45.1	0.8	0.8	0.9	0.3	30.3	0.8
Tl	0.0–0.5	0.2	0.2	0.1	33.8	0.2	0.2	0.2	0.0	10.6	0.2
V	7.0–56.0	27.9	27.0	6.9	24.8	27.8	29.6	29.8	6.3	21.2	29.8
Zn	16.9–2161.0	136.2	107.2	179.4	131.7	120.8	119.8	120.8	11.8	9.9	120.1

the above-mentioned laboratory, the PTEs studied in this work were determined with the following Detection Limits (ppm): As (0.1), Ba (0.5), Cd (0.01), Co (0.1), Cr (0.5), Cu (0.01), Hg (0.005), Mo (0.01), Ni (0.1), Pb (0.01), Sb (0.02), Se (0.1), Tl (0.02), V (2), Zn (0.01). Samples submitted were analyzed with the strictest quality control. Five blanks (analytical and method), five duplicates and ten analyses of standard reference materials (internal standards and OREAS45EA) were inserted in the sequences of samples providing a measure of background noise, accuracy, and precision.

A subset of the analyzed elements corresponding to PTEs was used for this study. This subset was chosen because it represented a set of typical contaminants (heavy metal(loid)s) found in environmental studies in Asturias (Albuquerque et al., 2017; Boente et al., 2016; Gallego et al., 2015), in addition the Risk-Based Soil Screening Levels (RBSSLs) for these contaminants are available for this region of Spain (BOPA, 2014). Furthermore, the dispersal of the concentrations of these contaminants never exceeded three orders of magnitude and thus provided readable proportions. Therefore, of the original list of 36 elements, the following 15 were examined (PTE group): As, Ba, Cd, Co, Cr, Cu, Hg, Mo, Ni, Pb, Sb, Se, Tl, V, and Zn.

2.3. Data transformation – compositional data and the closure problem

In geochemistry, compositional data is obtained by transforming each original raw concentration (i.e. mg/kg of an element in a sample) into proportions of a whole whose elements sum one or 100% (Pawlowsky-Glahn and Egozcue, 2006). However, the unfeasibility of analyzing all the elements in a given soil hinders the consideration of proportions. Indeed, this issue has been heavily debated and is referred to by researchers as the closure problem (Filzmoser et al., 2009b). In environmental science studies, it is generally accepted that the elements analyzed make up the entirety of the soil on the condition that a suitable

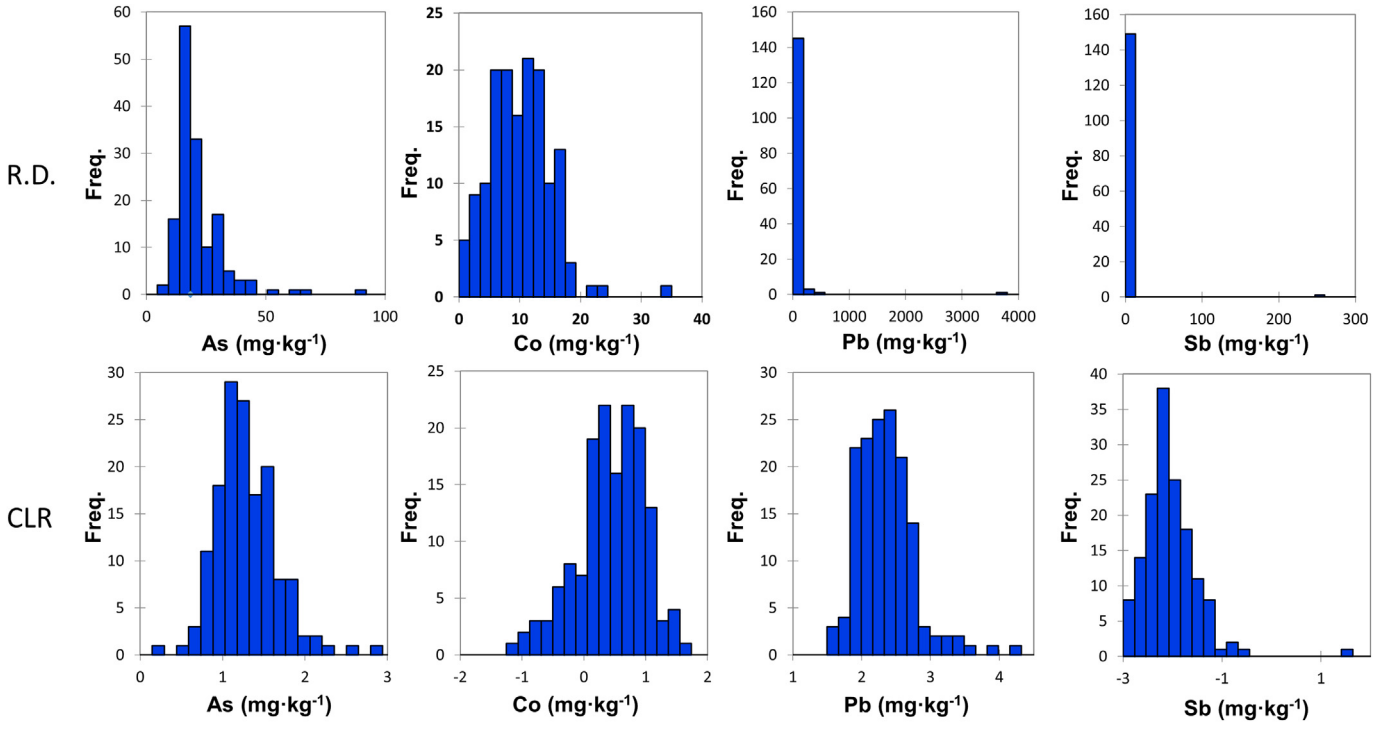

Fig. 3. As, Co, Pb and Sb histograms for raw data (R.D.) and *clr*-transformed data (CLR).

number of such elements is included in the study (Campbell et al., 2009; Reimann et al., 2012). Moreover, other authors work with subcompositions, defined as a subset of components of parts of a composition (Mateu-Figueras and Pawlowsky-Glahn, 2008; Pawlowsky-Glahn and Buccianti, 2011). Subcompositions are feasible when they respect the principles of compositional data (Greenacre and Lewi, 2009), including the sub-compositional coherence principle (Aitchison, 1986).

The most frequently used log-ratio transform functions (*alr*; *clr* and *ilr*) have both advantages and disadvantages, which are widely discussed in the literature. The *clr* transformation is the prevailing function in geochemical studies as it uses the geometric mean as normalizer parameter and it was chosen for the purposes of the present study (Pawlowsky, 1989; Pawlowsky and Burger, 1992; Pawlowsky et al., 1995).

The centered log-ratio transformation (*clr*) equation was adapted from (Aitchison, 1986):

$$clr(x) = \ln\left(\frac{C_j}{\sqrt[D]{\prod_{j=1}^{D} C_j}}\right) \quad (1)$$

where C_j is the concentration of pollutant j and D is the number of parts into which the composition is divided (in this case, the number of pollutants considered).

The back-transformation equation is computed as:

$$\overline{clr}(x) = \frac{e^{clr(x)}}{\sum_{j=1}^{D} e^{clr(x)}} \quad (2)$$

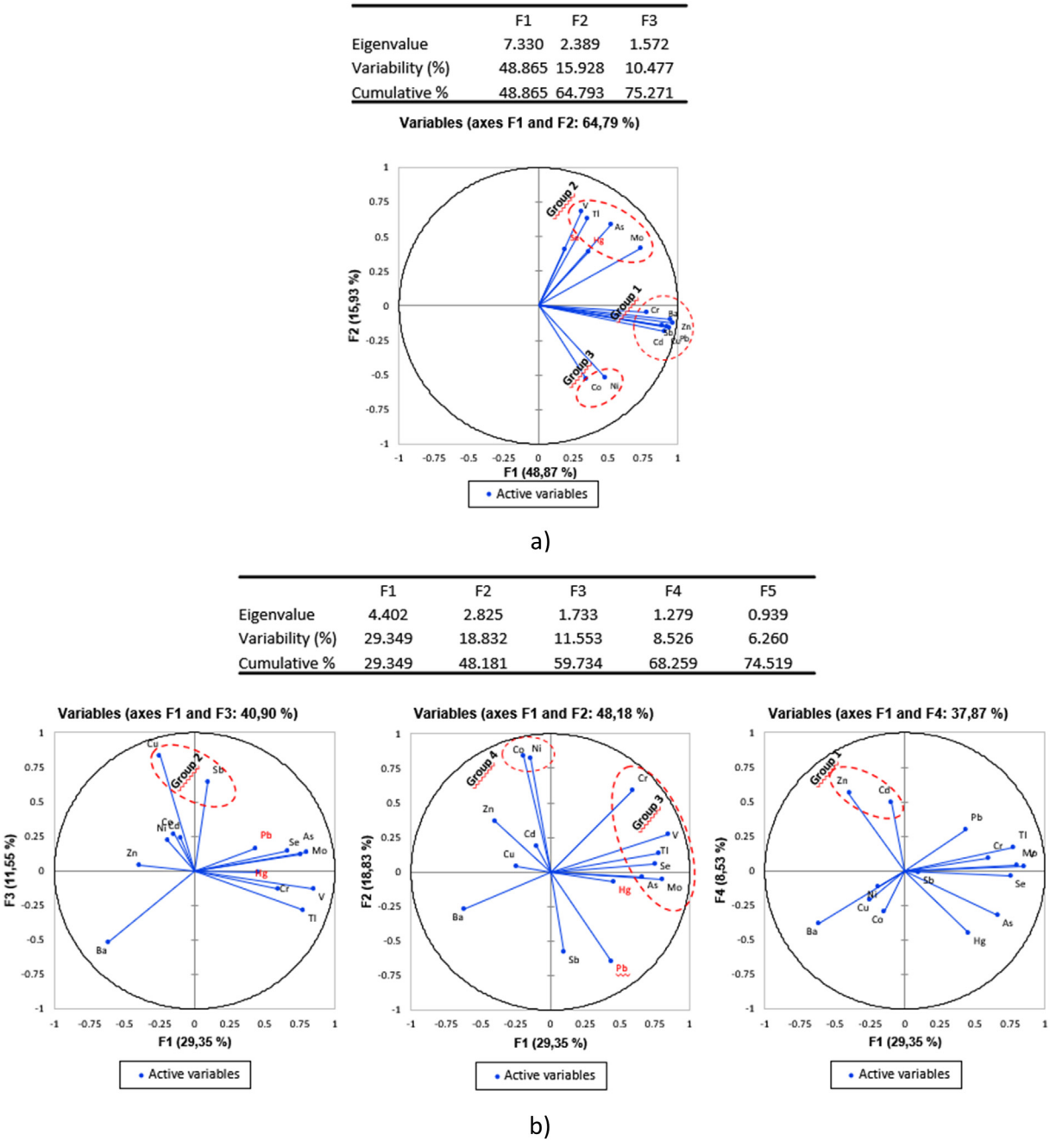

Fig. 4. a) PCA - Raw dataset; b) PCA - Compositional data.

where *e* represents the inverse function of the Napierian logarithm. This equation allows representation of the *clr*-transformed data as compositional data (proportions). This means that the sum of all the elements after back-transformation is equal to 1. The *clr* transformation and the calculation of its back-transformation were performed using CoDaPack v2.02.21 software.

2.4. Spatial modeling

The spatial characterization of PTE distribution was performed with the following two complementary objectives in mind. First, to define spatial clusters of PTE concentration. To accomplish this, the raw dataset was used, allowing to interpret contamination outbreaks and therefore locate the main sources of PTEs. Second, to define Relative Enrichment (RE) spots and thus, evaluate trends of enrichment. Indeed, rather than catch solely the PTEs content's enrichment, it was possible to approach the study of PTE's fate, by examining the changes in their proportions throughout the study area and therefore. The compositional dataset was used to tackle this issue, and spatial clusters of RE were computed.

A four-step methodology was adopted as follows:

- Principal Components Analysis (PCA) for reducing dimensionality and for evaluating variable association was performed. PCA is one of the most important multivariate statistical methods and it is widely used for data preprocessing and dimension reduction (raw and compositional data). The aim of PCA is to reduce the dimensionality of data while simultaneously preserving the within variability structure (variance-covariance) (e.g. Zuo et al., 2016). The analysis starts with *p* random attributes $X_1, X_2, \ldots, X_p$, where no assumption of multivariate normality is required. The axes of the constant ellipsoids correspond to the new synthesis variables, the principal components. The XlStat 2013.1.01 (XlStat software v. 2013.1.01, 2013) software was used for computational purposes.
- Selected attributes were subjected to a structural analysis, and experimental variograms were computed for both raw and compositional data. The variogram is a vector function used to calculate the spatial variation structure of regionalized variables (Matheron, 1963; Journel and Huijbregts, 1978; Gringarten and Deutsch, 2001), in accordance with the following equation:

$$\gamma(h) = \frac{1}{2N(h)} \sum_{2N(h)}^{N(h)} [Z(x_i) - Z(x_i + h)]^2 \quad (3)$$

Its argument is *h* (distance), where $Z(x_i)$ and $Z(x_i + h)$ are the numerical values of the observed variable at point x_i, and $x_i + h$. The number of pairs forming for an *h* distance is $N(h)$. Thus, it is the median value of the square of the differences between all pairs of points in the geometric field spaced at an *h* distance. The graphics of the obtained variograms provide an overview of the spatial structure of the variable. One of the parameters that provide such information is the nugget effect (C_o), which shows the behavior at the origin. The other two parameters are the sill (C_1) and the amplitude (A) which define the inertia used in the interpolation process and the influence radius of the variable, respectively.

- Spatial prediction through Ordinary Kriging (OK), aiming to predict the values for the variables at any arbitrary spatial location within the study region, was performed. The raw dataset was used to infer the concentration and PTE origin, as the compositional dataset was used for dissemination trend detection and local RE evaluation. Of note, geostatistics is a reference approach for the characterization of environmental hazards in contexts in which the information available is scarce. The primary application of geostatistics is to estimate and map environmental attributes in unsampled areas where Kriging is a generic name for a set of generalized least-squares regression algorithms. Ordinary Kriging (OK) accounts for local fluctuations of the mean by limiting the field of stationary of the mean to the local neighborhood (Goovaerts, 1997). For the computation, the SpaceStat Software V. 4.0.18, Biomedware (Biomedware: SpaceStat V. 4.0-.18. software, 2014) was used (Antunes and Albuquerque, 2013) (Fig. 6).
- Finally, Local G clustering was performed. This technique allows measurement of the degree of association that results from the concentration of weighted points (or region represented by a weighted point) and all other weighted points included within a radius of distance from the original and defining clusters of high (high-ring) and low (low-ring) significance. For computation, the Biomedware's SpaceStat V. 4.0–.18. software was used.

3. Results and discussion

3.1. Descriptive statistics

Descriptive statistics for raw and *clr*-transformed data were computed (Table 1). The raw data revealed considerable variability for some elements, which was of concern for As, Cd, Cu, Pb, Sb and Zn, whose maximum values surpassed the RBSSLs (BOPA, 2014). The 5% trimmed mean allowed to conclude that extreme values were concentrated mainly in the upper 2.5% intervals, as the remaining 97.5% can be approximated by the normal distribution. Once the *clr*-transformed data were applied, the associated standard deviation was clearly reduced and the mean, median and 5% trimmed mean tended to be similar. Indeed, the *clr* data showed a normal distribution as a result of diminishing the weight of outliers. This diminished weight enhanced the prediction of data proportions after the back-transformation of *clr* data, and compositional data were obtained.

On the basis of comparison of the histograms (Fig. 3) of the raw and compositional datasets, it is possible to reason that: a) when considering the raw dataset, asymmetric distributions are found for almost all the PTEs, and these distributions are biased mainly by the presence of outliers; b) the *clr*-transformed dataset shows an important feature as it allows the assumption of normality. Therefore, it was possible to conclude that the *clr*-transformed dataset and the compositional dataset (after *clr* back-transform) have two principal advantages, namely, they allow work with proportions and at the same time, improves data normalization.

Of note were the anomalous As, Cd, Cu, Pb, Sb and Zn concentrations, which greatly exceeded the RBSSLs (BOPA, 2014) (Table 1). These

Table 2
Experimental variogram parameters for the raw and compositional datasets: *A* (m) is the amplitude; C_0 represents the value of the nugget effect; C_1 and C_2, the value of the sill of the first and the second spherical structure respectively, and C_0(%Var) and $C_1 + C_2$ (% Var) the mutual variances weighing for nugget and sill respectively.

	Parameters	As	Cu	Hg	Pb	Zn
Raw data	A	2738	2575	1997	1376	1327
	C_0	0.356	0.664	0.401	0.488	0.330
	C_1	0.465	0.256	0.411	0.201	0.544
	C_2	0.260	0.110	1.17	0.339	0.172
	C_0 (%Var)	33	64	20	47	32
	$C_1 + C_2$ (%Var)	67	36	80	53	68
Comp. data	A	2700	2569	4758	2808	3903
	C_0	$2.77 \cdot 10^{-4}$	$1.63 \cdot 10^{-4}$	$5.93 \cdot 10^{-7}$	$9.90 \cdot 10^{-4}$	$1.47 \cdot 10^{-3}$
	C_1	$6.45 \cdot 10^{-4}$	$4.83 \cdot 10^{-4}$	$3.50 \cdot 10^{-7}$	$3.52 \cdot 10^{-3}$	$1.58 \cdot 10^{-3}$
	C_2	$1.14 \cdot 10^{-4}$	$8.11 \cdot 10^{-5}$	$6.90 \cdot 10^{-7}$	$5.35 \cdot 10^{-4}$	$4.18 \cdot 10^{-4}$
	C_0 (%Var)	27	22	36	20	42
	$C_1 + C_2$ (%Var)	73	78	64	80	58

elements are classic fingerprints of heavy industrial activity. However, the presence of Ba, Co, Cr, Hg, Mo, Ni, Se, Tl and V did not constitute an immediate risk to human health or the environment.

3.2. Multivariate statistics – principal components analysis

When running the raw dataset, PCA results revealed three groups (Fig. 4a): a) the first formed by Ba, Cd, Cr, Cu, Pb, Sb and Zn—a typical association of heavy metals; b) the second composed by As, Mo, Tl and V; and c) the third representing Co and Ni. Finally, Hg and Se showed independent behaviors, thereby possibly indicating different sources. On the other hand, when considering the compositional dataset, slight differences in the results were observed (Fig. 4b). The first-mentioned group (Ba, Cd, Cr, Cu, Pb, Sb and Zn) was split in two: a) the first comprising Cd and Zn; b) the second Cu and Sb. Furthermore, two more groups were identified, c) the third comprising As, V, Tl, Mo, Se and Cr; and d) the fourth Ni and Co. Mercury (Hg) and Pb were found to be independent. The PCA's results lead to conclude that the compositional dataset provides a fuller recognition of relevant contaminant associations. When setting a dependence on weight between elements, those which increase or decrease proportionally tend to be associated.

3.3. Spatial modeling – geostatistical approach

At this point, As, Cu, Hg, Pb, and Zn were chosen for spatial modeling purposes as they are core PTEs in contamination forecasts and representative of the most important groups identified (Fig. 4).

The spatial stochastic patterns of the five chosen PTEs were constructed following a three-step geostatistical modeling method.

3.3.1. Structural analysis and experimental variograms

The experimental variograms $\gamma_{(h)}$ (Table 2) were fitted to a theoretical model, $\hat{\gamma}_{(h)}$ (Isaaks and Srivastava, 1989). The adjusted parameters for the five PTEs of the theoretical variograms (raw and compositional datasets) (Fig. 5) allowed to observe that the isotropic variograms obtained generally showed a better fit for the compositional dataset. Indeed, the attributes showed a nugget effect below 40% of the total

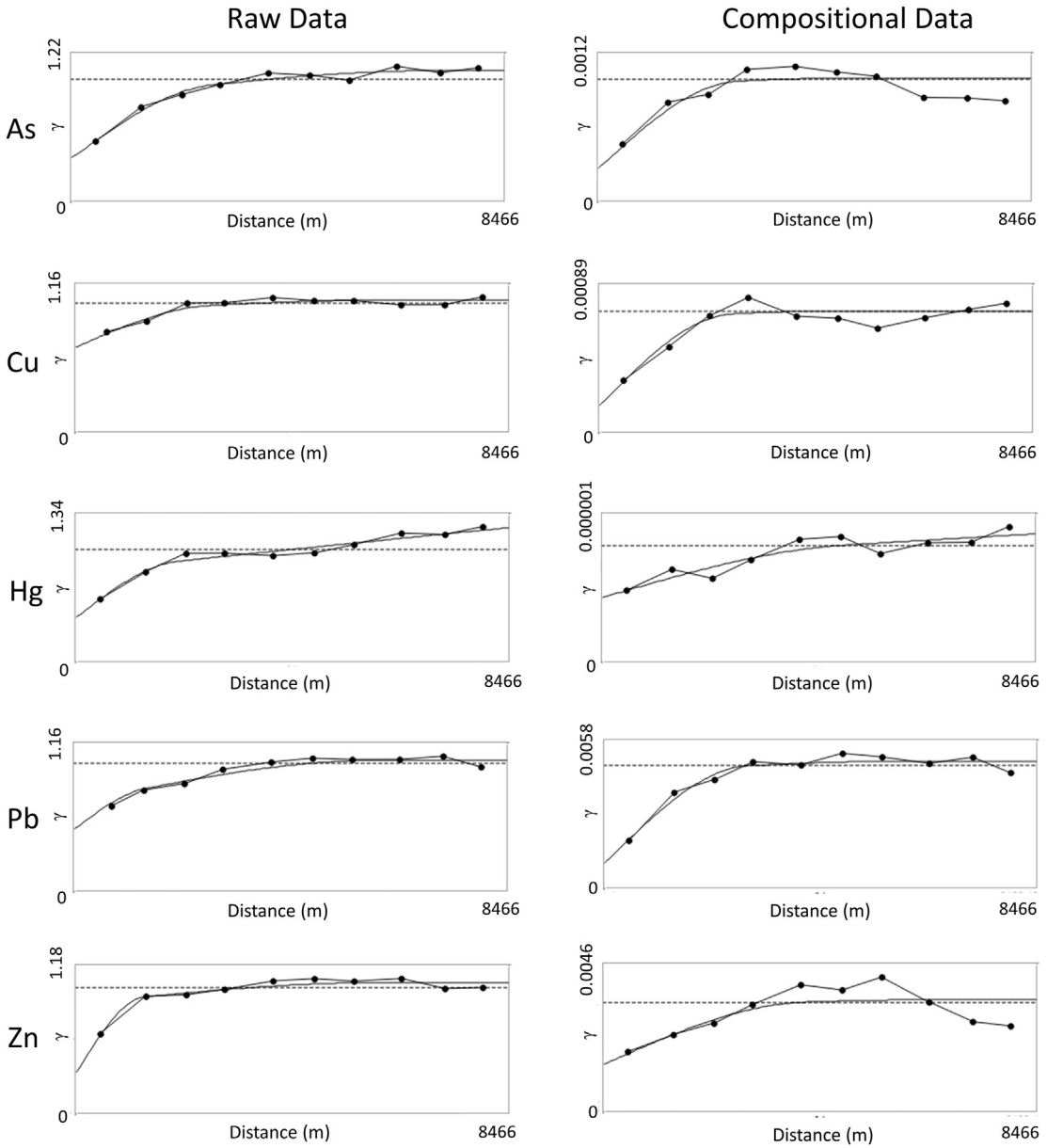

Fig. 5. Isotropic experimental variograms and fitted models for the raw and compositional datasets.

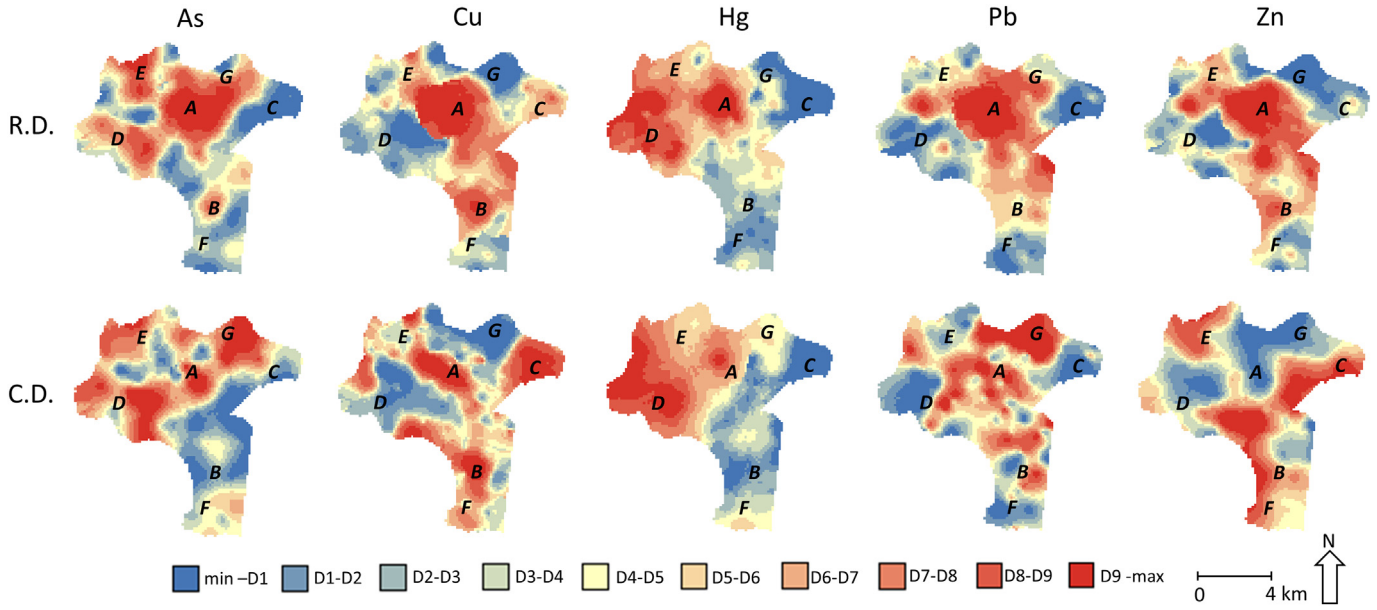

Fig. 6. Ordinary Kriging (OK) results. Raw data (R.D.) and compositional data (C.D.) respectively. The scale is expressed in deciles (D_i) of $mg \cdot kg^{-1}$ (R.D.) and of % (C.D.).

variance of all the attributes (Table 2). The error associated with the interpolation procedure (OK), is therefore minimized when using the compositional dataset.

3.3.2. Spatial prediction: ordinary kriging

Analysis of the outputs obtained revealed evident contrasts between the raw and the compositional dataset representations. Care must be taken when interpreting representations as they reflect distinct data. In this regard, the raw dataset mapping shows the estimated picture of PTE concentration distribution, thus indicating possible sources of these contaminants. In contrast, the compositional dataset mapping shows the spatial variability of PTE proportion, thus reflecting PTE's Relative Enrichment, and providing crucial information about the fate of these compounds within the study area. To facilitate the understanding of the results, the study area was divided into various zones of interest and interpreted as follows:

a) Considering the maps of the raw dataset (Fig. 6 - R.D.), high concentrations for all PTEs (Zn, Hg, As, Pb and Cu) in the central zone (zone *A-mainly urban/industrial land use*) can be observed, which coincides with the city of Langreo (Fig. 6). Moreover, Cu and Zn showed notable presence in the southern area (zone *B-mainly industrial land use*), where the mining industry (coal mines and processing) were located (Fig. 1). The Cu map shows a north-eastern red-colored site (zone *C-several land use*) coinciding with a former coal-mining area. On the other hand, high concentrations of Hg and As were observed in the western (zone *D-mainly rural use*) and northern (zone *E-mainly urban land use*) areas, which may be explained by the proximity to a derelict Hg mine (El Terronal site) whose impact has been widely discussed (e.g. Gallego et al., 2015; González-Fernández et al., 2018);
b) Concerning the compositional dataset (Fig. 6 - C.D.), Relative Enrichment in Cu, Pb and Zn were identified towards the south (zone *F-*

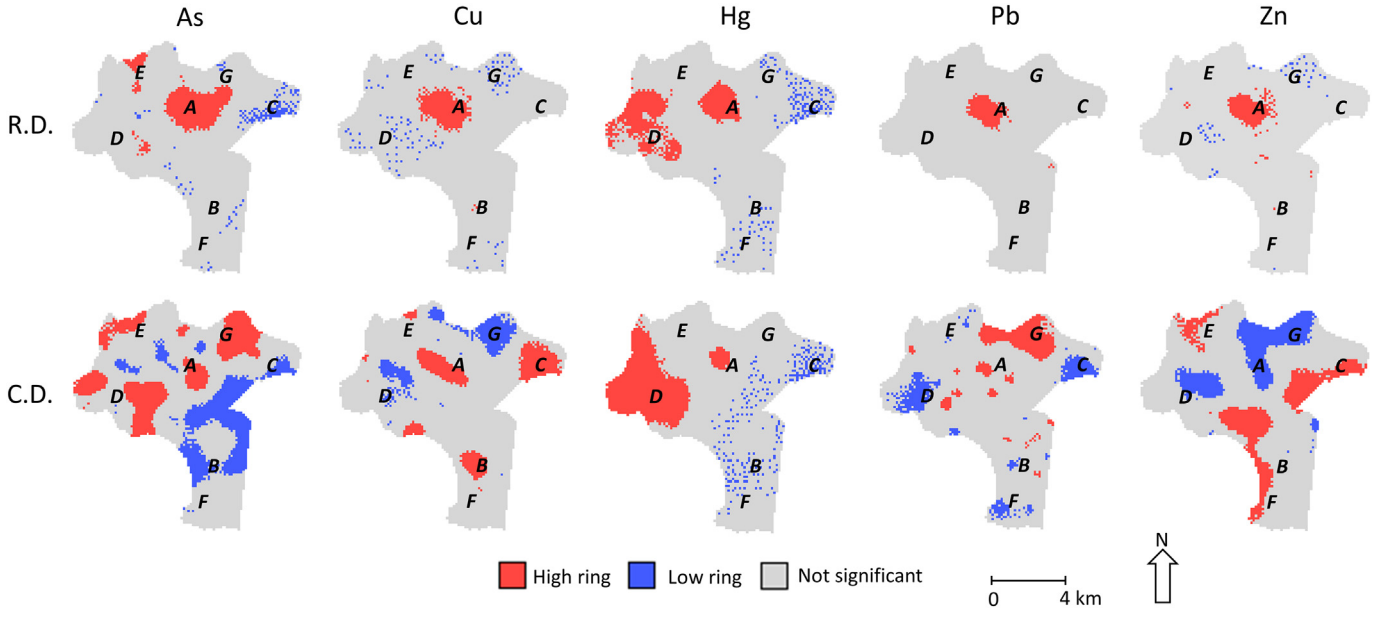

Fig. 7. Local G clusters. Raw data (R.D.) and compositional data (C.D.) respectively.

mainly rural use) and northeast (zone *G-mainly rural use*) of the area (Fig. 6), where the corresponding distribution was at its lowest level when using the raw data. Cu, Pb, and Zn showed a significant distribution throughout the area and therefore a marked RE.

3.3.3. Spatial prediction: local G clustering

To reinforce the findings of the previous section, a local G clustering was conducted to assess the level of association resulting from the concentration of weighted points (or region represented by a weighted point) and all other weighted points included within a radius from the original point. In this regard, a given zone was subdivided into n regions, $I = 1, 2, \ldots, n$, where each neighborhood is distinguished by a point whose Cartesian coordinates are known. Each i has a value x (a weight) taken from a variable X associated with it. The variable holds a natural origin and it is positive. The $G(i)$ statistic developed below allows the testing of hypotheses concerning the spatial concentration of the sum of x values associated with the j points within d of the ith point. The following statistic is obtained:

$$G_i(d) = \frac{\sum_{j=1}^{n} W_{ij}(d) X_i}{\sum_j^n x_j} \quad (4)$$

where W_{ij} is a symmetric one/zero spatial weight matrix with a value of 1 for all links defined as being within distance d of a given i; all other links are zero, including the link of point i to itself. The numerator is the sum of all x_j within d of i but not including x_i. The denominator is the sum of all x_j, excluding x_i (Getis and Ord, 1992).

The maps obtained (Fig. 7) provide a faster and more intuitive way to verify whether the problematic zones detected previously are indeed of concern. Thus, red areas (high ring) show the sites with the greatest accumulation of the PTEs, while the blue areas (low ring) represent zones with low accumulation (Fig. 7). The highest accumulation of PTEs, when considering the raw data clusters, was in the city center (high ring-zone A). The soils in this area were clearly affected by PTE deposition, presumably due to heavy industry and/or the transport of pollutants. However, examination of the significance of the spatial clusters obtained using the compositional data shows several differences. The central high ring (high significance) is now smaller, showing that the areas with the highest concentration of these PTEs (Zn, Hg, As, Pb and Cu) do not totally overlap with the corresponding higher proportions and indicating that PTE transport and RE occurs in a westerly and southerly direction.

4. Conclusions

The degree of PTE contamination in the soil of an industrial area can be characterized using two datasets, namely raw and compositional (*clr*-transformed followed by the back-transformation function). To exemplify the complementary attributes of these two types of dataset, 150 soil samples were collected, and 36 elements were analyzed in Langreo (80 km^2), a paradigmatic example of an industrial area affected by heavy metal and metalloid contamination. Univariate statistics allowed recognition of redundant information and the identification of outliers. The space of analysis was then reduced for both datasets by building the synthesis variables held by PCA. Five PTEs, namely Zn, Hg, As, Pb and Cu, were retained for spatial modeling due to their significance in the contamination forecast. Ordinary Kriging (OK) and Local G clustering allowed the construction of hazard maps, which facilitate the evaluation of the probable origin of PTEs (raw data) and their possible Relative Enrichment (compositional data).

The combination of raw and compositional data puts together PTEs concentration and respective proportions. This allows emphasizing not only the concentration's spatial distribution but also the relative enrichment trends, facts that would not be possible when using the traditional geostatistical approach that commonly uses solely raw data. This methodology facilitates the recognition and quantification of anthropogenic impacts and consequent implementation of adequate monitoring measures to environmental safeguard and feasible remediation solutions.

Regarding the Langreo area, it is extensively affected by its industrial and mining history. The following observations support this conclusion: 1. The city center is highly enriched in PTEs, which can be explained by heavy industry and pollutant transport, Pb being the main contaminant; 2. The spatial distribution of Cu indicates a strong association with coal mining and processing; and 3. Hg and As show enrichment in a northwesterly direction, which is linked to natural mineralization and former Hg mining and metallurgy. Future work would require an exhaustive study of covariates to shed light on PTE dynamics and to clarify the main sources of PTEs, as well as their RE throughout the study area.

The information gathered provides a basis for delimiting the polluted zones and the sources of pollutants, thus facilitating the development of specific air and soil monitoring activities, urban planning, and environmental policies.

Acknowledgements

C. Boente obtained a grant from the "Formación del Profesorado Universitario" program, financed by the "Ministerio de Educación, Cultura y Deporte de España" (FPU14/02215).

M.T.D Albuquerque acknowledges a scholarship 567 SFRH/BSAB/127907/2016 from the Foundation for Science and Technology (Portugal).

References

Aitchison, J., 1986. The statistical analysis of compositional data. J. R. Stat. Soc. 44: 139–177. https://doi.org/10.1007/978-94-009-4109-0.

Albuquerque, M.T.D., Gerassis, S., Sierra, C., Taboada, J., Martín, J.E., Antunes, I.M.H.R., Gallego, J.R., 2017. Developing a new Bayesian Risk Index for risk evaluation of soil contamination. Sci. Total Environ. 603–604:167–177. https://doi.org/10.1016/j.scitotenv.2017.06.068.

Alloway, B.J., 1990. The origins of heavy metals in soils. Heavy Metals in Soils, p. 339.

Antunes, I.M.H.R., Albuquerque, M.T.D., 2013. Using indicator kriging for the evaluation of arsenic potential contamination in an abandoned mining area (Portugal). Sci. Total Environ. 442:545–552. https://doi.org/10.1016/j.scitotenv.2012.10.010.

Biasioli, M., Barberis, R., Ajmone-Marsan, F., 2006. The influence of a large city on some soil properties and metals content. Sci. Total Environ. 356:154–164. https://doi.org/10.1016/j.scitotenv.2005.04.033.

Biomedware: SpaceStat V. 4.0-.18. software, 2014. https://www.biomedware.com/, Accessed date: 17 August 2017.

Boente, C., Sierra, C., Rodríguez-Valdés, E., Menéndez-Aguado, J.M., Gallego, J.R., 2016. Soil washing optimization by means of attributive analysis: case study for the removal of potentially toxic elements from soil contaminated with pyrite ash. J. Clean. Prod. https://doi.org/10.1016/j.jclepro.2016.11.007.

Boente, C., Matanzas, N., García-González, N., Rodríguez-Valdés, E., Gallego, J.R., 2017. Trace elements of concern affecting urban agriculture in industrialized areas: a multivariate approach. Chemosphere 183:546–556. https://doi.org/10.1016/j.chemosphere.2017.05.129.

BOPA, Boletín Oficial del Principado de Asturias, April 21, 2014. Generic Reference Levels for Heavy Metals in Soils From the Principality of Asturias, Spain. https://sede.asturias.es/portal/site/Asturias/menuitem.1003733838db7342ebc4e191100000f7/?vgnextoid=d7d79d16b61ee010VgnVCM1000000100007fRCRD&fecha=21/04/2014&refArticulo=2014-06617&i18n.http.lang=es, Accessed date: 15 December 2017.

Cachada, A., Dias, A.C., Pato, P., Mieiro, C., Rocha-Santos, T., Pereira, M.E., Da Silva, E.F., Duarte, A.C., 2013. Major inputs and mobility of potentially toxic elements contamination in urban areas. Environ. Monit. Assess. 185:279–294. https://doi.org/10.1007/s10661-012-2553-9.

Campbell, G.P., Curran, J.M., Miskelly, G.M., Coulson, S., Yaxley, G.M., Grunsky, E.C., Cox, S.C., 2009. Compositional data analysis for elemental data in forensic science. Forensic Sci. Int. 188:81–90. https://doi.org/10.1016/j.forsciint.2009.03.018.

Egozcue, J.J., Pawlowsky-Glahn, V., Mateu-Figueras, G., Barceló-Vidal, C., 2003. Isometric logratio transformations for compositional data analysis. Math. Geol. 35:279–300. https://doi.org/10.1023/A:1023818214614.

Fayiga, A.O., Saha, U.K., 2016. Soil pollution at outdoor shooting ranges: health effects, bioavailability and best management practices. Environ. Pollut. 216:135–145. https://doi.org/10.1016/j.envpol.2016.05.062.

Filzmoser, P., Hron, K., Reimann, C., 2009a. Principal component analysis for compositional data with outliers. Environmetrics:621–632 https://doi.org/10.1002/env.966.

Filzmoser, P., Hron, K., Reimann, C., 2009b. Univariate statistical analysis of environmental (compositional) data: problems and possibilities. Sci. Total Environ. 407:6100–6108. https://doi.org/10.1016/j.scitotenv.2009.08.008.

Gallego, J.R., Esquinas, N., Rodríguez-Valdés, E., Menéndez-Aguado, J.M., Sierra, C., 2015. Comprehensive waste characterization and organic pollution co-occurrence in a Hg and As mining and metallurgy brownfield. J. Hazard. Mater. 300:561–571. https://doi.org/10.1016/j.jhazmat.2015.07.029.

Gallego, J.R., Rodríguez-Valdés, E., Esquinas, N., Fernández-Braña, A., Afif, E., 2016. Insights into a 20-ha multi-contaminated brownfield megasite: an environmental forensics approach. Sci. Total Environ. 563–564:683–692. https://doi.org/10.1016/j.scitotenv.2015.09.153.

Getis, A., Ord, J.K., 1992. The analysis of spatial association by use of distance statistics. Geogr. Anal. 24:189–206. https://doi.org/10.1111/j.1538-4632.1992.tb00261.x.

González-Fernández, B., Rodríguez-Valdés, E., Boente, C., Menéndez-Casares, E., Fernández-Braña, A., Gallego, J.R., 2018. Long-term ongoing impact of arsenic contamination on the environmental compartments of a former mining-metallurgy area. Sci. Total Environ. 610–611:820–830. https://doi.org/10.1016/j.scitotenv.2017.08.135.

Goovaerts, P., 1997. Geostatistics for Natural Resources Evaluation. University Press, New York, Oxford.

Greenacre, M., Lewi, P., 2009. Distributional equivalence and subcompositional coherence in the analysis of compositional data, contingency tables and ratio-scale measurements. J. Classif. 26:29–54. https://doi.org/10.1007/s00357-009-9027-y.

Gringarten, E., Deutsch, C.V., 2001. Teacher's aide variogram interpretation and modeling. Math. Geol. 33:507–534. https://doi.org/10.1023/a:1011093014141.

Isaaks, E.H., Srivastava, R.M., 1989. An Introduction to Applied Geostatistics. University Press, New York, Oxford, pp. 278–322.

Journel, A.G., Huijbregts, C.J., 1978. Mining Geostatistics. Academic Press, San Diego.

Lark, R.M., Bishop, T.F., 2007. Cokriging particle size fractions of the soil. Eur. J. Soil Sci. 58: 763–774. https://doi.org/10.1111/j.1365-2389.2006.00866.x.

Li, Z., Ma, Z., van der Kuijp, T.J., Yuan, Z., Huang, L., 2014. A review of soil heavy metal pollution from mines in China: pollution and health risk assessment. Sci. Total Environ. https://doi.org/10.1016/j.scitotenv.2013.08.090.

Martínez, J., Saavedra, Á., García-Nieto, P.J., Piñeiro, J.I., Iglesias, C., Taboada, J., Sancho, J., Pastor, J., 2014. Air quality parameters outliers detection using functional data analysis in the Langreo urban area (Northern Spain). Appl. Math. Comput. 241:1–10. https://doi.org/10.1016/j.amc.2014.05.004.

Mateu-Figueras, G., Pawlowsky-Glahn, V., 2008. A critical approach to probability laws in geochemistry. Progress in Geomathematics:pp. 39–52 https://doi.org/10.1007/978-3-540-69496-0_4.

Matheron, G., 1963. Principles of geostatistics. Econ. Geol. 58:1246–1266. https://doi.org/10.2113/gsecongeo.58.8.1246.

McIlwaine, R., Doherty, R., Cox, S.F., Cave, M., 2016. The relationship between historical development and potentially toxic element concentrations in urban soils. Environ. Pollut. 220:1036–1049. https://doi.org/10.1016/j.envpol.2016.11.040.

Megido, L., Suárez-Peña, B., Negral, L., Castrillón, L., Fernández-Nava, Y., 2017. Suburban air quality: human health hazard assessment of potentially toxic elements in PM10. Chemosphere 177:284–291. https://doi.org/10.1016/j.chemosphere.2017.03.009.

Moen, J., Ale, B.J.M., 1998. Risk maps and communication. J. Hazard. Mater. 61, 271–278.

Odeh, I.O.A., Todd, A.J., Triantafilis, J., 2003. Spatial prediction of soil particle size fractions as compositional data. Soil Sci. 168, 501–515.

Olea, R.A., Raju, N.J., Egozcue, J.J., Pawlowsky-Glahn, V., Singh, S., 2017. Advancements in hydrochemistry mapping: methods and application to groundwater arsenic and iron concentrations in Varanasi, Uttar Pradesh, India. Stoch. Env. Res. Risk A.:1–19 https://doi.org/10.1007/s00477-017-1390-3.

Pawlowsky, V., 1989. Cokriging of regionalized compositions. Math. Geol. 21:513–521. https://doi.org/10.1007/BF00894666.

Pawlowsky, V., Burger, H., 1992. Spatial structure-analysis of regionalized compositions. Math. Geol. 24:675–691. https://doi.org/10.1007/BF00894233.

Pawlowsky, V., Olea, R.A., Davis, J., 1995. Estimation of regionalize compositions: a comparison of three methods. Math. Geol. 27, 105–127.

Pawlowsky-Glahn, V., Buccianti, A., 2011. Compositional Data Analysis: Theory and Applications. Wiley.

Pawlowsky-Glahn, V., Egozcue, J.J., 2006. Compositional data and their analysis: an introduction. Geol. Soc. Lond. Spec. Publ. 264:1–10. https://doi.org/10.1144/GSL.SP.2006.264.01.01.

Reimann, C., Filzmoser, P., Fabian, K., Hron, K., Birke, M., Demetriades, A., Dinelli, E., Ladenberger, A., Albanese, S., Andersson, M., Arnoldussen, A., Baritz, R., Batista, M.J., Bel-lan, A., Cicchella, D., De Vivo, B., De Vos, W., Duris, M., Dusza-Dobek, A., Eggen, O.A., Eklund, M., Ernstsen, V., Finne, T.E., Flight, D., Forrester, S., Fuchs, M., Fugedi, U., Gilucis, A., Gosar, M., Gregorauskiene, V., Gulan, A., Halamic, J., Haslinger, E., Hayoz, P., Hobiger, G., Hoffmann, R., Hoogewerff, J., Hrvatovic, H., Husnjak, S., Janik, L., Johnson, C.C., Jordan, G., Kirby, J., Kivisilla, J., Klos, V., Krone, F., Kwecko, P., Kuti, L., Lima, A., Locutura, J., Lucivjansky, P., Mackovych, D., Malyuk, B.I., Maquil, R., McLaughlin, M.J., Meuli, R.G., Miosic, N., Mol, G., Négrel, P., O'Connor, P., Oorts, K., Ottesen, R.T., Pasieczna, A., Petersell, V., Pfleiderer, S., Ponavic, M., Prazeres, C., Rauch, U., Salpeteur, Schedl, A., Scheib, A., Schoeters, I., Sefcik, P., Sellersjö, E., Skopljak, F., Slaninka, I., Šorša, A., Srvkota, R., Stafilov, T., Tarvainen, T., Trendavilov, V., Valera, P., Verougstraete, V., Vidojevic, D., Zissimos, A.M., Zomeni, Z., 2012. The concept of compositional data analysis in practice - total major element concentrations in agricultural and grazing land soils of Europe. Sci. Total Environ. 426: 196–210. https://doi.org/10.1016/j.scitotenv.2012.02.032.

XlStat software v. 2013.1.01, 2013. https://www.xlstat.com/en/, Accessed date: 15 September 2017.

Zuo, R., Carranza, E.J.M., Wang, J., 2016. Spatial analysis and visualization of exploration geochemical data. Earth Sci. Rev. 158:9–18. https://doi.org/10.1016/j.earscirev.2016.04.006.

Chapter III. New advances in remediation of soils polluted by potentially toxic elements

III.I Soil washing optimization by means of attributive analysis: Case study for the removal of potentially toxic elements from soil contaminated with pyrite ash

---

C. Boente, C. Sierra, E. Rodríguez-Valdés, J.M. Menéndez-Aguado, J.R. Gallego

Journal of Cleaner Production (2017)

Volume 142, January 2017, Pages 2693-2699

Rank: 28 out of 339 (1st Quartile) in *Environmental Science* (JCR)

Journal of Cleaner Production 142 (2017) 2693–2699

Contents lists available at ScienceDirect

Journal of Cleaner Production

journal homepage: www.elsevier.com/locate/jclepro

Soil washing optimization by means of attributive analysis: Case study for the removal of potentially toxic elements from soil contaminated with pyrite ash

C. Boente [a], C. Sierra [b, c, *], E. Rodríguez-Valdés [a], J.M. Menéndez-Aguado [a], J.R. Gallego [a]

[a] Environmental Technology, Biotechnology and Geochemistry Group, C/Gonzalo Gutiérrez Quirós s/n, 33600 Mieres, Asturias, Spain
[b] Escuela Superior Politécnica del Litoral, ESPOL, Facultad de Ciencias Naturales y Matemáticas, Campus Gustavo Galindo Km 30.5 Vía Perimetral, P.O. Box 09-01-5863, Guayaquil, Ecuador
[c] Departamento de Transportes, Tecnología de Procesos y Proyectos, Universidad de Cantabria, Campus de Torrelavega, Spain

ARTICLE INFO

Article history:
Received 9 February 2016
Received in revised form
31 October 2016
Accepted 1 November 2016
Available online 4 November 2016

Keywords:
Soil washing
Quality index
Pyrite ashes
Potentially toxic elements
Physical separation

ABSTRACT

This paper describes a feasibility study of physical soil washing techniques to separate potentially toxic elements, such as As, Cu, Hg, Pb and Sb, in a brownfield affected by pyrite ash disposal. To this end, complete pedological and geochemical analyses were conducted in order to determine the properties of the soil. Afterwards exhaustive lab-scale soil washing tests were performed with the aim to concentrate most of the contaminants into a small fraction of treated soil. The procedures used included gravity separation—heavy liquid assays—, hydrocycloning and wet and dry magnetic separation.

Within this context, grain-size classification proved effective only for the treatment of the sizes below 63 μm. Better results were obtained by heavy liquid separation, which was optimal at most grain sizes, except fractions of the soil between 1000 and 2000 μm, and below 63 μm. As regards magnetic separation, dry high-intensity magnetic separation was suitable for the treatment of grain sizes above 500 μm and gave yields similar to those achieved by heavy liquid assays in most cases. The results of the experiments were compared through the novel approach of attributive analysis, and the findings indicated that the separation procedures for pollutants yielded repeatable results. Moreover, an intuitive method of evaluating the performance of the separation techniques by introducing a "success score" was developed. This procedure takes into account not only the various scenarios contemplated by legislation but also the performance of each washing method for each element.

All things considered, in feasibility studies for soil washing methods and also for mineral processing purposes, both attributive analysis and the "success score" may be useful for selecting optimal operating conditions, thus facilitating the scale-up of the results. Moreover, the method presented could be used in any operating plant that aims to reduce emissions while at the same time maximizing product outputs.

1. Introduction

Sites that have been abandoned after the closure of heavy industries or after the relocation of the industry from urban to periurban areas are common in developed countries. In this context, the presence of certain trace elements usually implies a risk to the environment and human health.

Potentially Toxic Elements (PTEs) are elements of environmental concern usually characterized by their persistence in the environment and their readiness to bioaccumulate and biomagnify (Clemens, 2006). Although these elements occur naturally, they are concentrated in certain sites as a result of mining and industrial activities (e.g.: Sierra et al., 2014a; Gallego et al., 2016). They enter human, animal, and plant tissues (Adamo et al., 2014) via inhalation, intake, or manual manipulation, and they can bind to vital cellular components, thereby interfering with normal function and causing severe diseases.

Pyrite (FeS_2) is used to manufacture sulfuric acid, which is the largest-volume industrial chemical produced in the world (D'Aquin and Fell, 2012). This process includes the roasting of pyrite, a procedure that gives rise to a hazardous waste, namely pyrite ash or

* Corresponding author. Departamento de Transportes, Tecnología de Procesos y Proyectos, Universidad de Cantabria, Campus de Torrelavega, Spain.
E-mail address: carlos.sierra@unican.es (C. Sierra).

http://dx.doi.org/10.1016/j.jclepro.2016.11.007
0959-6526/

cinder, which comprises high concentrations of hematite and PTEs (Oliveira et al., 2012).

During the roasting of the pyrite, several physicochemical transformations also occur, resulting in the potential accumulation of trace elements, especially As, in the residue (Bulut et al., 2013). This scenario explains why inappropriately managed pyrite ash disposal has historically been a massive problem for soils and also for (ground) water (Yang et al., 2009, 2013). In this regard, an increasing number of studies have proposed methods to reduce/recycle trace elements such as As, Hg, Pb and Cu (Li et al., 2013; Xu et al., 2014; Wang et al., 2012; Di Maria et al., 2013; Sierra et al., 2014a).

In this context, many remediation techniques can be used to reduce or even eliminate soil contamination. Among them is the soil washing approach (Mann, 1999), a system that concentrates the polluting agents into a reduced volume fraction of the affected soil and generally results in decontamination of the matrix (Anderson et al., 1999). This method is relatively inexpensive, easy to implement, and highly versatile. Such features make this approach appropriate for mobile plants (on-site treatments) and for large-scale facilities (ex situ treatments) (Pearl et al., 2006; Fan et al., 2015).

Soil washing approaches are usually based on mineral processing technologies (Wills and Napier-Munn, 2006; Gupta and Yan, 2006) and can be divided into physical (the chemical properties of materials are not altered to achieve the separation), chemical (based on extracting the pollutants from the soil or dissolving them), and physico-chemical (combination of both) (Dermont et al., 2008) separation.

Before designing a full-scale washing plant, a feasibility analysis is required. At this stage, several laboratory and analytical determinations are performed to define the properties of both the pollutant and the soil (Abumaizar and Smith, 1999; Sierra et al., 2010). In the second step, pilot-scale experiments can be performed in conditions similar to those found in the field. Finally, if the results are satisfactory, the method can be implemented in the field (Cappuyns, 2013) once the entire life cycle of the project has been considered (Hou et al., 2014).

Given the preceding considerations, this paper describes a feasibility study of washing techniques in a soil severely affected by pyrite ash disposal. The soil pollution in the study site is relevant from the point of view of the volume of soil affected and also the concentrations of PTEs—mainly As and Pb, but also Cu, Hg and Sb present (Gallego et al., 2016). The study soil is made up of a mixture of natural aggregates (mostly silicic and organic) and pyrite ash. It is therefore assumed that these components have different sizes, densities and/or magnetic properties and are therefore amenable for separation treatments. In addition, the multicomponent pollution, typical in this sort of site, lends itself to the soil washing approach (Sierra et al., 2011). The specific objectives were as follows:

- To integrate the pedological and geochemical information of the polluted soil in order to define the element concentrations that exceeded the Risk-Based Soil Screening Levels (RBSSLs) and the soil fractions to which these pollutants were preferentially bound to.
- To use the information reported in the previous step to select the most appropriate soil washing techniques and to carry out a feasibility study to reduce the PTE content of the distinct soil fractions.
- To compare the results achieved by these techniques by means of attributive analysis in order determine the best operating conditions, and to develop a new index ("success score") in order to evaluate the effectiveness of the treatments, taking into account environmental standards.

2. Materials and methods

2.1. Site description and sampling

The Nitrastur complex is a derelict fertilizer plant in La Felguera (Asturias) that was closed in 1997. The site has been extensively described in a recent study (Gallego et al., 2016). In brief, it covers 200,000 m^2, of which approx. 70,000 m^2 are contaminated. More than half of this contamination corresponds to landfills comprised of pyrite ash, in addition to other iron and steel-type debris. Pyrite ash (around 80,000 m^3) has been reported to be the main source of pollution at this site. Together with other minor wastes at Nitrastur, pyrite ash has supplied the soil with PTEs over many years. Consequently, As, Pb, Cu, Sb and Hg concentrations exceed the soil screening levels of reference in many areas within the site.

In fact, the pollution of the soil at this site is highly heterogeneous, ranging from soils that show slight contamination to areas registering a mixture of pure waste and soil. In this regard, sampling was designed in such a way as to accurately represent the variability of the study site. For the purpose of this study, samples were selected from areas where soil aggregates are mixed with pyrite ash. To this end, a "macrosample" of about 50 kg was taken from several points across the Nitrastur site between a depth of 0 and 30 cm and using a Dutch auger (25 subsamples). The sample soil (a mixture of pyrite ash and natural soil) was passed through a 2-cm mesh screen in situ to remove rocks, gravel, and other large material.

2.2. Soil characterization

The pH of the sample was measured with a glass electrode in a suspension of soil and deionized water (1:2.5), and electrical conductivity was measured in the same extract (diluted 1:5). Organic matter content was determined by the ignition method (weight loss at 450 °C). Exchangeable cations (Ca, Mg, K and Na), extracted with 1 M NH_4Cl, and exchangeable Al, extracted with 1 M KCl, were determined by means of an atomic absorption/emission spectrophotometer (model AA200 Perkin Elmer) (Pansu and Gautheyrou, 2007). The effective cation exchange capacity (ECEC) was calculated as the sum of concentrations of exchangeable cations and Al.

A representative sample of the soil was soaked in water before being sieved into particle-size fractions of <63, 63–125, 125–250, 250–500, 500–1000 and 1000–2000 μm, and also a 63–500 μm fraction. Normalized sieves were placed in a column, and batches of 100 g of the material were put into a sieve shaker for 5 min with a water flow of 0.3 l/min (ASTM D-422-63, Standard Test Method for Particle-Size Analysis of Soils). The fractions were recovered with the help of a spray nozzle. They were then laid out in trays, dried at 30 °C (in order not to volatilize Hg), and finally weighed.

Representative samples of soil and soil fractions were subjected to chemical analyses by means of Inductively Coupled Plasma-Optical Emission Spectroscopy (ICP-OES). In order to standardize the conditions used for chemical attack, samples with a grain size >125 μm were ground in a RS100 Resch mill at 400 rpm for 40 s to obtain a smaller grain size. For chemical analyses, 1-g representative sub-samples of the diverse origins (soils, grain-size fractions, etc.) were subjected to a 1:1:1 "Aqua regia" digestion. The total concentrations of the elements of concern (As, Pb, Cu, Hg and Sb) in the digested material were determined by ICP-OES at the accredited (ISO 9002) laboratories Bureau Veritas (Vancouver, Canada).

2.3. Magnetic soil washing techniques

Given the nature of the pollutants studied, namely a hematite-rich waste formed as a result of the roasting of pyrite and also

containing significant amounts of goethite (Gallego et al., 2016), it was considered that high-intensity magnetic separation (HIMS) procedures would be feasible to treat the soil. Therefore, the efficiency of the dry and wet HIMS methods was tested for the grain-size intervals indicated above.

2.3.1. Dry-HIMS

Dry-HIMS is a soil washing technique based on rare earth permanent magnets, and it provides high recovery yields with low operating costs. This method efficiently removes weak magnetic pollutants and can achieve precise separations as a result of the absence of drag forces (Svoboda, 2004). The particularities of this technique make it necessary to previously dry the polluted soil. This drying process may imply high costs for soil washing operations, thus explaining why the approach has not been widely described in the literature. However, despite these potential limitations, this procedure is suitable for washing large soil particles (500–2000 μm) (Sierra et al., 2013).

In this context, a separation study by means of a rare earth magnetic separator (Model No L/p 10:30 of International Process Systems Inc.) was conducted. This high-force magnetic separator consists of a support frame, a magnetic roller, an idler roller, and a conveyor belt. The apparatus applies gravity and magnetic force (centripetal force) to separate particles on the basis of their magnetic properties. In this regard, the magnetic force keeps them attached to the conveyor belt, thereby resulting in a different discharge trajectory. The velocity of the roller in the factorial tests was set at 30, 60, and 90 rpm. The separation was visually assessed, and the test that showed the best performance (90 rpm) was analyzed.

2.3.2. Wet-HIMS

Wet-HIMS is suitable for the treatment of smaller grain sizes. It is straightforward to use and provides an excellent yield recovery and ratio of concentration (Mercier et al., 2001).

An OUTOTEC Laboratory WHIMS 3X4L apparatus, which has the capacity to separate paramagnetic (weakly magnetic) from non-magnetic materials, was used. The slurry feed was prepared by mixing 50 g of soil with 200 g of water. This slurry was then passed through a matrix canister (also known as a separating chamber) filled with steel spheres measuring12.5 or 6.5 mm in diameter (depending on the particle-size of the feed; 12.5-mm spheres are appropriate for soil particle sizes >125 μm, while 6.5-mm spheres are appropriate for those <125 μm).

In accordance with the manufacturer's specifications, the magnetic flux density was 2.16 T (max). The magnetic particles are retained by the magnetized spheres, while the non-magnetic components and the water pass across the matrix canister and are collected in a tray. Finally, the magnetic material retained on the spheres is washed out by turning off the equipment, thus reducing the magnetic field to zero. The variable magnetic field intensity of the equipment is adjusted through the coil input amperage (0–6 amps) (Sierra et al., 2014b). For all the tests in this study, 25% of the maximum output voltage was used because it provided the best performance for all the fractions studied.

2.4. Gravity washing techniques

Gravity separation of minerals is one of the oldest techniques for separating minerals; it does not call for the use of chemicals or excessive heating, thus making it environment-friendly. However, full-scale application is expensive, and treatment of the smallest grain sizes is usually complex. Despite these problems, specific devices have been developed by the industry (e.g. Model 50TPH - Dense Medium Drum Plant, HBR Limited) for soil washing purposes. Within this context, various studies have addressed soil washing of fine fraction (e.g. Klima and Kim, 1998), as well as the separation of organic matter (density <1.8 g/cm^3) from the siliciclastic fraction (density approx. 2.7 g/cm^3). In the present study, given the differences in density between the pyrite ash and the natural aggregates of the soil, gravity washing techniques were expected to be efficient.

2.4.1. Float-sink separation

Float-sink separation is a gravity concentration procedure that segregates particles with different specific gravities by immersing them in a fluid (heavy solutions, heavy liquids, semi-stable suspensions and ferrofluids) (Wills and Napier-Munn, 2006). In this regard, it is important to highlight that the differences in density between the polluting substances (e.g. pyrite ash) and the soil fraction to which they are bound (e.g., soil organic matter, silicic fractions or carbonates) are relevant. Within float-sink approaches, heavy liquid separation (HLS) is a straightforward means of assessing dense medium separation, and it is also used for other gravity washing techniques, such as spirals (Dallaire et al., 1978) and shaking tables, among others (Klima and Kim, 1998).

In the present study, the dense liquid was prepared in various proportions of chloroform (density of 1.49 g/cm^3 at 293 K) and bromoform (density of 2.82 g/cm^3 at 293 K). The pollutant-carrying fraction was heavy, so densities of 2.82 g/cm^3 (0% chloroform and 100% bromoform) and 2.69 g/cm^3 (10% chloroform and 90% bromoform) were used. As a previous step, preliminary tests allowed estimation of optimum residence times, mixture ratio of the liquids, and relative aggressiveness of the bromoform with the soil. Other densities (2.55 g/cm^3 and 2.42 g/cm^3) were also prepared and tested, but the results were poor (assessed by portable X-Ray Fluorescence equipment).

The liquid and soil were placed in a separating funnel. Particles with a density lower than that of the liquid floated, while those with a higher density sunk. Both dense and light materials were collected in separate trays by opening and closing a manual valve in the separating funnels. All samples were weighed and dried at low temperature (30 °C to minimize loss of Hg) to obtain dry weight subsamples for ICP-OES analyses.

2.4.2. Hydrocycloning

The hydrocyclone is the most widely used system for mineral treatment (Ma et al., 2013). It achieves the separation of heavy and light particles via a static piece of equipment that applies a centrifugal force to a liquid (commonly water) that contains the material. This device works in continuous flow regime (Yang et al., 2013). The material is introduced through instantaneous in-flow slurry (feed), which is tangentially pumped inside the cyclone, wherein the joint action of the centrifugal drag and gravity forces separate the particles on the basis of their grain size and density. This system determines whether an individual particle flows through the apex (underflow) or the upper part (overflow) of the hydrocyclone. The underflow and overflow comprise the outflow, the sum of which must be equal to the inflow; the lighter and finer particles pass through the overflow.

Regarding the current study, a hydrocycloning lab-scale plant (C700 Mozley) with a capacity to operate hydrocyclones from 10 to 50 mm in diameter was used. The solid concentration of the slurry feed used in the experiments was constant (20% per weight), whereas the apex diameters (9.5 mm and 6.5 mm) and working pressures (69 and 138 kPa) were combined (Nieuwoudt et al., 1990). The procedure was used to treat the grain size fraction of <63 μm, in accordance with the manufacturer's specifications. In all cases, after reaching a stationary regime, samples from the underflow and overflow were collected in borosilicate flasks and then weighed and dried in an oven at low temperature, thereby obtaining dry weight and representative subsamples for ICP-OES analyses.

2.5. Attributive analysis

Soil washing aims to concentrate a contaminant into a small volume of soil. However, multiple variables of each experiment make it difficult to assess the performance of the process. Thus, comparison of experiments calls for a tool with the capacity to define the quality of the same.

Such comparison has been possible thanks to a method based on attributive analysis that was successfully used in other studies (Sierra et al., 2010). The method was applied to a number of soil washing tests treating the same particle size but with distinct operational procedures. Since legislation establishes RBSSLs (Risk-Based Soil Screening Levels) for several scenarios, e.g. industrial and residential, the ensuing paragraphs describe how to calculate the quality index for an industrial soil (in the soils of study, only As and Pb exceeded the RBSSL for industrial use). All calculations in this section were performed using the software COS (Sierra et al., 2012).

First, R^i (%) was defined, which is the weight recovery in test "i". From the all the tests performed, the test with the minimum weight recovery is selected and defined as R^{min} (%).

Conditions for concentration must be established for every test and element (i.e. weight recovery smaller than element recovery). These conditions can occur in the mags, overflow and heavies or in the non-mags, underflow and lights. For both cases, the recovery for a given element is termed as Rec^i (%), and the test with the maximum recovery is denoted as Rec^{max} (%).

Accordingly, the quality index (also termed index of merit) Q^i_{As} for As was defined for test "i" using the following expression:

$$Q^i_{As} = \frac{R^{min}}{R^i} + \frac{Rec^i_{As}}{Rec^{max}_{As}}$$

Similarly, the quality index for Pb was calculated as:

$$Q^i_{Pb} = \frac{R^{min}}{R^i} + \frac{Rec^i_{Pb}}{Rec^{max}_{Pb}}$$

When dealing with more than one element, the expression can be generalized as the sum of Q^i for all the elements.

However, the "distance" between the concentrations of all these contaminants in the initial soil and the target value differs. Therefore, a weighting factor "A", which takes into account this fact (Sierra et al., 2010), for each contaminant is defined. Thus, for As and Pb:

$$A_{As} = \frac{Co_{As}(\text{ppm})}{RBSSL_{As}(\text{ppm})}$$

$$A_{Pb} = \frac{Co_{Pb}(\text{ppm})}{RBSSL_{Pb}(\text{ppm})}$$

where Co_{As} is the concentration of the element in the initial soil, and $RBSSL_{As}$ is the Risk- Based Soil Screening Level for As —of the region of Asturias (BOPA, 2014)—for the intended soil use (industrial or residential).

Furthermore, these coefficients are corrected on the basis of their contribution to total contamination. Thus, for As and Pb the corrected weighting factor A′ is:

$$A'_{As} = \frac{A_{As}}{A_{As} + A_{Pb}}$$

$$A'_{Pb} = \frac{A_{Pb}}{A_{As} + A_{Pb}}$$

Therefore, the particularized expression of the attributive analysis for the global quality index (Q_T) in the case of an industrial soil is defined as:

$$Q^{ind}_T = Q^i_{As} \cdot A'_{As} + Q^i_{Pb} \cdot A'_{Pb}$$

In the case of soil for residential use, the calculation of the quality index is analogous, but the expression will also include Cu, Hg and Sb (see results).

3. Results and discussion

3.1. Soil characterization

The pedological characterization (average of 25 representative subsamples collected in the study area, with a standard error below 5%) revealed a slightly acidic pH (6.5), low electrical conductivity (EC = 0.116 dS m^{-1}), low content of exchangeable base cations Mg and K (0.30 and 0.60 $cmol_+$ kg^{-1} respectively), moderate values for Ca and Na (15.29 and 1.92 $cmol_+$ kg^{-1} respectively), moderate Effective Cation Exchange Capacity (ECEC), and a moderate-high organic matter content in the upper horizon (9.66%).

On the other hand, for the composite bulk sample, the ICP-OES analyses (Table 1) revealed that the RBSSLs (BOPA, 2014) were surpassed by As, Pb and Sb for the industrial scenario, and by Cu, Hg and Sb for the residential context. As regards element concentration per fraction, As, Hg, Pb and Sb were above the standards for residential use in all the grain-size intervals; however, Cu was above the standards in only some intervals. Furthermore, when the most permissive industrial scenario was considered, As and Pb still exceeded the reference levels for most of the grain-size intervals.

Moreover, chemical analyses also showed significant amounts of Fe. This observation, together with the fact that many Fe-bearing minerals become magnetic when roasted (e.g. hematite to Fe_3O_4 or gamma Fe_2O_3), suggested the occurrence of ferro- ferri- or paramagnetic materials. This notion is consistent with pyrite ash being the main source of pollution in the soil. Consequently, magnetic separation was also performed. Furthermore, textural classification indicated a high proportion of fine particles (silty sand soil with 37.62% < 63 μm), which may hamper pollutant separation by conventional gravity concentration techniques.

3.2. Separation results

The experiments in this section included separation by classification (hydrocycloning), gravity concentration (heavy liquid tests), and high-intensity magnetic separation (HIMS).

Table 1
Particle-size distribution and element concentration of the bulk and grain size fractions (aqua-regia digestion and ICP-OES). RBSSL indicates Risk-Based Soil Screening Level. Results correspond to the average of 3 determinations with a standard error < 3%.

Grain size (μm)	Weight	Element (mg Kg^{-1})				
		As	Cu	Hg	Pb	Sb
1000–2000	10.78	864	743	15	2724	96
500–1000	7.88	1050	867	29	2729	125
250–500	18.74	376	280	15	2065	48
125–250	18.46	315	257	21	1199	43
63–125	6.52	394	325	27	1501	58
<63	37.62	1251	926	56	3134	126
63–500	43.72	370	291	21	1512	47
Bulk sample		801	618	33	2394	88
RBSSL	Industrial	200	4000	100	800	295
	Residential	40	400	10	400	25

Each set of tests was compared by means of the global quality index (Q_T). Using this mathematical procedure, the separation method that performed best for each grain-size interval was determined. The goal was to concentrate the pollutants and thus obtain a low weight recovery with a very high element recovery (in the concentrate).

In this respect, it is important to indicate that it is not possible to compare quality indexes for tests that do not share a common characteristic (i.e.: type of separator, operating conditions, or feed grain size). In the present study, to facilitate comparison, each set of tests used a common feed grain size. The results obtained are shown in Table 2.

With respect to the very coarse sand fraction (1000–2000 μm) and according to the manufacturer's specifications, only Wet-HIMS was appropriate. In this case, comparison with other tests was not possible, but separation by this technique gave high element recoveries and moderate weight recoveries.

For the coarse sand fraction (500–1000 μm), HLS and Dry- and Wet- HIMS were performed. HLS was carried out as an indicator of the maximum efficiency achievable by means of gravity washing, as this method is the most effective gravity concentration operation. That is to say, the results obtained using other techniques with industrial gravity equipment, namely jigs, shaking tables, spirals, and centrifugal concentrators, do not surpass those of HLS.

Regarding grain-size intervals, magnetic separation by Dry- and Wet-HIMS showed greater efficiency than HLS. Due to high weight recovery, the quality index for HLS was lower than that achieved with the other procedures. In this respect, Dry-HIMS showed the best separation performance. Moreover, Wet-HIMS also achieved respectable contaminant recoveries, but the weight recovery was excessively high and pollutant concentration was thus limited. In this regard, high recoveries were achieved for As, Cu and Sb, although with relatively small weight recoveries. The latter were insufficient to make the process efficient in a single stage. In contrast, the recovery of Pb and Hg was low, thereby suggesting that these metals did not bind to any magnetic particle.

Concerning the medium sand fraction (250–500 μm), Wet-HIMS and HLS were used under the same conditions as in the previous section whereas, following the manufacturer's instructions, Dry-HIMS was not used for this particle-size. In general terms, a reduction in weight recovery was observed, which was around 10% for HIMS. Moreover, element recoveries were higher for Wet-HIMS than for HLS. Thus, according to the quality indexes, the heaviest medium (2.82 g/cm^3) gave better results, although Wet-HIMS outperformed HLS. In contrast, when the previous set of experiments was repeated for the fine sand fraction (125–250 μm), the performance of HLS was superior to that of Wet-HIMS.

For the very fine sand fraction (63–125 μm), the results were similar to those of the two previous fractions; however, weight recovery for Wet-HIMS increased, thus allowing higher recoveries in the concentrate. This observation indicates that the effectiveness of Wet-HIMS diminishes with the finest materials.

In real-scale processing, it is common practice to screen material using a small number of meshes, thus cutting costs and increasing operability. Accordingly, given the similarities between the results obtained for the last three grain-size intervals, a composite sample (63–500 μm in size), which represented 43.72% of the total weight smaller than 2 mm, was subjected to both Wet-HIMS and HLS. In this case, HLS outperformed Wet-HIMS and even slightly improved on the results obtained in the previous sections by grain-size intervals.

The silted clayed fraction (<63 μm) had a great presence in the soil (37.62% of the weight <2 mm). Therefore classification by hydrocycloning, in addition to Wet-HIMS and HLS, was tested. For the hydrocycloning experiments, the overflow presented high concentrations of the contaminants, as expected. This observation

Table 2
Results grouped by grain-size intervals for the separation experiments. Q_T^{ind} indicates the quality index for industrial soil (calculated with As and Pb). Q_T^{res} indicates the quality index for residential soil (calculated with As, Pb, Cu, Hg and Sb). Results correspond to the average of 3 determinations with a standard error < 3%.

Grain-size fraction (μm)	Equipment	Conditions	Weight recovery in the concentrate (yield) (%)	Element recovery in the concentrate (%)					Q_T^{ind}	Q_T^{res}
				As	Pb	Cu	Hg	Sb		
1000–2000	Dry-HIMS	Roll speed: 90 rpm	51.7	88.5	62.0	89.1	49.5	94.5	–	–
500–1000	Dry-HIMS	Roll speed: 90 rpm	53.2	94.0	78.3	91.9	82.4	95.3	1.932	1.900
	Wet-HIMS	Ball diameter: 12.5 mm	78.9	97.3	95.4	95.9	94.9	98.8	1.670	1.664
	HLS	Density: 2.82 g/cm^3	65.2	90.9	97.9	92.5	95.7	96.5	1.771	1.775
250–500	Wet-HIMS	Density: 2.69 g/cm^3	63.0	90.0	97.5	91.8	90.6	96.2	1.789	1.797
		Ball diameter: 12.5 mm	42.0	86.4	81.1	89.6	81.3	94.3	1.241	1.252
	HLS	Density: 2.82 g/cm^3	10.9	58.7	82.9	62.7	49.0	78.5	1.807	1.741
		Density: 2.69 g/cm^3	12.5	61.8	84.7	67.6	63.7	77.7	1.713	1.660
125–250	Wet-HIMS	Ball diameter: 12.5 mm	35.4	91.3	85.7	83.2	70.4	95.1	1.216	1.215
	HLS	Density: 2.82 g/cm^3	7.6	52.9	78.2	56.5	33.2	73.8	1.722	1.652
		Density: 2.69 g/cm^3	8.6	51.7	72.3	54.7	39.1	69.6	1.574	1.523
63–125	Wet-HIMS	Ball diameter: 6.5 mm	52.1	97.1	95.2	95.3	87.7	97.3	1.111	1.112
	HLS	Density: 2.82 g/cm^3	5.8	45.9	70.6	50.3	22.5	59.0	1.587	1.515
		Density: 2.69 g/cm^3	7.6	49.6	71.8	52.0	35.3	61.8	1.371	1.314
<63	Wet-HIMS	Ball diameter: 6.5 mm	62.8	84.5	81.8	81.0	76.6	87.3	1.496	1.522
		Ball diameter: 6.5 mm Dual-pass for denses	74.6	92.1	90.4	89.0	87.2	93.3	1.502	1.536
	Hydrocyclone	Apex: 9.5 mm Pressure: 68.95 kPa	37.1	41.7	44.3	44.5	56.6	27.0	1.469	1.489
		Apex: 9.5 mm Pressure: 137.90 kPa	37.1	41.3	45.0	44.8	57.2	26.2	1.469	1.490
		Apex: 6.4 mm Pressure: 68.95 kPa	45.7	50.0	53.1	53.8	73.3	32.4	1.372	1.414
		Apex: 6.4 mm Pressure: 137.90 kPa	38.3	42.0	46.2	46.4	62.4	28.1	1.447	1.470
63–500	Wet-HIMS	Ball diameter: 12.5 mm	37.5	92.7	83.9	93.0	80.8	95.9	1.024	1.042
		Ball diameter: 6.5 mm	53.0	96.3	94.4	94.8	89.0	97.0	1.066	1.068
	HLS	Density: 2.82 g/cm^3	3.7	33.1	53.7	34.8	14.5	44.8	1.410	1.337
		Density: 2.69 g/cm^3	3.5	28.2	52.7	30.1	15.4	44.6	1.427	1.354

is coherent with the increasing concentration of pollutants in the smallest grain sizes. Moreover, the presence of organic matter acts as a heavy metal scavenger, forming a new complex of reduced density which tends to report to the underflow. Note that hydrocyclone classification is also affected by density.

HLS was also attempted, but middlings floated, forming a mat which retained the coarser middlings on the free surface of the heavy liquid, thus hindering separation. This observation could be explained by the fact that HLS is not effective at this size range because fine grains have a slow settling velocity as a result of the balance between the small downward forces and high friction forces created by the viscosity of the fluid (Wills and Napier-Munn, 2006).

Moreover, as the feed size reduced, the overall concentration efficiency of the magnetic separation decreased considerably, probably because dragging overcame magnetic forces, thus resulting in lower separation efficiency. This could be attributable to the dependence of the increasing force acting on a particle in a magnetic separator on the increasing size, thereby dramatically reducing the separation for the finest grain sizes (Svoboda, 2004). In order to improve the results for Wet-HIMS, the magnetic fraction was passed through the separator (dual-pass) a second time; however, no improvement was observed. In this respect, comparison of the quality indexes for this fraction revealed that Wet-HIMS showed optimum performance, registering the maximum recoveries; however, there was still excessive weight recovery.

3.3. Criterion according to the environmental standards

In this section, the results from the present study were compared with environmental standards. In this respect, a soil or fraction was considered decontaminated when the concentration of the contaminant was below the RBSSL. To this end, attention was devoted only to the contaminant concentration in the original soil (feed) and in the non-concentrated fraction (usually referred to as "tailings" in mineral processing), namely, the decontaminated soil.

The results regarding reduction of the concentration below RBSSLs are presented in Table 3. Therein, '0' indicates that the sample exceeded the RBSSL for both industrial and residential use (unsuccessful decontamination); '1' that it exceeded the RBSSL only for residential use; and '2' that it fell below the RBSSL for both industrial and residential use. When several conditions were used to treat a given fraction with certain technique, only the best results are included in Table 3.

The parameter "success score" per element was defined in order to assess difficulty in the separation (Table 3). Hence, by adding up the individual scores, as defined in the previous paragraph, the global score indicates the following order of success: Cu > Sb > Hg > Pb > As. Despite the satisfactory recoveries achieved, these results are a consequence not of deficient separation but of a high concentration of the element in the feed sample. Thus, the concentration of Cu was only 1.5 times higher than the RBSSL for the residential scenario, while the approximate concentration of Hg was 3.3, Sb 3.52, Pb 6 and As 20.

If the same procedure is followed per assay, the "success score" per test is obtained. In this respect, conclusions comparable to those obtained by attributive analysis were drawn. Thus, for the 500–1000 μm grain-size interval, both Wet- and Dry-HIMS gave similar yields, thereby complying with environmental standards. As regards the 500-250 μm and 250-125 μm fractions, Wet-HIMS and HLS scored equally. Concerning the 125-63 μm grain-size, Wet-HIMS clearly offered the best results. For the fraction <63 μm, small scores were obtained when compared with the other fractions, thus highlighting the difficulties encountered when treating this fraction. As a final point, it is important to note the good scores obtained for the 63–500 μm fraction, for which concentrations of the elements were below the RBSSLs in both scenarios. The results of the Wet-HIMS tests for this fraction pointed again to the feasibility of this method for scale-up purposes.

4. Conclusions

Part of the brownfield at Nitrastur comprises soil with an anomalous content of various PTEs, namely As, Cu, Fe, Hg, Pb and Sb, as a result of pyrite ash disposal. Here several soil washing procedures were tested, and attributive analysis was used to identify the method with the highest capacity to decontaminate several grain-size fractions of the polluted matrix.

Table 3
Success at reducing the concentration below RBSSL. '0' indicates that the sample exceeded the RBSSL for both industrial and residential use, '1' that it exceeded the RBSSL only for residential use, and '2' that it met the RBSSL for both scenarios.

Grain-size fraction (μm)	Equipment	Weight recovery in the less polluted fraction (%)	Success at reducing the concentration below the RBSSL					"Success score" per test
			As	Pb	Cu	Hg	Sb	
1000–2000	Feed		0	0	1	1	1	3
	Dry-HIMS	48.3	1	0	2	1	2	6
500–1000	Feed		0	0	1	1	1	3
	Dry-HIMS	46.8	1	0	2	2	2	7
	Wet-HIMS	78.9	1	1	2	2	2	8
	HLS	37.0	0	1	2	2	1	6
250–500	Feed		0	0	2	1	1	4
	Wet-HIMS	58.0	1	1	2	2	2	8
	HLS	89.1	0	2	2	2	2	8
125–250	Feed		0	0	2	1	1	4
	Wet-HIMS	64.6	1	2	2	1	2	8
	HLS	92.4	1	2	2	1	2	8
63–125	Feed		0	0	2	1	1	4
	Wet-HIMS	47.9	2	2	2	2	2	10
	HLS	94.2	1	2	2	2	1	8
<63	Feed		0	0	1	0	1	2
	Wet-HIMS	25.4	0	0	2	0	1	3
	Hydrocyclone	62.9	0	0	2	1	1	4
63–500	Feed		0	0	2	1	1	4
	Wet-HIMS	47.0	2	2	2	2	2	10
	HLS	96.5	1	2	2	1	2	8
"Success score" per element			12	17	39	27	31	

Separation by magnetism proved most appropriate for grain sizes >250 μm, becoming less effective for small particle sizes. In this respect, Wet-HIMS reduced all the contaminants for all the grain sizes tested, except the silted-clayed one (<63 μm, 37.62% of the material), to below the RBSSLs for industrial use. Furthermore, heavy liquid tests were performed in order to study the amenability of gravity separation for soil washing purposes. The study evidenced promising results, particularly for the very fine sand fraction (63–500 μm).

In this regard, the fraction <63 μm presented the most difficulty with respect to separation, probably because of the lower gravity forces, which were unable to overcome the viscous forces in the case of HLS and the lower magnetic forces that surpassed drag forces in the case of Wet-HIMS. Likewise, the organic matter present in the sample was also highlighted as a possible source of misclassification. Moreover, the tests also proved that the tailing fraction did not exceed the RBSSLs for most cases. This observation therefore indicates that this material can be disposed of directly without prior treatment.

In view of the aforementioned findings, it is concluded that the novel approach of attributive analysis offers coherent results when used to assess the performance of washing tests for soil affected by multicomponent pollution. Moreover, the "success score" provides complementary information to evaluate the results, taking into account not only the different scenarios contemplated in the RBSSLs but also the separation performance per element, that is to say the treatability of each element. The methodologies reported herein can be used not only for soil washing purposes, but also to support the design of efficient industrial plants, thus reducing final waste disposal and emissions while at the same time maximizing product outputs.

Acknowledgements

This research was funded by the project LIFE I + DARTS (LIFE11 ENV/ES/000547). Carlos Boente obtained a grant (FPU014/02215) from the "Formación del Profesorado Universitario" program, financed by the "Ministerio de Educación, Cultura y Deporte de España". Carlos Sierra received a Prometeo visiting faculty grant (20150359 BP) from the SENESCYT (Government of Ecuador).

References

Abumaizar, R.J., Smith, E.H., 1999. Heavy metal contaminants removal by soil washing. J. Hazard. Mater. 70, 71–86.
Adamo, P., Mingo, A., Coppola, I., Motti, R., Stinca, A., Agrelli, D., 2014. Plant colonization of brownfield soil and post-washing sludge: effect of organic amendment and environmental conditions. Int. J. Environ. Sci. Technol. 12, 1811–1824.
Anderson, R., Rasor, E., Van Ryn, F., 1999. Particle size separation via soil washing to obtain volume reduction. J. Hazard. Mater. 66, 89–98.
BOPA, Boletín Oficial del Principado de Asturias, 91, April 21, 2014. Generic reference levels for heavy metals in soils from Principality of Asturias, Spain. http://sede.asturias.es/bopa/2014/04/21/2014-06617.pdf (accessed Sept 2016).
Bulut, G., Yenial, Ü., Emiroğlu, E., Sirkeci, A.A., 2013. Arsenic removal from aqueous solution using pyrite. J. Clean. Prod. 84, 526–532.
Cappuyns, V., 2013. Environmental impacts of soil remediation activities: quantitative and qualitative tools applied on three case studies. J. Clean. Prod. 52, 145–154.
Clemens, S., 2006. Toxic metal accumulation, responses to exposure and mechanisms of tolerance in plants. Biochimie 88, 1707–1719.
Dallaire, R., Laplante, A.R., Elbrond, J., 1978. Humphrey's spiral tolerance to feed variations. Cim. Bull. 71, 128–134.
D'Aquin, G.E., Fell, R.C., 2012. Sulfur and sulphuric acid. In: Kent, J.A. (Ed.), Handbook of Industrial Chemistry and Biotechnology, twelfth ed. Springer, New York, pp. 997–1015.
Dermont, G., Bergeron, M., Mercier, G., Richer-Laflèche, M., 2008. Soil washing for metal removal: a review of physical/chemical technologies and field applications. J. Hazard. Mater. 152, 1–31.
Di Maria, F., Micale, C., Sordi, A., Cirulli, G., Marionni, M., 2013. Urban mining: quality and quantity of recyclable and recoverable material mechanically and physically extractable from residual waste. Waste Manag. 33, 2594–2599.
Fan, C.H., Zhang, Y.C., Du, B., He, L., Wang, J.H., 2015. Spectrum characteristics of leaching components from Co-Contaminated loess in ex-situ column washing reaction. Spectrosc. Spectr. Anal. 35, 447–452.
Gallego, J.R., Rodríguez-Valdés, E., Esquinas, N., Fernández-Braña, A., Afif, E., 2016. Insights into a 20-ha multi-contaminated brownfield megasite: an environmental forensics approach. Sci. Total Environ. 563, 683–692.
Gupta, A., Yan, D.S., 2006. Mineral Processing Design and Operation. Elsevier Science, Amsterdam.
Hou, D., Al-Tabbaa, A., Guthrie, P., Hellings, J., Gu, Q., 2014. Using a hybrid LCA method to evaluate the sustainability of sediment remediation at the London Olympic Park. J. Clean. Prod. 83, 87–95.
Klima, M.S., Kim, B.H., 1998. Dense-medium separation of heavy-metal particles from soil using a wide- angle hydrocyclone. J. Environ. Sci. Heal. Part A Toxic Hazard. Subst. Environ. Eng. 33, 1325–1340.
Li, Y.M., Lei, M., Chen, T. Bin, Yang, J., Zhou, X.Y., Wang, Y.W., 2013. Optimized EDTA washing procedure to decontaminate heavy metals from soils in iron and steel works sites. Asian J. Chem. 25, 37–41.
Ma, L., Yang, Q., Huang, Y., Qian, P., Wang, J.G., 2013. Pilot test on the removal of coke powder from quench oil using a hydrocyclone. Chem. Eng. Technol. 36, 696.
Mann, M.J., 1999. Full-scale and pilot-scale soil washing. J. Hazard. Mater. 66, 119–136.
Mercier, G., Duchesne, J., Blackburn, D., 2001. Prediction of metal removal efficiency from contaminated soils by physical methods. J. Environ. Eng. Rest. Va. 127, 348–358.
Nieuwoudt, D.J., Deventer, J.S.J. Van, Reuter, M.A., Ross, V.E., 1990. The influence of design variables on the flotation of pyrite in an air-sparged hydrocyclone. Min. Eng. 3, 483–499.
Oliveira, Marcos L.S., Ward, Colin R., Izquierdo, Maria, Sampaio, Carlos H., de Brum, Irineu A.S., Kautzmann, Rubens M., Sabedot, Sydney, Querol, Xavier, Silva, Luis F.O., 2012. Chemical composition and minerals in pyrite ash of an abandoned sulphuric acid production plant. Sci. Total. Environ. 430, 34–47.
Pansu, M., Gautheyrou, J., 2007. Handbook of Soil Analysis: Mineralogical, Organic and Inorganic Methods. Springer Science & Business Media.
Pearl, M., Pruijn, M., Bovendeur, J., 2006. The application of soil washing to the remediation of contaminated soils. Land Contam. Reclam. 14, 713–726.
Sierra, C., Gallego, J.R., Afif, E., Menéndez-Aguado, J.M., González-Coto, F., 2010. Analysis of soil washing effectiveness to remediate a brownfield polluted with pyrite ashes. J. Hazard. Mater 180, 602–608.
Sierra, C., Menéndez-Aguado, J.M., Afif, E., Carrero, M., Gallego, J.R., 2011. Feasibility study on the use of soil washing to remediate the As-Hg contamination at an ancient mining and metallurgy area. J. Hazard. Mater 196, 93–100.
Sierra, C., Gallego, J., Gutiérrez, S., Menéndez-Aguado, J.M., 2012. Concentration Optimization Software. Available at: https://www.researchgate.net/profile/Carlos_Sierra18/publications.
Sierra, C., Martínez, J., Menéndez-Aguado, J.M., Afif, E., Gallego, J.R., 2013. High intensity magnetic separation for the clean-up of a site polluted by lead metallurgy. J. Hazard. Mater. 248–249, 194–201.
Sierra, C., Boado, C., Saavedra, A., Ordóñez, C., Gallego, J.R., 2014a. Origin, patterns and anthropogenic accumulation of potentially toxic elements (PTEs) in surface sediments of the Avilés estuary (Asturias, northern Spain). Mar. Pollut. Bull. 86, 530–538.
Sierra, C., Martínez-Blanco, D., Blanco, J., Gallego, J.R., 2014b. Optimisation of magnetic separation: a case study for soil washing at a heavy metals polluted site. Chemosphere 107, 290–296.
Svoboda, J., 2004. Magnetic Techniques for the Treatment of Materials. Springer Science & Business Media.
Wang, J., Feng, X., Anderson, C.W.N., Xing, Y., Shang, L., 2012. Remediation of mercury contaminated sites - a review. J. Hazard. Mater. 221–222, 1–18.
Wills, B., Napier-Munn, T., 2006. Mineral Processing Technology: An Introduction to the Practical Aspects of Ore Treatment and Mineral Recovery. Butterworth-Heinemann.
Xu, J., Kleja, D.B., Biester, H., Lagerkvist, A., Kumpiene, J., 2014. Influence of particle size distribution, organic carbon, pH and chlorides on washing of mercury contaminated soil. Chemosphere 109, 99–105.
Yang, C., Chen, Y., Peng, P.A., Li, C., Chang, X., Wu, Y., 2009. Trace element transformations and partitioning during the roasting of pyrite ores in the sulfuric acid industry. J. Hazard. Mater. 167, 835–845.
Yang, Q., Li, Z.M., Lv, W.J., Wang, H.L., 2013. On the laboratory and field studies of removing fine particles suspended in wastewater using mini-hydrocyclone. Sep. Purif. Technol. 110, 93–100.

III.II Nanoscale zero-valent iron-assisted soil washing for the removal of potentially toxic elements

---

C. Boente, C. Sierra, D. Martínez-Blanco, J.M. Menéndez-Aguado, J.R. Gallego

Journal of Hazardous Materials (2018)

Volume 350, May 2018, Pages 55-65

Rank: 14 out of 109 (1st Quartile) in *Environmental Chemistry* (JCR)

Journal of Hazardous Materials 350 (2018) 55–65

Contents lists available at ScienceDirect

Journal of Hazardous Materials

journal homepage: www.elsevier.com/locate/jhazmat

Nanoscale zero-valent iron-assisted soil washing for the removal of potentially toxic elements

C. Boente[a], C. Sierra[b], D. Martínez-Blanco[c], J.M. Menéndez-Aguado[a], J.R. Gallego[a,*]

[a] INDUROT and Environmental Biotechnology & Geochemistry Group, University of Oviedo, C/Gonzalo Gutiérrez Quirós s/n, 33600 Mieres, Asturias, Spain
[b] Escuela Politécnica de Ingeniería de Minas y Energía, University of Cantabria, Boulevard Ronda Rufino Peón no 254, 39316 Torrelavega, Spain
[c] Servicio Científico-Técnico de Medidas Magnéticas, University of Oviedo, C/Gonzalo Gutiérrez Quirós. s/n, 33600 Mieres, Asturias, Spain

GRAPHICAL ABSTRACT

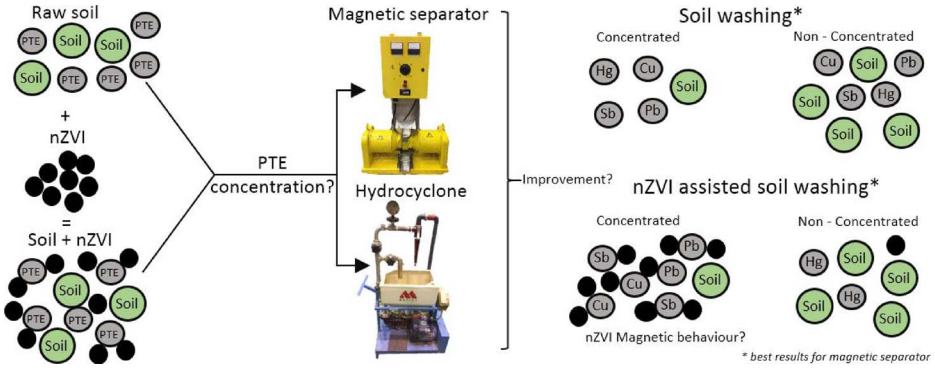

ARTICLE INFO

Keywords:
Soil remediation
Nanoscale zero-valent iron
Soil washing
PTEs

ABSTRACT

The present study focuses on soil washing enhancement via soil pretreatment with nanoscale zero-valent iron (nZVI) for the remediation of potentially toxic elements. To this end, soil polluted with As, Cu, Hg, Pb and Sb was partitioned into various grain sizes (500–2000, 125–500 and < 125 μm). The fractions were pretreated with nZVI and subsequently subjected, according to grain size, to Wet-High Intensity Magnetic Separation (WHIMS) or hydrocycloning. The results were compared with those obtained in the absence of nanoparticles.

An exhaustive characterization of the magnetic signal of the nanoparticles was done. This provided valuable information regarding potentially toxic elements (PTEs) fate, and allowed a metallurgical accounting correction considering the dilution effects caused by nanoparticle addition.

As a result, remarkable recovery yields were obtained for Cu, Pb and Sb, which concentrated with the nZVI in the magnetically separated fraction (WHIMS tests) and underflow (hydrocyclone tests). In contrast, Hg, concentrated in the non-magnetic fraction and overflow respectively, while the behavior of As was unaltered by the nZVI pretreatment. All things considered, the addition of nZVI enhanced the efficiency of soil washing, particularly for larger fractions (125–2000 μm). The proposed methodology lays the foundations for nanoparticle utilization in soil washing operations.

* Corresponding author.
E-mail address: jgallego@uniovi.es (J.R. Gallego).

https://doi.org/10.1016/j.jhazmat.2018.02.016
Received 2 November 2017; Received in revised form 24 January 2018; Accepted 5 February 2018
Available online 09 February 2018

1. Introduction

Potentially toxic elements (PTEs) are a major cause of contamination in soils of cities and rural areas. The concept of PTE encompasses a wide selection of elements (As, Cu, Hg, Pb, Zn, among others) that in high concentrations might cause severe damage to the environment and also to the human health [1,2]. Their persistence in the environment and the ease with which they bioaccumulate and biomagnify in living organisms make them pollutants of special concern [3]. PTEs may derive from natural sources or anthropogenic sources such as mining, industry or traffic [4,5]. In soils they usually appear linked to industrial and chemical waste, or even atmospheric deposition [6]. They enter tissues via ingestion, breathing and touching and cause severe diseases [7]. For all these reasons, their removal has been widely discussed in environmental research over recent decades [8–10].

Of all the remediation techniques available [11], soil washing is widely used [12,13]. It is based on concentrating the contaminants into a reduced volume fraction of the affected soil (or concentrated fraction), thereby leaving the matrix decontaminated (non-concentrated fraction) [14]. The method embraces two contaminant-removal technologies, namely, physical separation, which is based on mineral processing technologies, and chemical extraction, which is based on hydrometallurgy [15].

Here we focused on physical soil washing, that is to say, those procedures that do not alter the chemical properties of materials [12]. In these cases, separation is achieved by means of differences in the physical properties, namely particle size, density, magnetic susceptibility, or even physicochemical properties, as is the case of froth floatation, between the soil and the contaminant [16]. This technique has several advantages, including ease of deployment and versatility to be combined in sequence with other physical and chemical remediation methods [17]. In this context, some researchers have used remediation techniques that combine soil washing together with phytoremediation [18,19], stabilization [20], electrokinetics [21] or ultrasonics [22].

Moreover, the addition of certain compounds such as surfactants [23] and chelants to soil washing enhances PTE recovery [24]. In this respect, nanoscale zero-valent iron (nZVI) is the most commonly used nanomaterial for remediation purposes in Europe and the United States [25,26]. It is a non-toxic reactive metal (as a result of its large surface area, among other factors) that has found wide applications due to its abundance, low cost and ease of production [27]. This remediation material has been successfully applied for the removal of PTEs not only from soils [28–30] but from groundwater [31–34] and water runoff [35].

The applications of nZVI for PTE decontamination of soil are diverse. In this regard, this nanomaterial can be used to immobilize, sorb and capture these compounds [36]. Within this context, nanoparticles enhance soil washing by adsorption of the PTE-containing particles, thereby causing the formation of larger and heavier aggregates which are easier to separate [37]. Regarding magnetic separation, the high magnetic susceptibility of the newly formed aggregates allows the separation of otherwise non-magnetic particles [11,12].

This study aims to evaluate the effect of nZVI as a pre-treatment to a subsequent soil washing process. Thus, the specific objectives were as follows:

- To introduce a procedure that allows the measurement of the amount of natural Fe and nZVI present in each studied fraction.
- To develop a metallurgical accounting correction that circumvents the dilution effect that the addition of nZVI entails, thus facilitating the comparison of results between experiments with and without pretreatments.
- To ascertain the trace elements for which nZVI is selective, on the basis of their behavior in the separation equipment.

2. Materials and methods

2.1. Site description and soil sampling

Soil samples were collected from the old Hg mine of Olicio, in the surroundings of the Picos de Europa National Park (Asturias, Spain). The geology of the area is framed within the Cantabrian zone, specifically in the Ponga mantle [40]. The lithology comprises mainly paraconglomerates, white quartzites and siltstones from the Ordovician period [41]. The first evidence of cinnabar dates back to the late 19th century, but it was not until 1965 when underground mining began, persisting until the early 1970s, when the Hg crisis occurred. During these years, the extracted mineral was treated in a retort furnace, and ashes and tailings were mindlessly dumped in the confined valley of the Brengues stream [42].

These mining activities covered approximately 8000 m^2 of the valley with waste, thus enriching the surrounding soils in several PTEs, particularly Hg and As. Within this context, 25 bulk soil samples were collected at a depth of between 0 and 30 cm using a Dutch auger. These samples were then pooled into a single “macro sample” of about 50 kg, which was subsequently sieved through a 2-cm screen to remove rocks, gravel, and other large material.

2.2. Soil characterization and chemical analysis

This macro sample was divided obtaining representative subsamples of 500 g each, which were subjected to wet sieving in order to obtain particle-size fractions of < 125, 125–500 and 500–2000 µm. Thus, normalized sieves were placed in a column, and batches of 100 g of the material were placed in a sieve shaker for 5 min with a water flow of 0.3 l/min (ASTM D-422-63, Standard Test Method for Particle-Size Analysis of Soils). pH was measured with a glass electrode in a suspension of soil and deionized water (1:2.5).

Fractions were then laid out on glass trays, dried at 30 °C to prevent Hg volatilization, and finally weighed. Once all the material was meshed, each fraction was split into two equal and representative masses, which were used to perform the experiments with and without nZVI pretreatment.

To standardize the conditions used for chemical determinations, samples > 125 µm were ground in a RS100 Resch mill at 400 rpm for 40 s. Then, 1-g representative subsamples of the diverse origins (soils, grain-size fractions, etc.) were subjected to a 1:1:1 “Aqua regia” digestion. The total concentrations of Ag, Al, As, B, Ba, Bi, Ca, Cd, Co, Cr, Cu, Fe, Ga, Hg, K, La, Mg, Mn, Mo, Na, Ni, P, Pb, S, Sb, Sc, Sr, Th, Ti, Tl, V, W and Zn in the digested material were determined by Inductively Coupled Plasma-Optical Emission Spectroscopy (ICP-OES) at the accredited (ISO 9002) Bureau Veritas Laboratories (Vancouver, Canada).

Powder X-Ray diffraction (PXRD) patterns measured on a PANalytical X’Pert Pro MPD diffractometer with Cu $k_{\alpha 1}$ radiation (1.540598 Å) were used to determine the mineralogical composition of the soil. After determining the position of Bragg peaks observed over the range of 2θ = 5–90°, the minerals were identified using databases of the International Centre for Diffraction Data.

2.3. Nanoscale zero-valent iron pretreatment

A commercial air-stabilized aqueous solution of nZVI (NANOFER STAR-W), supplied by Nano Iron Rajhrad (Czech Republic), was used. This product comprises Fe (0): 14–18%, magnetite ($Fe^{2+}Fe_2{}^{3+}O_4{}^{2-}$): 2–6%, carbon (C): 0–1% and about 80% of water. None of these components are classified as hazardous according to 67/548/EEC and Regulation (EC) N° 1278/2008 (CLP). As quoted by the manufacturer, this product is optimal for the preparation of slurries for in-situ remediation purposes [43].

The addition of nanoparticles followed the same procedure for each of the three grain-sizes. Thus, the nZVI drum provided by the

manufacturer was first vigorously shaken in order to homogenize and suspend the nanoparticles. Then, 1 l of the homogenized liquid was removed from the barrel and mixed with 100 g of polluted soil. This mixture was stirred for 2 h at 400 rpm. The operation was repeated until 10 l of nanoparticle solution had been mixed with 1000 g of raw soil. This material was then laid in glass trays and air-dried at 30 °C in order to prevent nZVI oxidation and Hg evaporation.

Nanoparticles are highly susceptible to oxidation, mainly because of their large surface area. Nonetheless, oxidation was prevented with low drying temperatures and expeditious laboratory experiments. Constant monitoring of the magnetic signal of both soil Fe and nZVI was performed in order to assure the quality of the results.

Soil washing equipment was selected so as to fully exploit the physical properties of nZVI. In this regard, given the high magnetic susceptibility of HIMS, this technique was considered suitable, as was hydrocycloning in the case of the smallest fraction (< 125 μm). Experiments were performed with untreated and nZVI-pretreated soils for the three size fractions. Separation tests were performed in triplicate.

2.4. Magnetic characterization

To this end, about 100 mg of soil fractions were quartered and ground in an agate mortar in order to be compacted and later encapsulated into an acrylic pillbox. After that, the capsule was fixed to an acrylic rod using double-sided Scotch® tape and placed into the linear motor of a Microsense EV9 vibrating sample magnetometer (VSM). We then measured magnetic hysteresis loops (M(H)), which determine magnetization (M) as a function of the magnetic field (H) in a complete cycle between H_{max} = 20 kOe and H_{min} = −20 kOe at room temperature (RT).

Each previous hysteresis loop, defined on the basis of soil grain size and output voltage in the WHIMS, was by pairs corresponding to its mags (magnetically separated fraction) and non-mags (non-magnetically separated fraction) fraction. Thus, the hysteresis loops of each feed (nZVI-pretreated soil samples) were depicted by summing the loops of both the mags and non-mags fractions, which minimized the least-square root difference by means the evolutionary (genetic) method of Microsoft Excel Solver package. In the same manner, the hysteresis loops of each compound (soil treated with nZVI and mags and non-mags fractions) were fitted by adding the corresponding raw soil and pure nZVI, thus determining the percentage of the latter disseminated.

2.5. Wet-high intensity magnetic separation

WHIMS is suitable for the treatment of small grain sizes [44]. It is straightforward to use and provides an excellent yield recovery and ratio of concentration [44]. The OUTOTEC Laboratory WHIMS 3 × 4 L apparatus, which has the capacity to separate paramagnetic (weakly magnetic) from non-magnetic materials was used for the experiments.

The feed for the untreated soil was prepared by mixing 50 g of dried soil with 200 g of water (57.5 g in the case of soil pretreated with nZVI, which represents about 16% of Fe (0) and 230 g of water). This slurry was then passed through a matrix canister filled with steel spheres 12.5 mm or 6.5 mm in diameter (depending on the particle-size of the feed; 12.5-mm spheres are appropriate for soil particle sizes > 125 μm, while 6.5-mm spheres are appropriate for those < 125 μm).

The mags material was retained by the magnetized spheres, while the non-mags components and the water passed across the matrix canister and were collected in a tray. Finally, the magnetic material retained on the spheres was washed out by turning off the equipment, thus reducing the magnetic field to zero.

The variable magnetic field intensity of the equipment was adjusted through the coil input amperage (0–6 amps) [38]. WHIMS was set at 10%, 20%, 30% and 50% of the maximum output voltage for all three fractions (500–2000 μm, 125–500 μm and < 125 μm). Higher voltages may render the process economically unviable and may modify the magnetic properties of nZVI. Experiments were performed for untreated and nZVI-pretreated samples. After separation experiments, samples were dried at 30 °C, then ground and subsequently subjected to chemical determinations.

2.6. Hydrocycloning

The hydrocyclone is one of the most widely used systems for mineral treatment [45]. It separates heavy and light particles via a static piece of equipment that applies a centrifugal force to a liquid (commonly water) that contains the material. This device works in continuous flow mode [46]. The feed to this apparatus is introduced through instantaneous in-flow slurry (feed), which is tangentially pumped inside the cyclone, wherein the joint action of the centrifugal drag and gravity forces separate the particles on the basis of grain size and density [45]. This system determines whether an individual particle flows through the apex (underflow) or the overflow of the hydrocyclone [45,46]. The underflow and overflow comprise the outflow, the sum of which must be equal to the inflow; the lighter and finer particles report to the overflow.

Regarding the current study, a hydrocycloning lab-scale plant (C700 Mozley) with a capacity to operate hydrocyclones from 10 to 50 mm in diameter was used. The solid:water ratio of the slurry feed used in the experiments was constant (1:5), whereas the apex diameters (9.5 mm and 6.5 mm) and working pressures (69 and 138 kPa) were combined (e.g. [47]). The procedure was used to treat the grain size fraction < 125 μm, in accordance with the manufacturer's specifications. In all cases, after reaching a stationary regime, samples from the underflow and overflow were collected in borosilicate flasks and then weighed. Thereafter, they were dried at 30 °C, and representative subsamples were obtained for chemical determinations. Tests were performed in triplicate.

2.7. Evaluation of results

2.7.1. Corrected expressions for weight and element recoveries

The efficiency of the concentration operation was evaluated in terms of two concepts, namely weight recoveries and element recoveries [14]. Both concepts can be referred to any outflow from the WHIMS and hydrocyclone, irrespective of whether they correspond to the concentrated or non-concentrated fractions [48]. Nevertheless, all calculations in this study refer to the concentrated fraction, that is to say, the fraction in which element recovery was higher than weight recovery. In this case, this refers to the magnetic fraction of the WHIMS and the overflow of the hydrocyclone.

The concepts of weight recovery (WR) and element recovery (ER) used in this study were as defined by Wills [15]. These expressions are valid for any soil without nZVI pre-treatment, but nanoparticle addition entails a dilution effect that makes the correction of the above-mentioned equations necessary in terms of facilitating the comparison of results between experiments with and without pretreatments. In this respect, considering that the original amount of Fe of the soil was small (between 0.9–2.6% Fe, see Table 1) compared with that after nZVI pretreatment, the dilution effect was removed by subtracting the weight of Fe. Thus, the corrected weight recovery in the concentrated fraction (WR_c') would be:

$$WR_c' = \frac{w_c - w_c^{Fe}}{w_c + w_{nc} - w_c^{Fe} - w_{nc}^{Fe}} \quad (1)$$

where w_c is the weight of the concentrated fraction and w_{nc} the weight of the non-concentrated fraction, w_c^{Fe} and w_{nc}^{Fe} being the weight of Fe in these fractions respectively. The WR_{nc}' is calculated similarly.

The concentration of the other elements is also altered when the weight of Fe is removed, but this change does not appreciably affect the

Table 1
Particle-size distribution and element concentration of the bulk and initial grain-size fractions (aqua-regia digestion and ICP-OES analysis).

Grain-size fraction	Weight (%)	Element concentration											
		Al (%)	As (ppm)	Ca (%)	Cu (ppm)	Fe (%)	Hg (ppm)	K (%)	La (ppm)	Pb (ppm)	Sb (ppm)	V (ppm)	Y (ppm)
> 2000	50.4	–	–	–	–	–	–	–	–	–	–	–	–
500–2000	11.0	0.6	182.4	2.8	92.6	1.0	73.7	0.3	14.4	22.4	10.4	11.4	15.9
125–500	12.6	0.5	123.0	1.6	63.7	0.9	53.5	0.2	10.3	52.1	9.3	9.8	15.3
< 125	25.9	0.9	380.7	1.6	300.5	2.6	153.8	0.2	17.4	129.4	18.2	24.7	29.5
Bulk	–	0.7	249.0	2.4	88.0	1.6	100.6	0.3	14.0	46.0	13.0	17.0	23.0

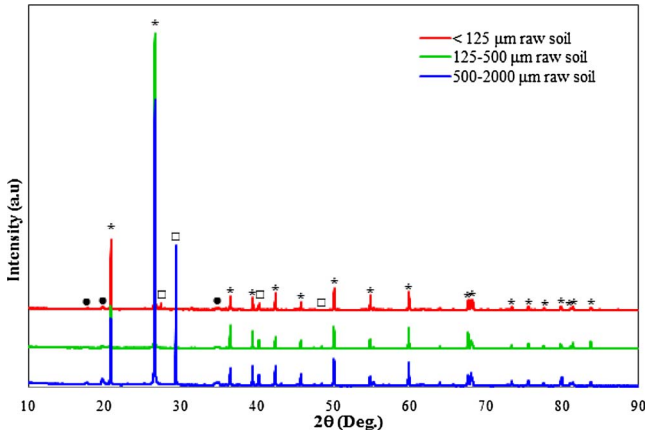

Fig. 1. X-ray diffraction patterns for the raw soil of grain size: 500–2000 µm (blue), 125–500 µm (green) and < 125 µm (red). Characteristic peaks of main crystalline phases identified are indicated as: quartz (*), calcite (□) and muscovite (●).(For interpretation of the references to colour in this figure legend, the reader is referred to the web version of this article).

comparability of the results. The corrected masses of element "i" in the concentrated ($w_c^{i\prime}$) and non-concentrated ($w_{nc}^{i\prime}$) fractions, [i_c] and [i_{nc}] being the concentration of the element "i" in the concentrated fraction, can be calculated as

$$w_c^{i\prime} = WR_c{}' \cdot [i_c] \quad (2)$$

$$w_{nc}^{i\prime} = WR_{nc}{}' \cdot [i_{nc}] \quad (3)$$

where [i_c] and [i_{nc}] is the concentration of element "i" in the concentrated or non-concentrated fraction respectively.

Finally, once $w_c^{i\prime}$ and $w_{nc}^{i\prime}$ have been calculated, the corrected element enrichment factor ($ER_c^{i\prime}$) for element "i" can be obtained as follows

$$ER_c^{i\prime} = \frac{w_c^{i\prime}}{w_c^{i\prime} + w_{nc}^{i\prime}} \quad (4)$$

2.7.2. Determination of nZVI fate by magnetic quantification

The magnetization of the WHIMS feed (M_s) corresponding to the original soil treated with nZVI, i.e. the blend of soil and nanoparticles obtained in the stirring tank before the separation test, was estimated using a linear combination of the measured signal of the original soil fraction (not treated with nanoparticles, denoted as M°) and the signal of the pure nZVI (M^{nZVI}). Thus, the magnetization for the mixture in a magnetic field, "i", can be calculated as:

$$M_s(H_i) = \%_s^{nZVI} \cdot M^{nzVI}(H_i) + (1 - \%_{Ms}^{nZVI}) \cdot M^0(H_i) \quad (5)$$

where the common factor, $\%_s^{nZVI}$, which minimizes the sum of square root difference between the two members for all applied magnetic fields "i" of the M(H) curve, represents the weight percentage of nZVI in the WHIMS feed. Likewise, once all the tests had been performed, magnetization values for the mags (M_M) and non-mags (M_{NM}) fractions were also modeled using analogous equations as follows:

$$M_M(H_i) = \%_M^{nZVI} \cdot M^{nzVI}(H_i) + (1 - \%_M^{nZVI}) \cdot M^0(H_i)$$
$$M_{NM}(H_i) = \%_{NM}^{nZVI} \cdot M^{nzVI}(H_i) + (1 - \%_{NM}^{nZVI}) \cdot M^0(H_i) \quad (6)$$

$\%_M^{nZVI}$ and $\%_{NM}^{nZVI}$ being the weight % of nZVI in the mags and non-mags fractions, respectively.

On the other hand, signals from the mags (M_M) and non-mags (M_{NM}) fractions were also used to reconstruct the previous feed signal (M_s) for each test. In this case, the least-square root fit of data was derived as:

$$M_s(H_i) = \%_M \cdot M_M(H_i) + (1 - \%_M) M_{NM}(H_i) \quad ((7))$$

where $\%_M$ is the proportion of magnetics in the mags. Finally, by combining Eq. (6) and (7), we can also calculate the weight percentage of nZVI in the feed belonging to each pair of mags and non-mags fractions, by means of:

$$\%_s^{nZVI} = \%_M \cdot \%_M^{nZVI} + (1 - \%_M) \cdot \%_{NM}^{nZVI} \quad (8)$$

3. Results and discussion

3.1. Textural and chemical characterization of the soil

X-ray diffraction results (Fig. 1) indicated that the soil samples were composed mainly of quartz (SiO_2), some calcite ($CaCO_3$), and muscovite ($KAl_2(AlSi_3O_{10})(OH)_2$), and probably also hematite (Fe_2O_3), with an unclear presence of dolomite ($CaMg(CO_3)_2$) and microcline ($KAlSi_3O_8$). Table 1 shows the element concentrations for the different grain sizes. pH values measured were slightly alkaline (around 7.5).

The coarser fraction (> 2000 µm) accounted for approximately 50%$_w$ of the bulk soil, followed by the fine fraction (< 125 µm), which accounted for roughly 26%$_w$. The 500–2000 µm and 125–500 µm fractions represented 11%$_w$ and 12%$_w$ respectively. The main potential toxicant in the bulk samples was Hg and to a lesser extent As, Cu and Sb. In the < 125 µm fraction, Pb played an important role.

Chemical determinations revealed that the abovementioned elements were the main environmental threats in the soil. However, the presence of other elements may indicate how they interact with other soil constituents. We therefore also included the following in our analysis: Al as representative of clays; Ca of carbonates; K of feldspars; La and Y of rare earth; V as neutral element (does not associate to any other); and Fe (main component of the nanoparticles).

3.2. Metallurgical accounting

First, corrected weight and element recoveries were calculated in order to compare the efficiency of soil washing with and without the nZVI pretreatment. The results corresponding to the WHIMS are shown in Table 2.

As can be observed, weight recoveries showed great variations after nZVI pretreatment. Thus, classical soil washing yielded corrected weight recoveries ranging from 3% to 20% in the concentrated fraction, whereas values for the pretreated soil ranged from 30% to 76%. In both cases, the greater the output voltage, the larger the weight recovery obtained. Simultaneously, higher voltages provided a slight improvement in element recoveries. In this respect, an increase in field intensity

Table 2
Results for WHIMS experiments. WR_c' designates the corrected weight recovery in the concentrated fraction and $ER_c^{i'}$ the corrected element recoveries for PTEs. In the case of Fe, uncorrected ERic values had to be used. Results correspond to the average of three measurements with a standard error < 3%.

Grain-size fraction (μm)	WHIMS Voltage (% of the maximum output)	Soil washing							nZVI-assisted soil washing						
		WR_c' (%)	ER_c^i	$ER_c^{i'}$					WR_c' (%)	ER_c^i	$ER_c^{i'}$				
			Fe	As	Cu	Hg	Pb	Sb		Fe	As	Cu	Hg	Pb	Sb
500–2000	**10**	8	3.22	24	19	4	14	18	55	14.30	59	76	37	62	61
	20	14	2.85	35	25	9	16	29	60	18.00	66	78	66	82	71
	30	17	3.17	41	40	6	36	38	69	14.10	75	94	45	86	82
	50	20	3.21	49	41	7	43	45	76	7.07	80	92	46	87	82
125–500	**10**	5	3.96	16	17	2	25	17	30	25.70	31	78	10	36	45
	20	6	4.10	20	13	3	20	20	43	21.70	44	85	21	50	60
	30	8	4.25	28	22	4	30	27	37	20.40	41	81	19	49	55
	50	10	4.14	36	30	5	40	31	51	20.90	56	89	27	62	70
< 125	**10**	3	7.24	9	8	4	11	12	35	21.80	37	59	39	42	43
	20	6	7.68	18	14	6	24	22	47	20.10	51	68	48	55	56
	30	7	7.41	17	14	7	19	22	60	17.40	60	75	65	66	67
	50	8	7.13	20	16	8	22	25	51	22.00	54	74	49	57	61

has to be seen as a trade-off between the previous facts, as well as the subsequent larger weight recovery in the concentrated fraction and higher power consumption.

Regarding the corrected element recoveries, significant improvement after nZVI pretreatment was achieved for all the elements studied. It is important to indicate that all element recoveries were corrected to minimize the effect of nanoparticle addition on the comparability of results with those of untreated samples. In this respect, Fe recovery was greatly increased for the nZVI-assisted concentration experiments as recoveries for this element cannot be corrected by subtracting the concentration of Fe.

In must be indicated that element recoveries rose in parallel to weight recovery. Since the aim of the concentration operation is to achieve high element recoveries for the smallest possible weight recoveries, a new trade-off between the two variables has to be established. This optimum could possibly be at around 30% of the maximum output voltage.

The best results in grain-size terms were obtained for the pretreated 500–2000 μm fraction (Table 2), with significantly high recoveries of Cu (> 90%), Pb (> 80%) and Sb (60–70%). Results were similar for the pretreated 125–500 μm fraction, Cu being the element with the greatest recovery (around 90%) for a repeatable mass of soil (30–40%). The previous experiments did not present appropriate concentration yields for the < 125 μm fraction. Therefore, a set of hydrocycloning tests was performed for this fraction (Table 3).

As occurred for the WHIMS assays, the immediate effect of nZVI pretreatment was an increase in weight and element recovery. However, although the pretreatment produced remarkable improvements in the hydrocycloning of this fraction (< 125 μm), the results were more modest than those of WHIMS. In this regard, smaller apex diameters translated into greater recoveries, although an increase in operating pressure did not lead to appreciable variations but may result in greater equipment abrasion. All things considered, although the performance of the separator was enhanced after nZVI pretreatment and certain selectiveness over Pb, Cu and Sb was observed, element recoveries as compared to weight recoveries were not as remarkable as in the WHIMS device, thus indicating poorer upgrading. These results are further discussed in the next section.

3.3. Nanoscale zero-valent Fe selectivity

nZVI Fe selectivity with regard to PTEs can be easily visualized by plotting $ER_c^{i'}$ vs. WR_c' and determining the separation between the represented points from the perfect splitting line ($ER_c^{i\prime} = WR_c\prime$). Thus, points along this line are undesirable since separation does not take place and, conversely, the further the distance of a point from the "perfect splitting" line, the better the concentration levels obtained.

Moreover, this line divides the figures into two triangles. The one on the top is the domain of the concentrated elements, that is to say, those elements that tend to accumulate in the mags fraction (WHIMS) or the overflow (hydrocyclone). In contrast, the area below the perfect splitting line comprises the elements that tend to accumulate in the non-mags fraction or in the underflow.

3.3.1. Wet-high intensity magnetic separation

In all experiments (Figs. 2–4) there are two clusters of points, the left one (circles) corresponding to traditional soil washing tests and the right one (crosses) to the nZVI-enhanced tests. Both clusters are clearly separated, thereby indicating that the addition of nanoparticles had a strong effect on the separation. Moreover, more elements scattered from the non-concentration line after nZVI pretreatment, thus revealing that the addition of this nanomaterial enhances concentration.

By size intervals, in the 500–2000 μm fraction (Fig. 2), nZVI pretreatment enhanced Cu, Pb and Sb concentration in the mags fraction

Table 3
Results for hydrocycloning experiments for the < 125 μm fraction under different conditions. WR_c' indicates the corrected weight recovery in the concentrated fraction. $ER_c^{i'}$ represents the corrected element recoveries for PTEs except for Fe (uncorrected). Results correspond to the average of three measurements with a standard error < 3%.

Assay conditions		Soil washing							nZVI-assisted soil washing						
Apex diameter (mm)	Pressure (kPa)	WR'c	ER_c^i (%)	$ER_c^{i'}$ (%)					WR'c	ER_c^i (%)	$ER_c^{i'}$ (%)				
			Fe	As	Cu	Hg	Pb	Sb		Fe	As	Cu	Hg	Pb	Sb
6.4	68.95	18	5.32	27	31	20	33	25	38	21.30	46	60	37	51	45
6.4	137.90	22	5.37	33	41	27	40	30	25	21.40	31	43	24	35	33
9.5	68.95	16	5.30	26	28	20	31	24	28	21.50	31	44	24	38	35
9.5	137.90	12	5.48	16	20	15	23	19	25	21.70	31	40	22	33	30

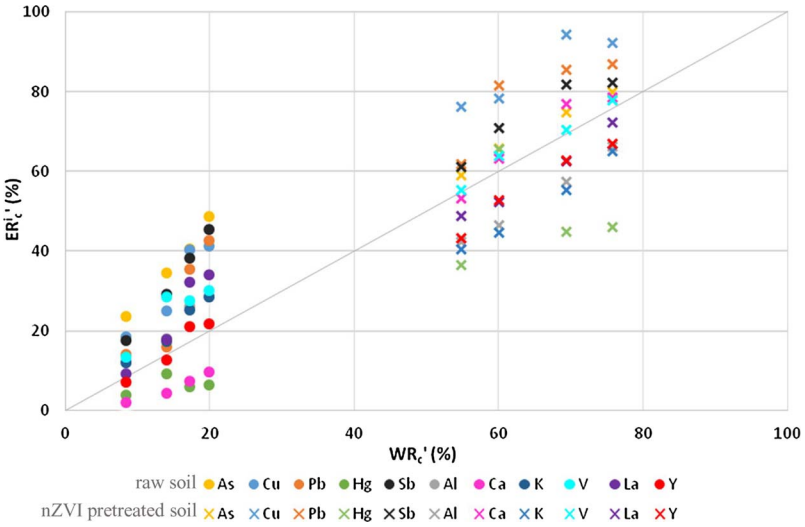

Fig. 2. Corrected element recovery vs. corrected weight recovery for the 500–2000 µm fraction after WHIMS. Crosses and circles and represent experiments with and without nZVI pretreatment, respectively. Vertical alignments correspond, from left to right, to increasing output voltages.

and Hg in the non-mags fraction; while As showed better yields in the untreated tests than under nZVI pretreatment. Moreover, Al, K, and La and Y, representative of clays, feldspars, rare earth, respectively and which were not concentrated in the mags fraction by traditional soil washing, concentrated in the non-mags fraction after addition of nZVI. Conversely, Ca, which is generally prone to concentrating in the non-mags fraction, lost this tendency. Finally, V seemed unaffected by nZVI pretreatment.

The 125–500 µm fraction (Fig. 3) showed similar results. Thus, Cu yielded better concentrations, as did Sb and Pb after pretreatment with nanoparticles. Note that all the PTEs accumulated in the mags fraction, with the exception of Hg, which was markedly concentrated in the non-mags fraction with other elements such as Al and rare earths. This observation suggests that nZVI repels Hg-containing particles (mostly of cinnabar).

The thickest fraction (< 125 µm) presented several differences with regards to the preceding ones (Fig. 4). Thus, it was difficult to concentrate any of the elements, the only exception being Cu. This observation could be explained as magnetic forces can be overcome by dragging forces for the smallest grain sizes [39]. Despite this drawback, the positive effects of nZVI on separation were once again observed.

All things considered, we conclude that the nanoparticles were selective for Cu, Pb and Sb in the 125–2000 µm size range. Moreover, Hg was also concentrated in this size interval but in the non-mags fraction. As regards the < 125 µm fraction, a certain degree of selectivity was observed but the separation efficiency diminished with grain size.

A proper discussion on PTEs mobility in soils is complex and commonly associated with adsorption and desorption processes as well as to precipitation with Al, Fe and Mn oxides (e.g.: [49,50]). In this context, in our case, we hypothesized the relevance of the amount of magnetite in the nanoparticles applied. In general, iron oxides adsorption capacities are greatly influenced by the redox conditions, the presence of other ions and the pH. Particularly, adsorption mechanisms of metals on magnetite are mainly due to the electrostatic attraction between the metallic ions and nanoparticles, being the hydrated ionic radius of cations a key parameter [51]. Magnetite is an amphoteric solid which may adsorb either negatively or positively charged species depending on pH variations. Magnetite surface has a positive charge at pH below 6.7–7 with prevalence of $FeOH^{2+}$ on its surface, and negative when the pH is higher and groups FeO^{-} are predominant [15]. As a consequence, for most PTEs (metals), magnetite adsorption efficiency increases with rising pH because they are prone to be in cationic form; on the contrary,

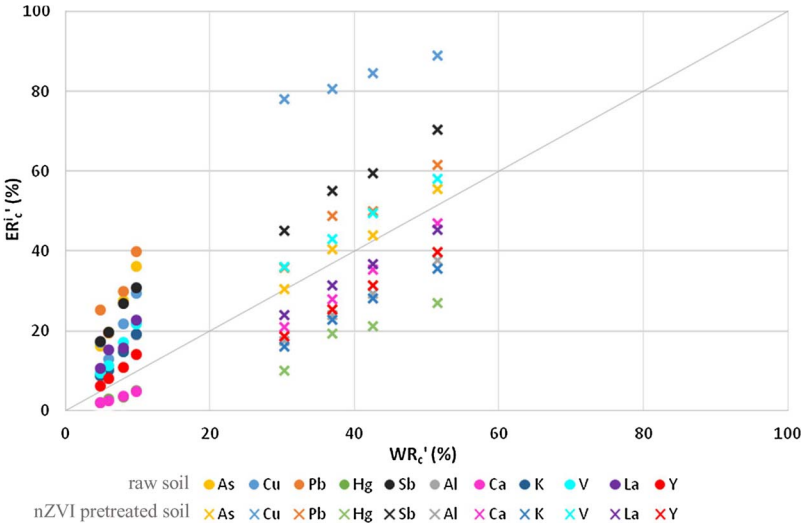

Fig. 3. Corrected element recovery vs. corrected weight recovery for the 125–500 µm fraction after WHIMS. Crosses and circles and represent experiments with and without nZVI pretreatment, respectively. Vertical alignments correspond, from left to right, to increasing output voltages.

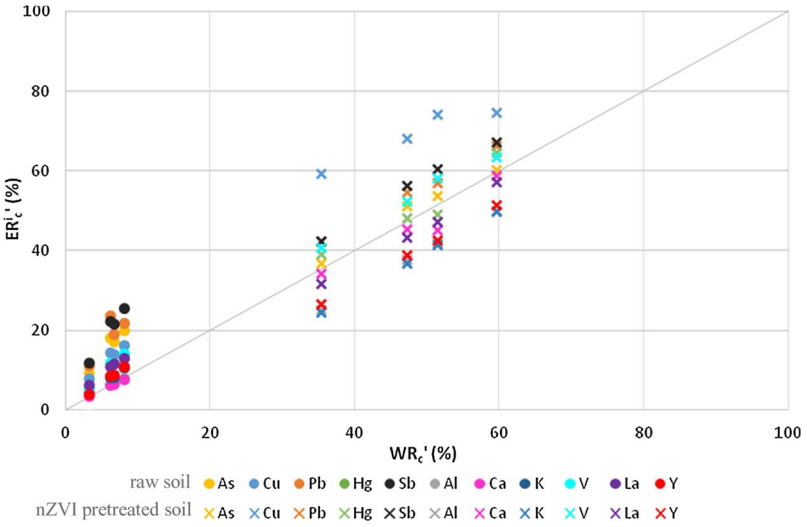

Fig. 4. Corrected element recovery vs. corrected weight recovery for the < 125 µm fraction after WHIMS. Crosses and circles and represent experiments with and without nZVI pretreatment, respectively. Vertical alignments correspond, from left to right, to increasing output voltages.

As is mostly present in the form of oxyanions [51,52] when the pH is slightly alkaline as occur in this work. Therefore, As behavior is different, as electrostatic repulsion between the arsenates and magnetite (with a net negative charge) hinders adsorption [53]. Moreover, As could co-precipitate with Fe (III) ions forming amorphous Fe arsenates and secondary oxidation minerals [54]. On the whole, maximum adsorption capacity of As on Fe oxides may occur at pH between 4 and 6 [55–57]. In addition, it has to be also pointed out that reliable adsorption determinations are complex at neutral or alkaline pH as a consequence of cations precipitation as hydroxides [51].

Concerning the preference of Hg for the non-mags fraction, it has to be considered that in the studied soil the Hg predominant form is cinnabar [48]. This mineral has mainly on its surface exposed hydroxyl sites and sulfide groups [58] which are negatively charged at pH above 3–4 [59] thus hindering sorption on magnetite surface.

3.3.2. Hydrocyclone

Given the unsatisfactory concentration yields obtained for the < 125 µm fraction, hydrocycloning was also tested. In this respect, a hydrocycloning test without nZVI pretreatment did not provide a significant improvement in separation yields. Moreover, samples pretreated with nZVI did not show a clear separation of elements, with all the points placed near or along the perfect splitting line and untreated and pretreated point clusters located very close as shown in Fig. 5.

In this respect, it must be commented that Cu was concentrated only when the nZVI particles were added. This observation suggests that the hydrocyclone showed less effectiveness as a concentrator compared with WHIMS even under nZVI pretreatment conditions. Regarding the interaction of nanoparticles with the PTEs, the positions of Cu and Hg showed variations with respect to the non-concentration line, as occurred for WHIMS, thereby evidencing that nZVI preferentially interacts with these two elements.

3.4. Magnetic quantifications

3.4.1. Magnetic signals of the nZVI, soil and feeds

Fig. 6 shows the hysteresis loops of: a) pure nZVI, b) raw soil and c) nZVI-pretreated soil when fed to the separating apparatus. Each hysteresis loop is depicted on the basis of soil grain-size: 500–2000 µm (blue), 125–500 µm (green) and < 125 µm (red).

In this respect, a relative low difference in magnetic susceptibility (below 0.5%) was observed in pure nZVI, as reflected by identical shape of the curves (Fig. 6a). This observation suggests that the distribution of the nanoparticles in the feed was homogeneous. Moreover, the hysteresis loops of the raw soil samples differed considerably in terms of both maximum magnetization value and form, with signals

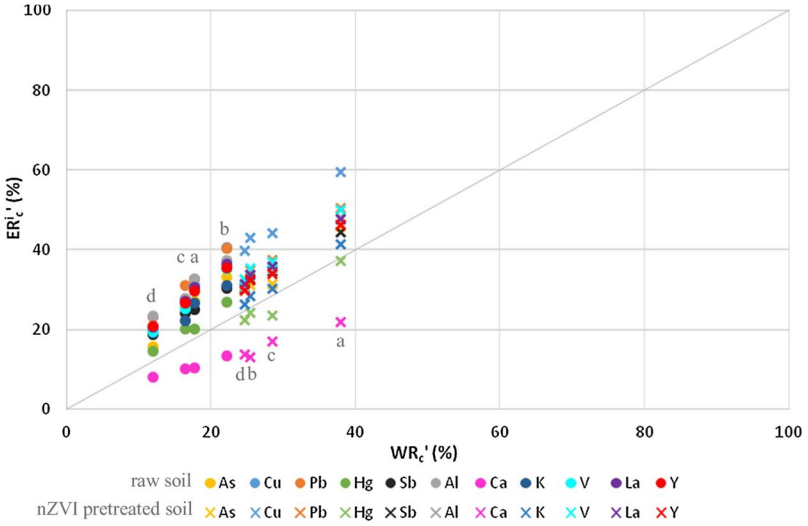

Fig. 5. Corrected element recovery vs. corrected weight recovery for the < 125 µm fraction after treatment with the hydrocyclone. Crosses and circles and represent experiments with and without nZVI pretreatment, respectively. Vertical alignments correspond to a) 6.4 mm apex diameter and 68.95 kPa; b) 6.4 mm apex diameter and 137.90 kPa; c) 9.5 mm apex diameter and 68.95 kPa; d) 9.5 mm apex diameter and 137.90 kPa.

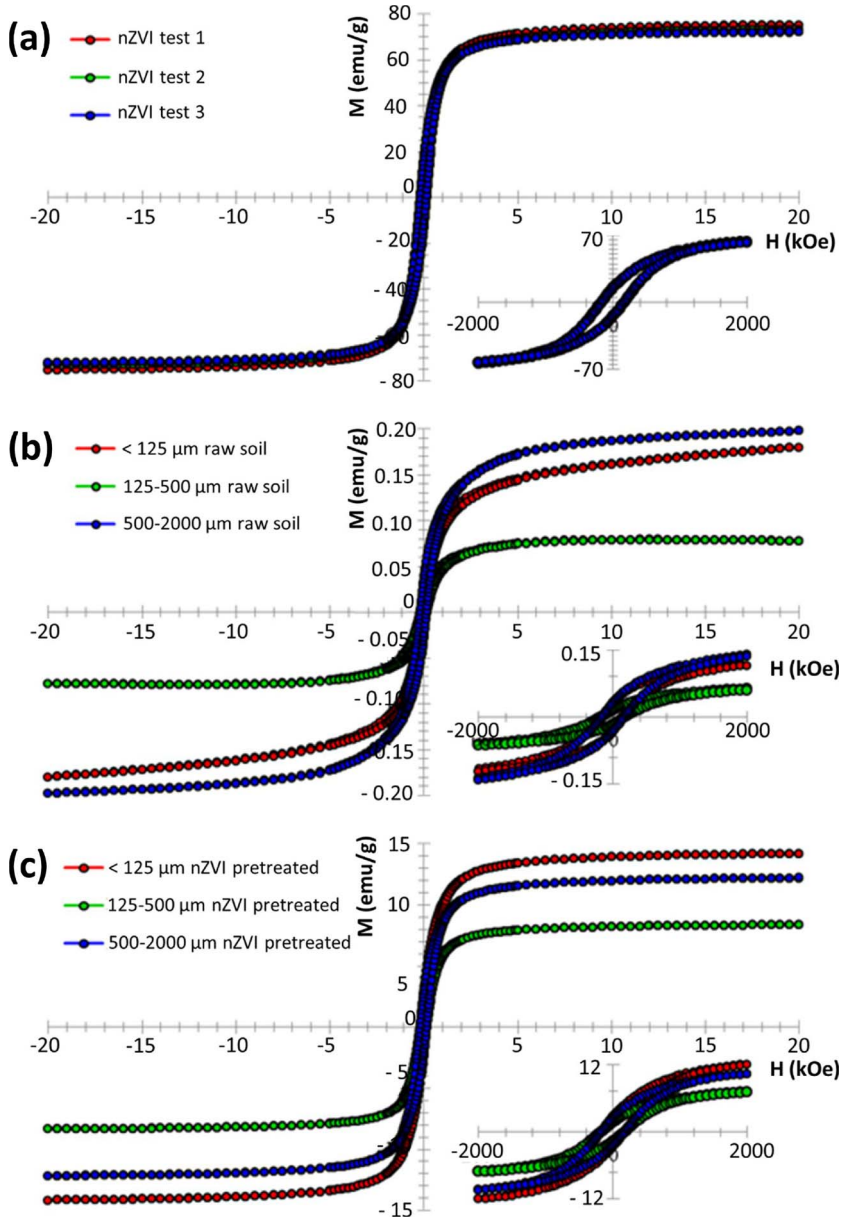

Fig. 6. Hysteresis loops of: a) pure nZVI, b) raw soil, and (c) nZVI pretreated soil. M, is the specific magnetization; and H, the magnetic field applied. Grain size: 500–2000 µm (blue), 125–500 µm (green) and < 125 µm (red). Bottom right loops indicate the magnification of the central section of the loop. (For interpretation of the references to colour in this figure legend and text, the reader is referred to the web version of this article).

approximately 1/400-1/1000 smaller than those registered for pure nZVI (Fig. 6b).

The medium fraction of the raw soil had a significantly smaller magnetic signal, while the larger fraction had the highest signal (Fig. 6b). Once the nZVI was added, the red line became the most prominent, thereby revealing that the < 125 µm grain-size fraction had the highest proportion of nZVI (Fig. 6c). Moreover, this figure evidences that aggregation of nZVI in the soil was heterogeneous, as curves showed different shapes and magnetic signals.

All things considered, the linear combination of the pure nZVI signal and that of the raw soil (Eq. 5) allowed the reconstruction of nZVI concentration in each feed. Thus, the magnetic signals indicated higher concentration for the finest grain size (18.52% < 125 µm), intermediate for the largest grain size (16.50%, 500–2000 µm) and lower for the medium grain size (11.27%, 125–500 µm). These results highlight how nanoparticle coalescence hinders the achievement of a homogenous soil-nanoparticle mixture.

Once the concentration experiments were completed, the magnetic signals of the mags and non-mags fractions were measured and the magnetic signal of the feed was reconstructed using Eq. 6. Figs. 7 and 8 show the signals of the two separated fractions (mags and non-mags) for all the experiments.

Regarding the hysteresis loops of the mags fraction, the maximum signal (corresponding to the highest concentration of nZVI) was obtained for the 500–2000 µm and 125–500 µm fractions at 30% of the maximum output voltage (Fig. 7, column C). When chemical analyses were taken into consideration, the highest element recoveries for relatively low weight recoveries were also obtained for this voltage. High element recoveries at this voltage suggest that nZVI acted as a PTE scavenger, as PTE recovery was related to the recovery of nZVI. This observation is also confirmed by the finding that the greater the magnetization (or nanoparticle content), the higher the recovery of Cu, Pb and Sb for a fixed grain size (Fig. 7, rows A', B' and C').

Furthermore, as shown in B' and C', increasing the maximum output voltage over 30% did not promote nZVI recovery—and subsequently more PTEs—in the mags fraction. Conversely, the magnetization for

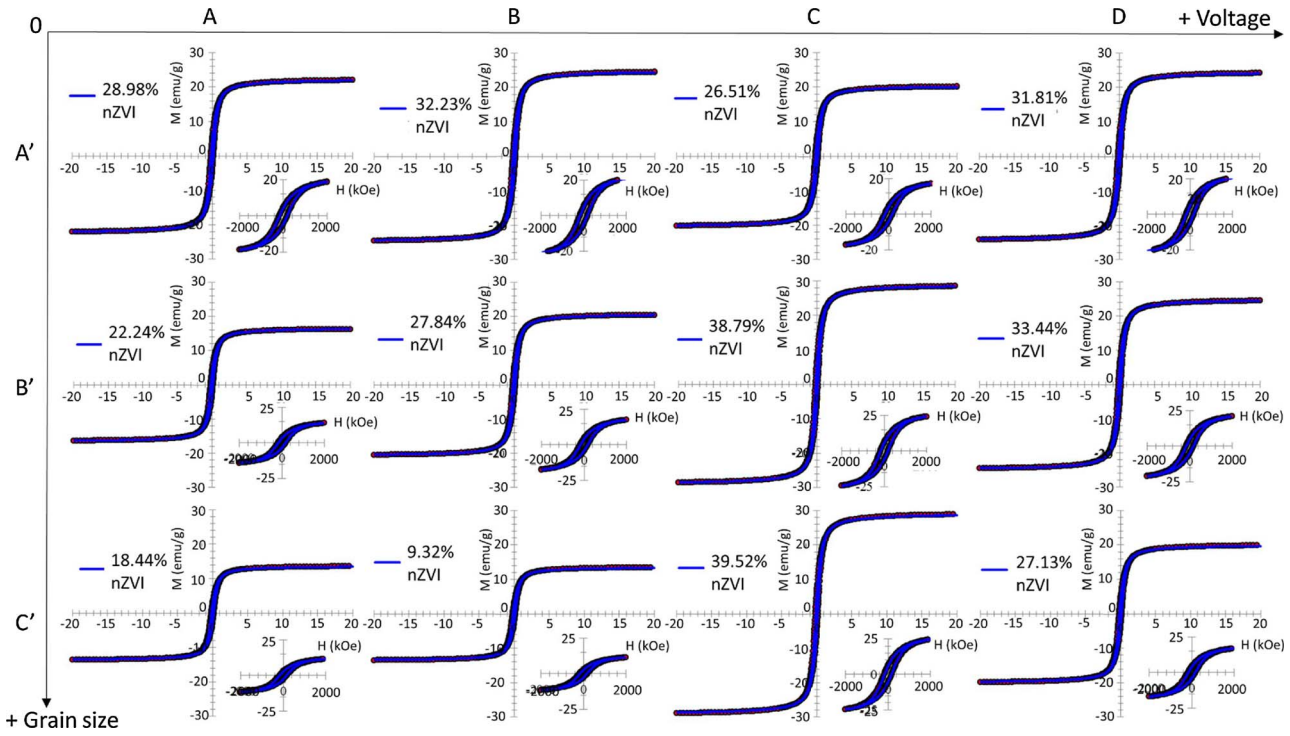

Fig. 7. M(H) curves for magnetic fractions of the feeds after WHIMS. Hysteresis loops are arranged in rows by grain size: A': < 125 μm, B': 125–500 μm and C': 500–2000 μm; and in columns by percentages of maximum output voltage: A (10%), B (20%), C (30%) and D (50%). Bottom right loops are the magnification of the central section of the loop. % values correspond to the weight % of nZVI in the mags fraction.

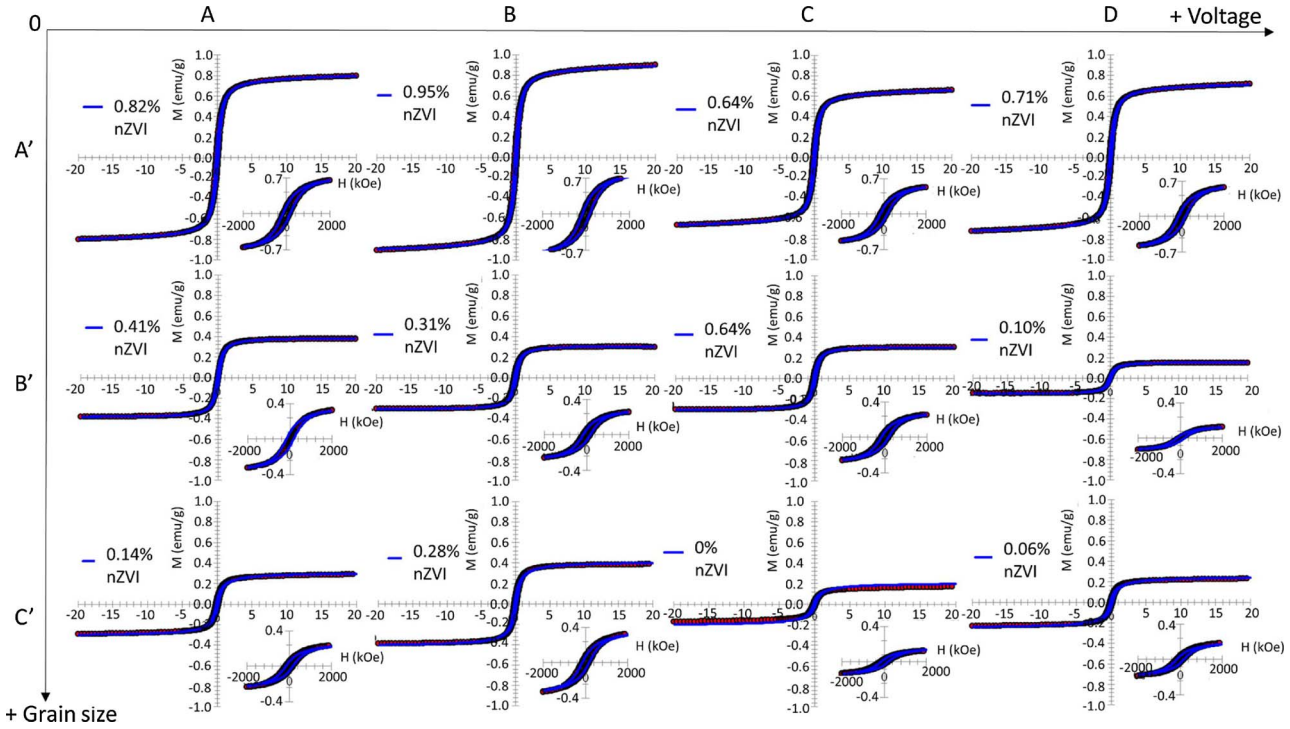

Fig. 8. M(H) curves for non-magnetic fractions of the feeds after WHIMS. Hysteresis loops are arranged in rows by grain size: A': < 125 μm, B': 500–125 μm and C': 500–2000 μm; and in columns by percentages of maximum output voltage: A (10%), B (20%), C (30%) and D (50%). Bottom right loops are the magnification of the central section of the loop. % values correspond to the weight % of nZVI in the non-mags fraction.

the < 125 μm fraction was minor at 30% voltage. This observation is consistent with previous findings (section 3.2), in which it was concluded that the metallurgical accounting revealed problems with the separation for this size. In fact, concerning the magnetic signals, these problems in the thickest fractions are also reflected in terms of the difference between the < 125 μm signals and the respective 500–2000 μm and 125–500 μm. In any case, for each experiment, almost all the nZVI was concentrated in the magnetic part (as revealed by the low percentages of nZVI in non-mags loops), thereby confirming a correlation between the accumulation of Cu, Pb, Sb in the mags fraction

Table 4
nZVI concentration derived from M(H) curves. $\%_M^{nZVI}$ and $\%_{NM}^{nZVI}$ are the percentages of nZVI in the mags and non-mags fractions, respectively, $\%_M$ is the proportion of magnetics in the mags fraction, and $\%_s^{nZVI}$ is the percentage of nZVI in each feed, calculated by means of Eq. 8.

Voltage (% of the maximum output)	2000–500 μm				125–500 μm				< 125 μm			
	$\%_M^{nZVI}$	$\%_{NM}^{nZVI}$	$\%_M$	$\%_s^{nZVI}$	$\%_M^{nZVI}$	$\%_{NM}^{nZVI}$	$\%_M$	$\%_s^{nZVI}$	$\%_M^{nZVI}$	$\%_{NM}^{nZVI}$	$\%_M$	$\%_s^{nZVI}$
10	18.44	0.14	89.42	**16.51**	22.24	0.41	49.75	**11.27**	28.98	0.82	62.86	**18.52**
20	18.26	0.28	90.24	**16.48**	27.84	0.31	39.81	**11.08**	32.23	0.95	56.17	**18.11**
30	39.52	0.00	41.81	**16.52**	38.79	0.31	28.48	**11.05**	26.51	0.64	69.11	**18.32**
50	27.13	0.06	60.76	**16.48**	33.44	0.10	33.50	**11.20**	31.81	0.71	57.27	**18.22**

(or Hg in the non-mags fraction).

Additionally, Fig. 8shows the signals of the non-mags for all the experiments. In this case it can be appreciated that the percentage of nZVI is lower than 1% in all the cases, evidencing that nZVI tends to accumulate in the magnetic fractions (Fig. 7). Moreover, this percentage decreases as the intensity of the magnetic field rises.

Finally, the ratio $\%_s^{nZVI}$ (i.e.; the percentage of nZVI in the soil feed) was calculated by means of Eq. 8, providing similar concentrations to those reconstructed with Eq. 5, as can be seen in Table 4. This ratio is a way of checking the robustness of the method of mixing and the innovative formulation presented.

4. Conclusions

Here we studied the effect of nZVI as a pretreatment to a subsequent soil washing process of soil affected by PTEs. To this end, various grain-size fractions were pretreated with nZVI and subjected to WHIMS or hydrocycloning. The study included an exhaustive chemical and magnetic characterization.

We introduced a correction of element recoveries in order to facilitate the comparison of results from experiments with and without nZVI pretreatment. In this respect, the equations proposed provided coherent results and successfully removed the dilution effect caused by nZVI addition.

Nanoparticle pretreatment performed before WHIMS provided satisfactory results, improving PTE concentrations for the 125–500 μm and 500–2000 μm grain-size fractions. However, concentration by hydrocycloning and WHIMS presented problems for the < 125 μm fraction. On the basis of these experiments, we conclude that nZVI preferentially interacts with Cu, Sb and Pb (making them report to the mags fraction) and Hg (which reported to the non-mags fraction). Unlike the previous elements, nanoparticles did not have a clear effect on As concentration.

Concerning the magnetic signals study, the hysteresis loops and proposed equations allowed us to determine the amount of nanoparticles present in each of the separated fractions. These results were essential to corroborate the contribution of nZVI to enhancing the concentration process, as well as to perform the metallurgical accounting correction. In this respect, we conclude that the larger the nZVI dose, the better the PTE recovery. Along the same lines, optimal operating conditions were deemed to be at 30% of the maximum output voltage, except in the < 125 μm fraction. In view of the aforementioned findings, we conclude that nZVI treatment prior to soil washing brings about an improvement in PTE recovery.

Acknowledgements

This work was supported by Project CTM2016-75894-P (MINECO). Carlos Boente obtained a grant from the “Formación del Profesorado Universitario” program, financed by the “Ministerio de Educación, Cultura y Deporte de España”. The authors thank the “Servicio Cientifico-Técnico de Medidas Magnéticas” of the University of Oviedo.

References

[1] M. Biasioli, H. Grcman, T. Kralj, F. Madrid, E. Díaz-Barrientos, F. Ajmone-Marsan, Potentially toxic elements contamination in urban soils: a comparison of three European cities, J. Environ. Qual. 36 (2007) 70–79, http://dx.doi.org/10.2134/jeq2006.0254.
[2] C. Huamain, Z. Chunrong, T. Cong, Z. Yongguan, Heavy status metal and in China : in soils pollution countermeasures, Ambio. 28 (1999) 130–134.
[3] S. Clemens, Toxic metal accumulation, responses to exposure and mechanisms of tolerance in plants, Biochimie. 88 (2006) 1707–1719, http://dx.doi.org/10.1016/j.biochi.2006.07.003.
[4] C.L.S. Wiseman, F. Zereini, W. Püttmann, Traffic-related trace element fate and uptake by plants cultivated in roadside soils in Toronto, Canada, Sci. Total Environ. 442 (2013) 86–95, http://dx.doi.org/10.1016/j.scitotenv.2012.10.051.
[5] C. Boente, N. Matanzas, N. García-González, E. Rodríguez-Valdés, J.R. Gallego, Trace elements of concern affecting urban agriculture in industrialized areas: A multivariate approach, Chemosphere 183 (2017) 546–556, http://dx.doi.org/10.1016/j.chemosphere.2017.05.129.
[6] A. Kabata-Pendias, Trace Elements in Soils and Plants, (2011), http://dx.doi.org/10.1201/b10158-25.
[7] L. Järup, Hazards of heavy metal contamination, Br. Med. Bull. 68 (2003) 167–182, http://dx.doi.org/10.1093/bmb/ldg032.
[8] M. Farrell, D.L. Jones, Use of composts in the remediation of heavy metal contaminated soil, J. Hazard. Mater. 175 (2010) 575–582, http://dx.doi.org/10.1016/j.jhazmat.2009.10.044.
[9] V.R. Ouhadi, R.N. Yong, N. Shariatmadari, S. Saeidijam, A.R. Goodarzi, M. Safari-Zanjani, Impact of carbonate on the efficiency of heavy metal removal from kaolinite soil by the electrokinetic soil remediation method, J. Hazard. Mater. 173 (2010) 87–94, http://dx.doi.org/10.1016/j.jhazmat.2009.08.052.
[10] A.M. Jiménez-Rodríguez, M.M. Durán-Barrantes, R. Borja, E. Sánchez, M.F. Colmenarejo, F. Raposo, Heavy metals removal from acid mine drainage water using biogenic hydrogen sulphide and effluent from anaerobic treatment: effect of pH, J. Hazard. Mater. 165 (2009) 759–765, http://dx.doi.org/10.1016/j.jhazmat.2008.10.053.
[11] Ra. Wuana, F.E. Okieimen, Heavy metals in contaminated soils: a review of sources, chemistry, risks and best available strategies for remediation, ISRN Ecol. 2011 (2011) 1–20, http://dx.doi.org/10.5402/2011/402647.
[12] G. Dermont, M. Bergeron, G. Mercier, M. Richer-Laflèche, Soil washing for metal removal: a review of physical/chemical technologies and field applications, J. Hazard. Mater. 152 (2008) 1–31, http://dx.doi.org/10.1016/j.jhazmat.2007.10.043.
[13] K.K. Fedje, L. Yillin, A.M. Strömvall, Remediation of metal polluted hotspot areas through enhanced soil washing - evaluation of leaching methods, J. Environ. Manage. 128 (2013) 489–496, http://dx.doi.org/10.1016/j.jenvman.2013.05.056.
[14] C. Sierra, J.R. Gallego, E. Afif, J.M. Menéndez-Aguado, F. González-Coto, Analysis of soil washing effectiveness to remediate a brownfield polluted with pyrite ashes, J. Hazard. Mater. 180 (2010) 602–608, http://dx.doi.org/10.1016/j.jhazmat.2010.04.075.
[15] B. Wills, J. Finch, Mineral Processing Technology:An Introduction to the Practical Aspects of Ore Treatment and Mineral Recovery, (2015), http://dx.doi.org/10.1016/B978-075064450-1/50003-5.
[16] R.J. Abumaizar, E.H. Smith, Heavy metal contaminants removal by soil washing, J. Hazard. Mater. 70 (1999) 71–86, http://dx.doi.org/10.1016/S0304-3894(99)00149-1.
[17] H. Freeman, E. Harris, Hazardous Waste Remediation: Innovative Treatment Technologies, (1995).
[18] M. Sung, C.Y. Lee, S.Z. Lee, Combined mild soil washing and compost-assisted phytoremediation in treatment of silt loams contaminated with copper, nickel, and chromium, J. Hazard. Mater. 190 (2011) 744–754, http://dx.doi.org/10.1016/j.jhazmat.2011.03.113.
[19] D. Komínková, M. Fabbricino, B. Gurung, M. Race, C. Tritto, A. Ponzo, Sequential application of soil washing and phytoremediation in the land of fires, J. Environ. Manage. 206 (2018) 1081–1089, http://dx.doi.org/10.1016/j.jenvman.2017.11.080.
[20] X. Yoo, J.- Beiyuan, Wang J, Tsang L, D.C.W. Baek, Bolan K, N.S. Li, A combination of ferric nitrate/EDDS-enhanced washing and sludge-derived biochar stabilization of metal-contaminated soils, Sci. Total Environ. 616–617 (2018) 572–582, http://dx.doi.org/10.1016/j.scitotenv.2017.10.310.
[21] K.R. Reddy, K. Maturi, C. Cameselle, Sequential electrokinetic remediation of mixed contaminants in low permeability soils, J. Environ. Eng. 135 (2009) 989–998,

http://dx.doi.org/10.1061/(ASCE)EE.1943-7870.0000077.
[22] B. Park, Y. Son, Ultrasonic and mechanical soil washing processes for the removal of heavy metals from soils, Ultrason. Sonochem. 35 (2017) 640–645, http://dx.doi.org/10.1016/j.ultsonch.2016.02.002.
[23] L.G. Torres, R.B. Lopez, M. Beltran, Removal of As, Cd, Cu, Ni, Pb, and Zn from a highly contaminated industrial soil using surfactant enhanced soil washing, Phys. Chem. Earth 37–39 (2012) 30–36, http://dx.doi.org/10.1016/j.pce.2011.02.003.
[24] A. Giannis, A. Nikolaou, D. Pentari, E. Gidarakos, Chelating agent-assisted electrokinetic removal of cadmium, lead and copper from contaminated soils, Environ. Pollut. 157 (2009) 3379–3386, http://dx.doi.org/10.1016/j.envpol.2009.06.030.
[25] E. Lefevre, N. Bossa, M.R. Wiesner, C.K. Gunsch, A review of the environmental implications of in situ remediation by nanoscale zero valent iron (nZVI): behavior, transport and impacts on microbial communities, Sci. Total Environ. 565 (2015) 889–901, http://dx.doi.org/10.1016/j.scitotenv.2016.02.003.
[26] R.M. Moattari, S. Rahimi, L. Rajabi, A.A. Derakhshan, M. Keyhani, Statistical investigation of lead removal with various functionalized carboxylate ferroxane nanoparticles, J. Hazard. Mater. 283 (2015) 276–291, http://dx.doi.org/10.1016/j.jhazmat.2014.08.025.
[27] F. Fu, D.D. Dionysiou, H. Liu, The use of zero-valent iron for groundwater remediation and wastewater treatment: A review, J. Hazard. Mater. 267 (2014) 194–205, http://dx.doi.org/10.1016/j.jhazmat.2013.12.062.
[28] M. Stefaniuk, P. Oleszczuk, Y.S. Ok, Review on nano zerovalent iron (nZVI): from synthesis to environmental applications, Chem. Eng. J. 287 (2016) 618–632, http://dx.doi.org/10.1016/j.cej.2015.11.046.
[29] R. Singh, V. Misra, R.P. Singh, Removal of cr(VI) by nanoscale zero-valent iron (nZVI) from soil contaminated with tannery wastes, Bull. Environ. Contam. Toxicol. 88 (2012) 210–214, http://dx.doi.org/10.1007/s00128-011-0425-6.
[30] C. Fajardo, M. Gil-Díaz, G. Costa, J. Alonso, A.M. Guerrero, M. Nande, M.C. Lobo, M. Martín, Residual impact of aged nZVI on heavy metal-polluted soils, Sci. Total Environ. 535 (2015) 79–84, http://dx.doi.org/10.1016/j.scitotenv.2015.03.067.
[31] X. Qiu, Z. Fang, X. Yan, F. Gu, F. Jiang, Emergency remediation of simulated chromium (VI)-polluted river by nanoscale zero-valent iron: laboratory study and numerical simulation, Chem. Eng. J. 193–194 (2012) 358–365, http://dx.doi.org/10.1016/j.cej.2012.04.067.
[32] V. Tanboonchuy, N. Grisdanurak, C.-H. Liao, Background species effect on aqueous arsenic removal by nano zero-valent iron using fractional factorial design, J. Hazard. Mater. 205 (2012) 40–46, http://dx.doi.org/10.1016/j.jhazmat.2011.11.090.
[33] R.A. Crane, T.B. Scott, Nanoscale zero-valent iron: future prospects for an emerging water treatment technology, J. Hazard. Mater. 211 (2012) 112–125, http://dx.doi.org/10.1016/j.jhazmat.2011.11.073.
[34] S.R. Kanel, B. Manning, L. Charlet, H. Choi, Removal of arsenic (III) from groundwater by nanoscale zero-valent iron, Environ. Sci. Technol. 39 (2005) 1291–1298, http://dx.doi.org/10.1021/es048991u.
[35] R. Rangsivek, M.R. Jekel, Removal of dissolved metals by zero-valent iron (ZVI): kinetics, equilibria, processes and implications for stormwater runoff treatment, Water Res. 39 (2005) 4153–4163, http://dx.doi.org/10.1016/j.watres.2005.07.040.
[36] D. O'Carroll, B. Sleep, M. Krol, H. Boparai, C. Kocur, Nanoscale zero valent iron and bimetallic particles for contaminated site remediation, Adv. Water Resour. 51 (2013) 104–122, http://dx.doi.org/10.1016/j.advwatres.2012.02.005.
[37] G.Z. Kyzas, K.A. Matis, Nanoadsorbents for pollutants removal: A review, J. Mol. Liq. 203 (2015) 159–168, http://dx.doi.org/10.1016/j.molliq.2015.01.004.
[38] C. Sierra, D. Martínez-Blanco, J. a Blanco, J.R. Gallego, Optimisation of magnetic separation: A case study for soil washing at a heavy metals polluted site, Chemosphere (2014), http://dx.doi.org/10.1016/j.chemosphere.2013.12.063.
[39] J. Svoboda, T. Fujita, Recent developments in magnetic methods of material separation, Min. Eng. 16 (2003) 785–792, http://dx.doi.org/10.1016/S0892-6875(03)00212-7.
[40] F. Lotze, Zur Gliderung der Varisziden der Iberischen Meseta, Geotekt. Forsch. 6 (1945) 78–92.
[41] M. Julivert, A. Marcos, Superimposed folding under flexural conditions in the Cantabrian zone (Hercynian Cordillera, Northwest Spain), Am. J. Sci. 273 (1973) 353–375, http://dx.doi.org/10.2475/ajs.273.5.353.
[42] C. Luque, M. Gutierrez-Claverol, La minería del mercurio en Asturias, Rasgos históricos, (2006).
[43] M. Gil-Díaz, J. Alonso, E. Rodríguez-Valdés, P. Pinilla, M.C. Lobo, Reducing the mobility of arsenic in brownfield soil using stabilised zero-valent iron nanoparticles, J. Environ. Sci. Health A Tox. Hazard. Subst. Environ. Eng. 49 (2014) 1361–1369, http://dx.doi.org/10.1080/10934529.2014.928248.
[44] G. Mercier, J. Duchesne, D. Blackburn, Prediction of metal removal efficiency from contaminated soils by physical methods, J. Environ. Eng. (Reston Virginia) 127 (2001) 348–358.
[45] L. Ma, Q. Yang, Y. Huang, P. Qian, J.G. Wang, Pilot test on the removal of coke powder from quench oil using a hydrocyclone, Chem. Eng. Technol. 36 (2013) 696 http://onlinelibrary.wiley.com doi/10.1002/ceat.201200316/abstract.
[46] Q. Yang, Z.M. Li, W.J. Lv, H.L. Wang, On the laboratory and field studies of removing fine particles suspended in wastewater using mini-hydrocyclone, Sep. Purif. Technol. 110 (2013) 93–100, http://dx.doi.org/10.1016/j.seppur.2013.03.025.
[47] D.J. Nieuwoudt, J.S.J. Van Deventer, M.A. Reuter, V.E. Ross, The influence of design variables on the flotation of pyrite in an air-sparged hydrocyclone, Min. Eng. 3 (1990) 483–499, http://dx.doi.org/10.1016/0892-6875(90)90041-9.
[48] C. Boente, C. Sierra, E. Rodríguez-Valdés, J.M. Menéndez-Aguado, J.R. Gallego, Soil washing optimization by means of attributive analysis: case study for the removal of potentially toxic elements from soil contaminated with pyrite ash, J. Clean. Prod. (2016), http://dx.doi.org/10.1016/j.jclepro.2016.11.007.
[49] A.G. Caporale, A. Violante, Chemical processes affecting the mobility of heavy metals and metalloids in soil environments, Curr. Pollut. Rep. 2 (2016) 15–27, http://dx.doi.org/10.1007/s40726-015-0024-y.
[50] M.B. Ogundiran, O. Osibanjo, Mobility and speciation of heavy metals in soils impacted by hazardous waste, Chem. Speciation Bioavailability 21 (2009) 59–69, http://dx.doi.org/10.3184/095422909X449481.
[51] L. Giraldo, A. Erto, J.C. Moreno-Piraján, Magnetite nanoparticles for removal of heavy metals from aqueous solutions: synthesis and characterization, in, Adsorption (2013) 465–474, http://dx.doi.org/10.1007/s10450-012-9468-1.
[52] X.S. Wang, H.J. Lu, F. Liu, J.J. Ren, Adsorption of lead(II) ions onto magnetite nanoparticles, Adsorpt. Sci. Technol. 26 (2011) 407–417.
[53] I. Carabante, Arsenic (V) adsorption on iron oxide, Implication for Soil Remediation and Water Purification, (2012).
[54] S. Fendorf, P.S. Nico, B.D. Koncar, Y. Massue, K.J. Tufano, Arsenic Chemistry in Soils and Sediments, Lawrence Berkeley Natl. Lab., 2010.
[55] C.H. Liu, Y.H. Chuang, T.Y. Chen, Y. Tian, H. Li, M.K. Wang, W. Zhang, Mechanism of arsenic adsorption on magnetite nanoparticles from water: thermodynamic and spectroscopic studies, environ, Sci. Technol. 49 (2015) 7726–7734, http://dx.doi.org/10.1021/acs.est.5b00381.
[56] S. Dixit, J. Hering, Comparison of arsenic (V) and arsenic (III) sorption onto iron oxide minerals: implications for arsenic mobility, Environ. Sci. Technol. 37 (2003) 4182–4189, http://dx.doi.org/10.1021/es030309t.
[57] S.M. Shaheen, C.D. Tsadilas, J. Rinklebe, A review of the distribution coefficients of trace elements in soils: influence of sorption system, element characteristics, and soil colloidal properties, Adv. Colloid Interface Sci. 201–202 (2013) 43–56, http://dx.doi.org/10.1016/j.cis.2013.10.005.
[58] H.L. Anderson, S.D. Balsley, P.V. Brady, Iodide retention by cinnabar (HgS) and chalcocite (Cu2S), sandia natl, Lab Sand (1995).
[59] P. Somasundaran, K.P. Ananthapadmanabhan, Handbook of Separation Process Technology, (1987), pp. 775–805.

Chapter IV. General Discussion

IV.I New advances in PTEs-contaminated soils' characterization: Sources identification and fate

The final aim of a characterization process is to identify pollutants, find their sources, and delimit their spatial distribution to define the contamination extent. First, it should be highlighted that a pollution case is a multivariate problem. This fact is a consequence of the existence of multitude of analytical variables that affect the presence of pollutants in the soils, namely, element concentration, pH, electrical conductivity, and bioavailability among others. However, the problem is more complex, and qualitative variables such as geography, orography, or geology also pose a great influence on the presence of PTEs in the soils. For all these reasons, the use of statistics, both univariate and multivariate, as well as a proper knowledge of geostatistics for spatial representation, are indispensable in the development of pollution characterization projects. All these methodologies, which were not designed originally for soil pollution, can be combined, adapted, and improved to be used effectively in this scientific field.

Descriptive statistics and normality problem on geochemical data

The first one is the descriptive statistics. Given a series of geochemical variables, it includes the calculus of the parameters such as the mean, median, range, standard deviation, or relative standard deviation, among others. They are useful as the first approximation in the identification of PTEs that do not follow a normal distribution. Experience tells us that it is difficult to find a Gaussian distribution when the distribution of a pollutant is studied mainly as consequence of the existence of outliers (Kleijnen, 2009). Outliers have in most cases an anthropogenic origin (Filzmoser et al., 2005). For some studies, outliers can be carefully removed considering the nature of the data.

Furthermore, the non-normality of the data hinders the use of the majority of geostatistical interpolation methods for spatial distribution studies. This is the case, for instance, in kriging, which prefers data normality (Kleijnen, 2009). However, it has been stated that it is possible to smooth out the problem of normality through transformations. Some examples are the logarithmic, the arcsine or Box-Cox transformations (Shumway et al., 2002). These set of procedures ease the achievement of normality conditions and support outliers' direct use in the dataset.

In this context, a flaw of most geostatistical softwares is not implementing a tool for data back-transformation. This is the case of Geographic Information Systems (GIS), which is more focused in other aspects. An exception is BioMedware's SpaceStat software (Goovaerts, 2001), which permits direct data back-transformation before kriging. Moreover, this software also allows to calibrate the parameters of the variogram, a basics for kriging analysis.

Multivariate statistics: The usefulness of Factor Analysis and Cluster Analysis

Multivariate statistics present a variety of possibilities. In this thesis, we emphasize on two of them: Factor Analysis (PCA) and Cluster Analysis (CA). In both articles of this chapter, the first stated to be an efficient tool for the grouping of elements. These were later associated to certain geologies or soil fractions. It has even been seen that there can be groups formed exclusively by PTEs, whether the pollutants have a strong presence in the soils. However, CA was efficiently used as a tool to classify samples, in terms of the grade of similarity among them, giving rise to areas of similitude in soil parameters or PTE content.

In any case, both tools are key factors for the interpretation of results, and they support the recognition of pollutants, as well as their interactions, patterns, origins, sources, delimitation of areas of affection, and so on. These are widely used in recent geochemical studies (Boente et al., 2019; Nogueira et al., 2018; Tume et al., 2019), and of course, both articles of Chapter II share the use of these multivariate methods that are considered mandatory in any characterization process.

The influence of the factor scale on the soil pollution assessment

The way to address the problem is radically different in terms of the scale considered. The study of characterization methodologies in this research was carried out at three levels of the administrative division of Spain: The local, municipal, and regional scales. Characterization works under Chapter II were focused on local and municipal contaminations problems, each independently, and both established a comparison with the regional scene (Asturias). This was so because the RBSSL for PTEs are designed for the regional scenario according to the current legislation of Spain.

For the local scale, areas of Jove and Lloreda (totaling 0.125 km^2) were selected. They are urban gardens located at the outskirts of Gijón, the most populated city of the

Principality of Asturias. Both study areas suffer problems of diffuse pollution as a result of an important industrial activity and traffic in the surroundings. These activities provoked an increase in the concentrations of PTEs and PAHs in the soils.

For the municipal scene, the complete Langreo municipality (approximately 80 km^2) was studied. This is a valley with a strong legacy linked to mining and industry. Unlike observed in an earlier study, pollution here is not uniquely diffused, but through dumping the pollutants from that are displaced by erosive agents. A strategy by way of perpendicular transects to the main river was adopted to carry out a representative sampling of this area. This allowed to study the pollution across the valleys without losing the desirable randomness for statistical and geostatistical methods.

In the current literature, there is a lack of indices and/or indicators that assess pollution levels from a legal or administrative point of view. For instance, the enrichment factors or geoaccumulation indices are built on the basis of the concepts of geochemical background or SSL (U.S. Environmental Protection Agency, 2007). However, as it was stated in Chapter I, the concept that finally determines whether a soil is polluted is the RBSSL.

Following this premise, the principal aim of the article with reference to a local area (Jove/Lloreda) is the creation of an indicator of pollution that considers the RBSSL and not the geochemical background or the SSL. It has been named as Soil Pollution Index (SPI). This mathematical expression is in fact a regionalized variable that evaluates the degree of pollution in a point considering the RBSSL of PTEs that are surpassed at least once in the study area. The result is a general overview about those areas that are more or less polluted, considering all PTEs as a group. Thus, the greater the value of the SPI, the greater the pollution of the point, as at least one RBSSL would have been surpassed in one or more points. Moreover, SPI can be introduced as a variable in kriging, allowing to estimate the value of the points that were not sampled, thus reducing the sampling costs.

Generally, it was corroborated that SPI worked properly in the case of Jove and Lloreda, as the areas that are highlighted by the SPI coincide with conclusions given by the univariate and multivariate statistical analysis. Therefore, a synergy has been created between methods and techniques, which allowed to assess the degree of soil affection by PTEs. In addition, in this work there were also considered the concentrations of PAHs, except for that of benzo(a)pyrene as it never surpassed the RBSSL, which in case of

organic pollutants are governed by national (and not regional) legislation in the Spanish case.

In case of the municipal scenario (Langreo), considering the RBSSL, something advanced was tried. Here, it was intended to perform a different data treatment which could provide a distinct vision of the problem, that is to say, a clarity that cannot be achieved with mere use of data on raw concentrations of PTEs. This was achieved by applying the theory of compositional data. The Centered Log-Ratio transformation (CLR) (Pawlowsky-Glahn and Egozcue, 2006; Tolosana-Delgado and McKinley, 2016) allowed to introduce a new concept presented in this thesis: Relative enrichment of a PTE. Given a number of PTEs (subcomposition), the relative enrichment of a certain PTE is the proportion of the PTE in the total subcomposition (Pawlowsky and Burger, 1992). This can be interpreted as a second use of the CLR transformation stated in McKinley et al., 2016: "*CLR is grounded to see the patterns of that element relative to the average behaviour of other elements at hand in the compositional dataset (by means of the geometric mean).*" In the case of Langreo, the chosen elements for the subcomposition were As, Cu, Hg, Pb, and Zn. Thus, each sampling point would have an assigned proportion for each PTE concentration within the subcomposition, 1 being the sum of all of them.

Again, this technique is compatible with kriging or any other geostatistical interpolation method for mapping the spatial distribution of a variable. In Langreo's work, a comparison between the mentioned compositional data and the raw data was established, mapping both of them. The results showed clear differences between them. Thus, the raw data interpolation showed the concentration of certain PTEs across the study area, but it did not reveal the level at which any given element was enriched. This fact was circumvented by the use of compositional data.

Consequently, results for Langreo indicated that, for instance, as occurs naturally in environmental studies, the representation of raw data highlights the urban core for all PTEs. This happens because the concentrations of PTEs are higher here due to human activity. However, the representation of the compositional approach displayed alternative zones that were not visible with the raw data. These are zones where each PTE is more enriched as compared with the rest of pollutants. This is very useful to discuss about the origins of the pollutants, to detect geological mineralizations or sources of PTEs, without resorting to classical pollution indices/indicators.

All things considered, the characterization tools presented in this chapter suppose a clear improvement for the soil pollution assessment and distribution. The tools supported the comprehension of the results and the discussion about the origins and fate of PTEs in real case studies, considering the current environmental legislations.

IV.II New advances in remediation of polluted soils: PTEs extraction

Soil washing is a remediation technique that has been the focus of Chapter III of the thesis. It is a methodology that has its origins in minerals processing. Washing methods are expected to concentrate pollutants into a volume of the initial soil that should be as reduced as possible. To this end, it takes advantage of certain properties of the target PTEs, as compared with those of the natural soil particles of the soils. Among the considered properties density, size, or magnetic susceptibility are the most common.

During this research, soil washing was used with two soils from different genesis. Both are officially declared as polluted soils in the Principality of Asturias. The first is the derelict fertilizer factory of Nitrastur (Langreo), whereas the second is the dump of the old mercury mine of Olicio (Cangas de Onís).

Improvements for classical soil washing: Methods for assessing experiments

Nitrastur was abandoned in the late 1990s, whereas Olicio's mine in early 1970s, and since then no remediation processes have been performed over them. Soils of the old industry present a problem associated with pyrite ash dumping. Pyrite cinders are dense and heavy metal-enriched by-product, which emerge as a result of the roasting of pyrite, required for the production of sulfuric acid (Gallego et al., 2016). This material was indiscriminately dumped in Nitrastur, increasing the concentration of the soil in several PTEs. It was observed that, up to five of them surpassed the RBSSL considerably. These are As, Cu, Hg, Pb, and Sb (Sierra et al., 2010).

With the intention of reducing the concentration of these contaminants, a classical soil washing design (without additives) was carried out. Magnetic (dry/wet high-intensity magnetic, Dry-HIMS/Wet-HIMS separators) and gravimetric (Hydrocycloning, HLS) techniques were selected, in terms of the grain size range of operability.

The remediation efficiency was assessed by the method of attributive analysis for the "concentrated" fraction. This is to say, for instance, for the "magnetic" or the "dense" fractions, depending on whether magnetic or gravimetric separation was performed. Attributive analysis maintains a balance between two variables: (1) weight recovery and (2) element recovery. Its goal is to maximize one and minimize the other in such a way that a very small volume of soil is obtained in which most pollutants are concentrated.

Conversely, the process leaves a large volume of treated soil mainly composed of soil matrix with pollutants concentration.

The final result of the attributive analysis is a quality index that indicates, within a test group, the most efficient one. All things considered, for the soil of Nitrastur it was observed that the best yields were obtained for the largest grain sizes and for the Wet-HIMS device, and also for HLS methods.

However, as stated earlier, the final aim of a remediation process is to obtain a large quantity of soil decontaminated, in which the levels of concentration of the decontaminant are below the RBSSL. Considering this, it is necessary to establish a method that compares the results of the experiments with the admissible levels of the concentration. Although it is true that the formulation of the attributive analysis considers the RBSSL, this quality index per se is not enough to ascertain whether the test is good enough to obtain a fraction of soil below the RBSSL.

The success score method, proposed in this thesis, is a very simple and intuitive methodology that offers a solution to this weakness. It consists in giving a punctuation to the concentrations of each contaminant individually in the feed, or polluted soil, and the concentrations of the clean soil fractions from the experiments: whether the soil (A or B) surpasses the RBSSL industrial and residential (success score = 0); whether it surpasses the residential, but not the industrial (Success Score = 1); or whether it is below both RBSSLs (Success Score = 2). The punctuation of all elements are summed and the success score for the experiment is obtained on one hand, and for the feed on the other. It is desirable that the experiment has a larger score than the feed as more RBSSL would have been reduced.

The advantage of both methods (attributive analysis and success score) is that they are not only applicable to soil washing, but also for every remediation methodology that provides a concentrated fraction of soil. However, it is strongly encouraged to maintain a balance between attributive analysis and Success Score. Regarding Nitrastur, in some cases the soil washing was able to keep the 50% of soil below the residential use RBSSL, thus reducing the quantity to half the total volume of polluted soil, which is ready to be subjected to a second remediation treatment, or to be transported to a landfill.

Nanoscale ZVI-assisted soil washing: The basis of a novel research line

The second study area was the soil of Olicio. It has a nature completely different to that of the Nitrastur's. Here, natural soil layers, more terrigenous, are intercalated with material from a soil heap that belongs to a mercury mine. This has created a soil presenting high concentrations of As, Cu, Hg, Pb, and Sb.

For this soil, it was decided to take one step further in the soil washing methodology. In this case, a dose of nanoscale ZVI (nZVI) was added to the original polluted soil. The use of this material as a complement to remediation procedures is rising in environmental science for multiple applications (Babaee et al., 2018; Gil-Díaz et al., 2014; Rajan, 2011), as Fe is not toxic or hazardous for the environment and its cost is relatively affordable (Zhang, 2003). Although it has been satisfactorily used for stabilization and pollutants found in water (Dong et al., 2017), never before has this material been used as an additive for a soil washing process. To fill this knowledge gap, this work has developed a technique of soil washing assisted by nZVI.

The expected effect is that contaminants are adsorbed onto the nanoparticles, forming aggregated larger and heavier fractions with increased magnetic susceptibility. As separation procedures both gravity separation, by means of hydrocycloning, and wet high-intensity magnetic separation were selected. A set of tests was conducted for three grain size fractions to determine the optimum grain size range for the different separation procedures. To make comparisons, exactly the same tests with polluted soils and without the addition of ZVI nanoparticles were carried out.

It is evident that the addition of nZVI should involve changes in soil washing yields. As a consequence of nZVI addition, element recoveries and weight recoveries may vary just by a simple distortion created by their mass. So, to make results comparable before and after their use, some calibrations on these equations may be required. These modifications can be included in the process of removal of Fe contaminants from all the fractions.

To perform these corrections, new equations for the magnetic quantification, based on their hysteresis curves were obtained. This magnetic study was useful to determine whether the dose of nZVI was correct, assess the efficiency of the nZVI-assisted soil washing, and trace nanoparticles movement throughout the process.

The graphical representation of weight recovery versus element recovery, for each PTE and tests, has been confirmed as a proper manner to check the efficiency of the concentration procedure. According to the theory presented in this thesis, the quality of the separation derives from the distance between a point in the graph and the $y = x$ line, which is the perfect quartering line. Each point in this line is undesirable. In other words, the greater the distance of a point to the line, the better the quality of the separation and the process of remediation. Thus, whether the distance of points to the line is larger for the nZVI-assisted soil washing than that for the classical soil washing, an improvement would have been achieved.

In case of the Olicio's soils, improvement was achieved for Cu, Sb, and Hg for Wet-HIMS tests. Here, the nZVI-assisted soil washing was much more efficient than the classical soil washing. Furthermore, the improvement was more relevant in the finer fractions (<500 μm), wherein the soil was more clayey and the concentration of PTEs tended to be higher. On the contrary, soil washing without additives, in turn, worked better for the larger fractions (>500 μm). This is suitable as the majority of PTEs tend to form aggregates on the finest grain sizes (Sierra et al., 2013). Regarding the gravimetric/size tests with the hydrocyclone also, an improvement was observed, but this was significantly lower.

IV.III References

Babaee, Y., Mulligan, C.N., Rahaman, M.S., 2018. Removal of arsenic (III) and arsenic (V) from aqueous solutions through adsorption by Fe/Cu nanoparticles. J. Chem. Technol. Biotechnol. 93. doi:10.1002/jctb.5320

Boente, C., Albuquerque, M.T.D., Gerassis, S., Rodríguez-Valdés, E., Gallego, J.R., 2019. A coupled multivariate statistics, geostatistical and machine-learning approach to address soil pollution in a prototypical Hg-mining site in a natural reserve. Chemosphere 218, 767–777. doi:10.1016/j.chemosphere.2018.11.172

Dong, H., Deng, J., Xie, Y., Zhang, C., Jiang, Z., Cheng, Y., Hou, K., Zeng, G., 2017. Stabilization of nanoscale zero-valent iron (nZVI) with modified biochar for Cr(VI) removal from aqueous solution. J. Hazard. Mater. doi:10.1016/j.jhazmat.2017.03.002

Filzmoser, P., Garrett, R.G., Reimann, C., 2005. Multivariate outlier detection in exploration geochemistry. Comput. Geosci. doi:10.1016/j.cageo.2004.11.013

Gallego, J.R., Rodríguez-Valdés, E., Esquinas, N., Fernández-Braña, A., Afif, E., 2016. Insights into a 20-ha multi-contaminated brownfield megasite: An environmental forensics approach. Sci. Total Environ. 563–564, 683–692. doi:10.1016/j.scitotenv.2015.09.153

Gil-Díaz, M., Alonso, J., Rodríguez-Valdés, E., Pinilla, P., Lobo, M.C., 2014. Reducing the mobility of arsenic in brownfield soil using stabilised zero-valent iron nanoparticles. J. Environ. Sci. Health. A. Tox. Hazard. Subst. Environ. Eng. 49, 1361–9. doi:10.1080/10934529.2014.928248

Kleijnen, J.P.C., 2009. Kriging metamodeling in simulation: A review. Eur. J. Oper. Res. doi:10.1016/j.ejor.2007.10.013

McKinley, J.M., Hron, K., Grunsky, E.C., Reimann, C., de Caritat, P., Filzmoser, P., van den Boogaart, K.G., Tolosana-Delgado, R., 2016. The single component geochemical map: Fact or fiction? J. Geochemical Explor. 162, 16–28. doi:10.1016/j.gexplo.2015.12.005

Nogueira, T.A.R., Abreu-Junior, C.H., Alleoni, L.R.F., He, Z., Soares, M.R., Santos Vieira, C. dos, Lessa, L.G.F., Capra, G.F., 2018. Background concentrations and quality

reference values for some potentially toxic elements in soils of São Paulo State, Brazil. J. Environ. Manage. doi:10.1016/j.jenvman.2018.05.048

Pawlowsky-Glahn, V., Egozcue, J.J., 2006. Compositional data and their analysis: an introduction. Geol. Soc. London, Spec. Publ. 264, 1–10. doi:10.1144/GSL.SP.2006.264.01.01

Rajan, C.S.R., 2011. Nanotechnology in Groundwater Remediation. Int. J. Environ. Sci. Dev. doi:10.7763/IJESD.2011.V2.121

Shumway, R.H., Azari, R.S., Kayhanian, M., 2002. Statistical approaches to estimating mean water quality concentrations with detection limits. Environ. Sci. Technol. doi:10.1021/es0111129

Sierra, C., Gallego, J.R., Afif, E., Menéndez-Aguado, J.M., González-Coto, F., 2010. Analysis of soil washing effectiveness to remediate a brownfield polluted with pyrite ashes. J. Hazard. Mater. 180, 602–8. doi:10.1016/j.jhazmat.2010.04.075

Sierra, C., Martínez, J., Menéndez-Aguado, J.M., Afif, E., Gallego, J.R., 2013. High intensity magnetic separation for the clean-up of a site polluted by lead metallurgy. J. Hazard. Mater. 248–249, 194–201. doi:10.1016/j.jhazmat.2013.01.011

Tolosana-Delgado, R., McKinley, J., 2016. Exploring the joint compositional variability of major components and trace elements in the Tellus soil geochemistry survey (Northern Ireland). Appl. Geochemistry 75, 263–276. doi:10.1016/j.apgeochem.2016.05.004

Tume, P., González, E., Reyes, F., Fuentes, J.P., Roca, N., Bech, J., Medina, G., 2019. Sources analysis and health risk assessment of trace elements in urban soils of Hualpen, Chile. Catena 175, 304–316. doi:10.1016/j.catena.2018.12.030

US Environmental Protection Agency, 2007. Soil Screening Guidance: User's Guide.

Zhang, W.X., 2003. Nanoscale iron particles for environmental remediation: An overview. J. Nanoparticle Res. doi:10.1023/A:1025520116015.

Chapter V. Conclusions

V.I General conclusions

The current research aimed to study methodologies to improve the characterization and remediation of soils polluted by PTEs. To that end, there were tools applied that are often used in other fields of science, and which were adapted here to be efficient as a solution to these environmental problems.

Some of the main general conclusions that could be drawn from the experiments are as follows:

- Soils are natural resources subjected to multitude of pollutants. Among them, there exist a series of inorganic pollutants named Potentially Toxic Elements (PTEs), which, given their high degree of toxicity, may compromise the human health or the environment when they reach certain concentrations.
- The evolution of the concentration of a pollutant at a point is determined by the concepts of geochemical background, Soil Screening Level (SSL), and Risk-Based Soil Screening Level (RBSSL). Although each depends on the others, it is the last one which eventually determines whether the soil is polluted, from the administrative point of view.
- Soils studied in this research were samples from the Principality of Asturias (Spain). Some of them are officially listed as polluted soils. However, it has been stated that there are many other soils in the region with concentrations that exceed the RBSSL. This research aims to encourage a revision of the Inventory of Polluted Soils, as well as to normalize the use of the risk assessment tools to study polluted soils in greater depth.

Conclusions concerning the improvement of the methodologies for the characterization of polluted soils

- The objectives of the characterization methodologies are: (1) to identify pollutants, (2) to study their spatial distribution, and (3) to find possible sources of pollutants or origins. In this context, the work scale is mandatory to achieve proper results. Thus, whereas for local or site scales it might be enough to deal with raw data through statistical and geostatistical analyses, regional scales may require an alternative treatment of data such as the use of enrichment factors or compositional data.
- Univariate and multivariate statistics are mandatory to determine the most hazardous elements as well as their associations. In this context, the validity of the Factorial Analysis has been stated for the recognition of elemental associations and the Cluster Analysis for the comparison of samples. However, geostatistics allow to represent the spatial distribution of any sort of data with geographical coordinates. Particularly, ordinary kriging is suitable for Gaussian distributions. However, there exist transformations (e.g., logarithmic or Box-Cox) that support the achievement of normality on data.
- The Soil Pollution Index (SPI) is a proper indicator to globally assess the degree of affection of a soil in terms of the RBSSL for PTEs.
- Graphical representation of raw data allow to distinguish the concentration of the pollutants across the study area. However, compositional data provide information on their Relative Enrichment. This is useful to determine natural or anthropogenic enrichments when there is an overall view of all the study variables.
- It has been stated that the synergy between all these tools, together with a proper geological and historical knowledge of the study area, allows to satisfy the objectives of the characterization process described earlier.

Conclusions concerning the improvements for the remediation of polluted soils

- This thesis states that soil washing is an efficient and versatile physico-chemical technique for the remediation of soils. Nevertheless, its on-field application requires mineral processing technologies the cost of which may be high.
- Attributive analysis is a mathematical tool that allows to assess the efficiency of the separation process and also to find the best performing assay. To do this, it establishes a balance between two parameters: weight recovery and element recovery. The aim is to maximize one and minimize the other, meaning the concentration of large quantities of pollutants in lesser volumes of soil. Moreover, the Success Score is an indicator that evaluates the concentration of PTEs in a soil that has been treated. It assigns a punctuation to the assay on the basis of whether the soil is below or above the RBSSL. Both proposals for the assessment of experimental assays are applicable to any sort of soil or remediation method that makes use of mineral processing technologies.
- This research lays the foundations for the nanoscale ZVI-assisted soil washing as an innovative remediation technology. It has been stated that soil washing improves its performance when a dose of nZVI is added to the polluted soil.
- The nZVI is an inert and non-contaminant material used in remediation. Nanoparticles adsorb the pollutants, forming aggregates with properties that may be exploited by mineral processing technologies.
- The attributive analysis equations were modified to adopt them to the particular case of the nZVI-assisted soil washing, allowing the evaluation of the experiments.
- Quantification through magnetic signals are a key aspect to identify the fate of the nanoparticles, as well as to evaluate the performance of the concentration operation.
- In case of the studied soils, magnetic separation yields better than the gravimetric separation at pilot scale to concentrate pollutants and to decontaminate soils.

V.II Conclusiones generales

En esta tesis se estudian herramientas y metodologías para mejorar los procesos de caracterización y remediación de terrenos contaminados por PTEs. Para ello, se han utilizado herramientas originariamente destinadas a otros campos de la ciencia y se han adaptado para dar solución a estos problemas.

Algunas de las conclusiones principales de tipo genérico que se pueden extraer de los trabajos desarrollados son:

- Los suelos son recursos naturales sometidos a multitud de agentes contaminantes. Entre ellos, existe una serie de contaminantes inorgánicos denominados elementos traza potencialmente tóxicos (Ing.: Potentially Toxic Elements, PTEs), que, por su alto grado de toxicidad, pueden comprometer la salud humana o el medioambiente si alcanzan determinadas concentraciones.
- La evolución de la concentración de un elemento en un punto viene determinada por los conceptos de nivel de fondo edafogeoquímico (Ing.: Geochemical Background), valor umbral (Ing.: Soil Screening Levels, SSL) y Nivel Genérico de Referencia (NGR) (Ing.: Risk Bassed Soil Screening Level, RBSSL). Aunque cada uno es dependiente del resto, es el último el que determina verdaderamente si un suelo está o no contaminado desde el punto de vista administrativo.
- Los suelos estudiados en la tesis pertenecen al Principado de Asturias. Algunos están catalogados oficialmente como suelos contaminados. Sin embargo, se ha demostrado que hay muchos otros cuyas concentraciones de PTEs están por encima de los Niveles Genéricos de Referencia. En la región existen multitud de suelos de estas características. Esta tesis pone de manifiesto la conveniencia de efectuar una revisión del Inventario de Suelos Contaminados, así como de normalizar el uso de las herramientas de análisis de riesgos para su el estudio de estos.

Conclusiones principales sobre mejora de los procesos de caracterización de suelos contaminados

- Los objetivos de los procesos de caracterización son la identificación de contaminantes, su distribución espacial y sus posibles fuentes u orígenes. La escala de trabajo es clave para conseguir los objetivos. Así, mientras que en una escala a nivel local, o de emplazamiento, puede ser suficiente con tratar los datos brutos mediante técnicas estadísticas y geoestadísticas, las escalas regionales pueden requerir algún tipo de tratamiento alternativo de los datos, como el uso de factores de enriquecimiento o datos composicionales.
- La estadística univariante y la multivariante son clave para determinar los elementos más peligrosos y sus asociaciones. En este sentido, se ha corroborado la validez del Análisis Factorial para conocer las asociaciones elementales, así como del Análisis Clúster para estudiar el grado de similitud de las muestras.
- La geoestadística es una herramienta que permite representar la distribución espacial de cualquier tipo de dato con coordenadas geográficas. Esto incluye concentración de contaminantes, datos composicionales o índices de contaminación. En particular, se ha constatado que el krigeado ordinario funciona muy bien con distribuciones gaussianas. Existen diversas transformaciones, como la logarítmica o la box-cox, que se pueden realizar para conseguir ésta distribución.
- El Índice de Contaminación del Suelo (ICS) (Ing.: Soil Pollution Index, SPI) es un indicador muy adecuado para evaluar, de manera global, el grado de afección de un suelo en base a los Niveles Genéricos de Referencia para Elementos Potencialmente Tóxicos.
- La representación espacial de datos brutos de concentración de elementos permite distinguir la distribución de los contaminantes en las áreas de estudio. La representación de datos composicionales, por el contrario, permite conocer el enriquecimiento relativo de los mismos. Esto último es útil para identificar enriquecimientos naturales o antrópicos cuando se tiene una visión global de todas las variables de estudio.
- Se ha constatado que la sinergia entre todas estas herramientas, así como la disposición de un buen conocimiento geológico e histórico del área de estudio, son eficaces a la hora de satisfacer los objetivos del proceso de caracterización anteriormente citados.

Conclusiones principales sobre mejoras de los procesos de remediación de suelos contaminados

- En esta tesis se ha constatado que el lavado de suelos es una técnica fisicoquímica, eficaz y versátil para el tratamiento de suelos, aunque para su desarrollo en campo se necesitan equipos de tratamiento de mineral cuyo coste puede llegar a ser elevado.
- El análisis atributivo es una herramienta matemática que permite evaluar la eficiencia de una separación y determinar el mejor ensayo. Para ello, se calculan dos parámetros: Rendimiento en peso y recuperación elemental, y se realiza un balance de ambos, buscando maximizar uno y minimizar el otro. El objetivo final de un proceso de concentración es la acumulación de la mayor cantidad posible de contaminante en una fracción muy pequeña de suelo.
- El índice de éxito (IE) (Ing.: Success Score) es un indicador que evalúa las concentraciones de PTEs del suelo tratado o limpio, y le otorga una puntuación en función de los elementos que se encuentran por debajo del Nivel Genérico de Referencia.
- Ambas propuestas para la evaluación de ensayos experimentales han demostrado ser eficaces y versátiles, siendo aplicables a cualquier tipo de suelo o tratamiento de remediación que emplee procesos mineralúrgicos.
- Esta tesis sienta las bases de la técnica del lavado de suelos asistido por nanopartículas como tecnología de remediación de suelos innovadora. Se ha demostrado que el lavado de suelos mejora sus prestaciones como técnica de remediación cuando se añade una dosis de nanopartículas de hierro cerovalente al suelo contaminado.
- El hierro cerovalente es un material inerte y no contaminante muy empleado en remediación. Las nanopartículas provocan un proceso de adsorción de los contaminantes a las mismas, formando un conjunto con propiedades que permiten ser explotadas por los equipos de concentración mineralúrgica.
- Las ecuaciones del análisis atributivo fueron modificadas para adaptarlas al caso particular de lavado de suelos con nanopartículas de hierro cerovalente, haciendo posible la valoración de estos ensayos.

- La cuantificación mediante señales magnéticas es un aspecto clave para conocer el destino de las nanopartículas, así como para evaluar el rendimiento de la operación de concentración.
- A nivel de escala piloto, para los suelos estudiados funciona mejor la separación magnética que la gravimétrica para concentrar contaminantes y descontaminar un suelo. El separador magnético de alta intensidad por vía húmeda se ha revelado como el equipo más eficaz.

Impact factor of scientific publications and other contributions

Compendium

Hereunder is revealed the impact factor of the publications that compound this thesis:

Publication 1:

Boente, C., Matanzas, N., García-González, N., Rodríguez-Valdés, E., Gallego, J.R., 2017. Trace elements of concern affecting urban agriculture in industrialized areas: A multivariate approach. Chemosphere 183, 546–556. doi:10.1016/j.chemosphere.2017.05.129

- IF 2017: 4.427
- Category: Environmental Chemistry
- Rank: 21 out of 109 (1st Quartile)

Publication 2:

Boente, C., Albuquerque, M.T.D., Fernández-Braña, A., Gerassis, S., Sierra, C., Gallego, J.R., 2018. Combining raw and compositional data to determine the spatial patterns of Potentially Toxic Elements in soils. Sci. Total Environ. 631–632, 1117–1126. doi:10.1016/j.scitotenv.2018.03.048

- IF 2017: 4.610
- Category: Environmental Chemistry
- Rank: 19 out of 109 (1st Quartile)

Publication 3:

Boente, C., Sierra, C., Rodríguez-Valdés, E., Menéndez-Aguado, J.M., Gallego, J.R., 2017. Soil washing optimization by means of attributive analysis: Case study for the removal of potentially toxic elements from soil contaminated with pyrite ash. J. Clean. Prod. doi:10.1016/j.jclepro.2016.11.007

- IF 2017: 5.651
- Category: Environmental Science
- Rank: 28 out of 339 (1st Quartile)

Publication 4:

Boente, C., Sierra, C., Martínez-Blanco, D., Menéndez-Aguado, J.M., Gallego, J.R., 2018. Nanoscale zero-valent iron-assisted soil washing for the removal of potentially toxic elements. J. Hazard. Mater. 350, 55–65. doi:10.1016/j.jhazmat.2018.02.016

- IF 2017: 6.434
- Category: Environmental Chemistry
- Rank: 14 out of 109 (1st Quartile)

Other works as first author

In addition to the four publications belonging the compendium, the author of the thesis has developed other works that have been published in journals or presented in reputable conferences across Europe. Here are described those works related to the matter of the thesis, being the student the first author:

Research papers:

1. Boente, C., Albuquerque, M.T.D., Gerassis, S., Rodríguez-Valdés, E., Gallego, J.R., 2019. A coupled multivariate statistics, geostatistical and machine-learning approach to address soil pollution in a prototypical Hg-mining site in a natural reserve. Chemosphere 218, 767–777. doi:10.1016/j.chemosphere.2018.11.172

2. Boente, C., Gerassis, S., Albuquerque, M.T.D., Taboada, J., Gallego, J.R., 2019. Local versus regional soil screening levels to identify potentially polluted areas. Math. Geosciences. Approved for publication. doi:10.1007/s11004-019-09792-x

3. Boente, C., Martín, I., Bel-Lán, A,. Gallego, J.R., 2019 A novel and synergistic geostatistical approach to identify sources and cores of potentially toxic elements in soils: An application in the region of Cantabria (Northern Spain). Geoderma. Under review.

Conference presentations:

1. Boente, C., Baragaño, D., Fernández-Braña, A., Gallego, J.R., 2019. Sources, fate and impact of polycyclic aromatic hydrocarbons in soils of a broad industrialized area in Northern Spain. AquaConSoil 2019. Antwerp, Belgium.
2. Boente, C., Albuquerque, MT.D., Gerassis, S., Taboada, J., Gallego, J.R., 2018. Optimizing soil screening levels for the delimitation of pollution risk areas in soils with high industrial density. GeoENV 2018. Belfast, United Kingdom.
3. Boente, C., Rodríguez-Valdés, E., Sierra, C., Gallego, J.R., Menéndez-Aguado, J.M., 2018. Mineral processing technologies for the remediation of soils polluted by trace elements. 2nd IRCSEEME. Mieres, Spain.
4. Boente, C., Sierra, C., Martínez, J., Rodríguez-Valdés, E., Afif, E., Rey, J., Gallego, J.R., 2018. Environmental threats of ancient Pb mining and metallurgical

activities in the Linares mining district (Southern Spain). 2nd IRCSEEME. Mieres, España

5. Boente, C., Matanzas, N., García-González, N., Rodríguez-Valdés, E., Gallego, J.R., 2017. Caracterización de contaminantes inorgánicos en los alrededores de una antigua mina de mercurio en Caunedo (Asturias). XII Congreso Nacional y XI Ibérico de Geoquímica. Linares, Spain.
6. Boente, C., Sierra, C., Menéndez-Aguado, J.M., Rodríguez-Valdés, E., Baragaño, D., Gallego, J.R., 2017. Remediation of an As-Hg polluted soil by means of enhanced soil washing with ZVI nanoparticles. AquaConSoil 2017. Lyon, France.
7. Boente, C., Gallego, J.R., Rodríguez-Valdés, E., Sierra, C., Menéndez-Aguado, J.M., 2016. Geostatistical approach to the 3D-Distribution of hazardous waste and polluted soil in a brownfield. XVI International Multidisciplinary Scientific GeoConference SGEM. Albena, Bulgary.

Other works as co-author

Research papers:

1. González-Fernández, B., Rodríguez-Valdés, E., Boente, C., Menéndez-Casares, E., Fernández-Braña, A., Gallego, J.R., 2018. Long-term ongoing impact of arsenic contamination on the environmental compartments of a former mining-metallurgy area. Sci. Total Environ. 610–611, 820–830. doi:10.1016/j.scitotenv.2017.08.135

2. Gerassis S., Albuquerque, M.T.D., García J., Boente, C., Giráldez E., Taboada, J., Martín, J.E., 2019. Understanding complex blasting operations: A structural equation model combining Bayesian networks and latent class clustering. Reliab. Eng. Syst. Safe. Accepted for publication.

3. Forján, R., Baragaño, D., Boente, C., Rodríguez-Valdés, E., Fernández-Iglesias, E., Gallego, J.R., 2019. Contribution of fluorite mining waste to mercury contamination in coastal systems. Mar. Pol. Bull. Under review.

4. Neiva, A.M.R., Albuquerque, M.T.D., Antunes, I.M.H.R., Carvalho, P.C.S., Santos, A.C.T., Boente, C., Cunha, P.P., Henriques, S.B.A., Pato, R.L., 2019, Assessment of metal and metalloid contamination in soils trough compositional data - the old Mortórios uranium mine area, central Portugal. Environ. Geochem. Health. Under review.

Conference presentations:

1. Albuquerque, M.T.D., Gerassis, S., Roque, N., Ribeiro, S., Boente, C., Ribeiro, M.M., 2019. Ecological modelling under climate change scenarios – a machine learning approach. 20th Annual Conference IAMG2019. Pennsylvania, USA.
2. Baragaño, D., Menéndez-Aguado, J.M., Marina, M., Boente, C., Sierra, C., Gallego, J.R., 2019. Enhanced magnetic separation with Fe-Ni nanoparticles: A novel tool for soil washing. AquaConSoil 2019. Antwerp, Belgium.
3. Sierra, C., Boente, C., Baragaño, D., Gallego, J.R., 2018. Nanoparticles pretreatment as a tool to enhance magnetic soil washing. Goldschmidt 2018. Boston, USA.

4. Baragaño, D., Rodríguez-Valdés, E., Peláez A.I., Boente, C., Matanzas, N., García, N., Gallego, J.R., 2018. Environmental Forensic Study and Remediation Feasibility in an Abandoned Industrial Site. 2nd IRCSEEME. Mieres, Spain.
5. Fernández-Braña, A., Boente, C., Afif, E., Gallego, J.R., 2017. Manejo de fondos geoquímicos y niveles genéricos de referencia de concentración de elementos traza en áreas afectadas por contaminación antropogénica difusa. XII Congreso Nacional y XI Ibérico de Geoquímica. Linares, Spain.
6. Gallego, J.R., Fernández-Braña, A., Boente, C., Afif, E., García, N., Colina, A., Rodríguez-Valdés, E., 2017. Management of soil geochemical backgrounds and threshold levels in areas affected by brownfields and diffuse anthropogenic pollution. AquaConSoil 2017. Lyon, France.
7. González-Fernández, B., Menéndez-Casares, E., Rodríguez-Valdés, E., Gallego, J.R., Boente, C., Fernández-Braña, A., 2016. Characterization of As-contaminated water in San Tirso River Valley (Asturias, Spain). IX Congreso Geológico de España. Huelva, Spain.